OAK RIDGE
NATIONAL LABORATORY
MANAGED BY UT-BATTELLE
FOR THE DEPARTMENT OF ENERGY

ORNL/TM-2006/609

Tensile and Creep-Rupture Evaluation of a New Heat of Haynes Alloy 25

February 2007

Prepared by
John P. Shingledecker, Principal Investigator
with Darryl B. Glanton, Ralph L. Martin, Brian L. Sparks, and Robert W. Swindeman

UT-BATTELLE
ORNL-27 (4-00)

ORNL/TM-2006/609

Tensile and Creep-Rupture Evaluation of a New Heat of Haynes Alloy 25

John P. Shingledecker[1], Principal Investigator
with
Darryl B. Glanton[1], Ralph L. Martin[1], Brian L. Sparks[1], Robert W. Swindeman[2]
[1]Oak Ridge National Laboratory, Materials Science and Technology Division, Oak Ridge, TN, USA
[2]Retired, Oak Ridge National Laboratory, Metals & Ceramics Division, Oak Ridge, TN, USA

February 2007

Prepared by
OAK RIDGE NATIONAL LABORATORY
P.O. Box 2008
Oak Ridge, Tennessee 37831-6285
managed by
UT-Battelle, LLC
for the
U.S. DEPARTMENT OF ENERGY
under contract DE-AC05-00OR22725

CONTENTS

LIST OF FIGURES

LIST OF TABLES

ACKNOWLEDGEMENTS

The authors would like to acknowledge the contributions of James F. King for his leadership on the program, Peyton Moore for his past leadership of the program, Roger Miller and Edgar Lara-Curzio for reviewing this report, Tim McGreevy for helpful discussions, Tom Geer for his assistance with metallography, Chris Stevens for performing some of the tensile tests, personnel from INL and LANL for providing the materials used in this study, Laura Riester for help with the elastic property measurements, and Christine Goudy for spending countless hours formatting this report.

ABSTRACT

From 1999 to 2006, a program was undertaken within the Materials Science and Technology Division, formerly the Metals and Ceramics Division, of Oak Ridge National Laboratory to characterize the tensile and creep-rupture properties of a newly produced heat of Haynes alloy 25 (L-605). Tensile properties from room temperature to 1100°C were evaluated for base material and welded joints aged up to 12,000 hours at 675°C. Creep and creep-rupture tests were conducted on base metal and cross-weldments from 650 to 950°C. Pressurized tubular creep tests were conducted to evaluate multiaxial creep-rupture response of the material. Over 800,000 hours of creep test data were generated during the test program with the longest rupture tests extending beyond 38,000 hours, and the longest creep-rate experiments exceeding 40,000 hours.

1. INTRODUCTION

Haynes alloy 25 (alloy 25), originally referenced as L-605, is a cobalt-based superalloy with good fabricability, high-temperature strength, and corrosion resistance. Most of the high-temperature data required for design of Haynes alloy 25 components, creep and tensile properties of base material and weldments, were summarized in 1970 by Swindeman [1]. All of the available literature was again reviewed by Swindeman in 1998 [2], and it was concluded that additional long-term data on a new heat of material would be needed for improved design and material analysis. Furthermore, it was recognized that new data on multiaxial creep effects would be useful, and therefore it was proposed that internally pressurized creep tests on tubular specimens of varying wall thicknesses be conducted. Based upon these recommendations, a test program to evaluate the tensile and creep properties of a new heat of alloy 25 was started. This report summarizes the results of this program, and an appendix containing the historical data (based largely on the summaries by Swindeman) and the data produced on this program is included.

2. BACKGROUND

A summary of the historical database for alloy 25 is provided in appendix subsections A.7 and A.8. Section A.7 contains the tensile data and section A.8 contains the stress and creep-rupture data. The tensile data are taken from the review of Slunder [3]. The data from Slunder's work includes references [1, 4, 14, 15, 16]. The stress and creep-rupture data are taken from Simmons and Cross [4], Baughman [5], Green et al. [6], Sandrock et al. [7], Conrad et al. [8], Flagella and McCullough [9], Yukawa and Sato [10], and Widmer et al. [11,12]. Stress-rupture data for weldments were included in some of the references: [1,4,5, and 8]. In general, the stress and creep-rupture data were of short duration. Only Widmer provided creep data beyond 10,000 hours. Over 200 tests are included in the historical database, but the total test durations for these tests are less than 200,000 hours.

A new heat of alloy 25 material was obtained for this study (details in section 3.0). Plate and bar product were evaluated. Dynamic elastic properties from room temperature to 1100°C were measured for the heat in the as-received mill-annealed condition and after aging at 675°C. Tensile tests from room temperature to 1100°C were performed on base metal and weldments aged up to 12,000 hours at 675°C. Creep and stress-rupture tests were conducted on base metal and weldments; this included aged material in addition to material in the as-received mill annealed condition. Creep-rupture test temperatures ranged from 650°C to 950°C for times in excess of 38,000 hours. Pressurized creep-rupture tests on tubular specimens were also conducted for two sizes of tubes at similar creep conditions.

3. MATERIAL AND SPECIMENS

The alloy 25 base metal material was received from Babcock & Wilcox of Ohio, Inc (Mound Laboratories) as 0.14-in. (3.3-mm) thick plate processed to meet the AMS 5537C specification. The vendor chemistry and the nominal composition of the alloy are given in Table 1. The vendor reported the following tensile properties: 67.5 ksi (465 MPa) yield strength, 114 ksi (786 MPa) ultimate strength, and 52 % elongation. Additional alloy 25 bar material, machined into the form of tubes, from the same heat of material was received from Idaho National Laboratory (INL) and Los Alamos National Laboratory (LANL). The grain size of the plate and the machined bar product were measured as an ASTM No. 4-5 (60-90 μm) and No. 7-8 (23-32 μm), respectively. Metallographic images of the as-received materials are shown in figure 3.1. Although the bar product had a finer average grain size than the plate, a number of larger grains similar in size to the plate grain size were observed in the bar material. Twining was evident within most grains, and in some areas it was difficult to differentiate grain boundaries from twin boundaries. All materials were received in the solution annealed condition, and the purchase specification required that the material have an ASTM grain size number of four or greater to reduce the materials susceptibility to hot cracking during welding.

Table 1. Composition of Haynes Alloy 25 used in this study

	Element (wt%)									
ID	C	Cr	Fe	Mn	Ni	P	S	Si	W	Co
Haynes Heat # 1860-8-1391	0.11	20.23	2.34	1.51	10.32	0.008	0.002	0.16	14.77	Bal.
AMS 5796C .035" Dia.Weld Wire Heat # 1860-8-1362	0.12	20.13	2.51	1.46	10.58	0.012	0.003	0.22	15.43	Bal.
Nominal Composition	0.10	20	3*	1.5	10	---	---	0.4*	15	51 (Bal)

*Maximum

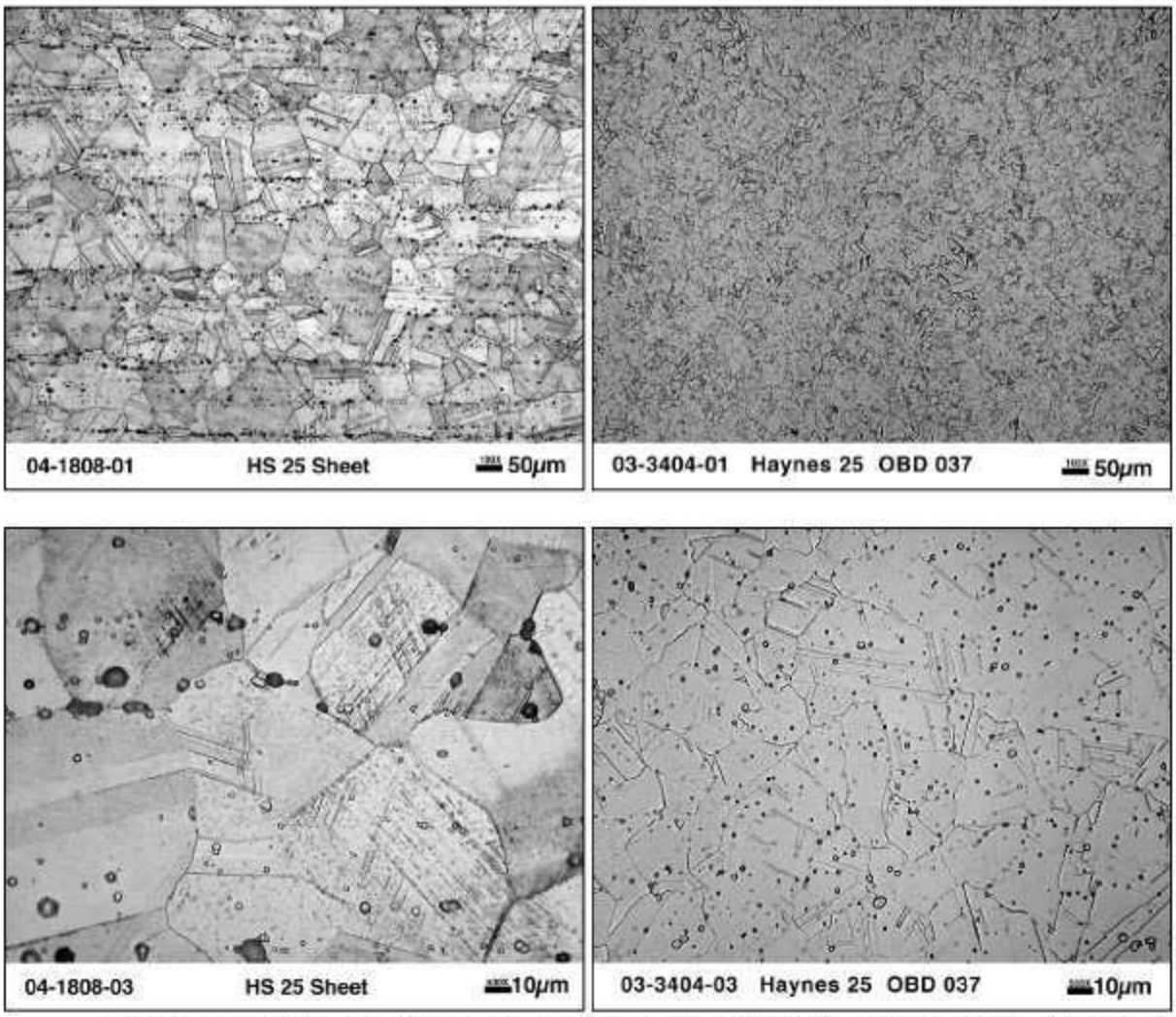

Figure 3.1. Metallographic images of the alloy 25 as-received material. sheet – left, machined bar (tube) – right.

The plate was sheared into several pieces and coupons were cut for the preparation of tensile and creep testing specimens. Plate-type specimens were machined with the uniform gage section parallel to the primary rolling direction of the sheet with dimensions shown in figure 3.2.

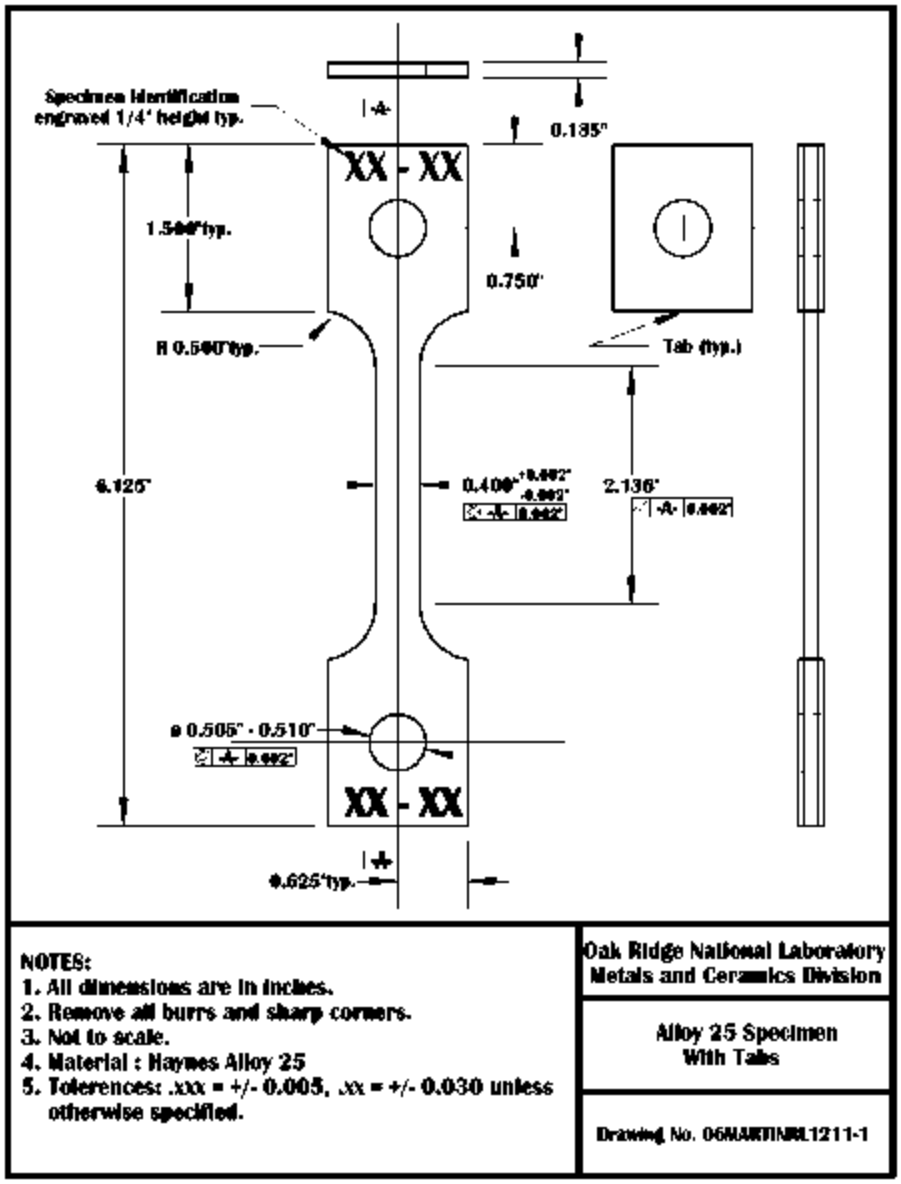

Figure 3.2. Specimen drawing for alloy 25 plate creep and tensile specimens.

Welded plate was received from Mound Laboratories as 0.14-in. (3.3-mm) thick sheet. This was the same plate material as supplied for base metal testing but containing a matching composition multi-pass gas tungsten arc weld (GTAW) transverse to the primary rolling direction. The weld filler metal heat met the AMS 5796C specification, and its composition is included in Table 1. Ten plates each 10 in. (250 mm) by 7 in. (178 mm) were supplied. The plates exhibited a slight angular distortion after welding. Coupons were cut from the plates oriented to place a transverse weld in the center of the reduced section of the plate specimen as shown in the example cutting plan in figure 3.3. The specimen design was the same as that used for testing the base metal with the exception of the weldment in the center of the gauge. Specimens were machined so that the pin-hole in each shoulder was perpendicular to the end of the sheet, and the weldment crown was not removed. After machining, specimens were placed in a three-point loading bend devise with the weldment crown resting on the center bend bar. The angular distortion was removed by flattening the specimens in the 3-point fixture. Tensile tests were performed on the flattened

bars. Short-term heat-treatments at 800°C did not cause significant changes in the room temperature tensile behavior indicating a minimal effect of flattening on tensile properties.

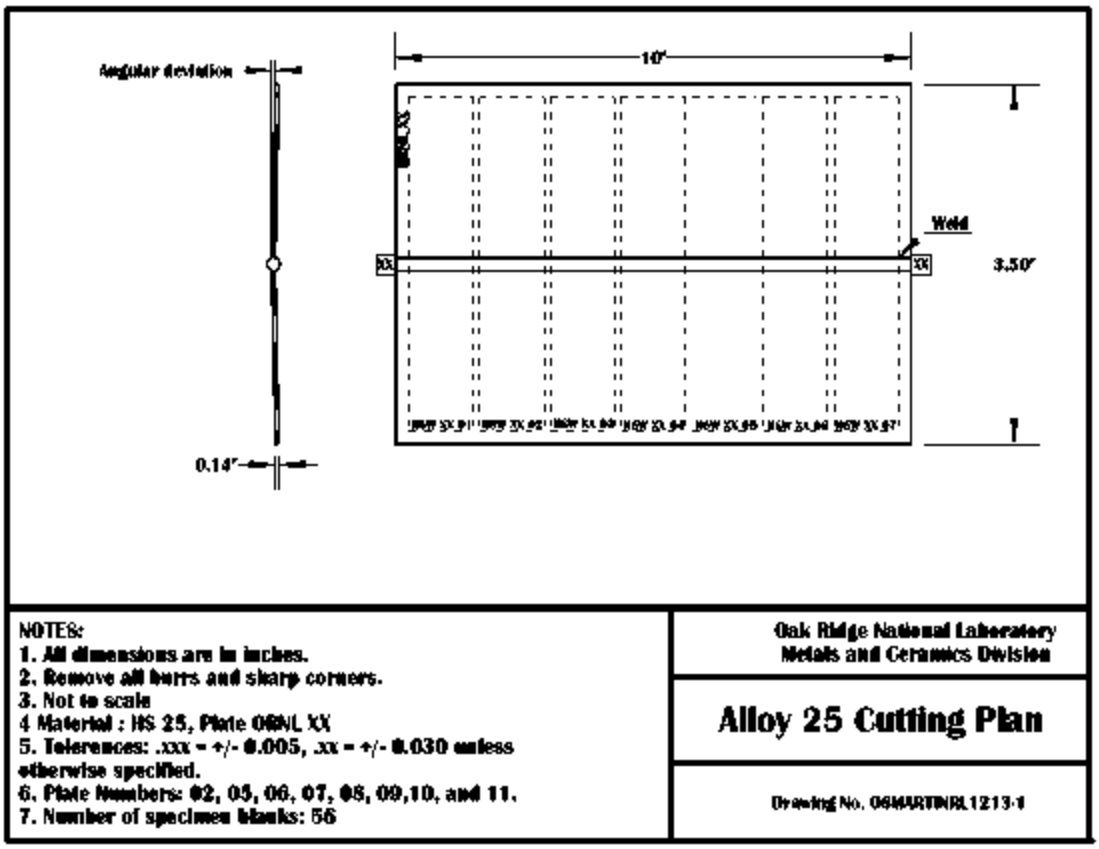

Figure 3.3. Example cutting plan for alloy 25 weldment specimens.

Tubular specimens machined from bar-stock were supplied by INL and LANL. Uniaxial weldment specimens for tensile and creep testing were machined in a similar configuration to the plate specimens as shown in figure 3.4. These specimens contained a matching filler metal multi-pass GTAW orbital weldment in the center of the gauge. The same heat of filler metal used in the plate specimens was used by both INL and LANL for these specimens. Due to the size of the bar stock, some specimens were machined with a 1.000 in. (25.00 mm) gauge length while others were similar to the plate specimens with a 2.140 in. (54.35 mm) gauge length. The curvature of the tube was left intact, as it was not practical to flatten the specimen without imparting a significant degree of cold work, and specialized grips were produced for long-term creep testing.

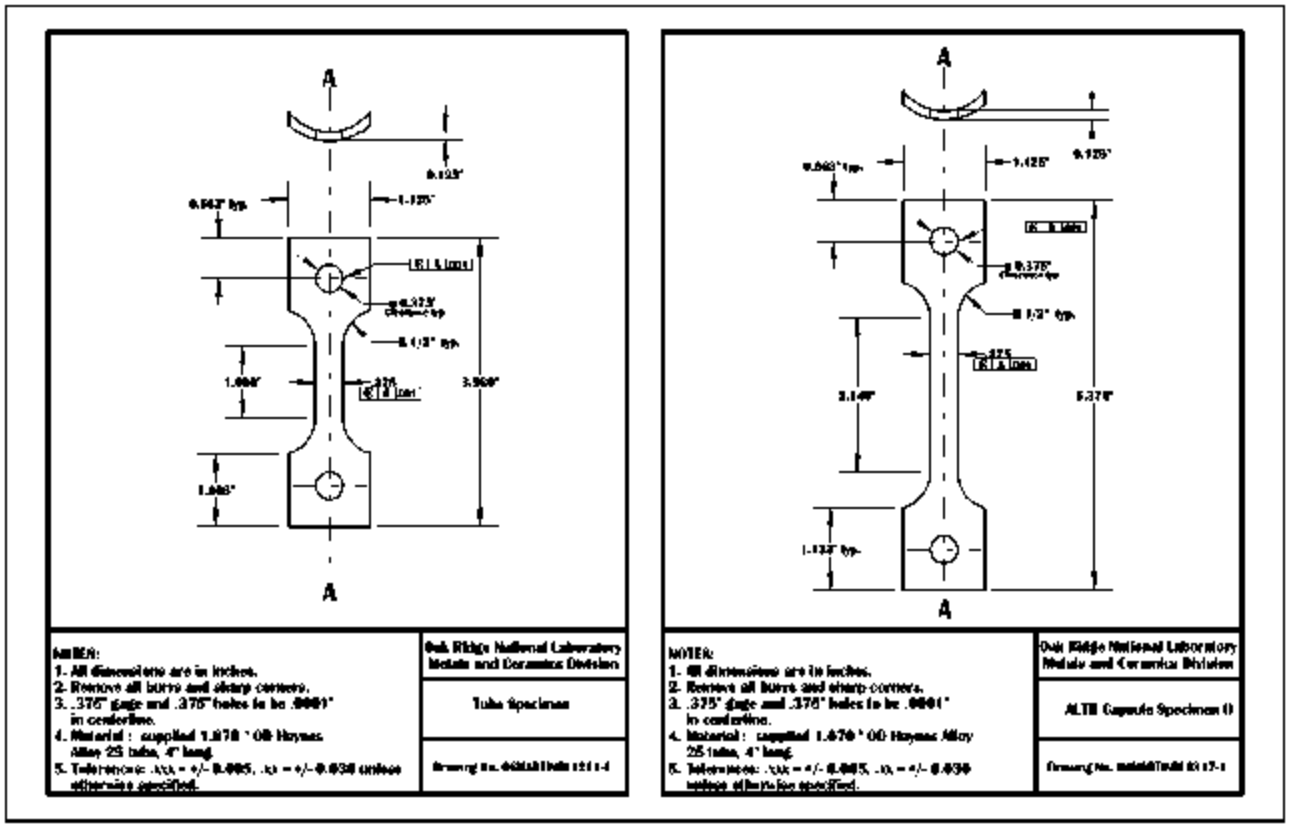

Figure 3.4. Uniaxial weldment specimens taken from tubular machined bar. Weldment crown was in center of gauge section similar to uniaxial plate specimens. The gauge length of some specimens was 1.000 in. (25.40 mm) as shown in the figure on the left, and other specimens were machined with a gauge length of 2.140 in. (54.35 mm) as shown on the right, depending on available material.

Tubular specimens machined from bar-stock for pressurized stress and creep-rupture testing were supplied by INL and LANL. Two sizes of tube with diameter (dia.) to wall thickness (t) ratios of dia/t = 10.76 and 13.15 were evaluated. Hemispherical end caps were welded on the ends of the tubes. A pressure stem was fabricated from Haynes 25 bar stock and welded into a hole in one of the caps to apply and control the pressure within the capsule. The length of the tubes between the weldments was approximately 3.5 to 4.5 times the nominal diameter of the tube.

Elastic property measurements of alloy 25 were performed using Resonant Ultrasound Spectroscopy (RUS). The RUS specimen configuration was a disc 0.708 in. (18 mm) in diameter and 0.118 in. (3 mm) in thickness as shown in figure 3.5.

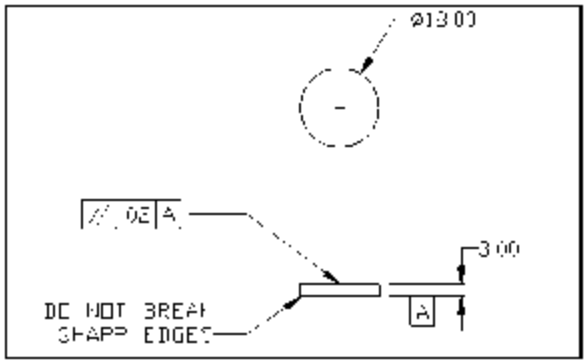

Figure 3.5. RUS alloy 25 specimen (dimensions in mm).

For aging studies, the machined specimens and fabricated tubular specimens were placed in quartz capsules, evacuated, and back-filled with a partial Ar-5%He atmosphere (~1/3 atm.). The quartz capsules were inserted into box furnaces and aged at various temperatures under close temperature control for up to 12,000 hours.

4. EXPERIMENTAL DETAILS

4.1 ELASTIC PROPERTY MEASUREMENTS

To determine the elastic constants (elastic modulus, shear modulus, and Poisson's ration) for this heat of alloy 25, Resonant Ultrasound Spectroscopy (RUS) testing was performed in an Argon atmosphere starting at room temperature (25°C) and at isothermal conditions at the following temperatures: 150, 300, 500, 650, 800, 900, 1000, and 1100°C for specimens removed from the as-received plate and plate aged for 6,000 hours at 675°C [17]. For each test, the specimen was heated to the desired temperature and a spectrum was obtained after soaking at that temperature for 30 minutes. The temperature was then raised and the process repeated. After completing the entire temperature range, the specimen was cooled to 25°C and another spectrum was obtained. The peak-fitting routine used to analyze the RUS spectrum determines a best-fit value for the elastic modulus (E) and the shear modulus (G) [18]. From these values, Poisson's ratio (ν) was determined by the relationship:

$$E = 2G(1+\nu) \qquad \text{equation 1}$$

Although the atmosphere was inert, a small oxide layer was visible after testing. Depending on its thickness, an oxide layer may affect the elastic measurements. Calculating the elastic constants after cooling (when the oxide layer is present) and comparing it to the initial room temperature constant is a standard method for determining the extent of an oxide layer effect. The difference between the pre- and post-test calculated elastic moduli were 2.2 and 1.0 percent for the unaged and aged material respectively, and no change was observed for Poisson's ratio. This indicates that the oxide layer had a negligible effect on the determined constants.

4.2 TENSILE TESTING

Tensile tests were performed on alloy 25 base metal (plate and bar product forms/specimens) and weldments in the as-received condition and after aging for various times and temperatures. The room temperature and elevated temperature tensile tests conformed to ASTM E8-00 and E 21-92, respectively. Tests were performed in electromechanical tensile machines equipped with digital data acquisition. All tests on the plate and plate weldment specimens were performed in extension control mode with an extension rate of 0.107 in/min, which corresponded to a nominal strain rate of 0.05/min on the specimen gauge section. For the bar cross-weldments, the tensile tests were performed in extension control with a nominal strain rate of 0.005/min. After yielding (one to two percent strain), the extension rate was increased to give a nominal strain rate of 0.05/min, and the test specimen was taken to failure. An ASTM class B1 or B2 extensometer was attached to the gauge section of the specimens for accurate measurement of strain. Yield strength (YS) was determined using the 0.2% offset method, the proportional limit was calculated by visual inspection of the tensile curve, ultimate tensile strength (UTS) and ultimate strain (strain at UTS) were calculated by the computer data acquisition system, and final elongation (EL) and reduction of area (RA) were determined by post-test measurements.

4.3 CREEP-RUPTURE TESTING

The creep-rupture testing procedures conformed to ASTM practice E139. For creep-rupture testing, dead-load and lever-arm machines were used with a maximum capacity of 22 kN (5,000 lbs). For temperatures of 800°C and lower, type K (Chromel-Alumel) thermocouples were used for temperature control and readout. For temperatures above 800°C, type S (Platinum-Platinum/Rhodium) thermocouples were used for control but type K thermocouples were sometimes used for set-up at the start of the test. Load cells were used to set and maintain the load within 0.5% of the target load for all creep-rupture and creep tests. Machine loads were adjusted when needed to accommodate potential changes due to the effect of lever arm travel. An extensometer was attached to the center 2 inches (50 mm) of the reduced section of the specimens. Depending on the test requirements, the ASTM extensometer type ranged from Class B-1 to Class C (ASTM E 83). Most testing was performed with extensometers calibrated to the Class B-2 category. The Class C extensometer was sometimes used for the weldment samples since the influence of the cross weld in the gage length produced some uncertainty as to the significance of the measured displacement. For tests above 900°C, oxidation of the specimen may have a significant influence on the creep-rupture properties, so testing at these conditions was performed in a flowing 99.99% purity Argon atmosphere. After testing, the specimen surfaces were tinted a light-green in color, which is indicative of a thin chromia based oxide scale typical in this alloy system. In contrast, the specimens tested in air all exhibited a dark black oxide layer after creep testing, which is evidence of a thicker oxide layer. For testing in Argon gas, the retort system excluded the use of typical creep extensometers for strain measurement and the high-temperature precluded the use of other strain measurement options. Thus, load-line displacement readings were taken manually at 48 to 72 hour increments and used to estimate the creep strain.

Several types of extension sensors were used on the extensometers. All were electronic and provided signals that could be read by a data acquisition system. For most tests, load and extension data were collected on a computer data acquisition system. Manual dial gage readings of the load line displacement were made on a weekly basis. Generally, these readings indicated larger displacements than readings from extensometers. The difference was attributed to creep strains accumulated in the shoulders of the specimens and displacement of the loading pins. Post test readings of the displacement on the specimen reduced sections generally confirmed the accuracy of the extension measurements.

For pressurized creep testing of the tubular specimens (removed from bar stock), the ORNL pressure-burst facility was used. Figure 4.3.1 shows a schematic representation of one test rig in the facility. A high-pressure oil-less pump supplied Ar-0.5%He gas to the test facility. A 7,500 psi safety pressure relief valve was used to limit pressure in case of an emergency. Specimen pressure was controlled manually using a series of valves. A digital pressure transducer, in line with the specimen, was used to monitor pressure at all times. In order to maintain a constant pressure within the capsule throughout the test, an accumulator was used so the system could be isolated from the supply pump. The main pump was only used during the test when the pressure deviated from the target pressure by more than +/- 50 psi. Generally, this was not needed because the accumulator had sufficient volume to keep the tube pressure within the specified range. Fluctuations in room temperature could also cause increases or decreases in the test system pressure. Insulating the accumulators reduced these fluctuations, and only in the case of the very long-term tests were one or two manual changes in pressure to the accumulators required.

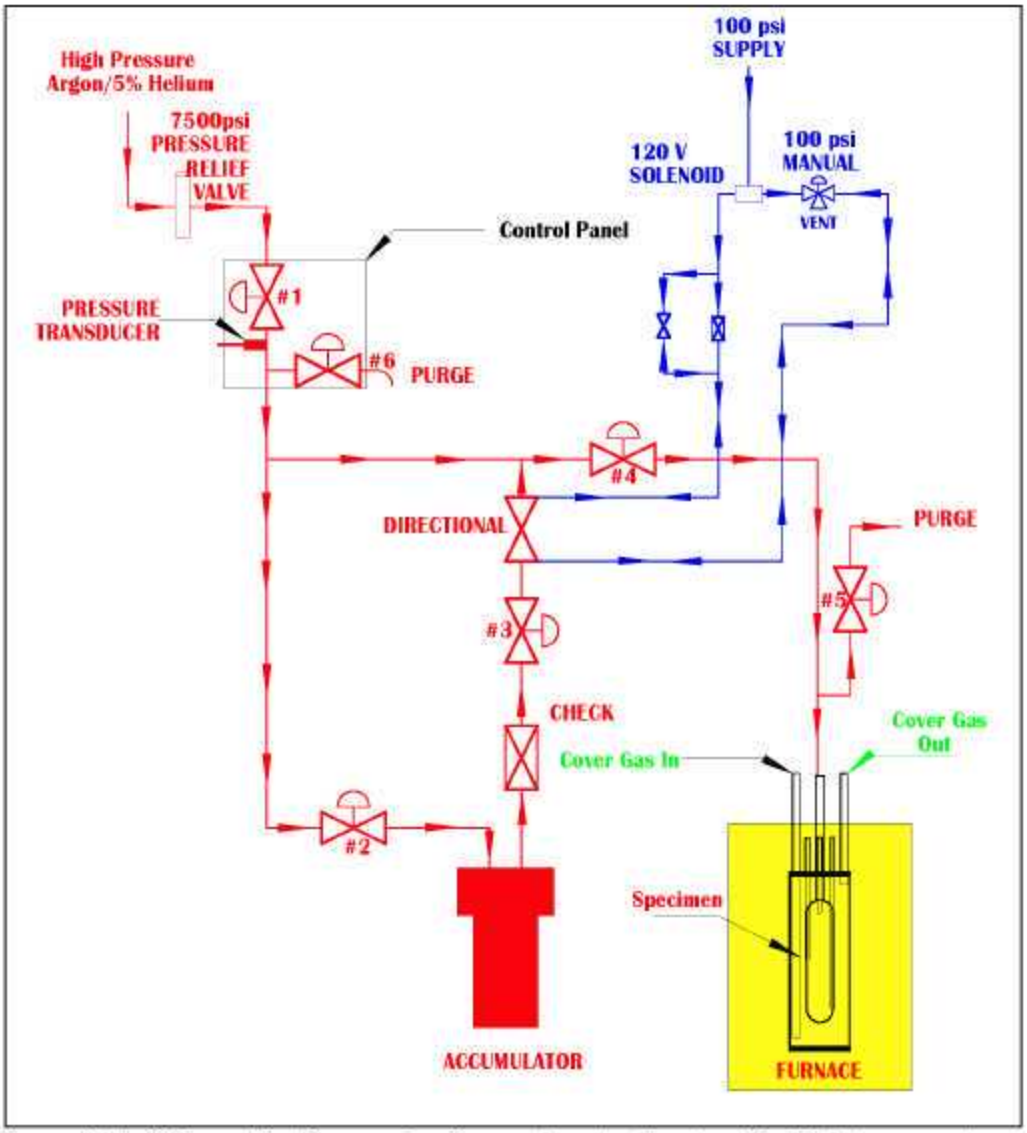

Figure 4.3.1. Schematic of pressurization and control system for high-temperature pressurized creep testing of tubular specimens.

A detailed schematic of the set-up within the furnace is shown in figure 4.3.2. A 304L stainless steel can was used to hold the specimen during the test. The can was used for three reasons: (1) to allow for the use of an inert cover gas (99.99% Ar) to minimize oxidation effects when testing at high temperature; (2) to protect the furnace and heating elements in case the specimen ruptured; (3) to assist in providing uniform temperature across the entire specimen. A Haynes 25 pressure-stem was welded (fillet weld) with Haynes 25 filler metal (GTAW process) to the can lid. This pressure-stem was welded to standard stainless steel high-pressure tubing to connect to the system outside of the furnace. The stainless steel lid was sealed to the can using 308L stainless steel wire.

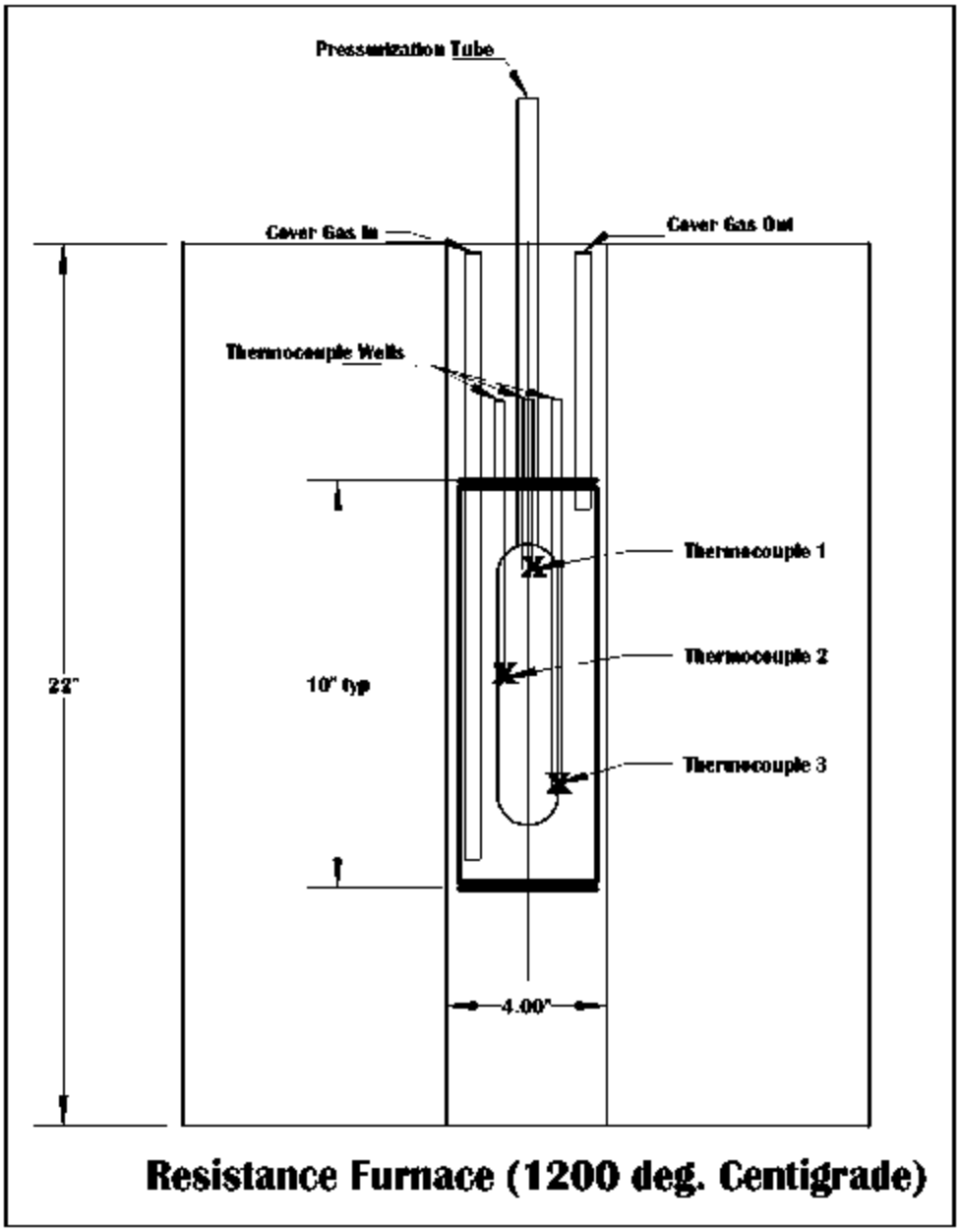

Figure 4.3.2. Furnace detail for high-temperature pressurized creep testing showing the tubular specimen, the thermocouple placement, the stainless steel canister, the gas inlet and outlet, and the pressure stem.

Metallic sheathed thermocouples were fed into the stainless steel canister through Swagelok fittings and ceramic-insulated thermocouples were fed in through stainless steel wells which were bent to touch the specimen surface. The difference in temperature readings between the sheathed thermocouples and the thermocouples in the stainless steel wells were less than 1°C. For these tests, three sheathed and three ceramic-sheathed thermocouples (two placed in each location as indicated in figure 4.3.2), were used to measure temperature. As with the uniaxial tensile testing, type K (Chromel-Alumel) thermocouples were used for temperatures of 800°C and lower while type S (Platinum-Platinum/Rhodium) thermocouples were used for testing at 850°C and above. In a few cases, tests of short duration (less than 200 hours) at 850°C were performed using type K thermocouples where temperature drift is not significant. A computer data acquisition system recorded the temperature (six thermocouples), the pressure, and time at

0.1 hr intervals. This data collection rate was increased when the pressure dropped below a predetermined value to record the rupture or leak rate. An accumulator shut-off valve was closed at this point so the entire gas volume of the accumulator did not leak through the specimen on rupture. When these events happened, the system sent an alarm to a staff member to manually check the system for specimen rupture.

The test procedure used was as follows. After the specimen was welded to the can top, the specimen was pressurized at room temperature to the test pressure and held for 24 hours to check for leaks. If a leak was detected, the welds and fittings were evaluated for leaks, the problem was corrected, and the process was repeated. After successful pressurization, the specimen was de-pressurized and the can lid was welded onto the can sealing the specimen inside the canister. The system was purged and the specimen was pressurized with Ar-0.5%He gas again for 24 hours. During this time, flowing Argon gas was introduced into the can. After 24 hours, the pressure in the capsule was lowered a minimum of 1000 psi below the intended test pressure, the data acquisition system was started, and the furnace was started. The temperature was gradually raised and the pressure adjusted to stay a minimum of 1000 psi below the test pressure. Once the capsule had reached the test temperature and the total temperature gradient was less than 5°C (< +/- 2.5°C intended test temperature), the pressure was raised to the test pressure and the test was started. In addition to the computer data acquisition system, the data was also recorded on a chart recorder and periodic manual readings were made. The pressure drop limit was set at 50psi; that is when the pressure dropped 50psi below the test pressure, the data acquisition rate was increased, the supply from the accumulator was stopped, and an alarm was sent out. If the pressure continued to decrease, then this point was taken as the rupture time.

To measure the rupture strain of the tubular specimens, the diameter of the specimen was measured after testing. This worked well for small longitudinal ruptures along the tube axis, but in some cases the specimen had a 'fishmouth' type rupture with a large opening. In these cases, the largest circumference was measured and the final diameter was calculated.

4.4 POST-TEST ANALYSIS

A select number of specimens (sheet and tubes) were visually examined using a digital stereo microscope. Others were sectioned and areas of interest were prepared metallographically by mounting the sectioned samples in epoxy, grinding using 220 and 600 SiC grit sandpaper, and polishing using 6, 3, and 1 μm diamond paste. Samples were etched for metallographic examination using glyceregia.

5. ELASTIC PROPERTIES RESULTS AND DISCUSSION

The measured elastic constants as a function of temperature for alloy 25 before and after aging at 675°C for 6,000 hour are tabulated in the appendix (A.1). The elastic modulus (E) for these two material conditions is plotted along with the dynamic modulus data from the Haynes 25 product brochure [19] in figure 5.1. The shear modulus (G) and bulk modulus (K) are plotted as a function of temperature in figure 5.2, and Poisson's ratio (v) values for the two conditions are plotted in figure 5.3.

The RUS measured elastic moduli are slightly higher than the Haynes data over the entire temperature range. The difference in modulus is generally less than 4%, which is small considering a different measurement technique and/or product form was likely used for generating the Haynes data. The plot also shows that the elastic modulus for aged material is 2 to 3 percent higher below 650°C compared to the unaged material. This difference is smaller above 800°C. The small change in elastic modulus for the aged material at the lower temperatures may be due to a change in the matrix composition between the unaged and aged material. Examination of the TTT diagram, figure 5.3, for Haynes 25 shows that aging for 6,000 hours at 675°C results in the precipitation of the Co_3W and Co_2W phases in addition to carbide phases. Precipitation of the intermetallic phases may appreciable change the bulk composition of the Co matrix resulting in a slight change in elastic properties. In addition to differences in elastic modulus, some small differences are observed in Poisson's ratio at the lower temperatures. Above the aging temperature, especially at 900 to 1100°C, both the elastic modulus and Poisson's ratio do not show noticeable differences. Closer examination of figure 5.2 shows that the differences in Poisson's ratio and elastic modulus below 800°C are the result of small changes in the shear modulus, which is consistently higher for the aged material at low temperatures. No trends are observed for bulk modulus for the unaged and aged conditions. This indicates that any possible aging effect on elastic properties (due to long-term exposure at 675°C) is small and restricted to temperatures below 650°C.

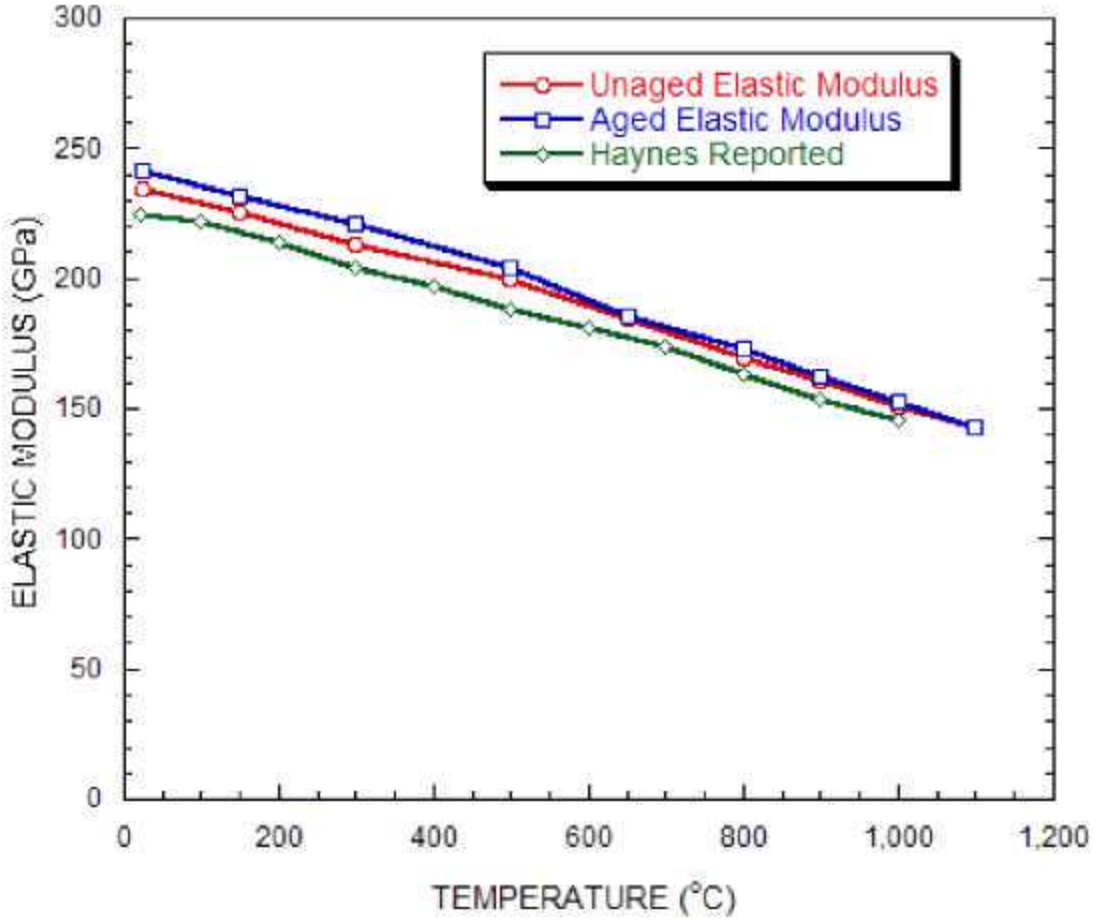

Figure 5.1. Plot of elastic modulus vs. temperature for this heat of alloy 25(aged = aged at 675°C for 6,000 hours) and compared to the Haynes Datasheet data [15].

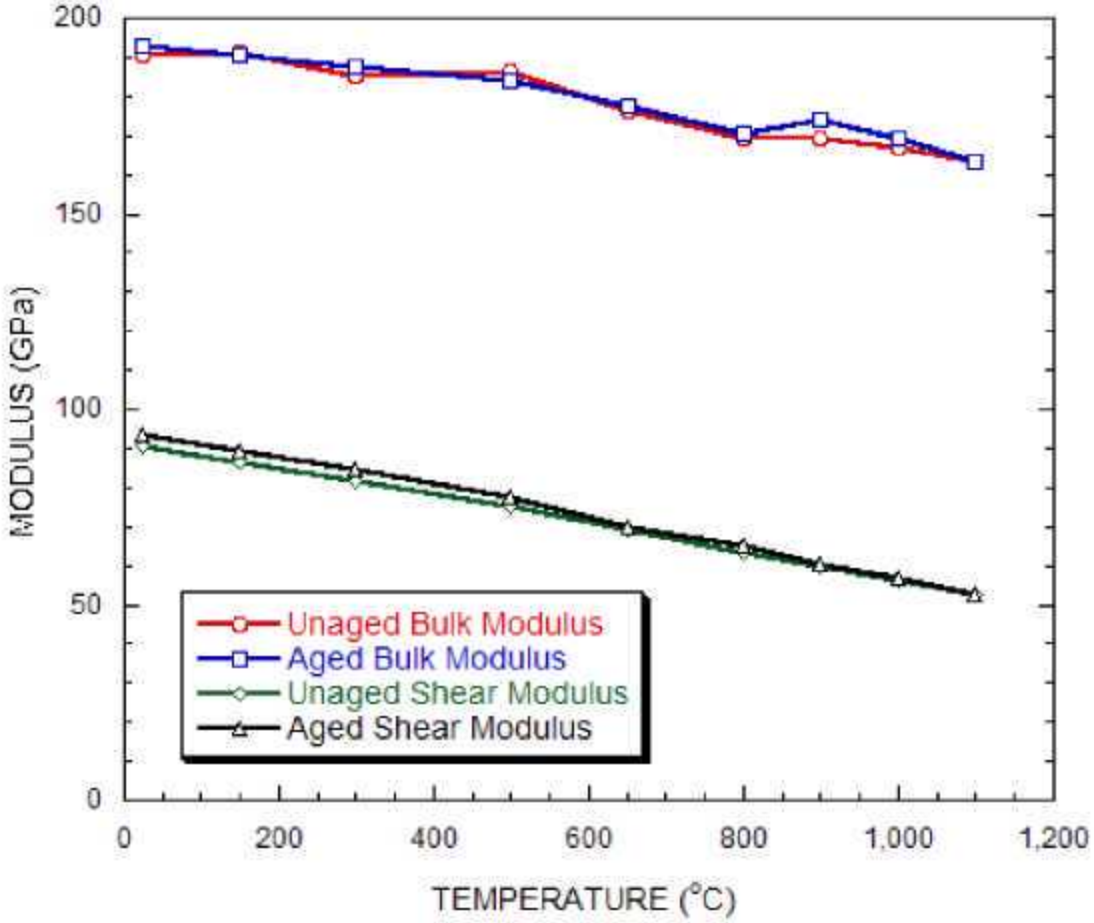

Figure 5.2. Plot of shear (G) and bulk (K) modulus vs. temperature for this heat of alloy 25 (aged = aged at 675°C for 6,000 hours).

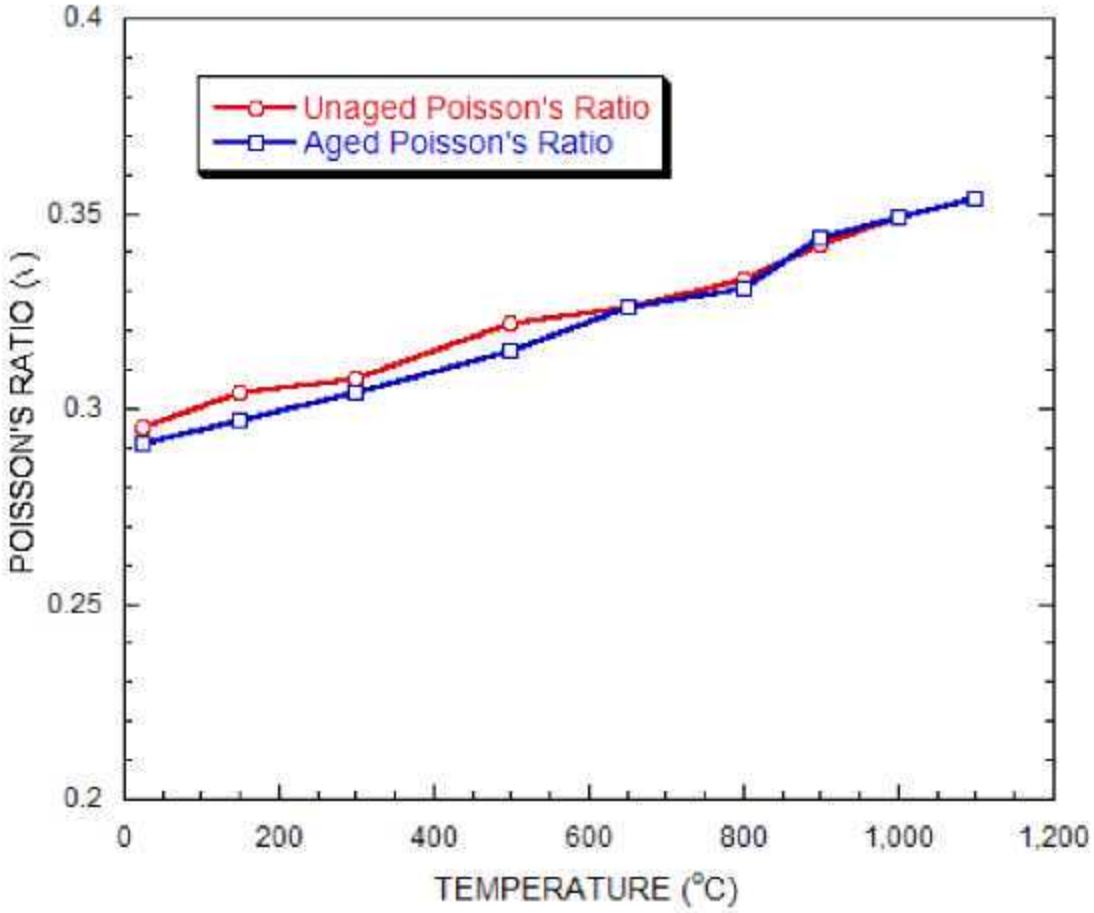

Figure 5.3. Plot of Poisson's ratio vs. temperature for this heat of alloy 25 (aged = aged at 675°C for 6,000 hours).

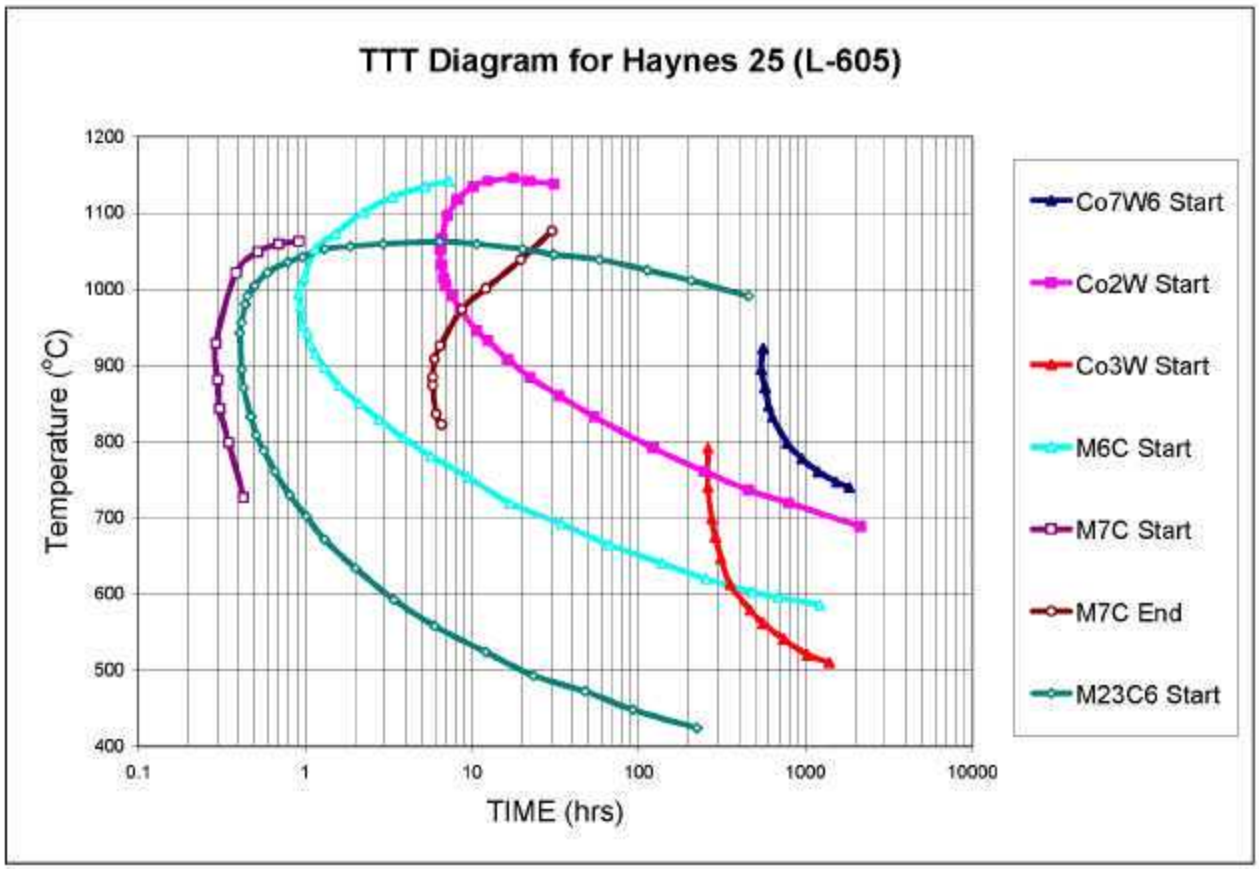

Figure 5.4. Reconstructed TTT diagram for Haynes alloy 25. Data taken from ref [10].

6.0 TENSILE PROPERTIES RESULTS AND DISCUSSION

Tensile properties were measured on sheet (base metal: BM), sheet cross-weldment (WM), and bar cross-weldment (bar WM) specimens in the as-received (annealed or as-welded) condition and in various aged conditions. The tabular tensile data can be found in the tables of appendix A.2. Table A.2.1 gives the tensile properties of the base metal while Table A.2.2 contains the weldment data. The most prominent aging conditions were 6,000 and 12,000 hours at 675°C. These conditions were chosen, in part, on the TTT diagram (figure 5.3) to cause precipitation of the $M_{23}C_6$ and M_6C carbides as well as the Co_3W intermetallic phase. The formation of the Co_2W Laves phase has also been reported at 700°C for short times and extension of this curve of the TTT diagram suggests this condition would precipitate this phase as well. The precipitation of the carbide and intermetallic phases has long been known to embrittle alloy 25 causing a decrease in the tensile and impact ductility [13-16]. However, most of these studies investigated short-time aging conditions at temperatures of 760°C and higher, and thus a lower temperature longer-time aging condition at 675°C was chosen for this study.

Figure 6.1 shows the yield strength (YS) and ultimate tensile strength (UTS) as function of temperature for alloy 25 base metal and weldments including aging at 675°C for 6,000 and 12,000 hours. Examination of the plot shows that for each aging condition, the sheet base metal (BM) and the weldment (WM) had the same properties. Since all of the sheet weldment test specimens broke in the base metal, it is expected that the base metal will govern properties. In the machining of the specimens, the weld crown was not removed, thus the weld metal was essentially mechanically reinforced due to a larger cross-sectional area. However, the heat-affected zone (HAZ) of the weldment is not reinforced. Therefore, the tensile data show that welding does not degrade the room and high-temperature tensile properties of Haynes alloy 25. A few tests on the bar weldments (Bar WM) were conducted at room temperature and at 650°C. In general, these showed the YS and UTS were slightly higher compared to the as-received and aged sheet products, but one data point fell slightly below the data for the sheet pieces. In contrast to the data for sheet pieces, the non-aged bar materials failed in the weldment, so these data are measures of weldment strength. The higher yield strength of the bar material may be due to a grain size effect. The grain size of the bar is finer, figure 3.1, compared to the sheet material. Generally, finer grain size, for the same material, results in higher low-temperature yield strength. Under this assumption of higher strength in the bar, the initial yielding of the bar specimen may have occurred in the weldment region eventually causing failure in the weldment whereas initial yielding in the sheet weldment was in the base metal leading to failure in the base metal. After aging, the bar weldments failed in the base metal similar to the sheet product. All of the data fell within typical scatter for tensile data. Thus, the data suggest that the bar product may have slightly better unaged tensile properties compared to sheet product, but there are no sufficient data to determine whether or not these differences are statistically significant.

Figure 6.1 also shows the dramatic effect aging has on alloy 25 strength. Aging at 675°C for 6,000 hours improves the YS of the material by about 300MPa from room temperature to 650°C. The magnitude of this effect decreases with further increasing temperature and no difference in YS is observed at 1,000°C. A similar but less dramatic effect is observed for the UTS. At room temperature, little difference is observed, but the UTS is improved in the range of 300 to 800°C by about 100 MPa. As with YS, aging at 675°C has no effect on UTS at 1,000°C and above. Also, aging for 12,000 hours at 675°C does not cause further changes in YS and UTS.

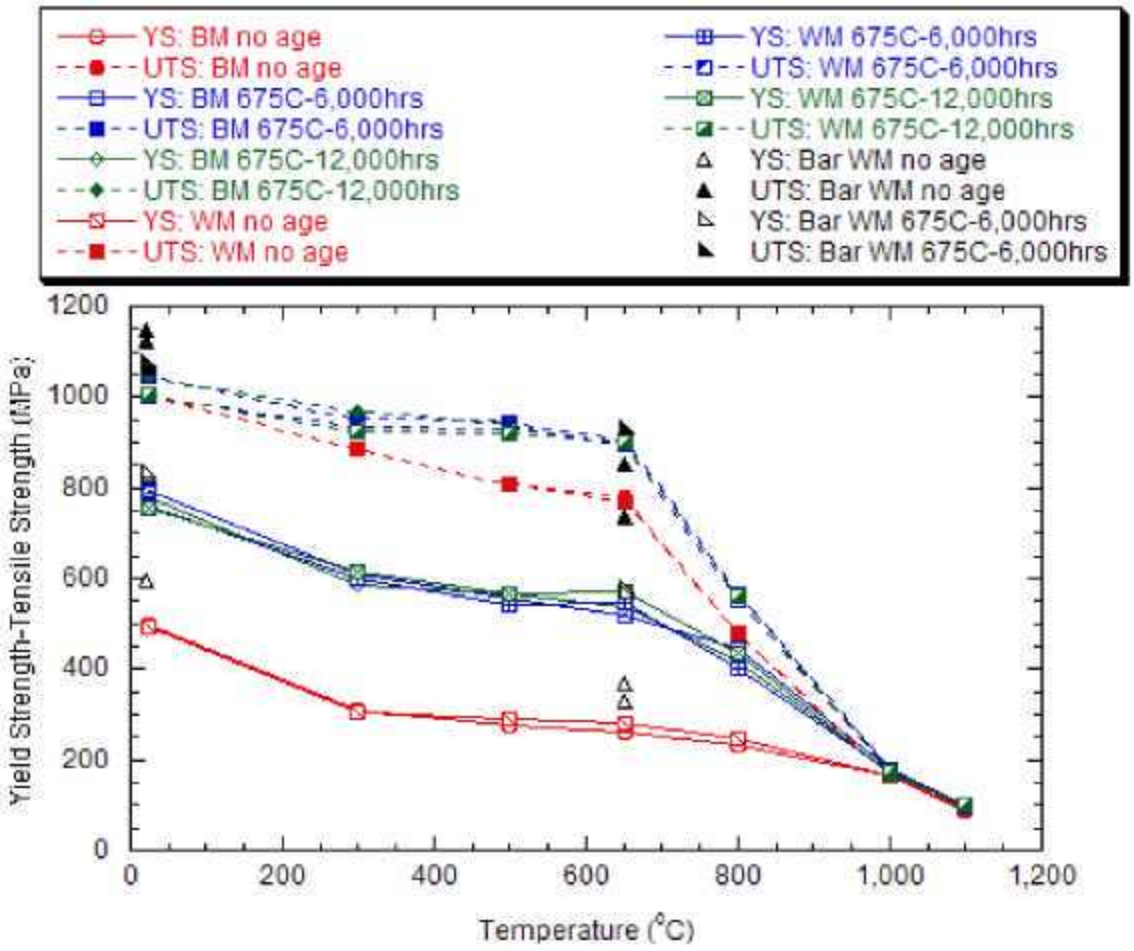

Figure 6.1. Measured Yield Strength (YS) and Ultimate Tensile Strength (UTS) as a function of temperature for base metal (BM) and weldments (WM) of Haynes alloy 25 sheet and cross-weldments of Haynes alloy 25 bar product in the as-received condition and after aging at 675°C for 6,000 and 12,000 hours.

Figure 6.2 is a plot of the tensile ductility, elongation (EL) and reduction of area (RA), for the all the material conditions. Similar to the strength data, no difference is observed for any aging condition between sheet BM and WM. However, the Bar WM does show lower ductility for the as-welded condition, which is due to localized failure in the weldment. After aging, the Bar WM is equivalent to the BM and WM. In the unaged condition, alloy 25 has good tensile ductility with EL above 45% and RA above 35% for all temperatures tested. However, after aging at 675°C for 6,000 hours, the tensile ductility at room temperature to 800°C is significantly reduced below 20%. Unlike strength, further aging for 12,000 hours at 675°C shows slightly more loss of ductility below 800°C, generally less than 15%. The effect is most pronounced at room temperature where ductility is less than 10%. At 1000°C and above, the aging effect is less with all ductilities measuring beyond 25%.

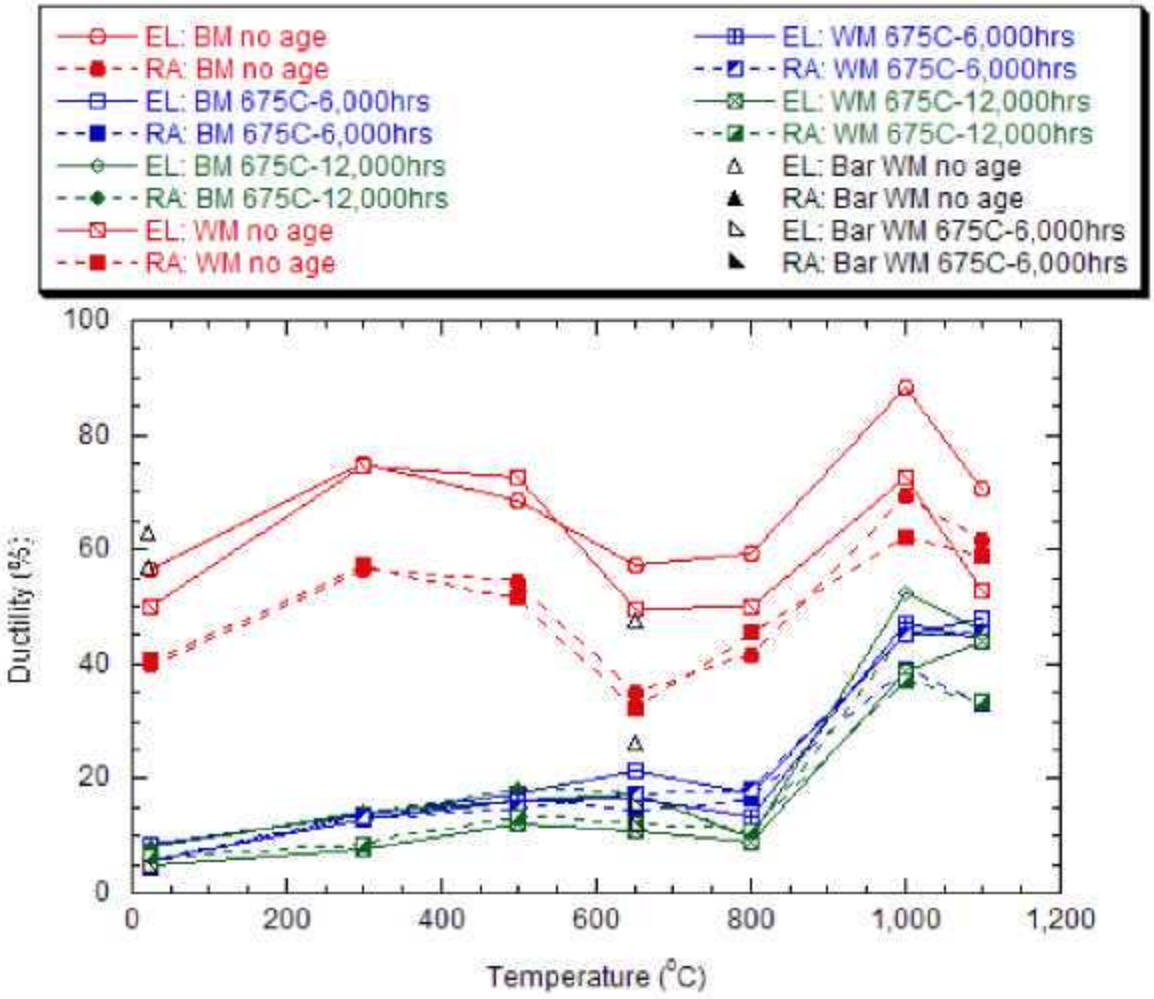

Figure 6.2. Measured ductility, elongation (EL) and reduction of area (RA), as a function of temperature for base metal (BM) and weldments (WM) of Haynes alloy 25 sheet and cross-weldments of Haynes alloy 25 bar product in the as-received condition and after aging at 675°C for 6,000 and 12,000 hours.

In addition to total elongation (EL), the uniform elongation (strain at the UTS) is also tabulated in the appendix. The difference in EL and uniform EL can be used as a measure of tensile behavior by the equation:

$$Difference(\%) = \frac{EL - UniformEL}{EL} 100 \qquad \text{equation 2}$$

When the difference between EL and uniform EL is very small (less than 10%), the material breaks at or near the UTS, and the material behavior is characterized as strain hardening. When the difference is close to 100%, all deformation is due to strain softening (after yielding, the strength begins to drop). Examination of the stress-strain tensile curves, individually plotted in appendix A.5, show that alloy 25 can show both types of behavior. Figure 6.3 is a plot of EL for all material conditions (aged and unaged) and the difference in EL and uniform EL (%) for these test data. Regardless of the value of EL (which varies significantly due to aging as already shown), the difference is only a function of testing

temperature. From room temperature to 650°C, the difference is less than 10%, which shows alloy 25 exhibits strain hardening without strain softening. At 1000 and 1100°C, the EL and difference are close to the same value showing strain softening dominates. At 800°C, the material exhibits a mixture of strain softening and strain hardening.

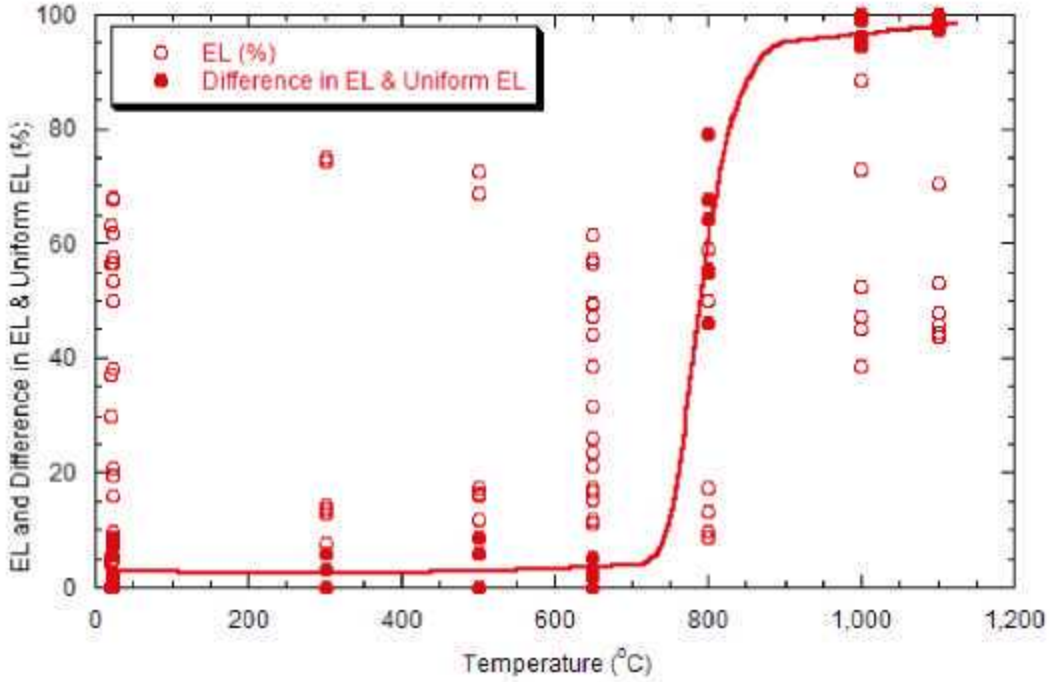

Figure 6.3.Tensile Elongation and the Difference in Uniform Elongation and Elongation as a function of temperature for alloy 25 unaged and aged sheet and bar products. The difference in EL and uniform EL is a measure of deformation due to strain softening. 0% = no strain softening (strain hardening), 100% = only strain softening (no strain hardening).

Shorter-term aging experiments were conducted at 675°C (in addition to the 6,000 and 12,000 hour aged material) on sheet BM to evaluate the kinetics of strength and ductility change. Figure 6.4 shows the room temperature tensile strength and ductility changes with aging time at 675°C. Figure 6.5 shows the tensile strength and ductility at 650°C after aging at 675°C for various times. Bourgette conducted room temperature and 650°C tensile tests after aging at 650°C [14]. These data are included on the plot for comparison. A general Johnson-Mehl-Avrami (JMA) type equation [20] was fit to the strength (S) and ductility (D) data as a function of time (t) as follows:

$$\frac{S - S_{Max}}{S_{Max} - S_{Min}} = 1 - \exp(kt^n) \qquad \text{equation 3}$$

$$\frac{D - D_{Max}}{D_{Max} - D_{Min}} = 1 - \exp(kt^n) \qquad \text{equation 4}$$

where the strength or ductility is bounded by maximum and minimum values (subscript Max or Min) and the kinetics of the change depend on the power law terms k and n. The calculated values for k and n for YS, EL, and RA are listed in Table 2. The n values for EL and RA are negative (inverse JMA) since ductility decreases with aging time. The n-value was found to be 1.1 to 1.2 for room temperature YS, EL, and RA, 1.1 for 650°C YS, and 0.7 to 1.0 for 650°C EL and RA.

Table 2. Calculated kinetic constants for alloy 25 strength and ductility aged at 675°C

Test Temp	YS		EL		RA	
	k	n	k	n	k	n
23	-6.003E-04	1.1052	-515.15	-1.1835	-789.80	-1.2280
650	-4.643E-04	1.1016	-77.14	-0.7374	-764.38	-0.9949

Examination of figures 6.4 and 6.5 and the kinetic constants show that the major change in room temperature and elevated temperature strength and ductility occurs from ~100 to 400 hours at 675°C. The TTT diagram for Haynes 25 shows this is the time when the Co_3W intermetallic forms. Additionally, the M_6C carbide is predicted to start its formation at ~50 hours at this temperature as well. Thus it is not possible to determine the exact cause of ductility loss at 675°C without a more detailed study of the microstructure. McKamey and George have studied the impact ductility of Haynes 25 at 675°C and have concluded that observed increases in hardness and decreases in ductility are due to the formation of carbides and intermetallics, but the two phenomena are not directly related. Their work suggests that grain boundary precipitates affect ductility while intragranular precipitates effect hardness [21]. The kinetic constants in Table 2 suggest that different precipitates (or the same precipitates that precipitate at different location and times) are responsible for changes in strength and ductility. The value of n should be independent of temperature for the same nucleation mechanism. The n-values for YS, EL, and RA are the same for room temperature and YS at 650°C, but ductility at 650°C is governed by a different n-value suggesting a different precipitate (or location) is contributing to the loss of high-temperature ductility. Current work is being undertaken to carefully examine these specimens to better characterize the precipitates, their morphology, and location as a function of time and temperature.

The data plotted from Bourgette in figures 6.4 and 6.5 show much lower strength and higher ductility at room temperature for alloy 25. At room temperature, these data do show a small increase in strength and loss of ductility with aging time that is similar to the data in this study. These data are shifted to slightly longer times, which may be due to differences in chemistry, thermal history, and aging at 650°C instead of 675°C. Unfortunately, the high-temperature data are too limited to infer any trends.

Short-term 1,000 hour aging treatments were carried out at 700 and 750°C in addition to the aging studies conducted at 675°C. Room temperature tensile tests were performed on the 1,000 hour aged material and are compared to the 1,000 hour aged data from the historical database in appendix A.7 (Table A.7.3). Figure 6.6 is a plot of these data. In general this heat of material shows higher room temperature YS and UTS after aging compared with the historical dataset. The ductility appears to fit the trend of the historical database with EL and RA measurements lower than lower-temperature aged material and higher than higher-temperature aged material after 1,000 hours.

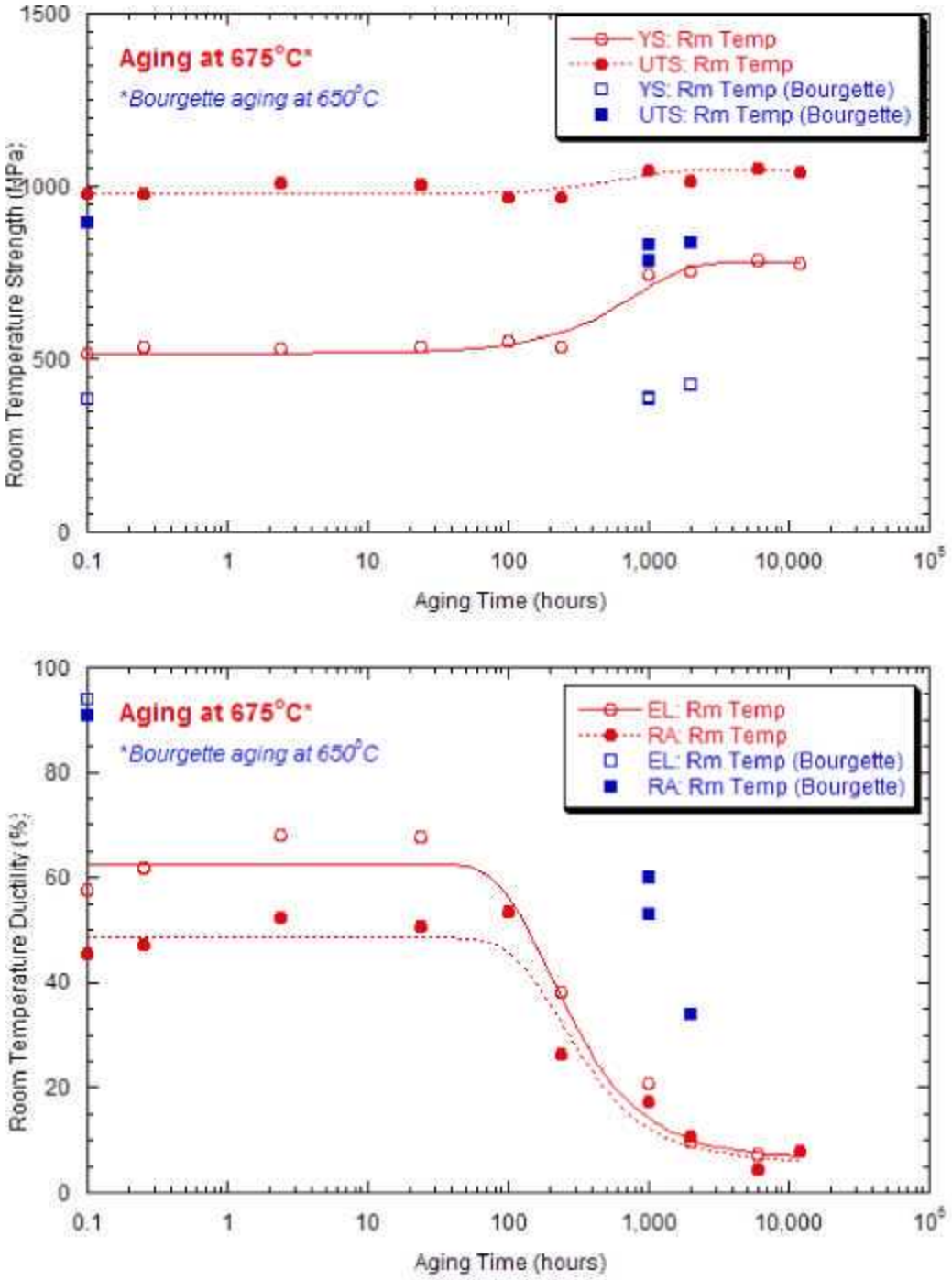

Figure 6.4. Room temperature tensile strength and ductility as a function of aging time at 675°C for alloy 25. Data from Bourgette aged at 650°C is plotted for comparison [14].

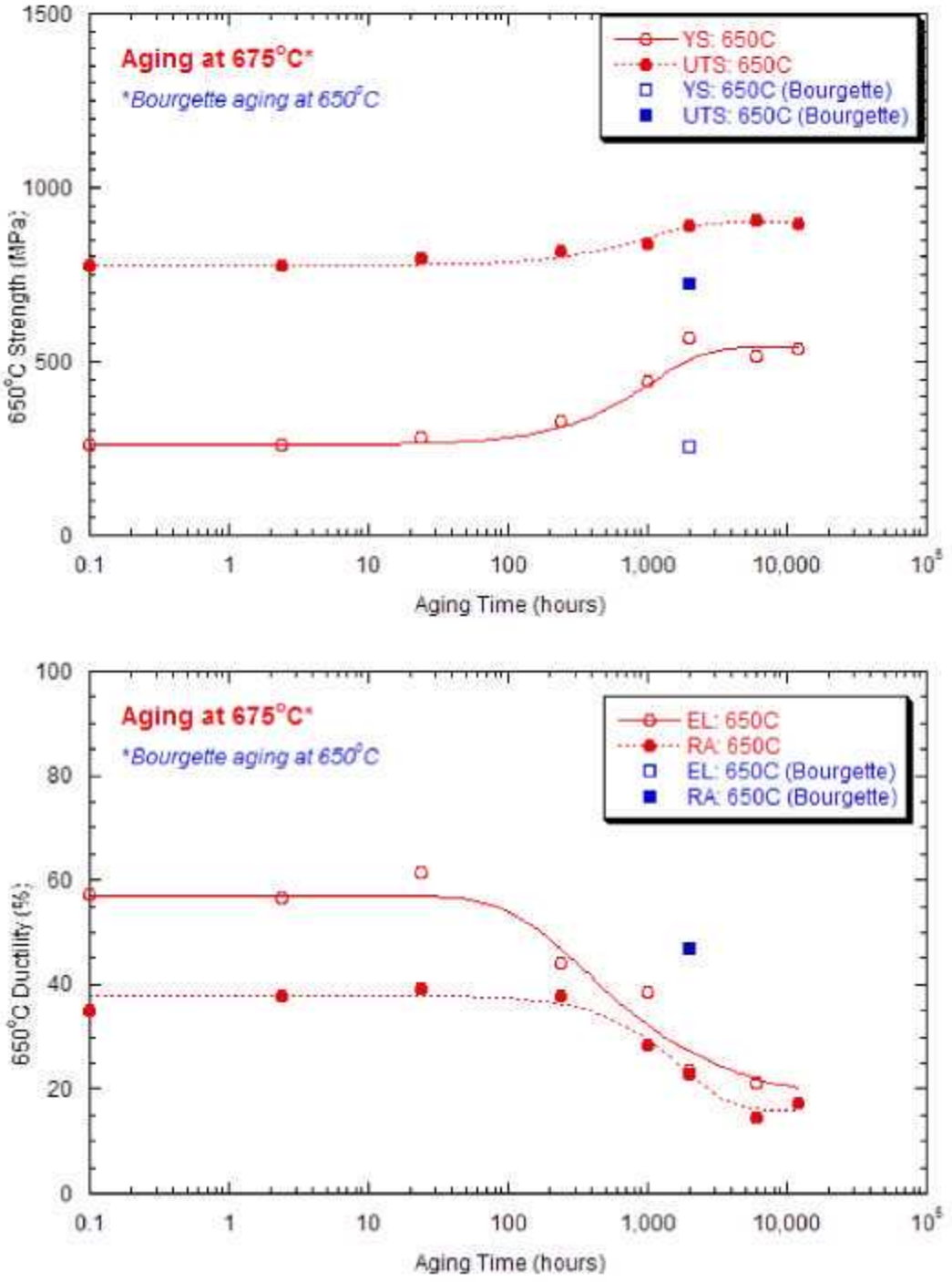

Figure 6.5. Tensile strength and ductility at 650°C, as a function of aging time at 675°C for alloy 25. Data from Bourgette aged at 650°C is plotted for comparison [14].

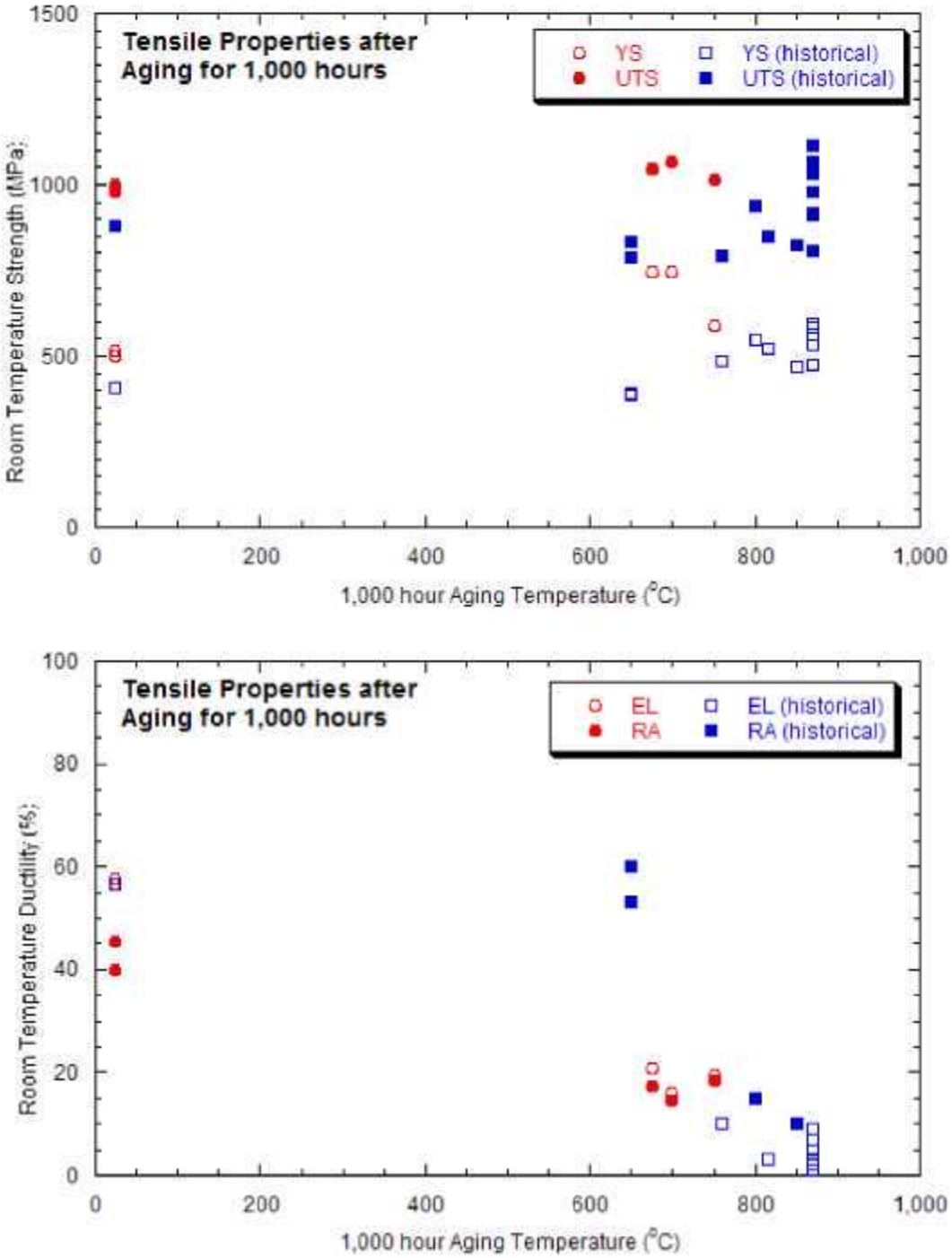

Figure 6.6. Room temperature tensile properties as a function of 1,000 hour aging temperature.

Figures 6.7 and 6.8 compare the measured tensile properties of the unaged sheet to the annealed historical database in appendix section A.7 (Table A.7.1). For YS and UTS, the current heat of material followed the general trend of the database. The strength values were average or slightly higher than average from room temperature to 650°C. At 800°C to 1100°C, the YS and UTS data fell within the scatter of the historical dataset.

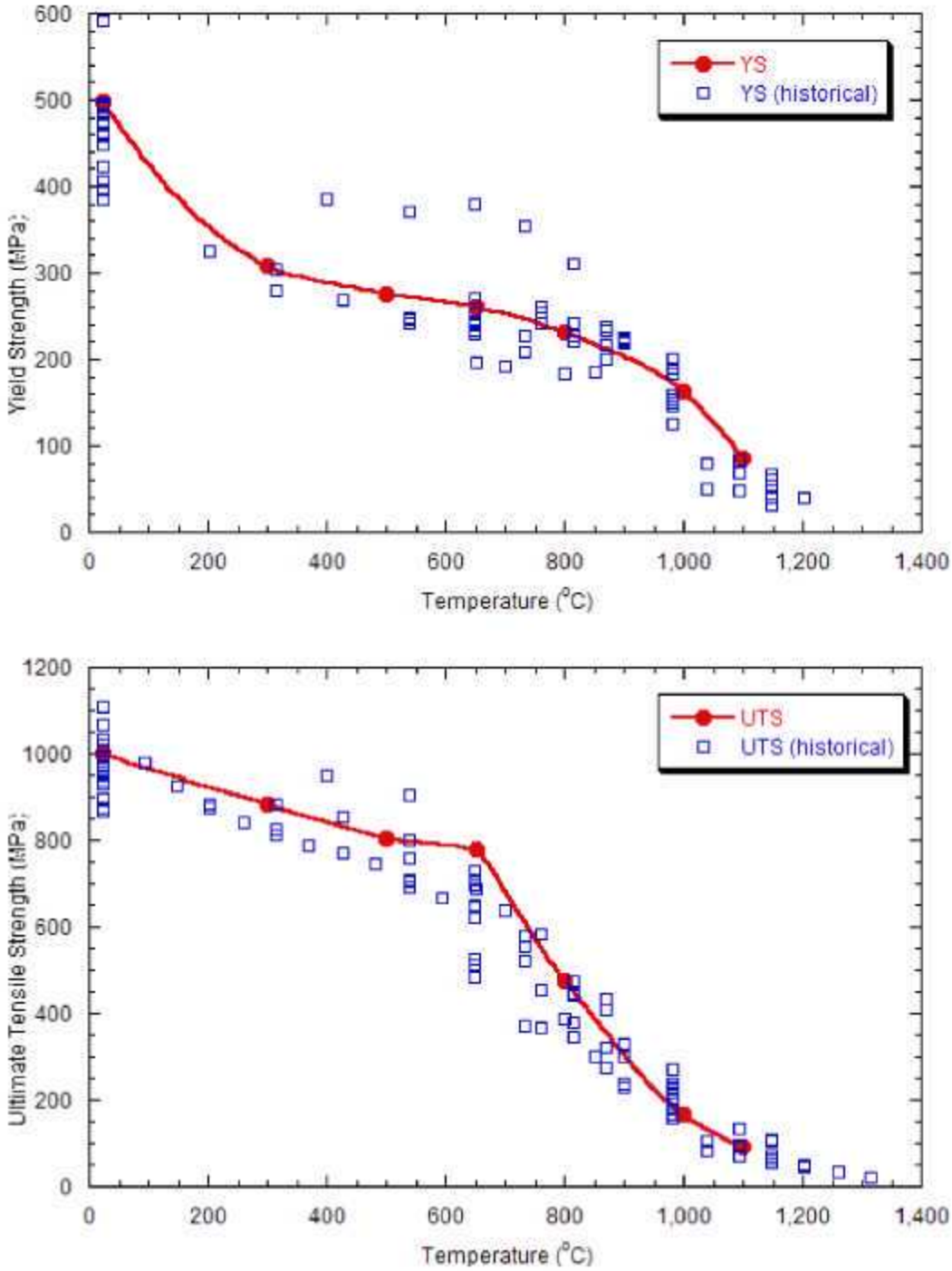

Figure 6.7. Measured Yield Strength (YS) and Ultimate Tensile Strength (UTS) for Haynes alloy 25 sheet (as-received, no aging) as a function of temperature compared to the historical database for annealed alloy 25.

Elongation (EL) values for this heat followed the typical trend in the historical database up to 650°C, but EL values at 800°C to 1100°C were higher than any others reported in the historical database. Although the historical database does not contain RA values, the RA was plotted for this heat of material in figure 6.8, and the RA showed the identical trend to EL. Since EL is not specimen geometry independent (EL

for the same material may vary depending on GL), RA is generally a better measure of ductility. Since both ductility measures show the same trend, the EL result is not due to specimen design. The reason for improved high-temperature ductility without a corresponding decrease in strength is not obvious, but improved melting practices and heat-treatments to produce a finer grain size, compared to older air-melting practices and coarse grain sizes in the historical database, may be reasons for the discrepancy with the historical dataset. The ductility data are consistent with a number of individual studies on alloy 25, summarized in ref [28], which show the material does exhibit a tensile ductility minimum around 760°C (1400°F). This is attributed to fracture behavior. "At low temperatures below the ductility minimum, crack propagation is transgranular in nature whereas at the minimum it is intergranular in nature failing by wedge-shaped voids and grain boundary shear. At higher temperatures the intergranular fracture mode continues but thermal recovery allows for blunting of the crack tips and improves ductility [28]."

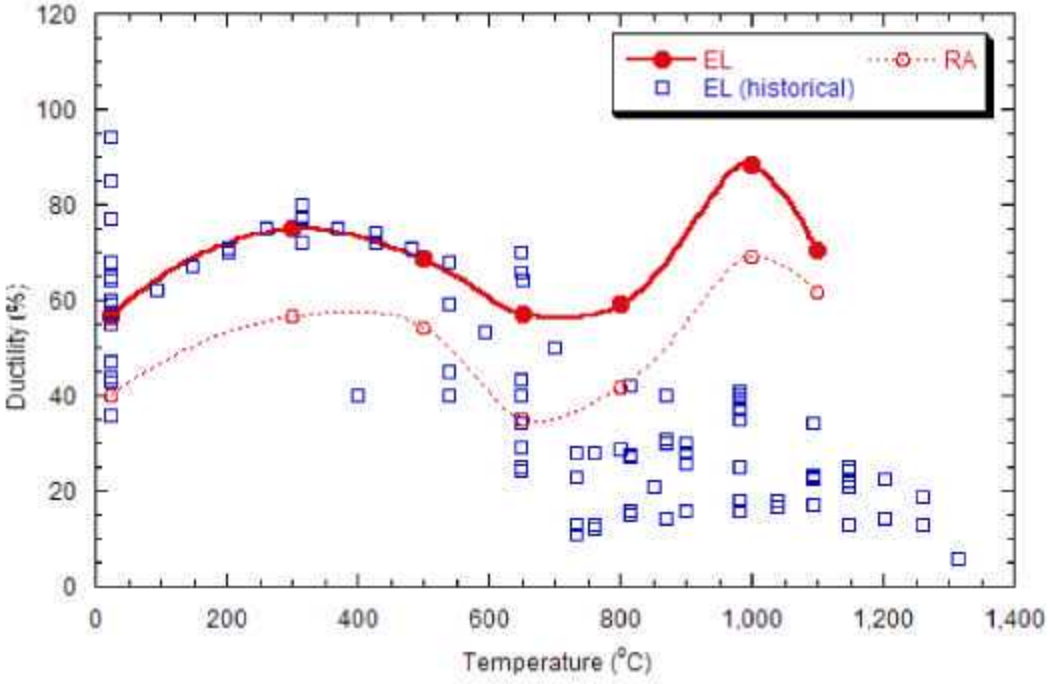

Figure 6.8. Measured ductility for Haynes alloy 25 sheet (as-received, no aging) as a function of temperature compared to the historical database for annealed alloy 25.

The historical dataset contains data on weldments (Table A.7.2). These data are for thinner sheet product and all reported failures occurred in the weld metal. For the current sheet and bar weldment, most failures were in the base metal, although a few of the bar data were in the weld. As discussed previously, this is mainly due to the mechanical reinforcement provided by the weldment crown (which was not removed). Thus, a comparison with the historical weld data is not appropriate. However, no HAZ failures were found in the current tensile dataset which does indicate the welding process did not have a detrimental effect on tensile properties. Figures 6.9 and 6.10 compare the weldment tensile data to the historical database. As expected, these data shows better YS and UTS compared to the historical data for the entire temperature range. For EL and RA, the trend is similar; at 650°C and above, the current welded sheet and bar show better ductility compared to the historical data.

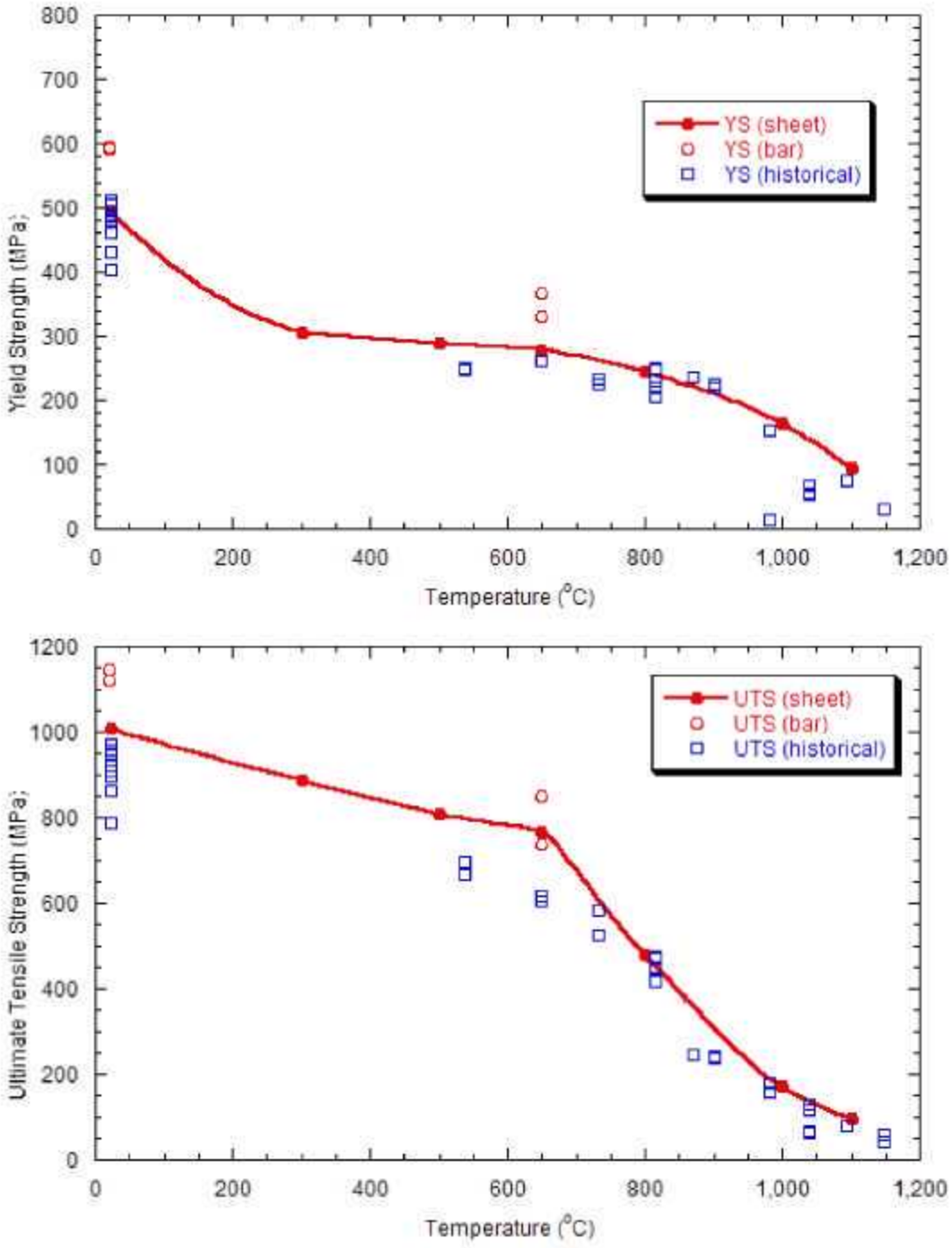

Figure 6.9. Measured Yield Strength (YS) and Ultimate Tensile Strength (UTS) for Haynes alloy 25 sheet weldments (no aging) as a function of temperature compared to the historical database for alloy 25 weldments.

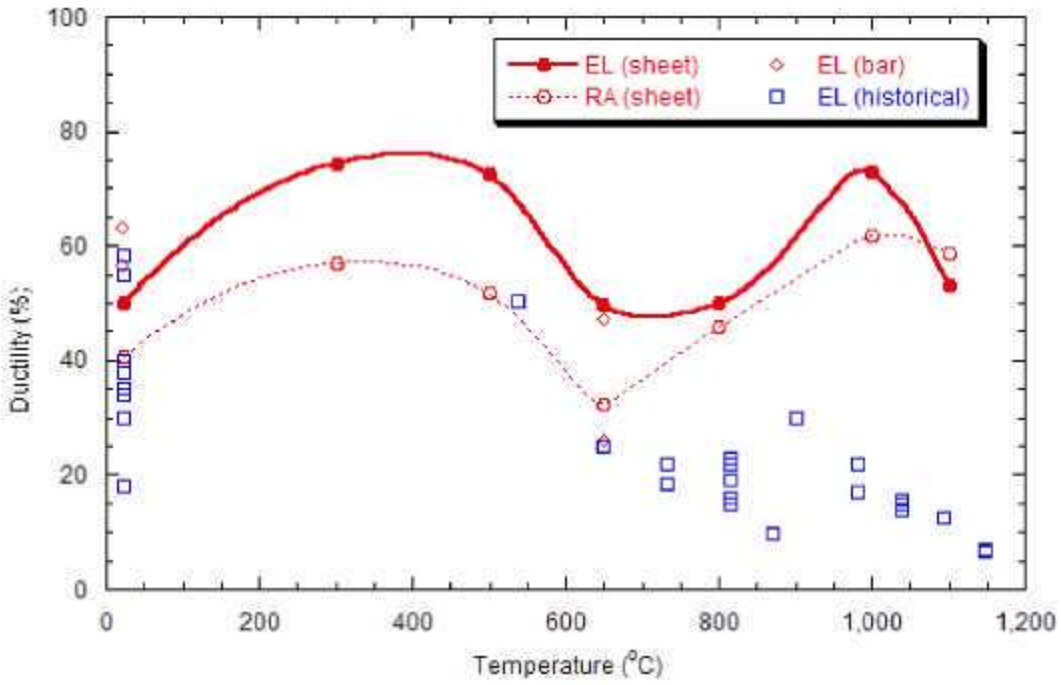

Figure 6.10. Measured ductility for Haynes alloy 25 sheet weldments (no aging) as a function of temperature compared to the historical database for alloy 25 weldments.

7. CREEP PROPERTIES RESULTS AND DISCUSSION

Uniaxial creep and creep-rupture tests were performed on alloy 25 sheet and weldments in the unaged and aged for 6,000 hour at 675°C condition and alloy 25 bar weldments in the unaged condition. Tests were conducted from 600°C to 950°C for times exceeding 40,000 hours. The results of these tests are presented in tabular form in appendix section A.3 (Tables A.3.1 and A.3.2). The corresponding creep strain versus time curves are included in appendix A.6. Tubular creep-rupture tests (internally pressurized tubular specimens machined from bar stock) were conducted from 675°C to 950°C for times exceeding 22,000 hours. Internal pressures ranged from 8.3 to 42.7 MPa (1,200 to 6,200 psi).

7.1 UNIAXIAL RUPTURE RESULTS

The uniaxial rupture results for all material conditions; unaged sheet (Base Metal or BM), sheet pre-aged before testing for 6,000 hour at 675°C (Aged Base Metal or BM-Aged), sheet or bar weldments (Weld Metal or WM), and sheet weldments pre-aged before testing for 6,000 hour at 675°C (Aged Weld Metal or WM-Aged), are plotted using the Larson-Miller Parameter (LMP) approach in figure 7.1. The LMP is defined as follows, where t_r = rupture life (hours), T = temperature (°C), and C = constant:

$$LMP = (273+T)[\log (t_r) + C] \qquad \text{equation 5}$$

Previous work has shown the historical HS-25 database to be best fit using a constant between 16.7 and 17.5 [2]. A constant of C=17 was used for the plot in figure 7.1. This gave a standard error of estimate (SEE) in the difference between the log time calculated from the LMP and the actual time to rupture of 0.18. Evaluation of the rupture data in figure 7.1 shows no obvious trend in rupture life as a function of material condition. All data fall in a tight scatter band with overlapping data for each material condition. Thus it was concluded that aging at 675°C and welding have no deleterious effects on the rupture strength of alloy 25.

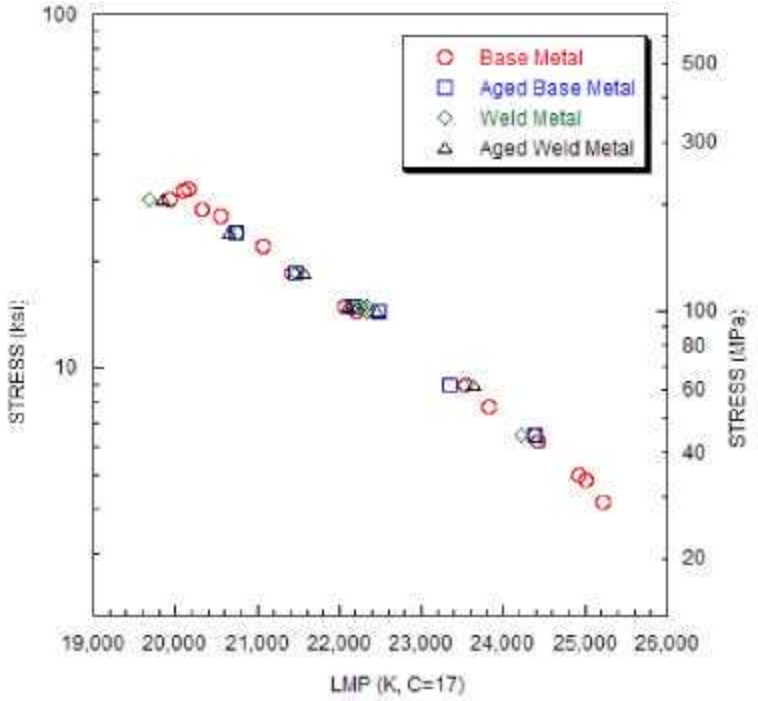

Figure 7.1. Larson-Miller Parameter (LMP) vs. Stress (log scale) for all material conditions.

Figure 7.2 is a LMP plot for the current uniaxial dataset and the historical rupture dataset. A second order polynomial is fit through all of the data on the plot. The historical dataset shows significant variation about this best fit line, but the current heat of tested material shows a good correlation to the line with only slight deviations for the highest and lowest stress tests conducted on this heat of alloy 25. These data are re-plotted in figure 7.3 as actual rupture life versus predicted rupture life by the LMP method. A one to one (straight line) correlation is an exact fit. Dotted lines are included in the plot to indicate the bounds for data within a factor of ±2 in life. Most data points for all material conditions fall within the plus or minus factor of two in life while many data points in the historical dataset fall outside of this range. The entire range of actual versus predicted times for the historical dataset is about plus or minus a factor of thirty (range of over two log cycles) in life. From this plot, it is concluded that an LMP fit of all the uniaxial rupture data, including the historical dataset, shows very good correlation with current heat of alloy 25, but using the historical dataset for design may be problematic due to the large variations in rupture times.

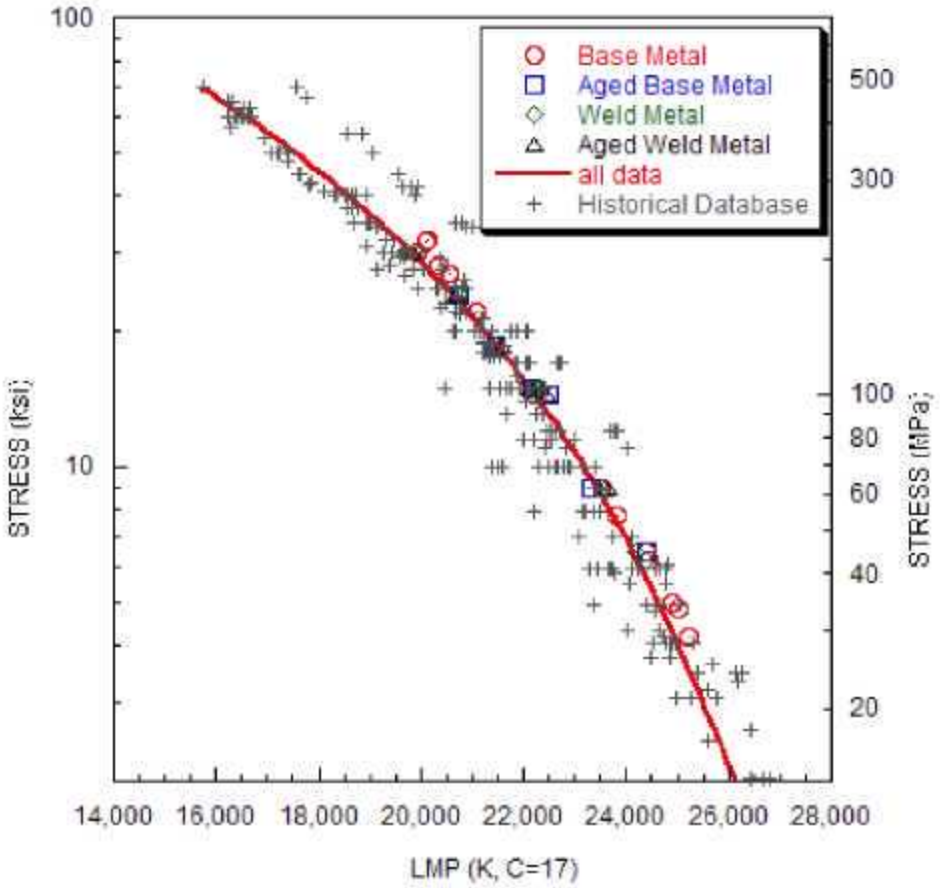

Figure 7.2. Larson-Miller Parameter (LMP) vs. Stress (log scale) for all material conditions and the historical database.

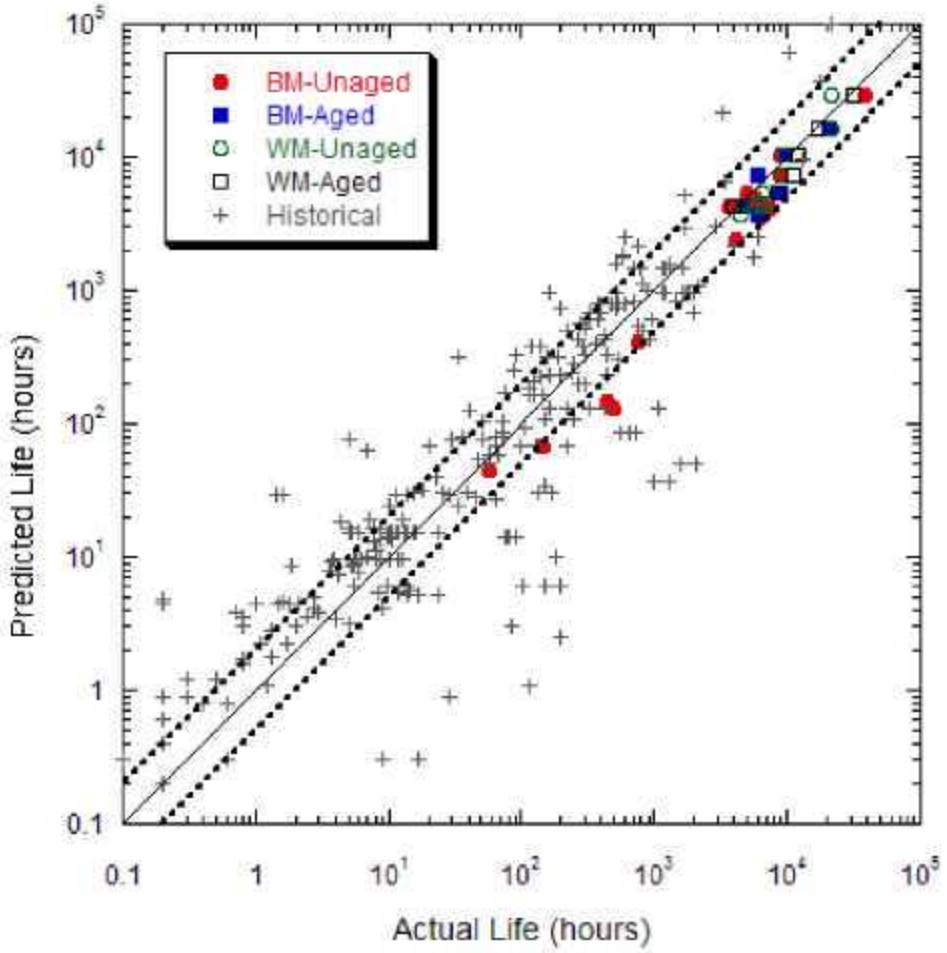

Figure 7.3. Actual life versus predicted life (LMP analysis). Dotted lines are plus or minus a factor of two on life.

Rupture ductility (post-test elongation) as a function of rupture life is plotted for all material conditions and the historical dataset in figure 7.4. Most of the historical dataset is based on short-time data, which gives highly variable results in terms of rupture ductility. For test times of 0.1 to 1,000 hours, the ductility of the historical dataset ranges from 2 to 35%, and the few rupture points beyond 1,000 hours the range is 2 to 15%. The current heat of material shows similar behavior where ~100 hour tests gave 50% elongation, ~1,000 hours gave 20 to 30% elongation, 5,000 to 10,000 hour tests resulted in 5 to 15%, and ruptures beyond 10,000 hours resulted in ductilities of 2 to 6%.

In figure 7.4, the rupture elongation measurements for each material condition overlap one another and no effect can be seen. However, examination of creep curves in the appendix A.6, revealed a few noticeable trends. The general trend for all the data is captured in figure 7.5. First, as already stated by LMP analysis, rupture life was not significantly affected by material condition (less than a factor of two in life). Second, when comparing base and welded material (either comparing unaged to unaged or aged to aged) the weld specimen showed slightly less creep strain for a given time. This is attributed to increased resistance to creep deformation in the cross weldment location. The strength of the weldment is a function of both weldment mechanical properties and geometry. As with the tensile tests, the weldment was mechanically reinforced because the weld crown was not removed which contributes to a portion of the gauge length having improved creep resistance. The third trend observed is the aging effect. Aging at 675°C for 6,000 hours reduces the minimum creep rate and lowers the creep strain at a given time

compared to identical tests on unaged material. The degree of this effect is a function of testing temperature. Generally, the effect is large (large differences between creep rates and strains) at low temperatures near or below the aging temperature, but the effect is minimal at the highest temperatures tested.

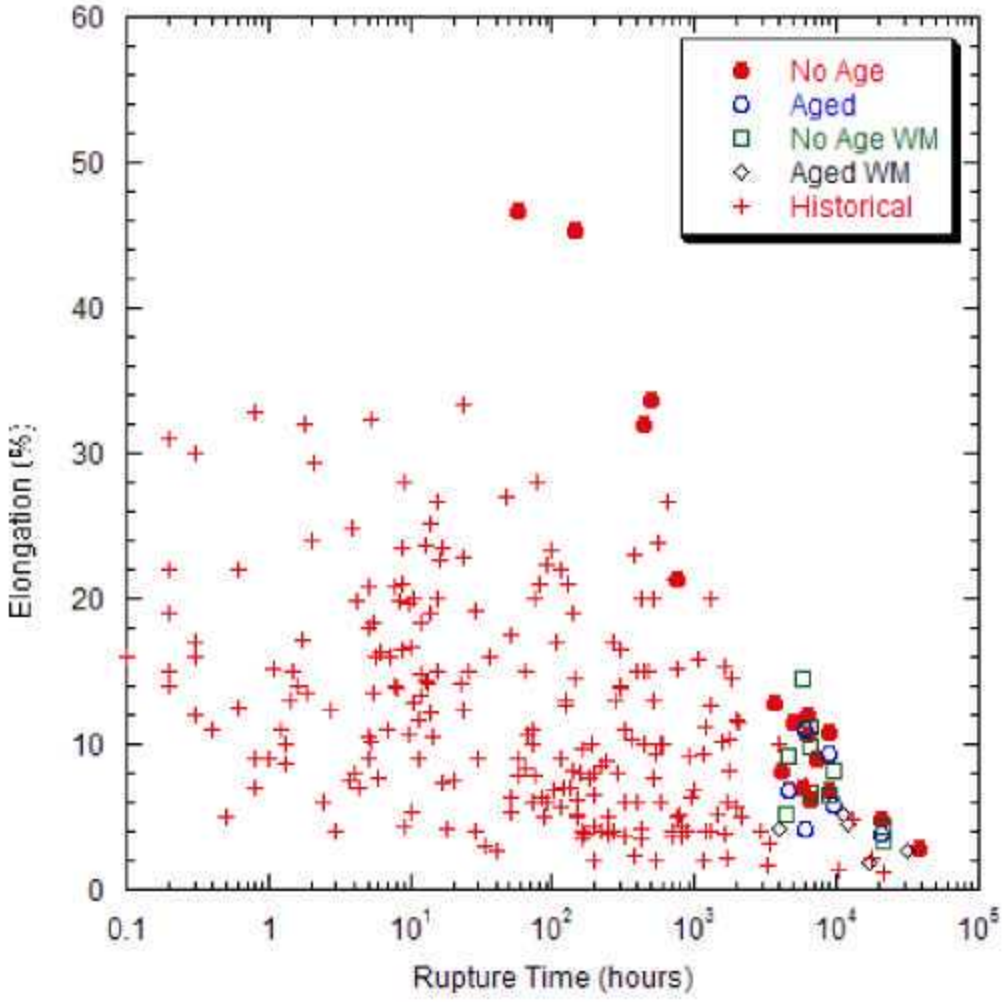

Figure 7.4. Rupture ductility as a function of rupture time for all material conditions compared to the historical database.

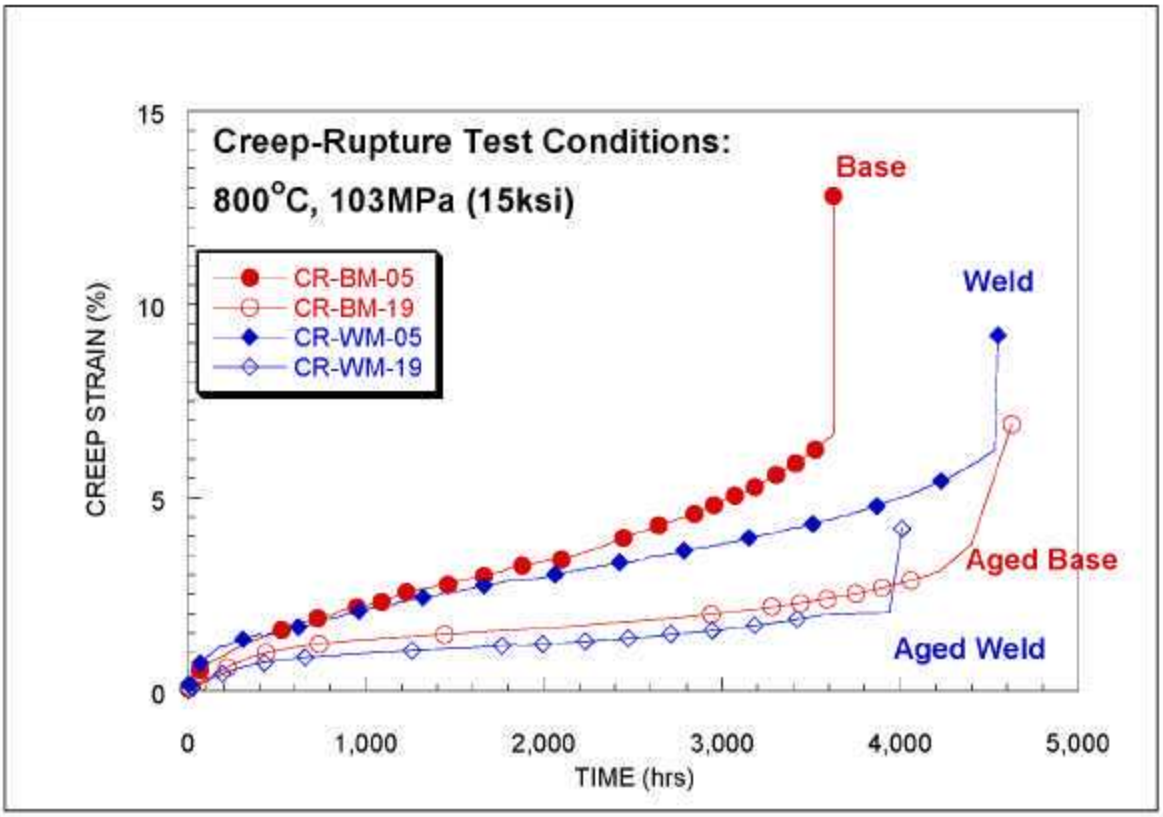

Figure 7.5. Creep curves (time vs. creep strain) for the four material conditions tested at 800°C and 103 MPa (15 ksi).

7.2 PRESSURIZED TUBE RUPTURE RESULTS

To evaluate the internally pressurized tube creep-rupture test results, the rupture life of the capsule was compared to the expected life using the fit of the rupture data in figure 7.2 and assuming the stress distribution in the tubular specimen could be modeled as an infinitely long tube. For a thick-walled tube with an internal pressure P, an internal radius R_i, and an external radius R_o, the elastic hoop stress (σ_{hoop}), axial stress (σ_{axial}), and radial stress (σ_{radial}) were calculated at any radial location (r) by Lame, per the following equations [22]:

$$\sigma_{hoop} = P \times \frac{R_i^2}{R_o^2 - R_i^2}\left(1 + \frac{R_o^2}{r^2}\right) \qquad \text{equation 6}$$

$$\sigma_{axial} = P \times \frac{R_i^2}{R_o^2 - R_i^2} \qquad \text{equation 7}$$

$$\sigma_{radial} = P \times \frac{R_i^2}{R_o^2 - R_i^2}\left(1 - \frac{R_o^2}{r^2}\right) \qquad \text{equation 8}$$

When creep deformation is considered, the Lame equations may not be applicable depending on the wall thickness. During creep, high stresses can relax. When this happens, the stresses are transferred to lower stress areas within the structure. The speed and the degree at which this happens are governed by the creep properties of the material. For simplicity, Bailey assumed the material's creep behavior could be modeled using only steady-state creep with a power-law dependence. Using this assumption, for a power-law exponent of n, the stress distribution is described as follows [22]:

$$\sigma_{hoop} = P \times \frac{[(2-n)/n](R_o/r)^{2/n} + 1}{(R_o/R_i)^{2/n} - 1} \qquad \text{equation 9}$$

$$\sigma_{axial} = P \times \frac{[(1-n)/n](R_o/r)^{2/n} + 1}{(R_o/R_i)^{2/n} - 1} \qquad \text{equation 10}$$

$$\sigma_{radial} = -P \times \frac{(R_o/r)^{2/n} - 1}{(R_o/R_i)^{2/n} - 1} \qquad \text{equation 11}$$

When n equals 1, i.e. when the creep-rate has a linear stress dependence, then the Bailey solution becomes the Lame solution.

In order to evaluate the internally pressurized tube rupture data using the Lame and Bailey equations, a single stress value for each test is needed. Two criteria (yield surfaces) were used: the Von Mises (VM) and the Stress Intensity (SI). The VM takes into account all three stresses (radial, axial, and hoop):

$$\sigma_{VM} = \sqrt{\frac{(\sigma_1 - \sigma_2)^2 + (\sigma_2 - \sigma_3)^2 + (\sigma_3 - \sigma_1)^2}{2}} \qquad \text{equation 12}$$

The SI is simply two times the Tresca stress or the maximum principal stress minus the minimum principal stress:

$$\sigma_{SI} = \sigma_{max} - \sigma_{min} \qquad \text{equation 13}$$

An alternative approach to evaluating rupture in structures is the reference stress approach [23]. The reference stress approach is based on a limit load analysis of a perfectly plastic material. The basis assumption in this approach is that there are similarities between creep and plasticity. For a structure subjected to complex loading in creep, after sufficient time, internal stresses will redistribute and reach a steady-state condition that can be described by the plastic solution (limit load) for the structure. The result of the limit load analysis for a given geometry combined with a yield criteria (typically Tresca) is a single reference stress ($\sigma_{reference}$), which governs the creep deformation in the structure and is independent of material (as long as the material is not creep brittle) [24]. For an infinitely long tube, the reference stress (Tresca) is [24]:

$$\sigma_{reference} = \frac{P}{\ln(R_o/R_i)} \qquad \text{equation 14}$$

This equation has been shown to give the best correlation with available experimental data compared to various ASME Boiler and Pressure Vessel (B&PV) Code rules for cylindrical sections with varying wall thickness that have crept under internal pressure [25]. The use of the equation was recently (2005) accepted in the ASME B&PV Code Section I as an alternative method for determining wall thickness of tubes and pipe in boilers.

The VM criterion was applied to the inner diameter (ID) and outer diameter (OD) stresses calculated for both the Lame and Bailey solutions. A value of n=8 was used for the creep calculations. This value was determined by evaluating the creep data for this heat of alloy 25 (discussed later in this section) and is consistent with other observations of creep in the alloy [29, 30]. Furthermore, the analysis is very sensitive to n only in the range of n=1 to n=4. Changing n from 6 to 10 has little effect on calculated stresses. The SI was applied to the ID and OD for the Bailey creep solution, and the reference stress was also evaluated. The rupture time for each stress calculated by each method was then compared with the predicted rupture life for that stress value by evaluation of the LMP fit of the uniaxial data. Figures 7.6 and 7.7 show the results for each analysis as actual life versus predicted life. A one-to-one correlation is a perfect fit of the data, and dashed lines at a factor of plus or minus two in life are included on each plot. Several ruptures are identified in each plot. For the standard tube without any pre-aging and exhibiting a longitudinal rupture originating in the tube, the identification is No Age. For a standard tube without pre-aging that had a rupture initiate in the tubular specimen weldment, the identification is No Age-WM. For a standard tube without pre-aging that had a rupture in the tubular specimen cap, the identification is "No Age – Cap". For the tube specimens pre-aged for 6,000 hours at 675°C, the identification is "Aged".

Each plot also includes a fit of a straight line (power-law fit on log-log plot) to see how well each model followed a one-to-one correlation. This line was fit to a censored dataset. To censor the dataset, the non-typical ruptures were removed (No Age-WM and No Age-Cap) and the rupture results on aged capsule test conducted at 750°C were also removed due to observed aging effects in creep deformation. The aged capsules tested at 850 to 950°C were included in the censored dataset along with the typical ruptures of unaged material because it was judged that aging at 675°C had little effect on creep behavior at and above 850°C. This was based on experimental observations of creep deformation of aged material in uniaxial creep tests where creep rates were similar at the highest testing temperatures (850°C and above) regardless of aging condition. A comparison of the tube ruptures, later in this section, with the uniaxial data shows that the 750°C test on aged material exhibited consistently longer life than expected compared to the aged tubes tested at 850°C and above which were within the scatter of the data.

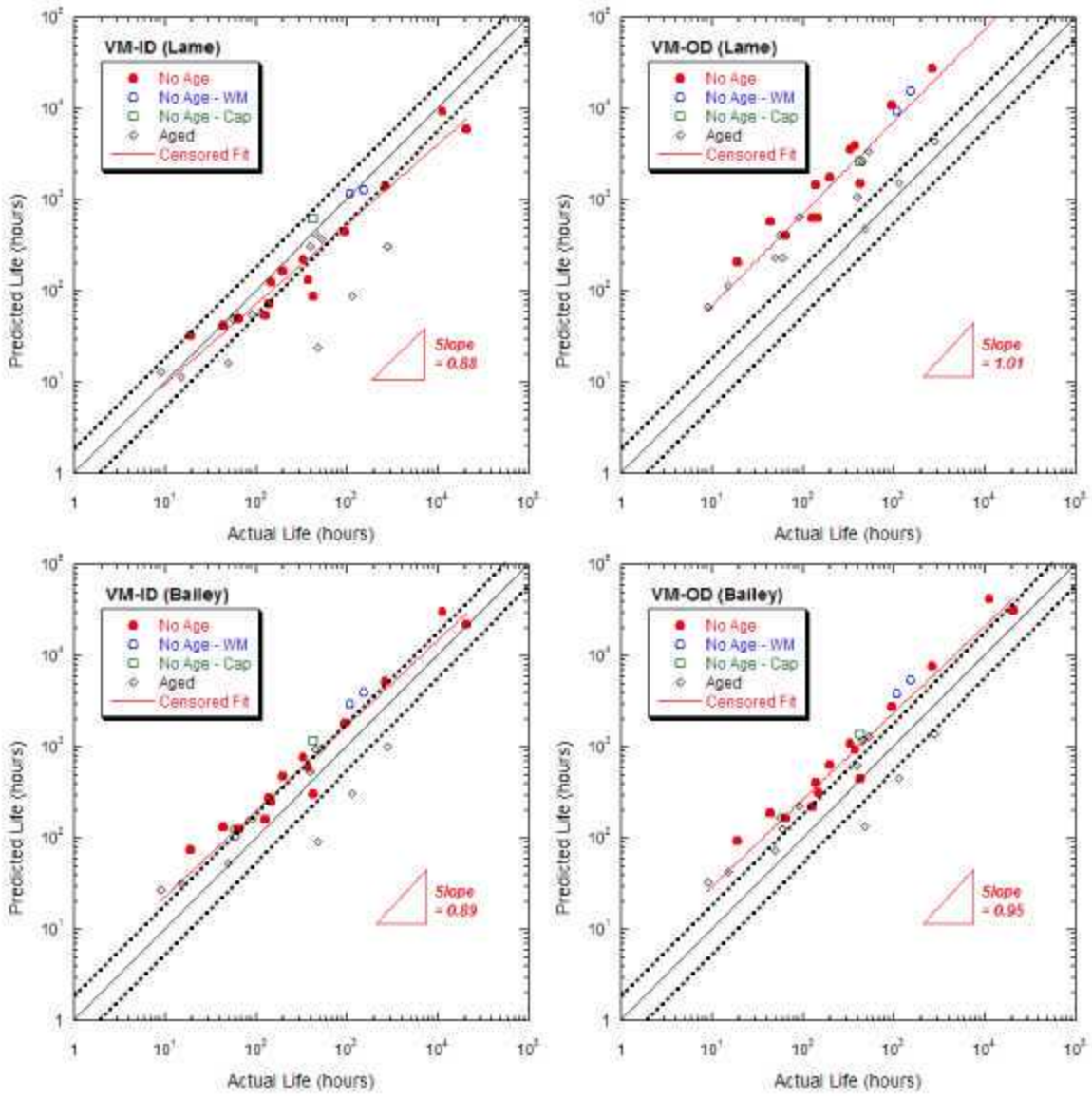

Figure 7.6. Actual vs. predicted life for pressurized tube creep-rupture tests analyzed using the Von Mises (VM) stress criterion for the inner (ID) and outer (OD) diameter elastic (Lame) and steady-state creep (Bailey) solutions. Slope is shown for a fit of the censored dataset.

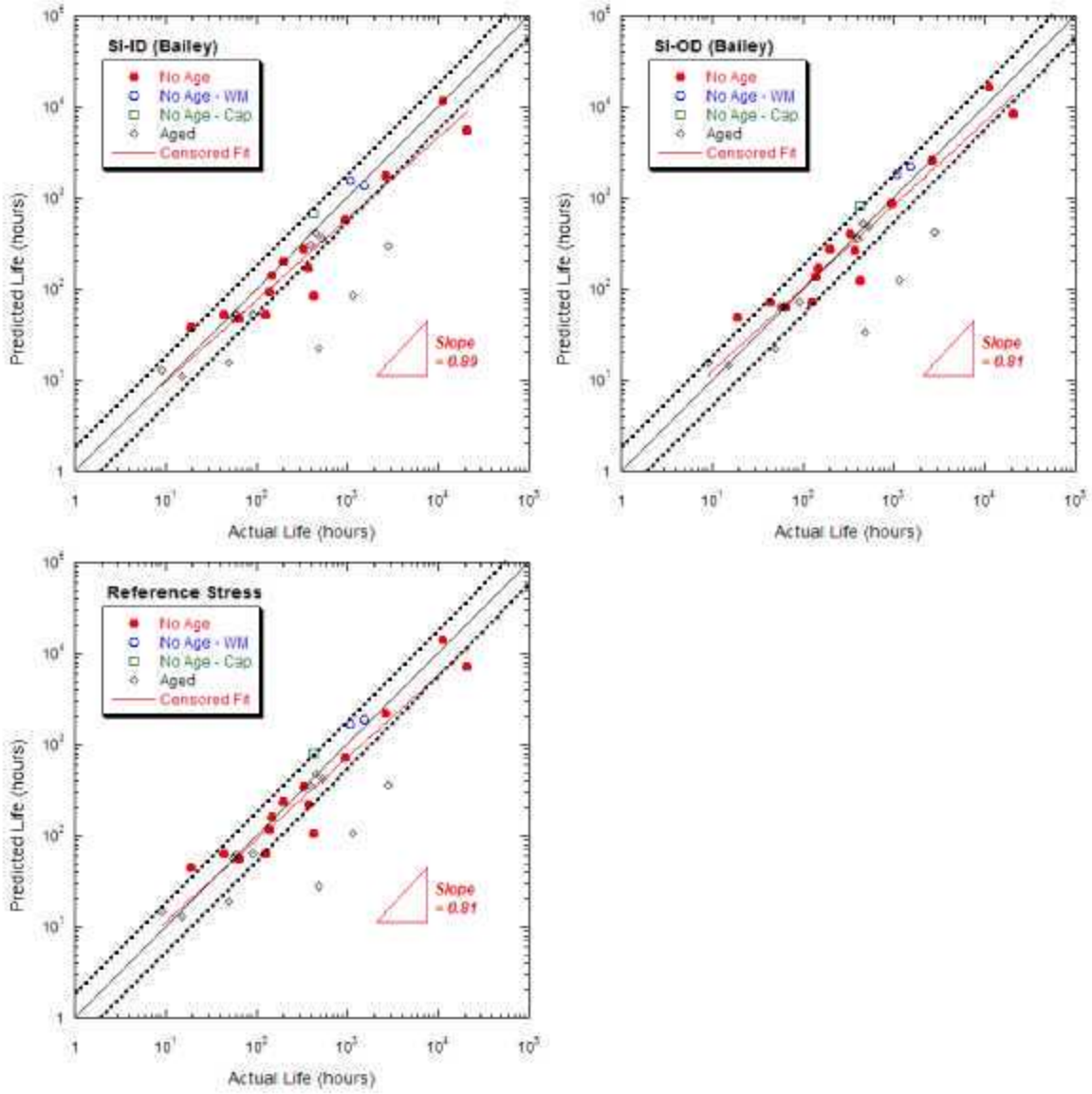

Figure 7.7. Actual vs. predicted life for pressurized tube creep-rupture tests analyzed using the stress intensity (SI) stress criterion (Tresca) for the inner (ID) and outer (OD) diameter steady-state creep (Bailey) solutions and for the reference stress solution (Tresca). Slope is shown for a fit of the censored dataset.

To evaluate the various stress criteria and models, the standard error of estimate (SEE) for log actual life and log predicted life was calculated for all of the rupture data and for the censored dataset. These results are tabulated with the calculated slopes for a fit of the censored dataset in Table 3. Visual examination of VM-OD (Lame), VM-ID (Bailey), and VM-OD (Bailey) plots show most of the data are above the one to one line and above the factor of two line. The VM-OD (Lame) showed the highest SEE for either dataset corroborating the visual inspection although it had the only slope close to one. The VM (Bailey) solutions appear to show good SEE for the entire dataset, but when the dataset is censored, little improvement is made in the SEE. This shows that the good SEE for the entire dataset is due to the location of the non-typical data and not due to a good representation of rupture data.

Table 3. Standard error of estimate* (SEE) for tube rupture results

	VM-ID (Lame)	VM-OD (Lame)	VM-ID (Bailey)	VM-OD (Bailey)	SI-ID (Bailey)	SI-OD (Bailey)	Ref. Stress
SEE	0.45	0.83	0.37	0.44	0.45	0.38	0.40
SEE (censored)	0.29	0.87	0.31	0.43	**0.27**	**0.21**	**0.23**
Slope (censored)	0.88	1.01	0.89	0.95	0.89	0.81	0.81

**SEE calculated for log actual life and log predicted life based on LMP fit of uniaxial data*

The VM-ID (Lame) shows better correlation than the other VM results, but 8 censored data points fall below the factor of 2 band.

The SI-ID and –OD (Bailey) results show improved SEE for the entire dataset and for the censored datasets. For the ID, 5 censored data points fall below the factor of 2 band while for the OD 3 fall below and 1 falls above the band. The SEE for the SI-OD (Bailey) is the lowest of any analysis of the data, but the slope of the SI-ID (Bailey) censored dataset is slightly closer to one.

The reference stress approach results in a SEE between the SI (Bailey) solutions. Four censored data points fall below the band while one falls above the band. The slope and SEE is very close to the SI-OD (Bailey).

Based on these data, it is clear that the Lame solutions give a poor representation of the rupture data and the VM criteria, regardless of the stress calculation, gives a less accurate result compared to the Tresca based SI and reference stress solutions. The SI-ID (Bailey) gives a good fit of the data and a conservative estimation on life. The SI-OD (Bailey) and the reference stress (Tresca) give the best fits of the tubular creep data to the uniaxial creep data.

Microstructural observations of ruptured tubes appear to support the Tresca based creep solutions. Figure 7.8 shows the microstructure of a tube after pressurized creep testing. Extensive inner (ID) and outer (OD) diameter cracking are observed. Additionally, intergranular cavitation is observed through the entire wall of the tube. Although there is a stress gradient through the wall of the tube, the SI criteria for the creep (Bailey) solutions results in similar stress values on the ID and the OD of the tubes. In contrast, the Von Mises criteria applied to the elastic solution results in large differences in stress values at the OD and ID of the tube. Assuming that crack/cavitation initiation is controlled by the one of the chosen criteria, the Von Mises stress (elastic solution) supports crack initiation on the tube ID. The SI applied to the creep solution (Bailey) results in small through wall differences or a uniform controlling stress. The reference stress, by definition, supports a single relaxed stress value that controls rupture. The calculated reference stress is very similar to both the ID and OD SI Bailey stresses. The micrographs indicate that the controlling stress is not an ID or an OD localized effect.

The ID and OD crack depth and spacing was measured for a number of ruptured tubes by quantitative metallographic observations. As shown in figure 7.9, no obvious trend for spacing or depth was observed. From this, it appears the Tresca-based creep solutions have a better physical basis for controlling rupture than the Von Mises criteria applied to the elastic solutions.

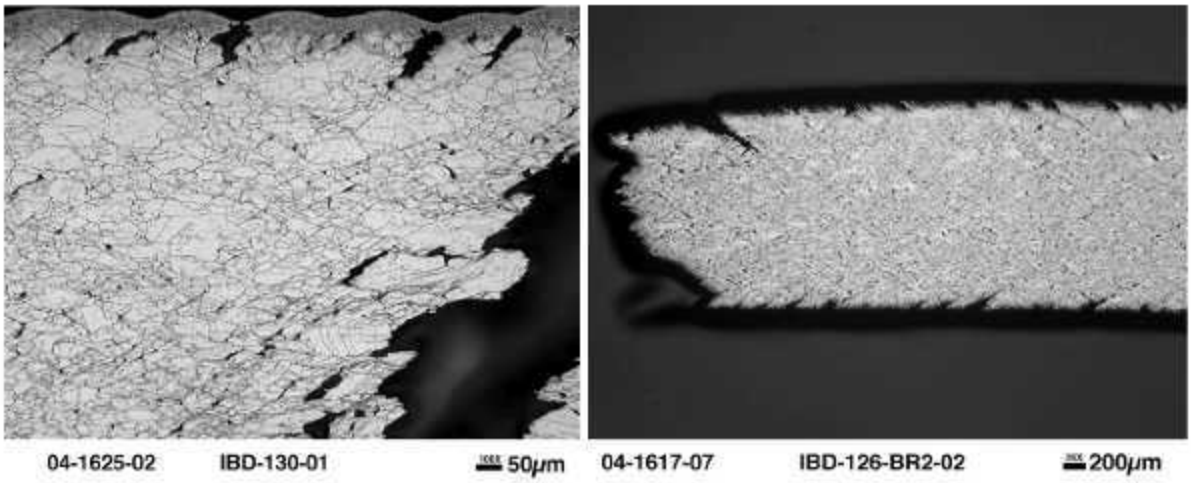

Figure 7.8. Typical micrograph of a region near the creep fracture of a pressurized tubular creep specimen. Extensive inner and outer diameter cracking is observed in addition to intergranular cavitation.

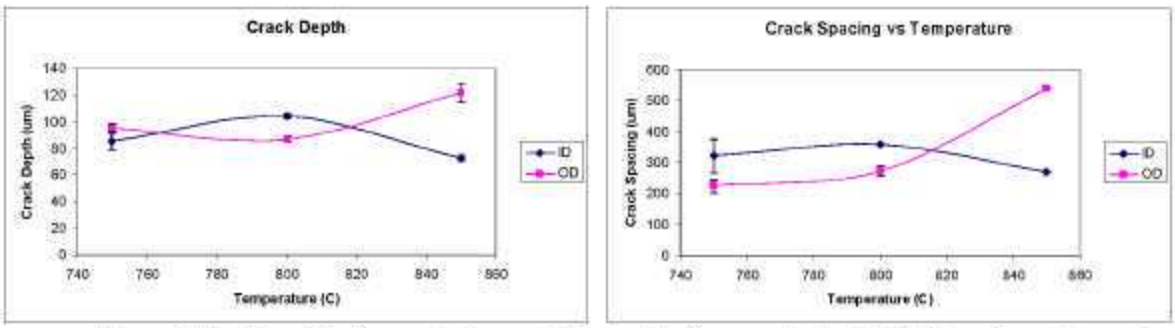

Figure 7.9. Quantitative metallographic results for crack depth (left) and crack spacing (right) as a function of test temperature and location (ID and OD) for selected tubular specimens.

7.3 SUMMARY OF ALL RUPTURE RESULTS

All of the rupture data produced on the program are plotted in figures 7.10, 7.11, and 7.12. The reference stress was used to calculate the stress for the internally pressurized tube tests. The nomenclature is as follows: "Unaged" – unaged sheet, "Aged" – sheet pre-aged for 6,000 hours at 675°C, "Unaged WM" – unaged sheet and bar cross-weldments, "Aged WM" - sheet cross-weldments pre-aged for 6,000 hours at 675°C, "Unaged Tube" – unaged pressurized tubular tests (all rupture types), "Aged Tube" - pressurized tubular tests pre-aged for 6,000 hours at 675°C, and "Isotherm" – isotherm from LMP fit of all uniaxial data. Ongoing tests are identified by arrows.

Evaluation of all the plots show the data scatter is very minimal for most temperatures. At 750°C, the effect of aging on the pressurized tubular tests is clearly identified, but the longer-term uniaxial data on aged material show this is most likely a short-term effect. At 800 and 850°C, a large amount of data is available which shows very good fits of the isothermal rupture curves, even for the non-typical ruptures in the tubular creep tests. The worst fit of the data is at 950°C where two of the tubular ruptures were at shorter-times than predicted. For the longest term test, this was due to a rupture in the cap of the specimen. Thus the fit is actually better than it appears.

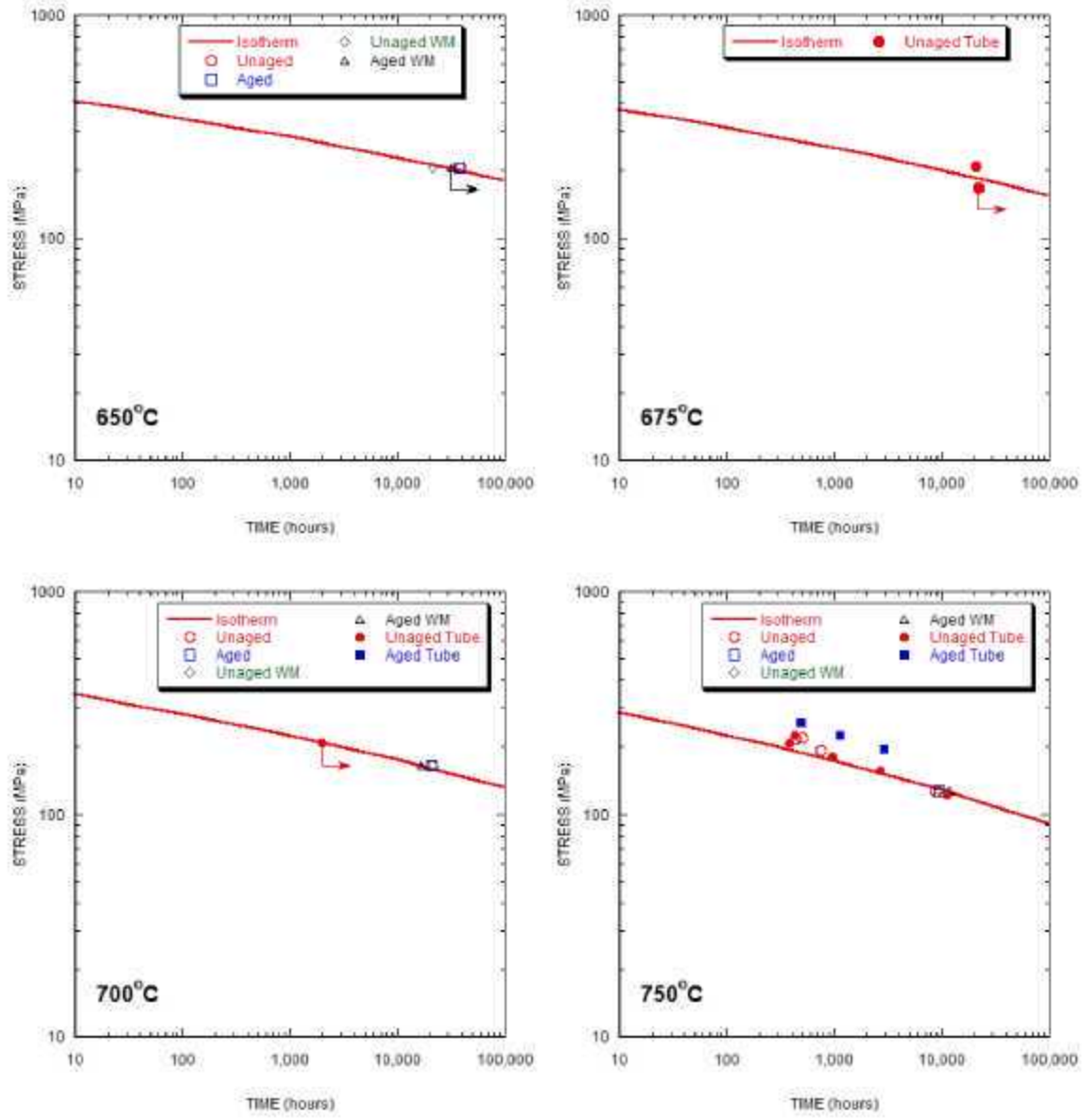

Figure 7.10. Plots of isothermal rupture data from 650 to 750°C. The solid line is based on LMP analysis of entire dataset including historical data.

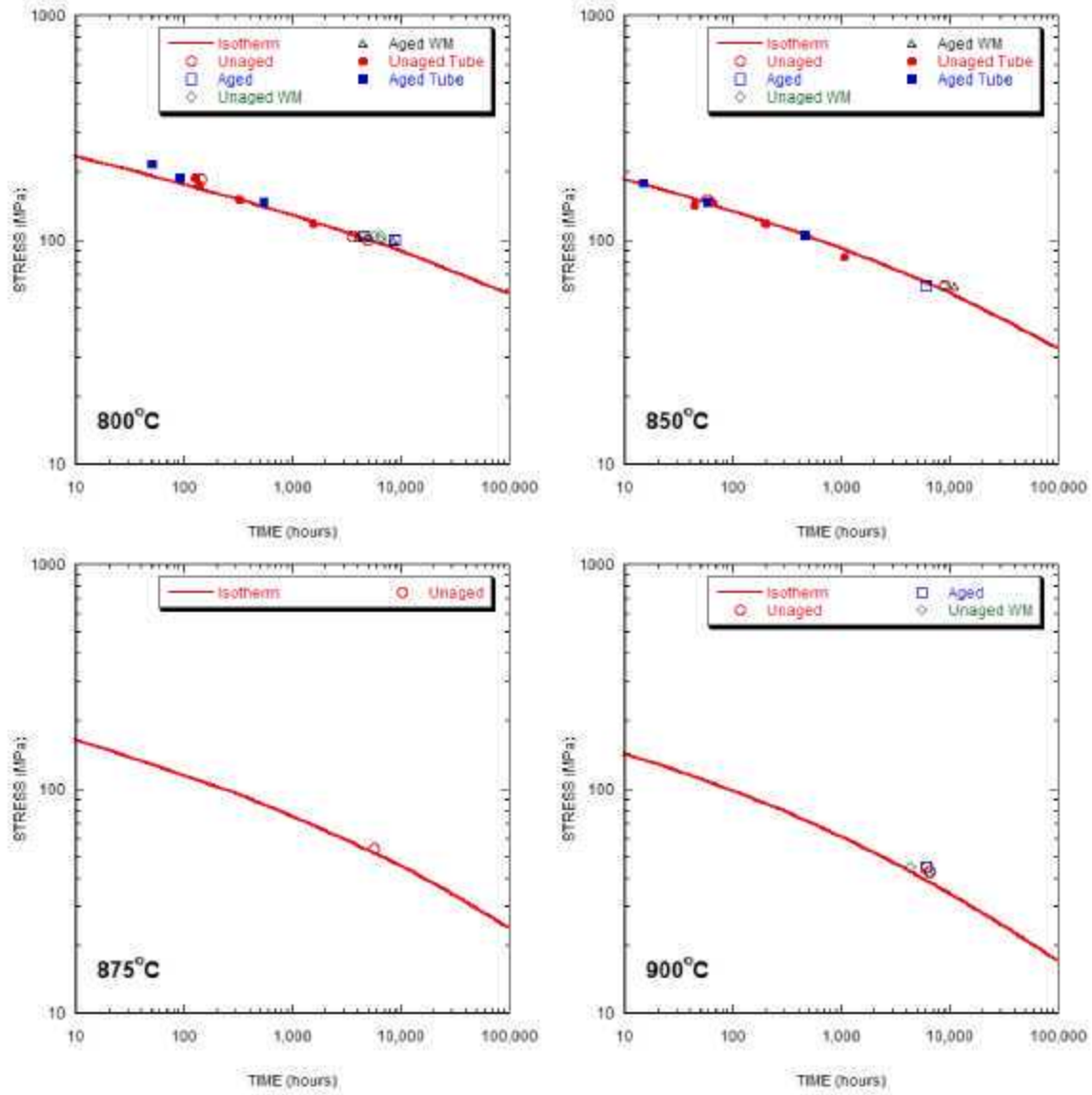

Figure 7.11. Plots of isothermal rupture data from 800 to 900°C. The solid line is based on LMP analysis of entire dataset including historical data.

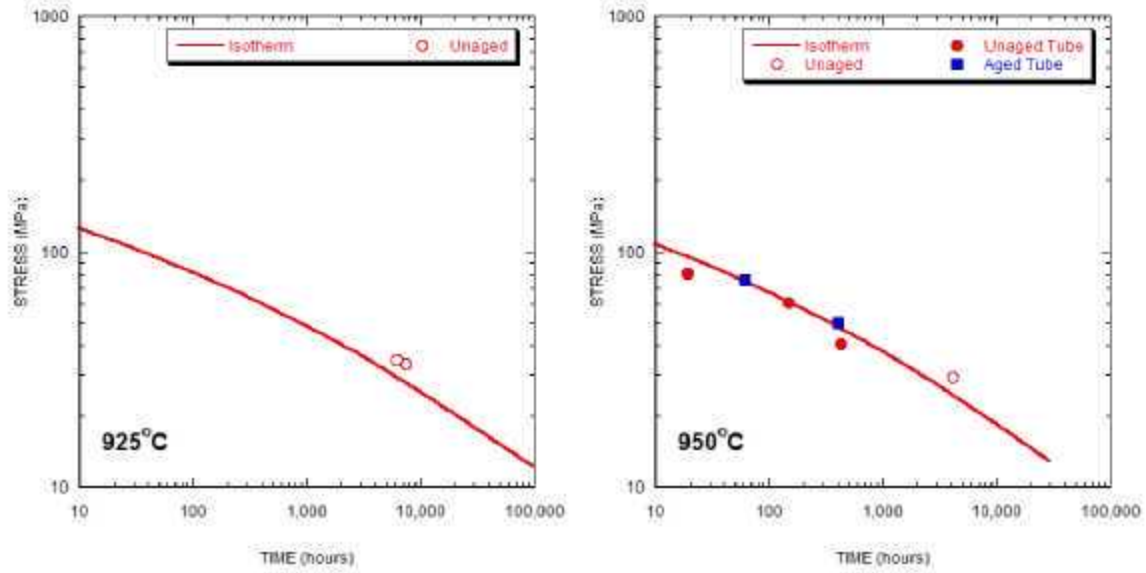

Figure 7.12. Plots of isothermal rupture data at 925 and 950°C. The solid line is based on LMP analysis of entire dataset including historical data.

7.4 CREEP-RATE ANALYSIS

In addition to creep-rupture tests, creep tests to determine the steady state or minimum creep rates of alloy 25 at lower temperatures (600 to 700°C) were performed. The minimum creep rates are plotted as function of stress for various temperatures from the historical database in figure 7.13.

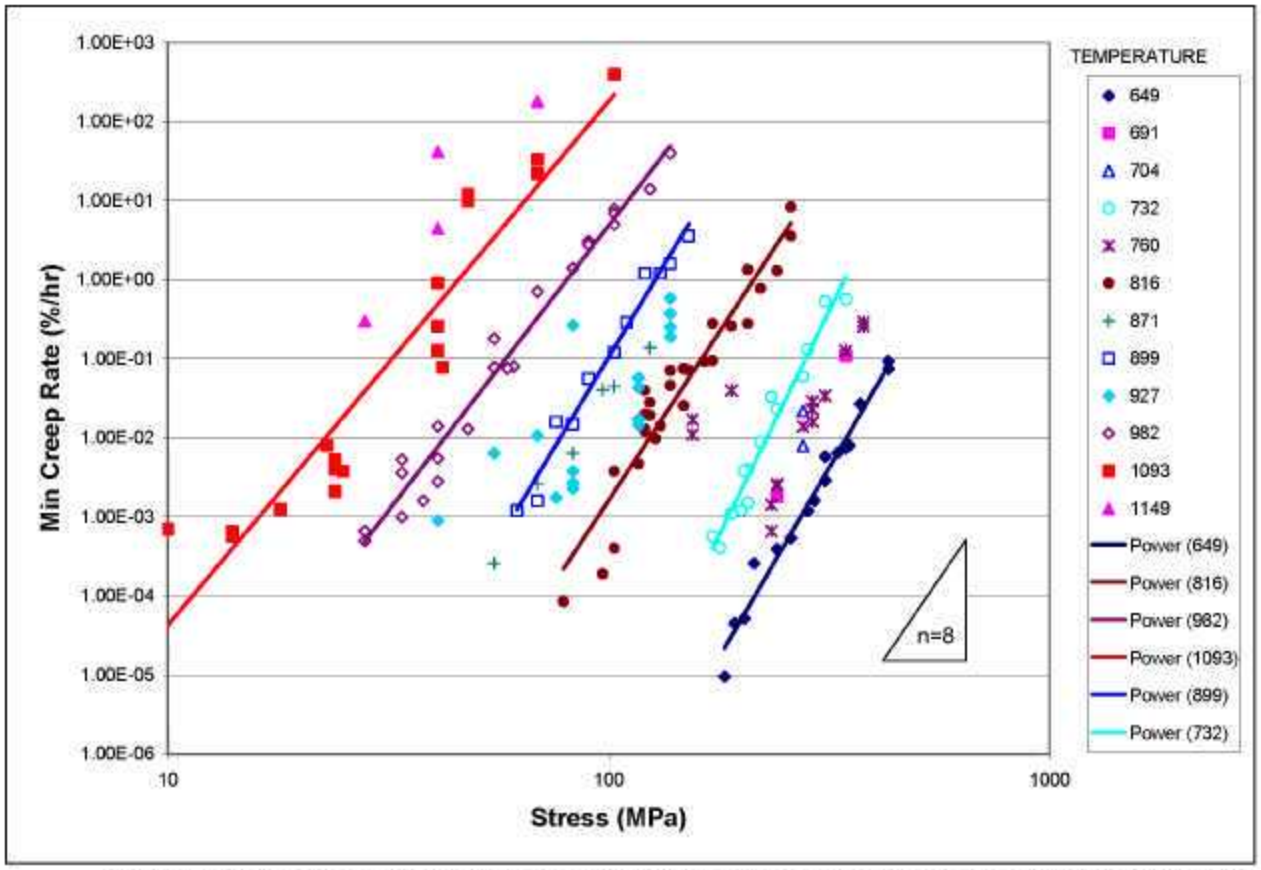

Figure 7.13. Minimum creep rate versus stress for various temperatures. All data taken from the historical dataset.

Some data are available for 649°C, but most data is for 732°C and above. The power-law dependence of the isothermal minimum creep rate data (ε_{min}) data is variable and the power law exponent (n), given by the relation:

$$\dot{\varepsilon}_{min} \propto \sigma^{n} \qquad \text{equation 15}$$

varies between n=6.5 and n=11.5. In this study, creep testing was performed over a large range of temperatures and stresses for a variety of material conditions. Few isothermal creep conditions had more than two or three different stress levels for the same material condition, so a creep rate analysis was performed on the historical dataset for comparison with the current dataset.

It is assumed the temperature dependence of creep can be described by an Arrhenius relationship:

$$\dot{\varepsilon}_{min} \propto D_o \exp(-Q/RT) \qquad \text{equation 16}$$

where T is absolute temperature, D_o is the pre-exponential diffusion constant, Q is the activation energy for creep, and R is the universal gas constant. A phenomenological description of minimum creep rate as function of temperature (T) and stress (σ) can be developed from relations 15 and 16 as follows [26, 27]:

$$\dot{\varepsilon}_{min} = A\sigma^{n} \exp(-Q/RT) \qquad \text{equation 17}$$

where A is constant, n is the power-law exponent, Q is the activation energy for creep, and R is the universal gas constant. Figure 7.14 is an Arrhenius plot of minimum creep rate divided by stress to the n power. From the analysis of these data, Q and A were determined, and, a diffusion compensated minimum creep rate parameter [min creep rate / Aexp(-Q/RT)] was calculated.

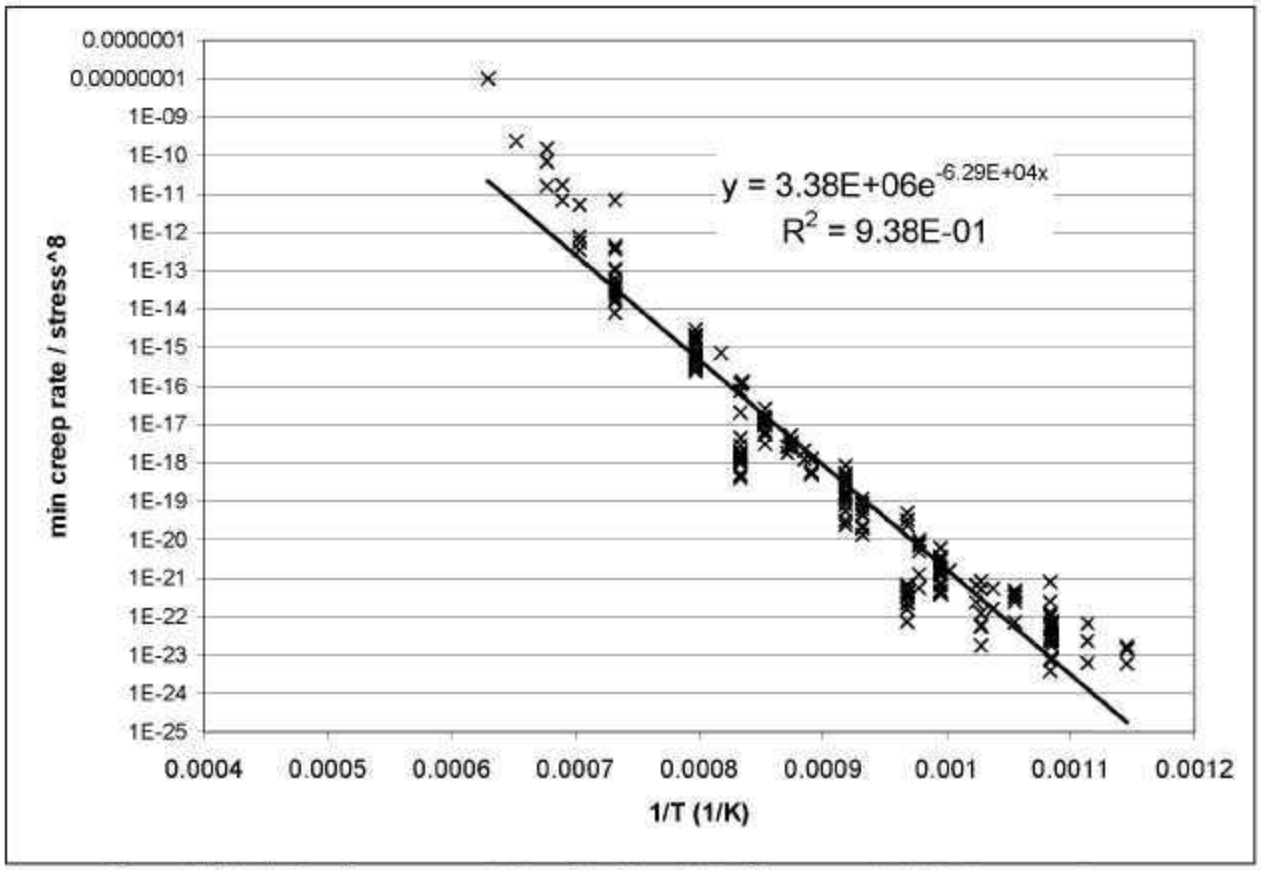

Figure 7.14. Activation energy determination plot of inverse absolute temperature versus minimum creep rate divided by stress^n (n=8).

This parameter is plotted versus stress for all data including all material conditions and the historical data in figure 7.15.

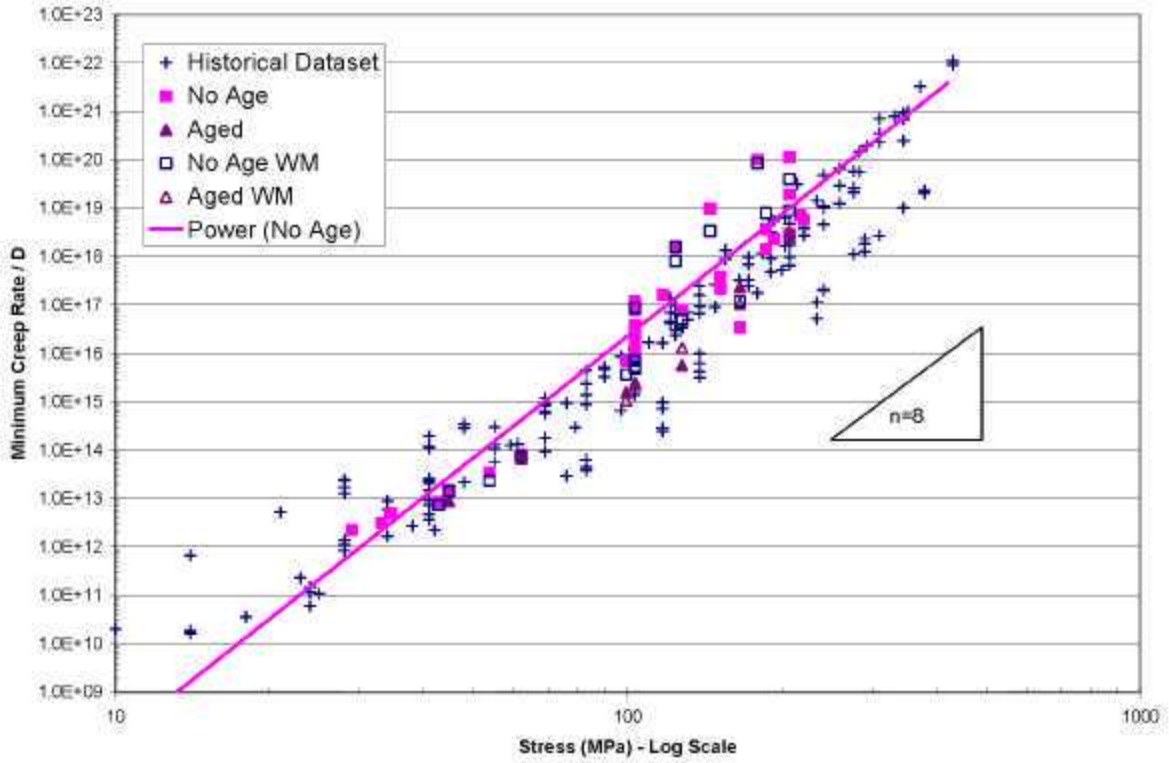

Figure 7.15. Stress versus diffusion compensated minimum creep rate (min. creep rate / $D_o exp(-Q/RT)$ for all material conditions. Fit of the data give a power-law exponent of n=8.4.

A power-law was fit to the No Age uniaxial creep data from the creep rate and creep-rupture tests in figure 7.15. The slope of fit matched the creep rates calculated from the historical dataset and the power-law exponent was found to be n=8 (fit value, n=8.4). This is in good agreement with literature results, were Tanaka et. al [29, 30] studied the effect of microstructure and aging heat-treatments on the creep behavior of alloy 25 at 816 to 1038°C and found that the power-law exponent was n=8 regardless of heat-treatment or test conditions. In general, the diffusion compensated creep rates for all material conditions matched those of the historical dataset. The aged data generally showed slightly lower creep rates at stress levels of 100MPa or greater. The data at lower stresses is limited but shows comparable results. From this analysis, a power-law exponent of n=8 was judged to be a good representation over a broad range of stresses and temperatures for alloy 25, and this value was used in the analysis of the pressurized tube rupture results.

8. CONCLUSIONS

An extensive tensile and creep study has produced a large database of high-temperature mechanical properties for a new heat of Haynes alloy 25. The database contains properties for sheet and bar products including material with GTAW weldments and material aged at 675 to 850°C for times up to 12,000 hours. An appendix is included in the report with all the data generated throughout the program as well as a collection of historical creep and tensile data on the alloy

Tensile results show this heat of alloy 25 to have yield strength and ultimate tensile strength values comparable to those reported in the historical database. Tensile ductility was comparable for lower temperatures and appears better than the historical database at 800°C and above. Welding did not cause a reduction in tensile properties (strength or ductility). Aging at 675°C caused a dramatic increase in yield strength, a modest increase in ultimate tensile strength, and a significant decrease in tensile ductility at both room temperature and at 650°C. The strength and ductility changes with time were accurately described by a Johnson-Mehl-Avarmi (JMA) type equation, which indicated different phases and/or location of phases may be the source of changes in strength and ductility.

Creep-rupture tests showed welding and aging at 675°C for 6,000 hours did not effect uniaxial rupture life for tests conducted from 650°C to 950°C. The Larson-Miller Parameter (LMP) was used to accurately describe the rupture strength for all material conditions. This heat showed much less scatter in rupture time compared to the historical database. The rupture ductility data matched the historical dataset where at long times ductility decreased. Tubular creep tests were conducted by internally pressurizing tubes of varying wall thicknesses. The rupture lives of these tests were evaluated by a number of methods which showed the steady-state creep analysis (Bailey) of I.D. and O.D. stresses and the reference stress solution for an infinitely long cylinder gave very good correlation with predicted life. Microstructural evaluation of ruptured tubes showed these fits have a physical basis. Evaluation of the creep-rates showed that for the broad range of stresses and temperatures, a power-law exponent of n=8 described the minimum creep rate behavior of the alloy. Overall, over 800,000 hours of creep data, with the longest test times exceeding 40,000 hours, were produced to augment the historical database which had less than 200,000 hours of creep data.

REFERENCES

[1] R.W. Swindeman, "Some Creep-Rupture Data for Newer Heats of Haynes Alloy No. 25 (L-605)," ORNL-TM-3028, Oak Ridge National Laboratory, Oak Ridge, TN, 1970.

[2] R. W. Swindeman, "Review of the Mechanical Behavior of Haynes Alloy No. 25," Attachment to Letter to J. P. Moore, Oak Ridge National Laboratory, July 1998.

[3] C. S. Slunder, "Short-Time Tensile Properties of the Co-20Cr-15W-10Ni Cobalt-Base Alloy (L-605)," DMIC-Memo-179, September, 1963.

[4] W.F. Simmons and H.C. Cross, "Report on The Elevated-Temperature Properties of Selected Super-Strength Alloys," Spec. Tech. Publ. No. 160, American Society for Testing and Materials, Philadelphia, 1954.

[5] B.A. Baughman, "Gas Atmosphere Effects on Materials," WASC-TR-59-511 (PB-161980), May 1960.

[6] A. Greene, H. Sieber, D. Wells, and T. Wolfe, "Research Investigations on Mechanical Properties of Nickel and Cobalt-Base Alloys for Inclusion in Military Handbook-5," AD-418639, March 1963.

[7] G. D. Sandrock, R.L. Ashbrook, and J.C. Freche, "Effect of Variations in Silicon and Iron Content on Embrittlement of a Cobalt-Base Alloy (L-605)," NASA-TN-D-2989, September 1965.

[8] H. Conrad, E. Barnett, and J. White, "Correlation and Interpretation of High Temperature Mechanical Properties of Certain Superalloys," pp. 1-9 to 1-29 in Joint International Conference on Creep, The Institute of Mechanical Engineers, London, 1963.

[9] P. N. Flagella and W. L. McCullough, "Stress-Rupture and Creep Behavior of Haynes Alloy No. 25 at 1440, 1700, and 2000°F in Air," TID-24045 (GE-NMP-67-181 AD-468683), June 1965.

[10] N. Yukawa and K. Sato, "The Correlation between Microstructure and Stress-Rupture Properties of a Co-Cr-Ni-W (HS-25) Alloy," pp. 680-686 in Proceedings of the International Conference on the Strength of Metals and Alloys, The Japan Institute of Metals, Omachi, Japan, 1968.

[11] R. Widmer, J. M. Dhosi, A Mullendore, and N. J. Grant, "Mechanisms Associated with Long Time Creep Phenomena," Part I, AFML-TR-65-181 (AD-468683), June 1965.

[12] R. Widmer, J.M. Dhosi, and N.J. Grant, "Mechanisms Associated with Long Time Creep Phenomena," Part II, AFML-TR-65-181 (AD-815679), March 1967.

[13] S.T. Wlodek, "Embrittlement of a Co-Cr-W (L-605) Alloy," Trans. ASM, American Society for Metals, 56, 287-303, 1963.

[14] D.T. Bourgette, "Effect of Aging Time and Temperature on the Impact and Tensile Behavior of L-605 – A Cobalt Base Alloy," ORNL-TM-3734, Oak Ridge National Laboratory, Oak Ridge, TN, 1973.

[15] H.E. McCoy and D.T. Bourgette, "Influence of Aging on the Impact Properties of Hastelloy N, Haynes Alloy No. 25, and Haynes Alloy No. 188," ORNL-TM-4380, Oak Ridge National Laboratory, Oak Ridge, TN. 1973.

[16] J. P. Hammond, "Effect of Long-Term Aging at 815°C on the Tensile Properties and Microstructural Stability of Four Cobalt- and Nickel-Base Superalloys," ORNL-5174, Oak Ridge National Laboratory, Oak Ridge, TN, 1976.

[17] J. P. Shingledecker, L. Riester. ORNL/CF-05/10, Oak Ridge National Laboratory, Oak Ridge, TN, 2005.

[18] M. Radovic, E. Lara-Curzio, L. Riester. "Comparison of different experimental techniques for determination of elastic properties of solids." *Materials Science and Engineering A*. A386 (2004) 56-70.

[19] "Haynes® 25 alloy Product Brochure." H-3057D, 2004 Haynes, Intl., www.haynesintl.com.

[20] D. A Porter, K. E. Easterling. Phase Transformations in Metals and Alloys. Chapman & Hall, London, 1992.

[21] C. McKamey, E. George. "Mechanical Properties of Haynes Alloy 25 Before and After Aging at 550-850°C." *Attachment to letter No. 0706-14-05, J.F.King to John Dowicki, July 8, 2005.*

[22] I.Finnie and W. R. Heller. Creep of Engineering Materials. McGraw-Hill 1959. 182-184.

[23] R. K. Penny, D .L. Marriott. Design for Creep. 1995 Chapman & Hall, London, UK.

[24] *Boiler Materials for Ultrasupercritical Coal Power Plants – Task 8, An Overview of Reference Stress Approach,* NETL/DOE/OCDO, 2003. USC T-6.

[25] J. D. Fishburn. "A Single Technically Consistent Design Formula for the Thickness of Cylindrical Sections Under Internal Pressure." *Proceedings of 2005 ASME Pressure Vessels and Piping Division Conference, July 17-21, Denver, CO USA*. PVP2005-71026.

[26] T. H. Courtney. Mechanical Behavior of Materials. 2nd Ed. McGraw-Hill 2000.

[27] F. R. N. Nabarro, H. L. deVilliers. The Physics of Creep. Taylor & Francis Ltd 1995.

[28] W.D. Klopp. Aerospace Structural Metals Handbook. L-605, CODE 4302, March 1986. 1-37.

[29] M. Tanaka, H. Iizuka, M. Tagami. "Effects of grain-boundary configuration on the high-temperature creep strength of cobalt-base L-605 alloys." *Journal of Materials Science* 24 (1989) 2421-2428.

[30] M. Tanaka, H. Iizuka "Effects of high-temperature ageing on the creep-rupture properties of cobalt-base L-605 alloys." *Journal of Materials Science* 25 (1990) 5199-5206.

APPENDIX A. DATA TABLES AND FIGURES

The appendix has eight sections. The first four sections (A.1-A.4) contain the tabular elastic, tensile, creep, and rupture data produced during this program (Haynes alloy 25 heat # 1860-8-1391). The fifth and sixth sections (A.5, A.6) contain the stress-strain and the creep strain versus time curves used to generate the tabular data in the previous sections. The final two sections (A.7 and A.8) contain the historical tensile and creep data used throughout the report; these data are based largely on the work of Swindeman [2].

A.1 TABULAR ELASTIC PROPERTIES

Table A.1.1. Elastic properties of Haynes alloy 25 (Heat # 1860-8-1391) before and after aging at 675°C for 6,000 hours

RUS Measured Properties of HS-25								
	Unaged				Aged 6,000 hours 675°C			
Temperature (°C)	Elastic Modulus (GPa)	Shear Modulus (GPa)	Bulk Modulus (GPa)	Poisson's Ratio	Elastic Modulus (GPa)	Shear Modulus (GPa)	Bulk Modulus (GPa)	Poisson's Ratio
25	234.7	90.6	190.8	0.295	241.5	93.5	192.7	0.291
150	225.1	86.3	191.0	0.304	232.1	89.5	190.4	0.297
300	213.4	81.6	185.2	0.308	220.7	84.6	187.7	0.304
500	199.4	75.4	186.6	0.322	204.0	77.6	184.1	0.315
650	184.3	69.5	176.2	0.326	185.6	70.0	177.8	0.326
800	169.6	63.6	169.2	0.333	173.3	65.1	170.7	0.331
900	160.4	59.7	169.5	0.342	162.4	60.4	173.8	0.344
1000	151.2	56.1	166.6	0.349	153.0	56.7	169.3	0.349
1100	143.0	52.8	163.3	0.354	143.3	52.9	163.2	0.354

Note 1: Measurement made by Resonant Ultrasound Spectroscopy (RUS)

A.2 TABULAR TENSILE PROPERTIES

Table A.2.1. Tensile properties of Haynes alloy 25 (Heat # 1860-8-1391)

Test ID	Product Form	Aging Temp (°C)	Aging Time (hours)	Test Temp (°C)	Prop Limit (MPa)	Yield Strength (MPa)	Ultimate Tensile Strength (MPa)	Uniform Elong (%)	Elong (%)	Red of Area (%)	Failure Location
TT-BM-01	Sheet	none	none	23	272	499	1000	56 6	56 6	39 9	GL
TT-BM-02	Sheet	none	none	300	196	308	884	72 5	74 9	56 6	GL
TT-BM-03	Sheet	none	none	500	165	276	806	64 6	68 7	54 4	GL
TT-BM-04	Sheet	none	none	650	218	261	778	54 1	57 2	35 1	GL
TT-BM-05	Sheet	none	none	800	167	232	477	26 2	59 1	41 6	GL
TT-BM-06	Sheet	none	none	1000	65	163	167	3 8	88 5	69 2	GL
TT-BM-07	Sheet	none	none	1100	27	86	92	1 7	70 4	61 7	GL
TT-BM-08	Sheet	675	6000	23	365	789	1053	7 3	7 3	4 4	GL, GM
TT-BM-08B	Sheet	675	6000	23	549	792	1045	8 4	8 4	5 8	GL
TT-BM-09	Sheet	675	6000	300	379	610	955	13 7	13 7	13 8	GL
TT-BM-10	Sheet	675	6000	500	421	558	945	17 3	17 3	16 1	GL
TT-BM-11	Sheet	675	6000	650	338	516	907	21 3	21 3	14 7	GL
TT-BM-12	Sheet	675	6000	800	269	445	565	3 6	17 3	16 6	GL
TT-BM-13	Sheet	675	6000	1000		178	179		45 2	39 0	GL
TT-BM-14	Sheet	675	6000	1100	62	101	101		47 9	32 9	GL
TT-BM-15	Sheet	675	12000	23	483	778	1043	7 9	7 9	8 1	GL
TT-BM-16	Sheet	675	12000	300	379	585	969	14 3	14 3	13 8	GL
TT-BM-17	Sheet	675	12000	500	331	566	938	16 1	16 1	18 0	GL
TT-BM-18	Sheet	675	12000	650	276	536	897	17 3	17 3	17 5	GL
TT-BM-19	Sheet	675	12000	800	221	414	553	3 5	9 8	10 3	GL
TT-BM-20	Sheet	675	12000	1000	83	174	175	2 0	52 4	45 2	GL
TT-BM-21	Sheet	675	12000	1100	48	99	99	0 4	45 8	45 0	GL
HS-03-01a	Sheet	none	none	23	386	518	978	56 0	57 5	45 6	GL
HS-03-02a	Sheet	675	0 25	23	524	537	978	61 0	62 0	47 4	GL
HS-03-07a	Sheet	675	2 4	23	462	532	1009	63 0	68 2	52 4	GL
HS-03-05a	Sheet	675	24	23	476	536	1008	62 0	67 8	50 8	GL
HS-03-09a	Sheet	675	100	23	434	552	969	53 0	53 5	53 4	GL
HS-03-03a	Sheet	675	240	23	421	536	970	38 0	38 4	26 3	GL
HS-03-01b	Sheet	675	1000	23	510	744	1047	20 9	20 9	17 4	GL
HS-03-01a	Sheet	675	2000	23	496	756	1017	9 8	9 8	10 7	GL
HS-03-08a	Sheet	675	2 4	650	207	260	776	56 6	56 6	37 9	GL
HS-03-06a	Sheet	675	24	650	207	280	795	61 4	61 4	39 4	GL
HS-03-04a	Sheet	675	240	650	221	328	818	44 2	44 2	38 0	GL
HS-03-02b	Sheet	675	1000	650	345	445	837	38 6	38 6	28 6	GL
HS-03-02a	Sheet	675	2000	650	345	568	891	23 6	23 6	22 9	GL
HS-03-10a	Sheet	700	1000	23	503	744	1066	16 1	16 1	14 6	GL
HS-03-11a	Sheet	750	1000	23	441	587	1014	19 6	19 6	18 3	GL

*Failure Location GL=gauge length, GM=gauge mark, WM=weld metal, BM=base metal, HAZ=heat affected zone

Table A.2.2. Tensile properties of Haynes alloy 25 GTA weldments

Test ID	Product Form	Aging Temp (°C)	Aging Time (hours)	Test Temp (°C)	Prop Limit (MPa)	Yield Strength (MPa)	Ultimate Tensile Strength (MPa)	Uniform Elong (%)	Elong (%)	Red of Area (%)	Failure Location
TT-WM-01	Sheet Weld	none	none	23		496	1008	50 0	50 0	40 7	BM
TT-WM-02	Sheet Weld	none	none	300	219	307	888	70 0	74 5	57 1	BM
TT-WM-03	Sheet Weld	none	none	500	196	289	809	66 2	72 5	51 7	BM
TT-WM-04	Sheet Weld	none	none	650	191	279	768	49 7	49 7	32 4	BM
TT-WM-05	Sheet Weld	none	none	800	153	245	480	22 5	50 0	45 7	BM
TT-WM-06	Sheet Weld	none	none	1000	90	165	170	4 0	72 8	62 0	BM
TT-WM-07	Sheet Weld	none	none	1100	54	94	96	1 5	53 0	58 7	BM
TT-WM-08	Sheet Weld	675	6000	23	552	762	1004	5 6	5 6	5 2	BM
TT-WM-09	Sheet Weld	675	6000	300	448	601	936	12 8	12 8	13 2	BM
TT-WM-10	Sheet Weld	675	6000	500	372	542	927	16 3	16 3	15 0	BM
TT-WM-11	Sheet Weld	675	6000	650	241	549	895	16 7	16 7	17 5	BM
TT-WM-12	Sheet Weld	675	6000	800		402	554	7 2	13 4	18 3	BM
TT-WM-13	Sheet Weld	675	6000	1000	83	174	177	0 5	47 3	45 2	BM
TT-WM-14	Sheet Weld	675	6000	1100	48	99	99	0 5	44 5	45 5	BM
TT-WM-15	Sheet Weld	675	12000	23	414	753	1009	5 0	5 0	6 3	BM
TT-WM-16	Sheet Weld	675	12000	300	372	615	926	7 6	7 8	8 4	BM
TT-WM-17	Sheet Weld	675	12000	500	310	564	918	12 0	12 0	13 3	BM
TT-WM-18	Sheet Weld	675	12000	650	310	572	899	11 0	11 0	12 2	BM
TT-WM-19	Sheet Weld	675	12000	800	193	438	562	2 8	8 7	10 9	BM
TT-WM-20	Sheet Weld	675	12000	1000		171	172	0 3	38 6	37 1	BM
TT-WM-21	Sheet Weld	675	12000	1100		101	101	0 3	43 8	33 4	BM
LWT-1	Bar Weld	none	none	20		595	1147	629 0	63 1		WM
AWT-1	Bar Weld	none	none	20		593	1122	53 7	56 8		WM
LWT-2	Bar Weld	none	none	650		330	736	25 5	26 2		WM
AWT-2	Bar Weld	none	none	650		367	851	47 7	47 4		WM
LWT-3	Bar Weld	850	50	20		533	1012	30 0	30 0		WM
AWT-3	Bar Weld	850	50	20		559	1051	37 2	37 3		WM
LWT-4	Bar Weld	850	50	650		538	831	31 7	31 7		WM
AWT-4	Bar Weld	850	50	650		352	873	49 2	49 3		WM
LWT-5	Bar Weld	675	6000	20		822	1058	4 5	4 5		BM
AWT-5	Bar Weld	675	6000	20		634	1073	4 3	4 3		BM
LWT-6	Bar Weld	675	6000	650		575	929	11 8	11 8		BM
AWT-6	Bar Weld	675	6000	650		564	931	15 1	15 4		BM

*Failure Location GL=gauge length, GM=gauge mark, WM=weld metal, BM=base metal, HAZ=heat affected zone

A.3 TABULAR UNIAXIAL CREEP AND CREEP-RUPTURE DATA

Table A.3.1. Creep and stress-rupture data for Haynes alloy 25 (Heat # 1860-8-1391)

Test ID	Product Form	Aging Temp. (°C)	Aging Time (hours)	Test Temp. (°C)	Stress (MPa)	Rupture Life (hours) *stopped or ongoing*	Minimum Creep Rate (%/hr)	Elong. (%)	Red. of Area (%)
CR-BM-01	sheet	none	none	650	206.8	38557.0	2.60E-05	2.8	4.5
CR-BM-02	sheet	none	none	700	165.5	20637.0	1.00E-05	4.9	3.9
CR-BM-03	sheet	none	none	750	127.6	8786.0	5.30E-04	10.9	8.3
CR-BM-04	sheet	none	none	800	99.3	4983.0	8.50E-04	11.5	10.2
CR-BM-05	sheet	none	none	800	103.4	3626.0	1.10E-03	12.8	12.2
CR-BM-06	sheet	none	none	850	62.1	8975.0	1.30E-04	6.9	2.7
CR-BM-07	sheet	none	none	875	53.8	5763.0	1.90E-04	7.0	5.0
CR-BM-08	sheet	none	none	900	44.8	6232.0	2.70E-04	12.0	8.4
CR-BM-09	sheet	none	none	900	42.7	6585.0	1.50E-04	6.1	5.7
CR-BM-11*	sheet	none	none	925	34.5	6253.0	*2.70E-04*	10.6	8.8
CR-BM-12*	sheet	none	none	925	33.1	7436.8	*1.70E-04*	9.0	6.5
CR-BM-14*	sheet	none	none	950	29.0	4095.0	*3.60E-04*	8.1	9.3
TN30440	sheet	none	none	750	220.6	498.4	3.90E-02	33.6	25.2
TN29885	sheet	none	none	800	186.2	144.4	1.70E-01	45.3	47.6
TN30215	sheet	none	none	750	217.2	436.8	4.90E-02	32.0	32.7
TN30420	sheet	none	none	850	151.7	57.6	3.60E-01	46.7	48.3
TN30138	sheet	none	none	750	193.1	745.0	1.60E-02	21.3	19.7
MG-13	sheet	none	none	600	179.3	*9000.0*	1.8E-05		
MG-14	sheet	none	none	600	206.8	12311.0	2.0E-05		
MG-15	sheet	none	none	625	144.8	*30000.0*	1.3E-05		
MG-17	sheet	none	none	625	206.8	12614.0	2.1E-05		
MG-18	sheet	none	none	650	124.1	10507.0	4.5E-05		
MG-21	sheet	none	none	650	186.2	11080.0	4.2E-05		
MG-22	sheet	none	none	675	103.4	11117.0	4.2E-06		
MG-24	sheet	none	none	675	151.7	*38000.0*	1.6E-05		
MG22b	sheet	none	none	675	103.4	15976.0	5.5E-06		
				675	0.0	16262.0			
				675	103.4	20591.0	5.70E-06		
				700	103.4	22892.0	6.80E-06		
				725	103.4	24496.0	2.10E-05		
				700	103.4	25574.0	1.10E-05		
				675	103.4	39841.0	6.30E-06		
				675	117.2	*42000.0*	8.70E-06		

** Testing was performed in Argon, load line displacement was used to estimate minimum creep rate*

Table A.3.1. Creep and stress-rupture data for Haynes alloy 25 (continued)

Test ID	Product Form	Aging Temp. (°C)	Aging Time (hours)	Test Temp. (°C)	Stress (MPa)	*Rupture Life (hours) stopped or ongoing*	Minimum Creep Rate (%/hr)	Elong. (%)	Red. of Area (%)
CR-BM-15	sheet	675	6000	650	206.8	*38300.0*	2.50E-05		
CR-BM-16	sheet	675	6000	700	165.5	20670	6.90E-05	3.8	3.1
CR-BM-17	sheet	675	6000	750	127.6	9536	3.90E-05	5.8	4.8
CR-BM-18	sheet	675	6000	800	99.3	8863	1.90E-04	9.3	7.1
CR-BM-19	sheet	675	6000	800	103.4	4626	3.00E-04	6.9	6.4
CR-BM-20	sheet	675	6000	850	62.1	6092	1.30E-04	4.2	1.2
CR-BM-22	sheet	675	6000	900	44.8	6105	1.60E-04	11.0	5.1

Table A.3.2. Creep* and stress-rupture data for Haynes alloy 25 weldments (Heat # 1860-8-1391)

Test ID	Product Form	Aging Temp. (°C)	Aging Time (hours)	Test Temp. (°C)	Stress (MPa)	Rupture Life (hours) stopped or ongoing	Minimum Creep Rate (%/hr)	Elong. (%)	Red. of Area (%)	Failure Location
CR-WM-01	sheet weld	none	none	650	206.8	21532	3.48E-04	3.3	1.7	BM
CR-WM-02	sheet weld	none	none	700	165.5	21339.3	3.45E-05	4.4	1.9	BM
CR-WM-03	sheet weld	none	none	750	127.6	9588	3.50E-04	8.1	9.6	BM
CR-WM-04	sheet weld	none	none	800	99.3	6620	4.40E-04	6.7	10.3	BM
CR-WM-05	sheet weld	none	none	800	103.4	4550	8.40E-04	9.2	5.4	BM
CR-WM-06	sheet weld	none	none	850	62.1	8710	1.20E-04	6.5	4.1	BM
CR-WM-07	sheet weld	none	none	875	53.8	6000	1.30E-04			
CR-WM-08	sheet weld	none	none	900	44.8	4372	2.50E-04	5.2	1.2	BM
CR-WM-09	sheet weld	none	none	900	42.7	6470	1.30E-04	9.8	7.2	BM
MG-01	sheet weld	none	none	600	179.3	32128	1.5E-05			
MG-03	sheet weld	none	none	625	144.8	32440	4.5E-06			
MG-06	sheet weld	none	none	650	124.1	11782	1.4E-05			
MG-09	sheet weld	none	none	650	186.2	10292	7.0E-05			
MG-10	sheet weld	none	none	675	103.4	11295	4.6E-06			
CR-WM-15	sheet weld	675	6000	650	206.8	32136	1.30E-05	2.6	2.1	BM
CR-WM-16	sheet weld	675	6000	700	165.5	16896	3.10E-05	1.8	1.0	HAZ
CR-WM-17	sheet weld	675	6000	750	127.6	11990	8.10E-05	4.5	3.1	BM
CR-WM-18	sheet weld	675	6000	800	99.3	8568	1.30E-04			BM
CR-WM-19	sheet weld	675	6000	800	103.4	4011	2.60E-04	4.2	6.2	BM
CR-WM-20	sheet weld	675	6000	850	62.1	11117	1.10E-04	5.2	2.4	BM
LWC-8	bar weld	none	none	650	206.8	8326.0				
LWC-9	bar weld	none	none	800	103.4	6464.1	6.34E-04	11.2	27.3	BM
AWC-7	bar weld	none	none	650	124.1	8326.0	7.12E-06			
AWC-8	bar weld	none	none	650	206.8	8186.0	7.99E-05			
AWC-9	bar weld	none	none	800	103.4	5718.9	5.71E-04	14.5	19.2	BM

**Note: Min. Creep Rate is based on displacement of a 2" specimen gauge length with a GTAW weldment in the center of the gauge*

A.4 TABULAR PRESSURIZED TUBE RUPTURE DATA

Table A.4.1. Rupture data for Haynes alloy 25 pressurized creep tests on tubes

Test ID	Diameter : thickness ratio	Aging Temp (°C)	Aging Time (hours)	Temperature (°C)	Pressure (psi)	Rupture Life (hours) *Ongoing*	Rupture Location	Hoop Strain at Failure (%)
LTP-1	10.76	none	none	675	5,000	*22114.0*	*In Test*	
LTP-2	10.76	none	none	750	3,645	11147.8	Tube	7.1
PB-IM-01	10.76	none	none	750	4,700	2707.6	Tube	13.8
PB-IM-02	10.76	none	none	750	5,400	958.4	Tube	12.6
PB-IM-03	10.76	none	none	750	6,200	383.0	Tube	18.9
PB-IM-04	10.76	none	none	800	3,500	1550.2	Weld	11.8
PB-IM-05	10.76	none	none	800	4,500	328.8	Tube	26.4
PB-IM-06	10.76	none	none	800	5,200	138.1	Tube	38.2
PB-IM-07	10.76	none	none	850	2,500	1071.0	Weld	6.0
PB-IM-08	10.76	none	none	850	3,500	199.8	Tube	30.7
PB-IM-09	10.76	none	none	850	4,300	43.8	Tube	38.6
PB-IM-10	10.76	none	none	950	1,200	432.2	End Cap	9.8
PB-IM-11	10.76	none	none	950	1,800	147.2	Tube	42.4
PB-IM-12	10.76	none	none	950	2,400	19.4	Tube	56.2
LTS-1	13.15	none	none	675	5,000	21002.0	Tube	
LTS-2	13.15	none	none	700	5,000	*2000.0*	*In Test*	
PB-OM-01	13.15	none	none	750	5,400	426.3	Tube	21.9
PB-OM-02	13.15	none	none	800	4,500	125.7	Tube	38.9
PB-OM-03	13.15	none	none	850	3,500	65.0	Tube	38.4
PB-OM-04	13.15	675	6000	750	4,700	2880.0	Tube	2.9
PB-OM-05	13.15	675	6000	750	5,400	1143.3	Tube	1.6
PB-OM-06	13.15	675	6000	750	6,200	495.8	Tube	2.5
PB-OM-07	13.15	675	6000	800	3,500	545.9	Tube	12.3
PB-OM-08	13.15	675	6000	800	4,500	92.1	Tube	22.1
PB-OM-09	13.15	675	6000	800	5,200	50.3	Tube	24.0
PB-OM-10	13.15	675	6000	850	2,500	459.9	Tube	19.0
PB-OM-11	13.15	675	6000	850	3,500	57.8	Tube	23.5
PB-OM-12	13.15	675	6000	850	4,300	15.2	Tube	32.6
PB-OM-13	13.15	675	6000	950	1,200	404.5	Tube	14.0
PB-OM-14	13.15	675	6000	950	1,800	60.4	Tube	18.0
PB-OM-15	13.15	675	6000	950	2,400	9.1	Tube	29.3

A.5 STRESS-STRAIN CURVES

Test ID	Product Form	Aging Temp. (°C)	Aging Time (hours)	Test Temp. (°C)	Prop. Limit (MPa)	Yield Strength (MPa)	Ultimate Tensile Strength (MPa)	Uniform Elong. (%)	Elong. (%)	Red. of Area (%)	Failure Location
TT-BM-01	Sheet	none	none	23	272	499	1000	56.6	56.6	39.9	GL

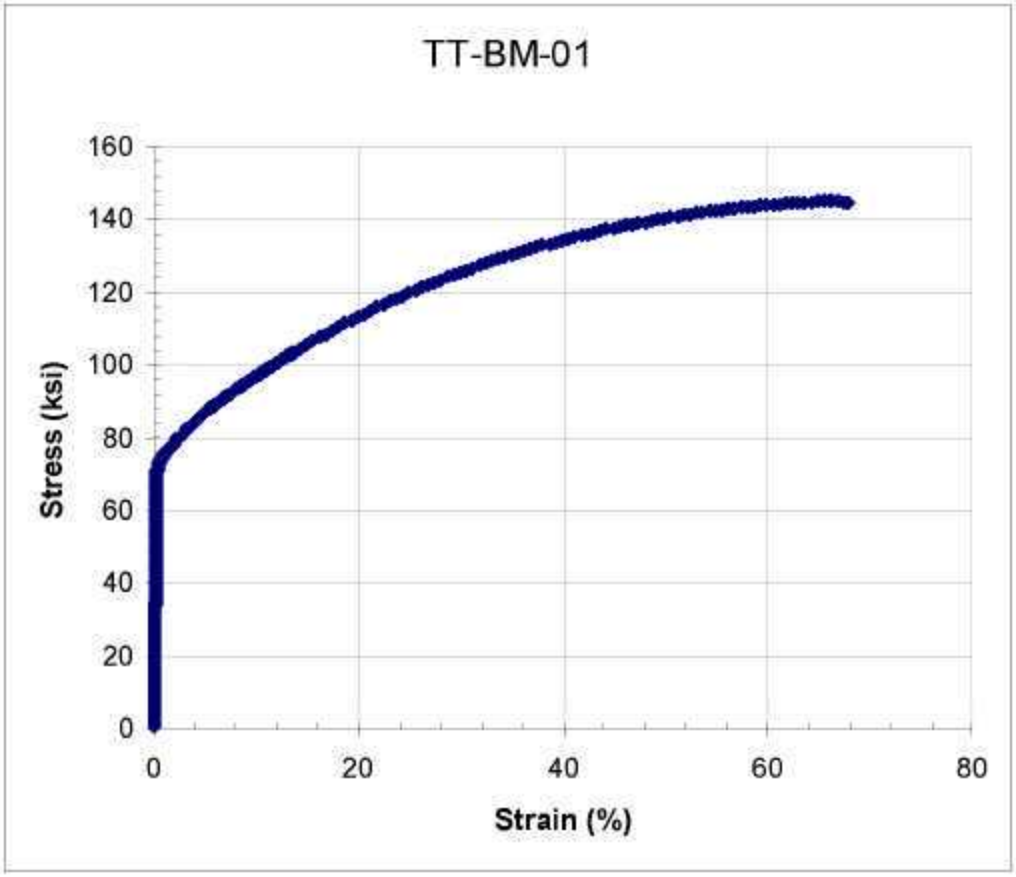

Test ID	Product Form	Aging Temp. (°C)	Aging Time (hours)	Test Temp. (°C)	Prop. Limit (MPa)	Yield Strength (MPa)	Ultimate Tensile Strength (MPa)	Uniform Elong. (%)	Elong. (%)	Red. of Area (%)	Failure Location
TT-BM-02	Sheet	none	none	300	196	308	884	72.5	74.9	56.6	GL

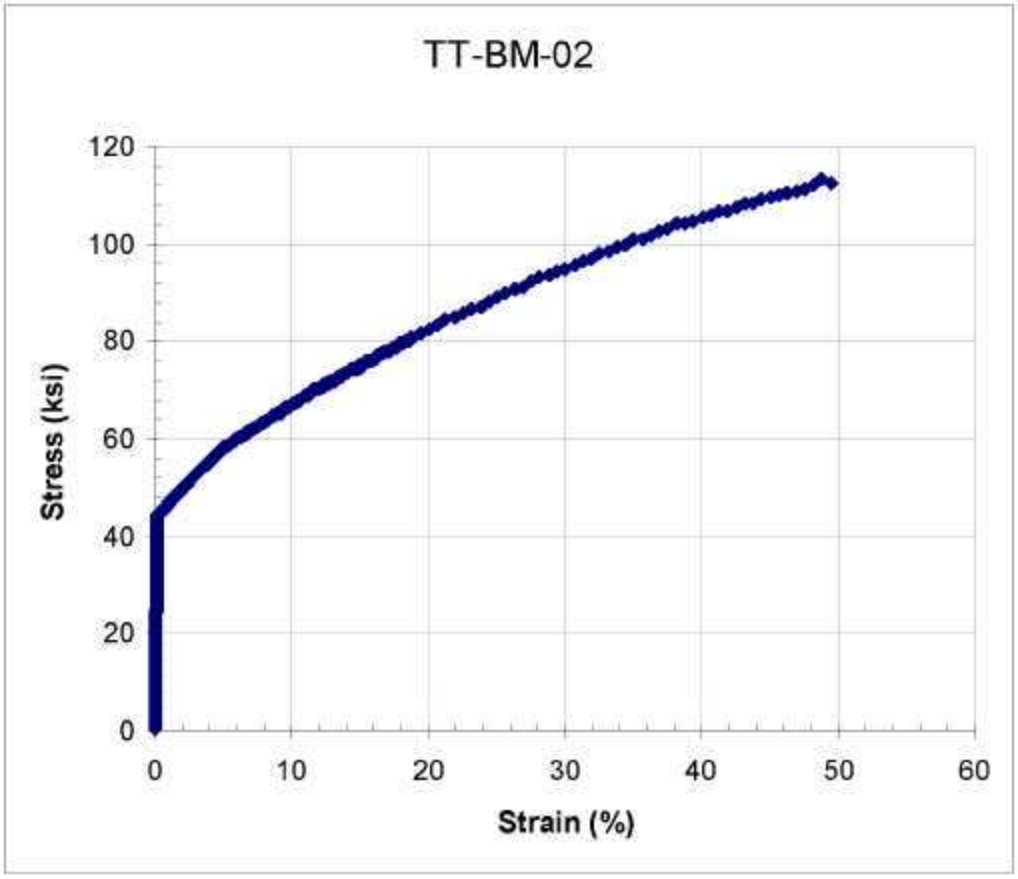

Test ID	Product Form	Aging Temp. (°C)	Aging Time (hours)	Test Temp. (°C)	Prop. Limit (MPa)	Yield Strength (MPa)	Ultimate Tensile Strength (MPa)	Uniform Elong. (%)	Elong. (%)	Red. of Area (%)	Failure Location
TT-BM-03	Sheet	none	none	500	165	276	806	64.6	68.7	54.4	GL

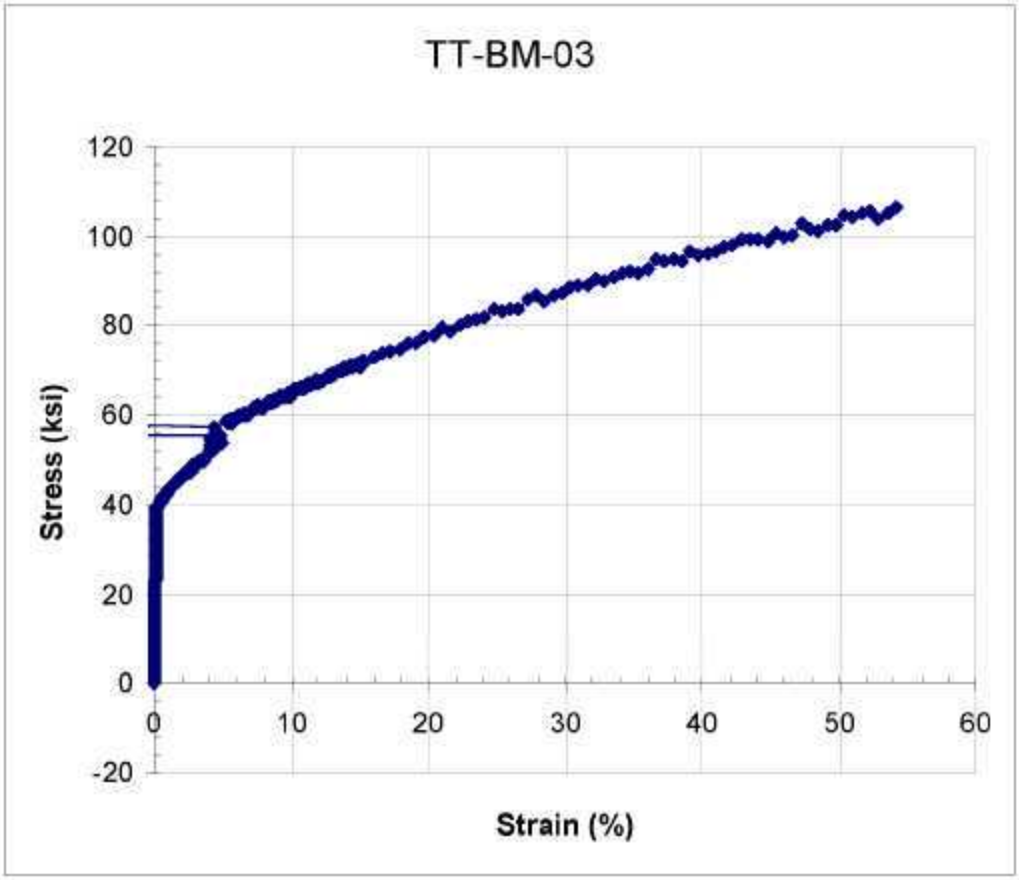

Test ID	Product Form	Aging Temp. (°C)	Aging Time (hours)	Test Temp. (°C)	Prop. Limit (MPa)	Yield Strength (MPa)	Ultimate Tensile Strength (MPa)	Uniform Elong. (%)	Elong. (%)	Red. of Area (%)	Failure Location
TT-BM-04	Sheet	none	none	650	218	261	778	54.1	57.2	35.1	GL

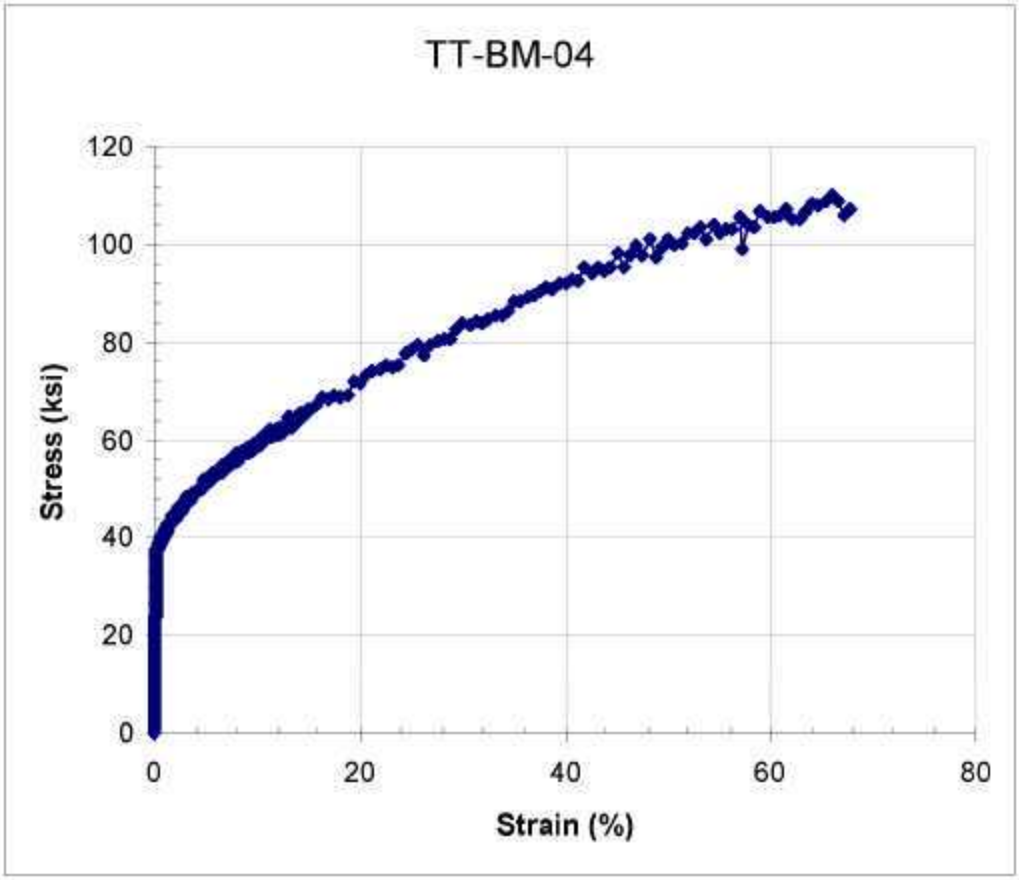

Test ID	Product Form	Aging Temp. (°C)	Aging Time (hours)	Test Temp. (°C)	Prop. Limit (MPa)	Yield Strength (MPa)	Ultimate Tensile Strength (MPa)	Uniform Elong. (%)	Elong. (%)	Red. of Area (%)	Failure Location
TT-BM-05	Sheet	none	none	800	187	232	477	26.2	59.1	41.6	GL

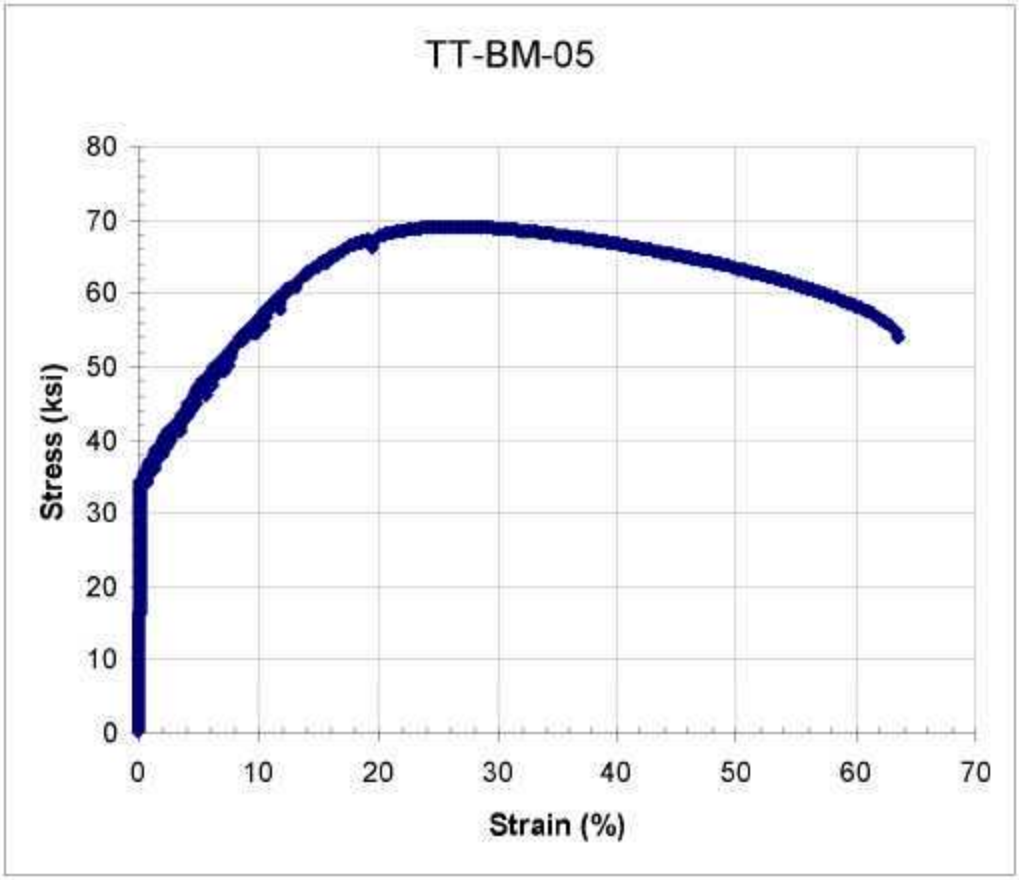

Test ID	Product Form	Aging Temp. (°C)	Aging Time (hours)	Test Temp. (°C)	Prop. Limit (MPa)	Yield Strength (MPa)	Ultimate Tensile Strength (MPa)	Uniform Elong. (%)	Elong. (%)	Red. of Area (%)	Failure Location
TT-BM-06	Sheet	none	none	1000	65	163	167	3.8	88.5	69.2	GL

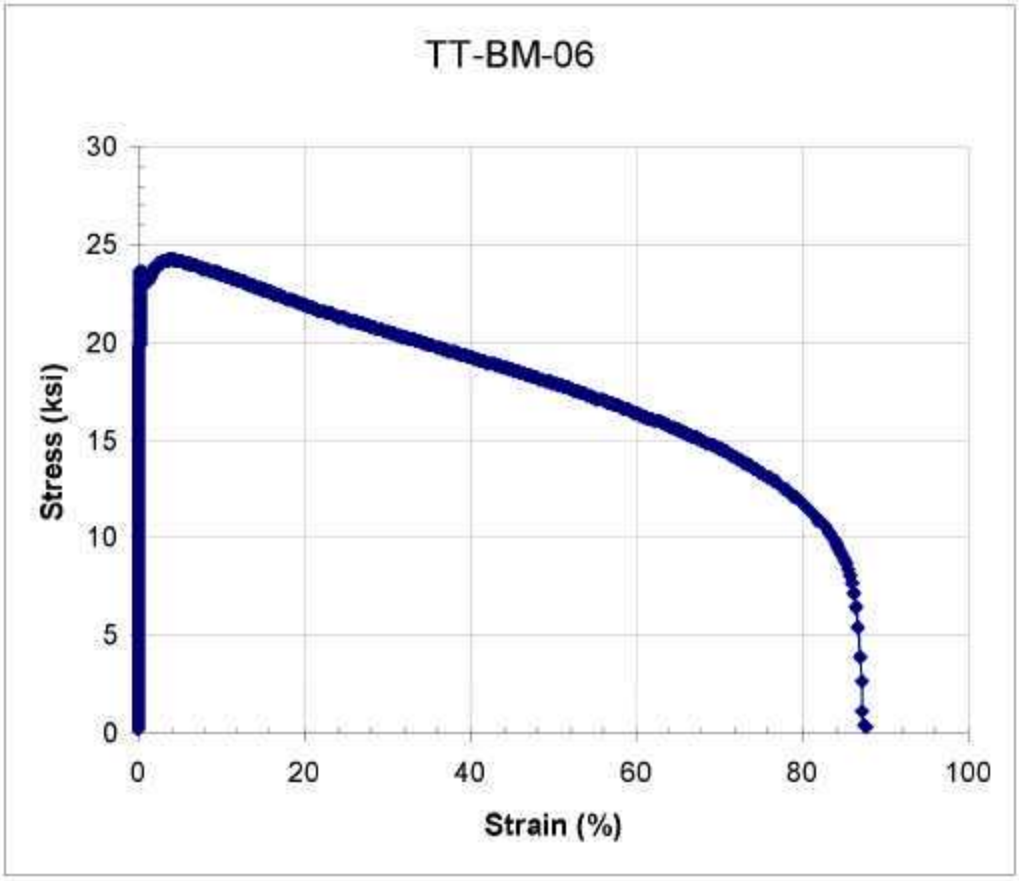

Test ID	Product Form	Aging Temp. (°C)	Aging Time (hours)	Test Temp. (°C)	Prop. Limit (MPa)	Yield Strength (MPa)	Ultimate Tensile Strength (MPa)	Uniform Elong. (%)	Elong. (%)	Red. of Area (%)	Failure Location
TT-BM-07	Sheet	none	none	1100	27	86	92	1.7	70.4	61.7	GL

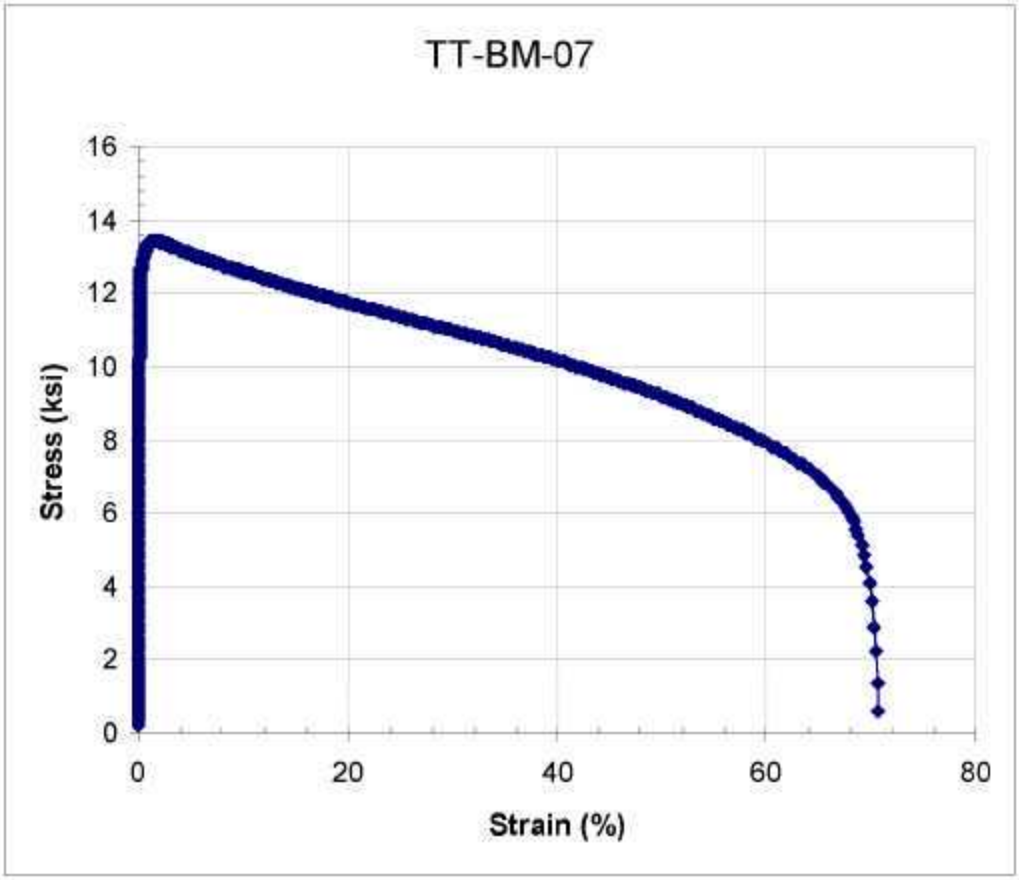

Test ID	Product Form	Aging Temp. (°C)	Aging Time (hours)	Test Temp. (°C)	Prop. Limit (MPa)	Yield Strength (MPa)	Ultimate Tensile Strength (MPa)	Uniform Elong. (%)	Elong. (%)	Red. of Area (%)	Failure Location
TT-BM-08	Sheet	675	6000	23	365	789	1053	7.3	7.3	4.4	GL, GM

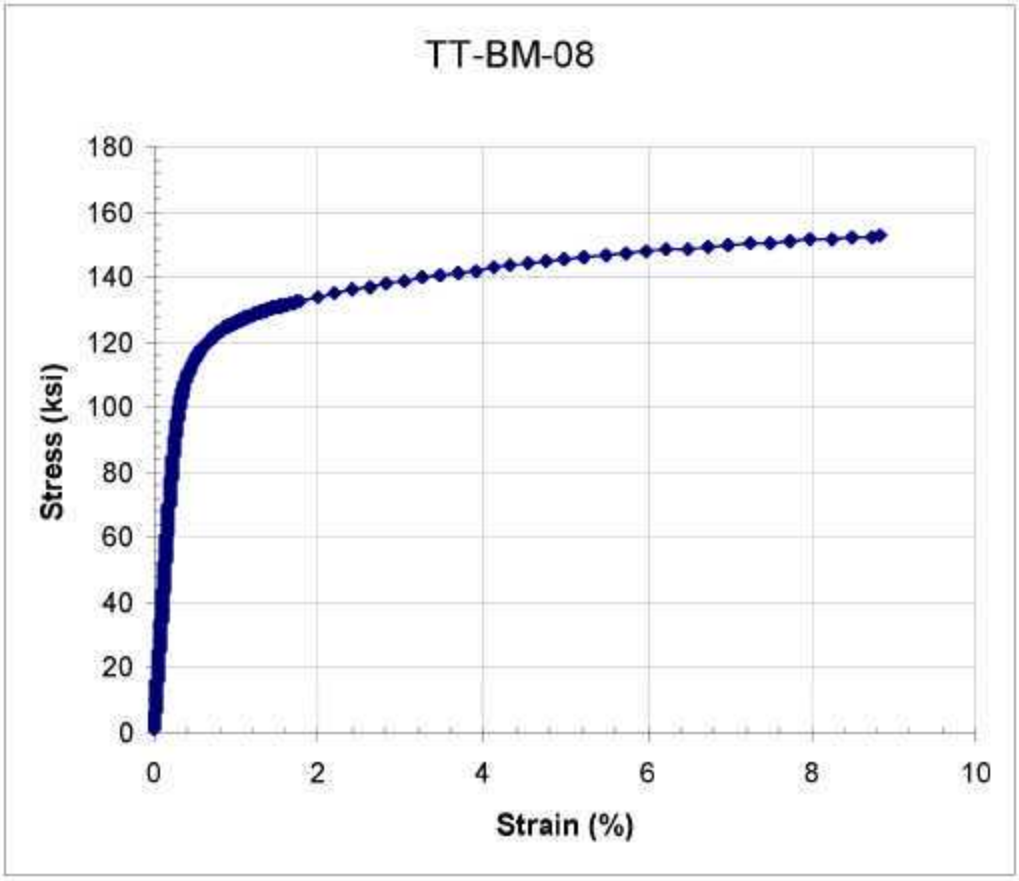

Test ID	Product Form	Aging Temp. (°C)	Aging Time (hours)	Test Temp. (°C)	Prop. Limit (MPa)	Yield Strength (MPa)	Ultimate Tensile Strength (MPa)	Uniform Elong. (%)	Elong. (%)	Red. of Area (%)	Failure Location
TT-BM-08B	Sheet	675	6000	23	549	792	1045	8.4	8.4	5.8	GL

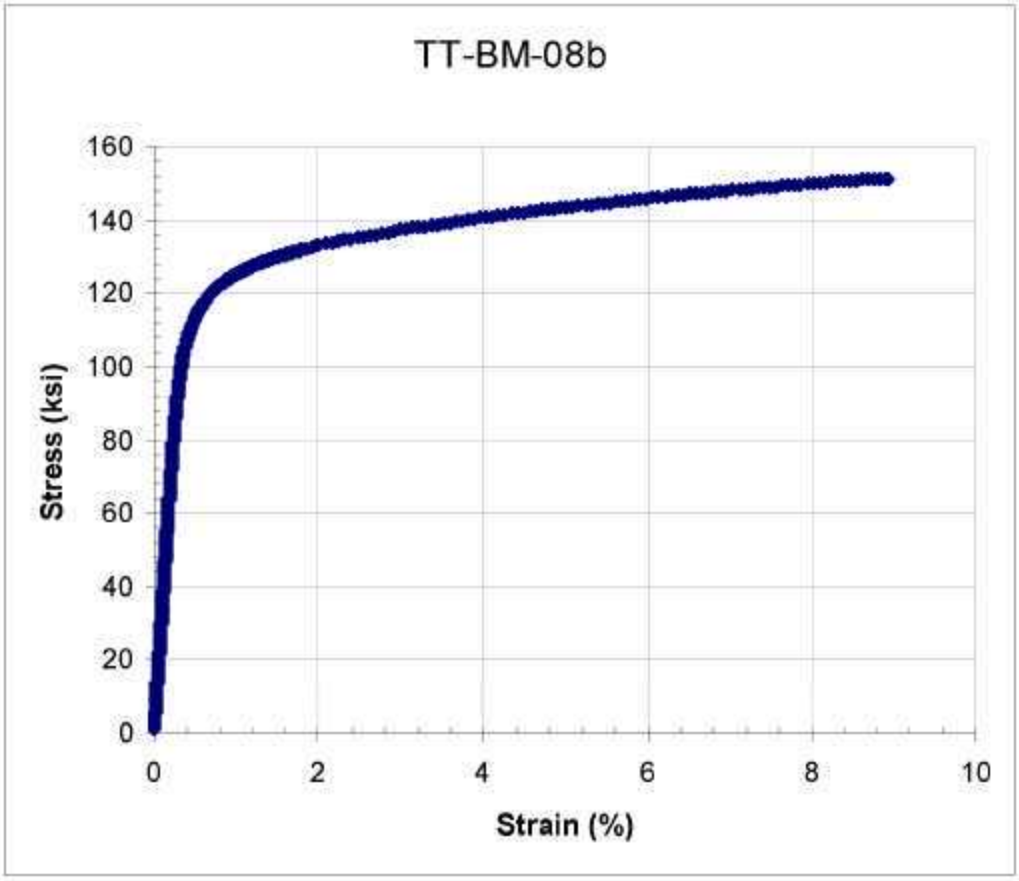

Test ID	Product Form	Aging Temp. (°C)	Aging Time (hours)	Test Temp. (°C)	Prop. Limit (MPa)	Yield Strength (MPa)	Ultimate Tensile Strength (MPa)	Uniform Elong. (%)	Elong. (%)	Red. of Area (%)	Failure Location
TT-BM-09	Sheet	675	6000	300	379	610	955	13.7	13.7	13.8	GL

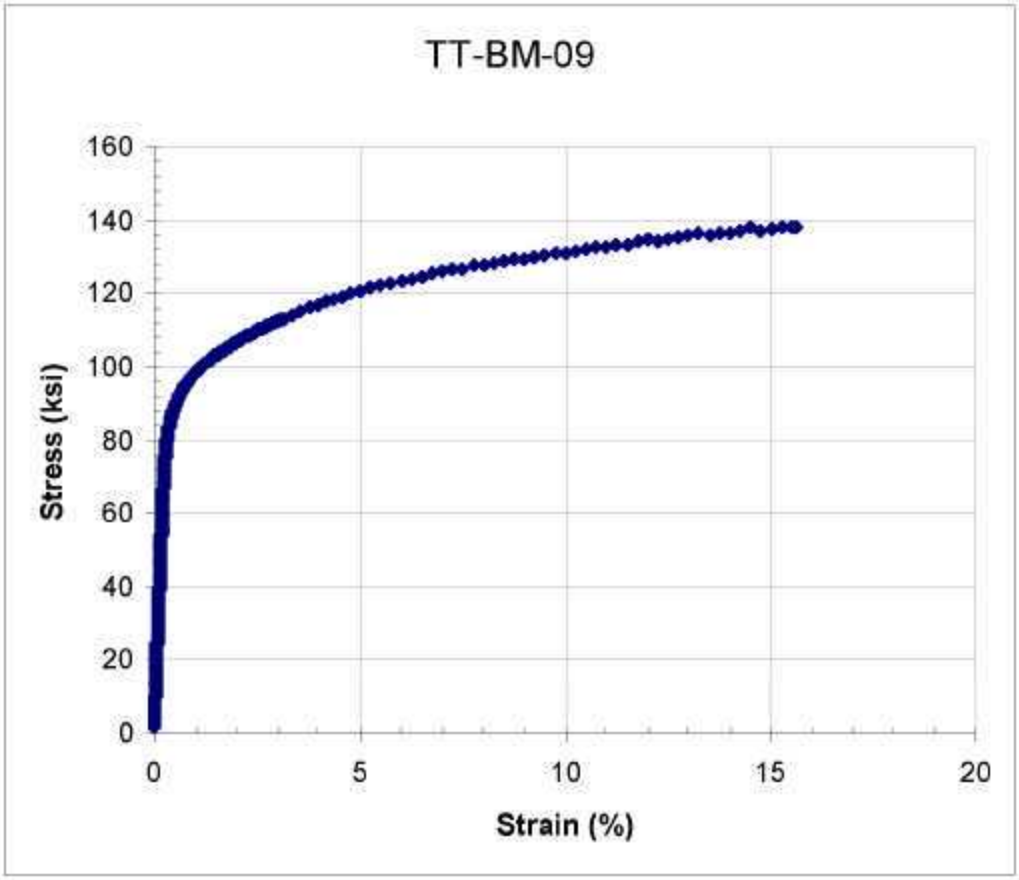

Test ID	Product Form	Aging Temp. (°C)	Aging Time (hours)	Test Temp. (°C)	Prop. Limit (MPa)	Yield Strength (MPa)	Ultimate Tensile Strength (MPa)	Uniform Elong. (%)	Elong. (%)	Red. of Area (%)	Failure Location
TT-BM-10	Sheet	675	6000	500	421	558	945	17.3	17.3	16.1	GL

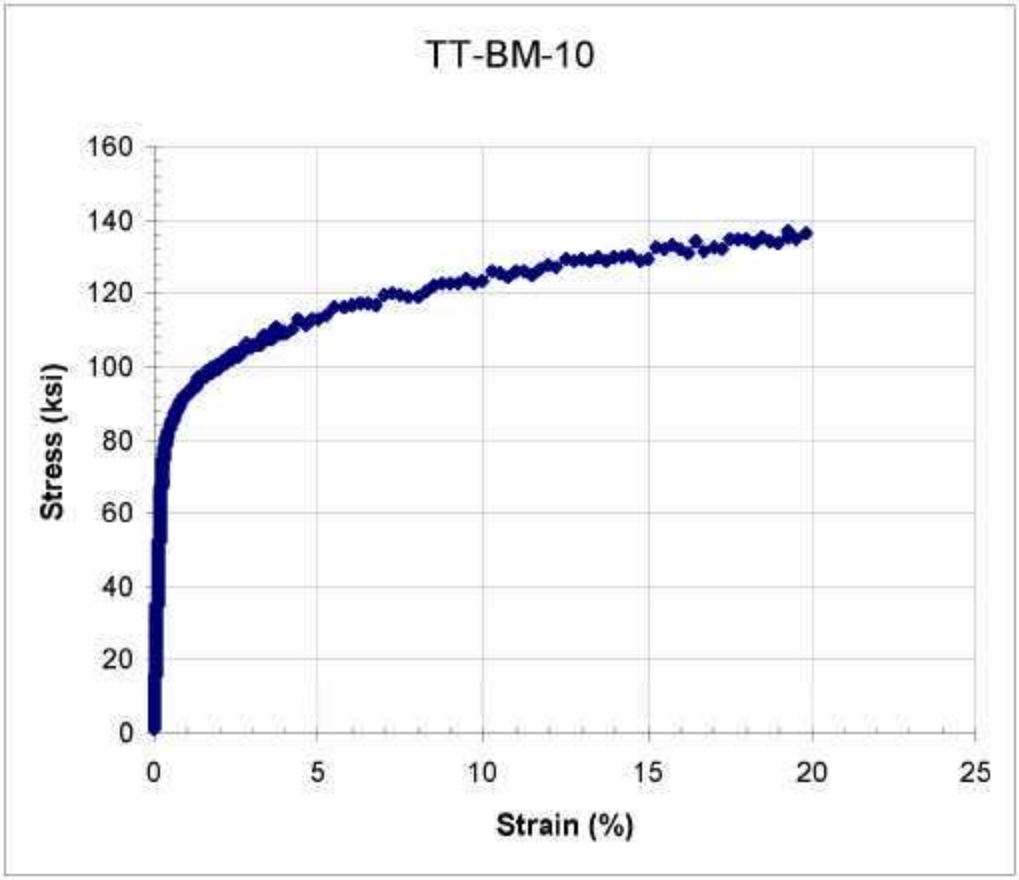

Test ID	Product Form	Aging Temp. (°C)	Aging Time (hours)	Test Temp. (°C)	Prop. Limit (MPa)	Yield Strength (MPa)	Ultimate Tensile Strength (MPa)	Uniform Elong. (%)	Elong. (%)	Red. of Area (%)	Failure Location
TT-BM-11	Sheet	675	6000	650	338	516	907	21.3	21.3	14.7	GL

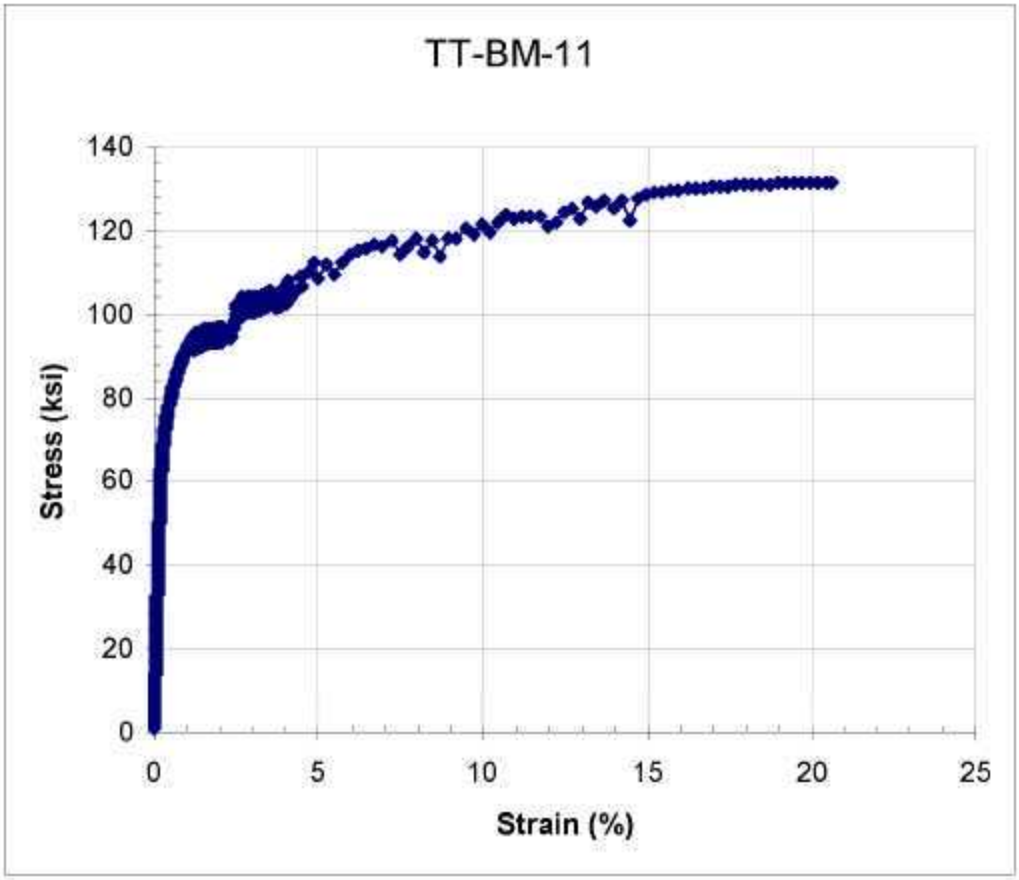

Test ID	Product Form	Aging Temp. (°C)	Aging Time (hours)	Test Temp. (°C)	Prop. Limit (MPa)	Yield Strength (MPa)	Ultimate Tensile Strength (MPa)	Uniform Elong. (%)	Elong. (%)	Red. of Area (%)	Failure Location
TT-BM-12	Sheet	675	6000	800	269	445	565	3.6	17.3	16.6	GL

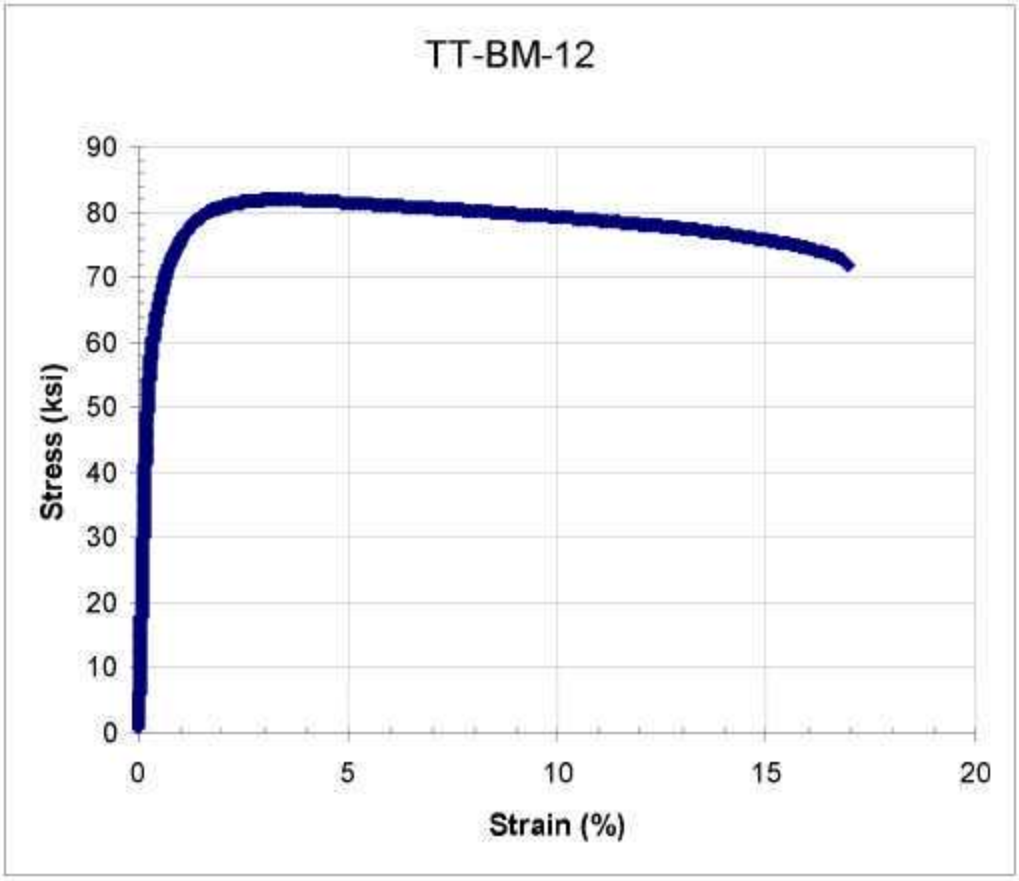

Test ID	Product Form	Aging Temp. (°C)	Aging Time (hours)	Test Temp. (°C)	Prop. Limit (MPa)	Yield Strength (MPa)	Ultimate Tensile Strength (MPa)	Uniform Elong. (%)	Elong. (%)	Red. of Area (%)	Failure Location
TT-BM-13	Sheet	675	6000	1000		178	179		45.2	39.0	GL

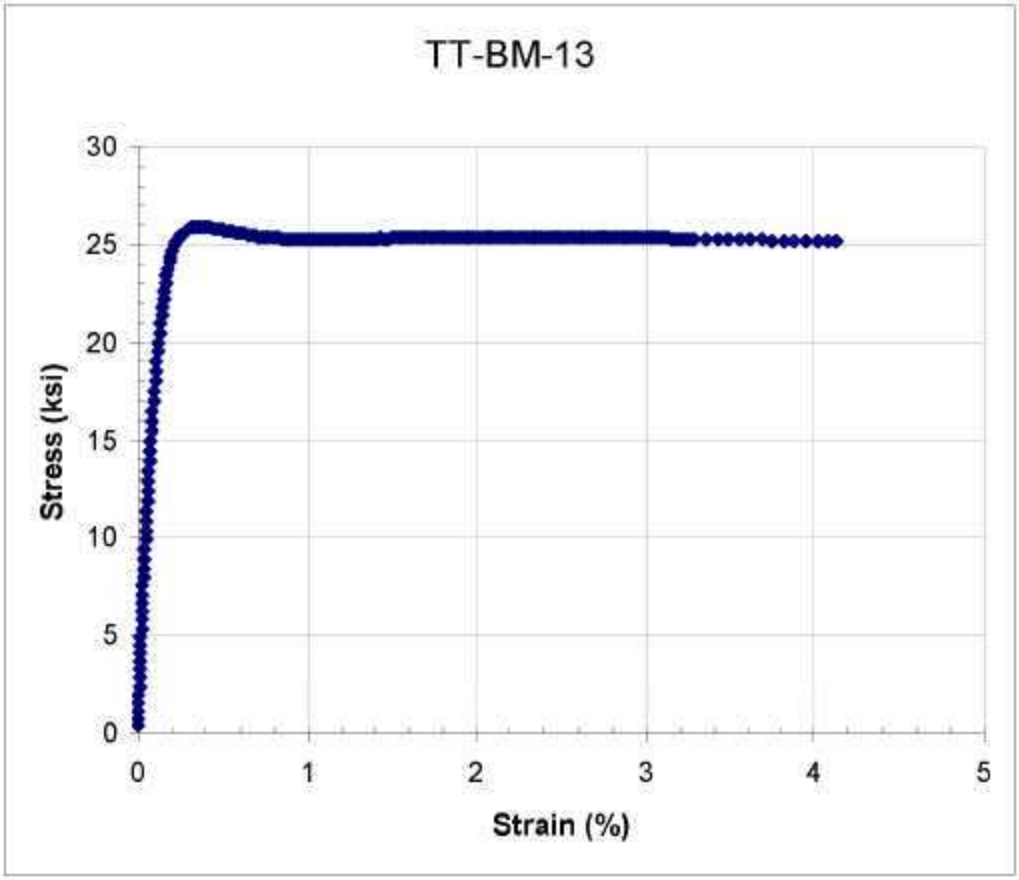

Test ID	Product Form	Aging Temp. (°C)	Aging Time (hours)	Test Temp. (°C)	Prop. Limit (MPa)	Yield Strength (MPa)	Ultimate Tensile Strength (MPa)	Uniform Elong. (%)	Elong. (%)	Red. of Area (%)	Failure Location
TT-BM-14	Sheet	675	6000	1100	62	101	101		47.9	32.9	GL

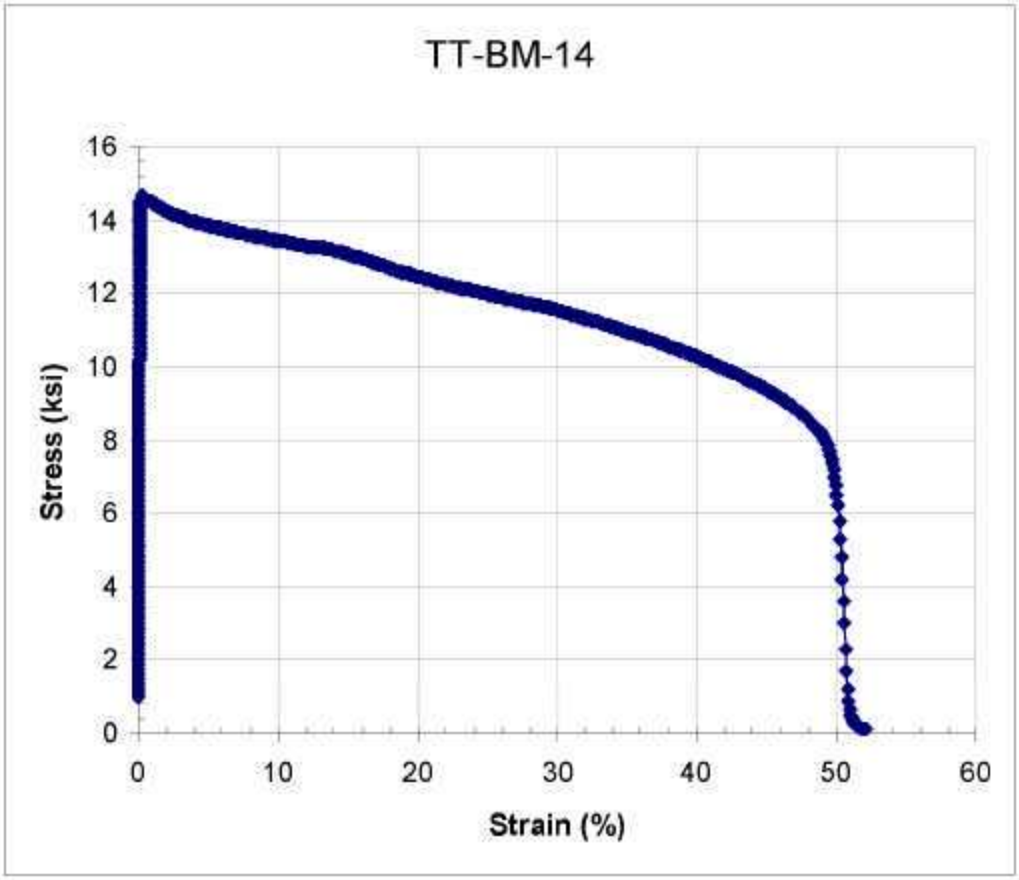

Test ID	Product Form	Aging Temp. (°C)	Aging Time (hours)	Test Temp. (°C)	Prop. Limit (MPa)	Yield Strength (MPa)	Ultimate Tensile Strength (MPa)	Uniform Elong. (%)	Elong. (%)	Red. of Area (%)	Failure Location
TT-BM-15	Sheet	675	12000	23	483	778	1043	7.9	7.9	8.1	GL

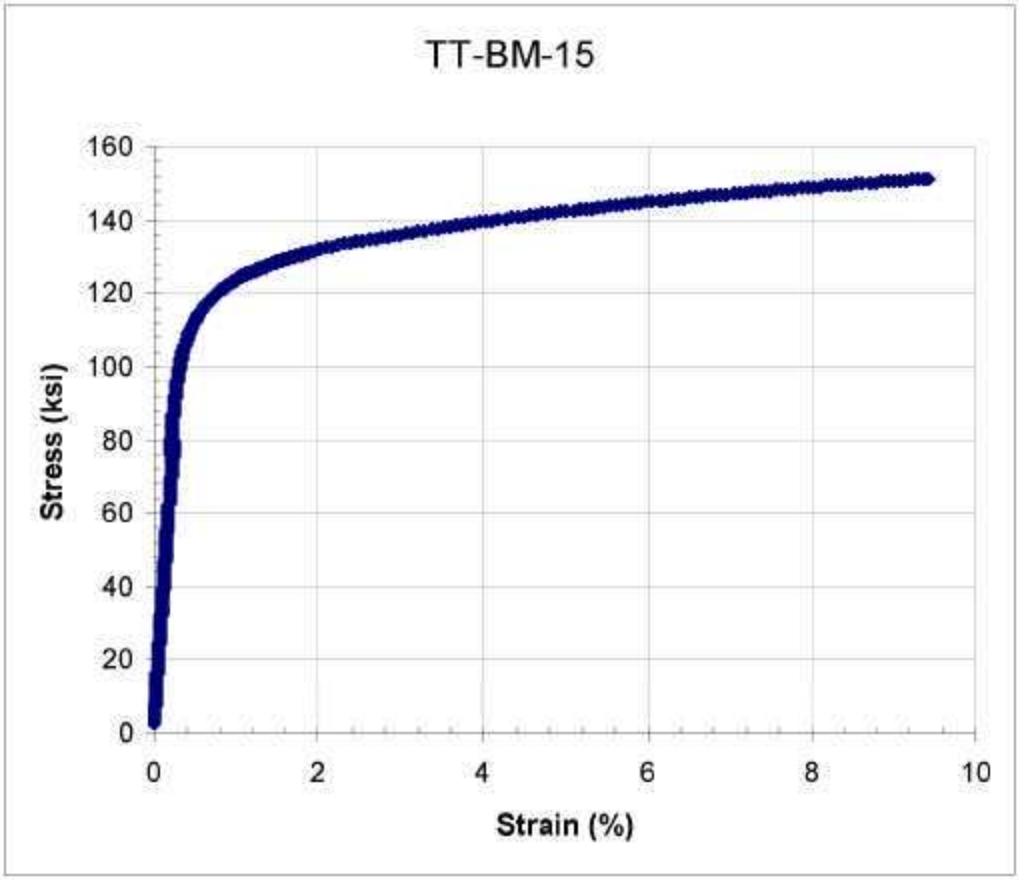

Test ID	Product Form	Aging Temp. (°C)	Aging Time (hours)	Test Temp. (°C)	Prop. Limit (MPa)	Yield Strength (MPa)	Ultimate Tensile Strength (MPa)	Uniform Elong. (%)	Elong. (%)	Red. of Area (%)	Failure Location
TT-BM-16	Sheet	675	12000	300	379	585	969	14.3	14.3	13.8	GL

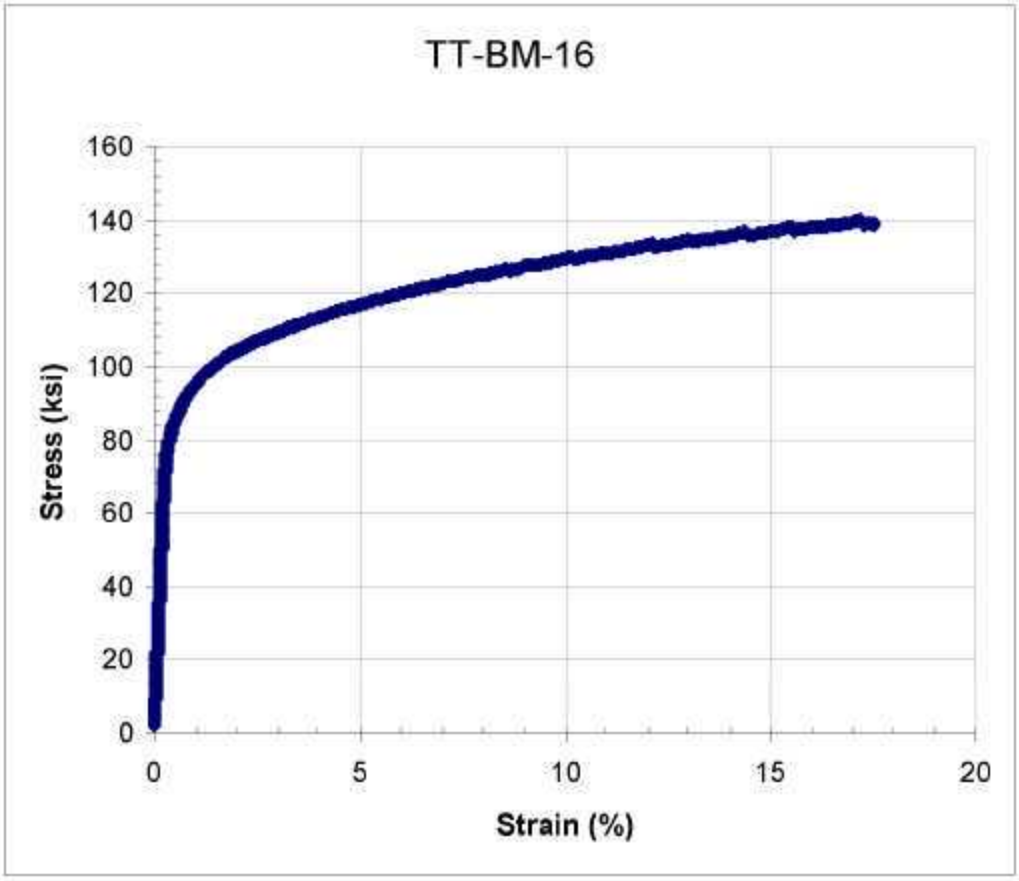

Test ID	Product Form	Aging Temp. (°C)	Aging Time (hours)	Test Temp. (°C)	Prop. Limit (MPa)	Yield Strength (MPa)	Ultimate Tensile Strength (MPa)	Uniform Elong. (%)	Elong. (%)	Red. of Area (%)	Failure Location
TT-BM-17	Sheet	675	12000	500	331	566	938	16.1	16.1	18.0	GL

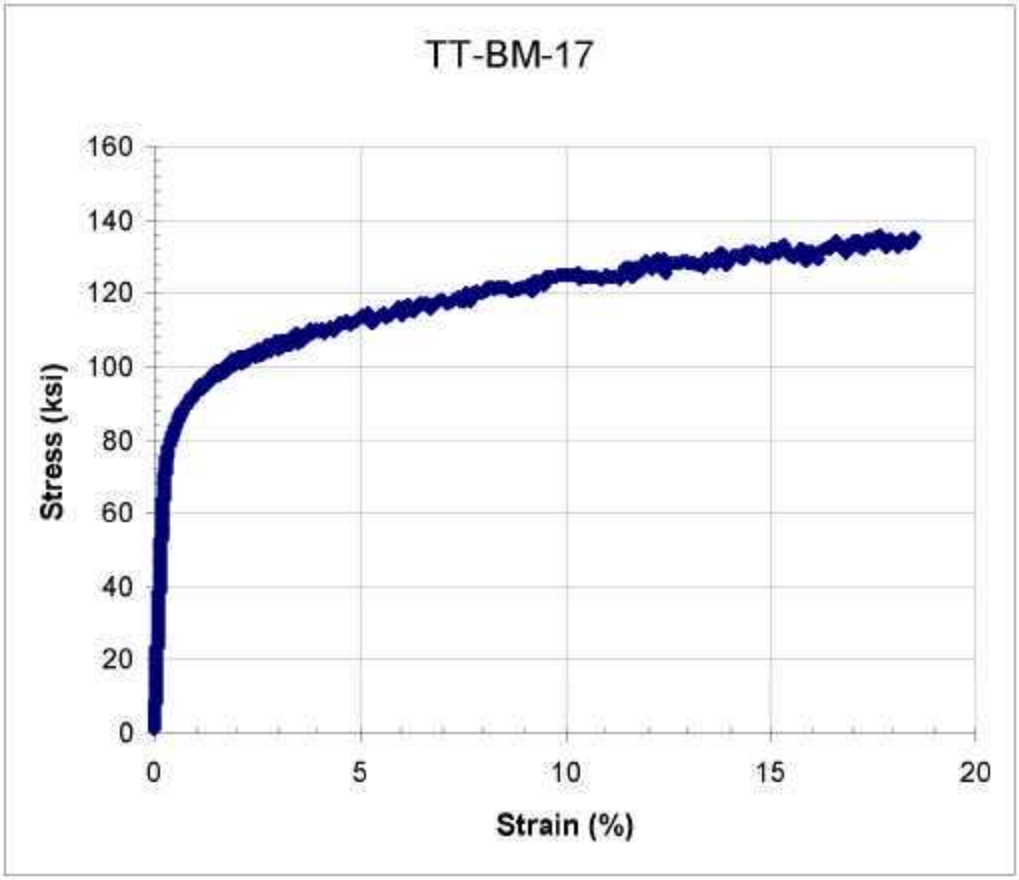

Test ID	Product Form	Aging Temp. (°C)	Aging Time (hours)	Test Temp. (°C)	Prop. Limit (MPa)	Yield Strength (MPa)	Ultimate Tensile Strength (MPa)	Uniform Elong. (%)	Elong. (%)	Red. of Area (%)	Failure Location
TT-BM-18	Sheet	675	12000	650	276	536	897	17.3	17.3	17.5	GL

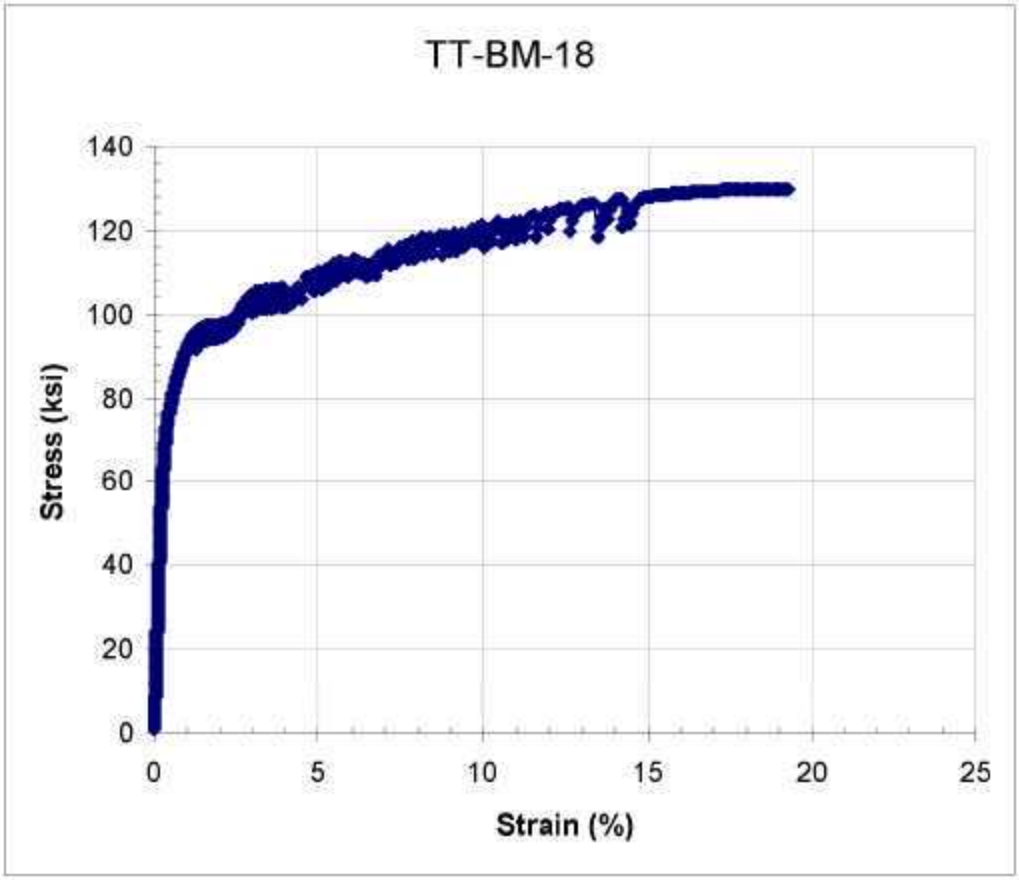

Test ID	Product Form	Aging Temp. (°C)	Aging Time (hours)	Test Temp. (°C)	Prop. Limit (MPa)	Yield Strength (MPa)	Ultimate Tensile Strength (MPa)	Uniform Elong. (%)	Elong. (%)	Red. of Area (%)	Failure Location
TT-BM-19	Sheet	675	12000	800	221	414	553	3.5	9.8	10.3	GL

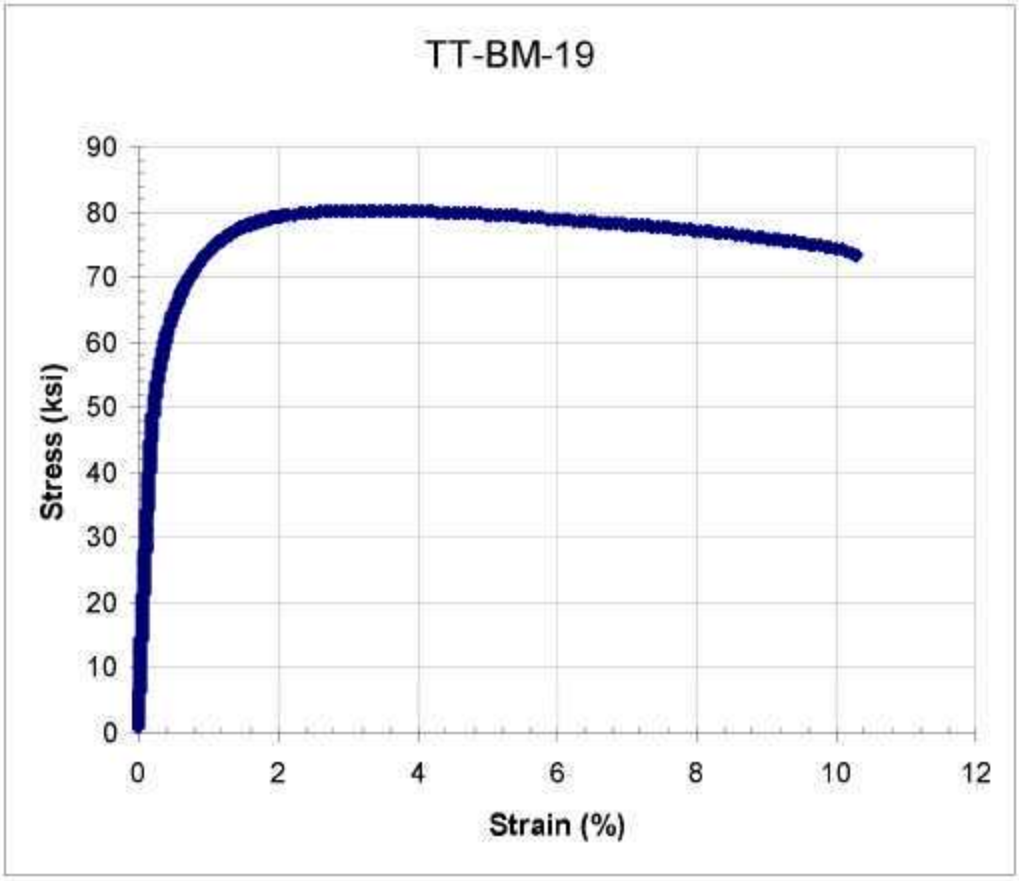

Test ID	Product Form	Aging Temp. (°C)	Aging Time (hours)	Test Temp. (°C)	Prop. Limit (MPa)	Yield Strength (MPa)	Ultimate Tensile Strength (MPa)	Uniform Elong. (%)	Elong. (%)	Red. of Area (%)	Failure Location
TT-BM-20	Sheet	675	12000	1000	83	174	175	2.0	52.4	45.2	GL

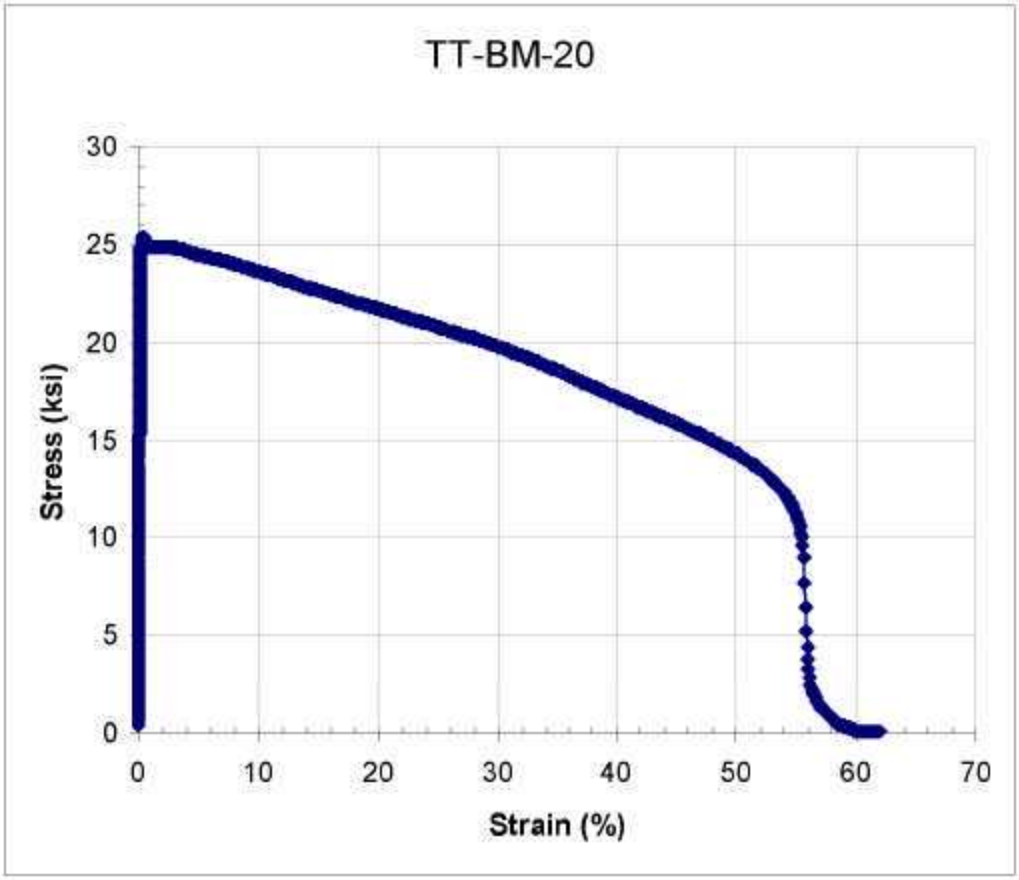

Test ID	Product Form	Aging Temp. (°C)	Aging Time (hours)	Test Temp. (°C)	Prop. Limit (MPa)	Yield Strength (MPa)	Ultimate Tensile Strength (MPa)	Uniform Elong. (%)	Elong. (%)	Red. of Area (%)	Failure Location
TT-BM-21	Sheet	675	12000	1100	48	99	99	0.4	45.8	45.0	GL

Test ID	Product Form	Aging Temp. (°C)	Aging Time (hours)	Test Temp. (°C)	Prop. Limit (MPa)	Yield Strength (MPa)	Ultimate Tensile Strength (MPa)	Uniform Elong. (%)	Elong. (%)	Red. of Area (%)	Failure Location
HS-03-07a	Sheet	675	2.4	23	462	532	1009	63.0	68.2	52.4	GL

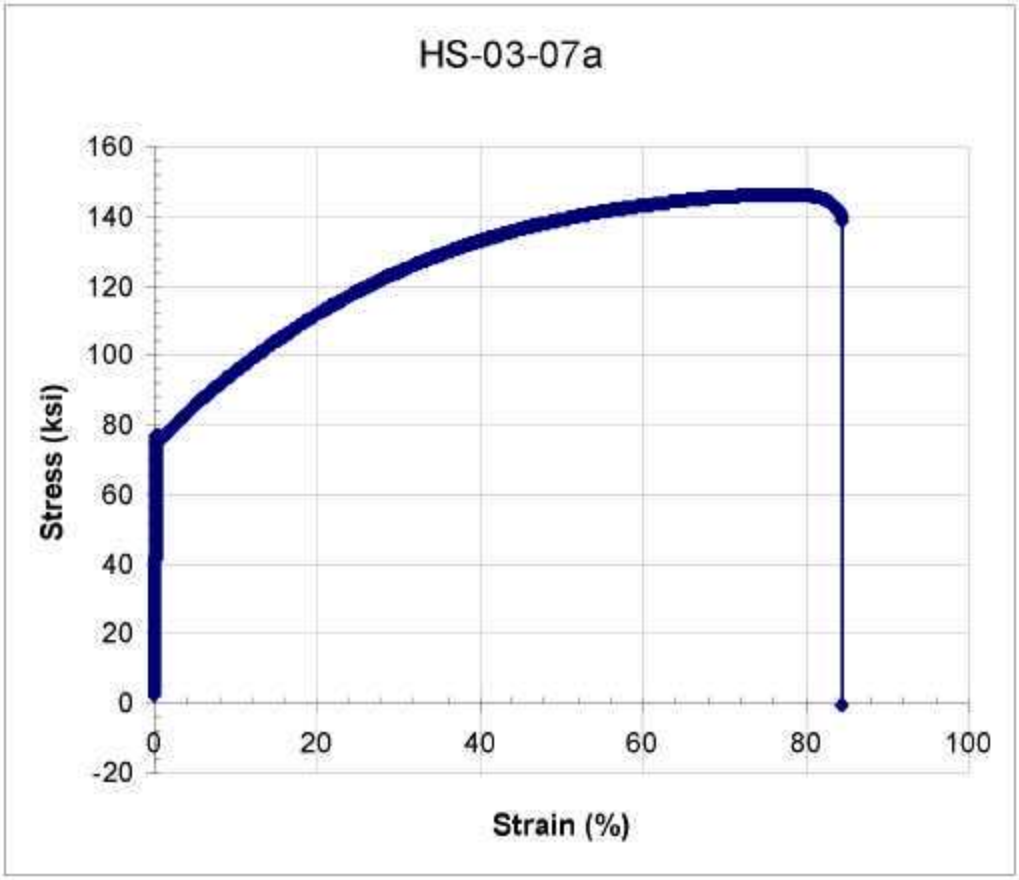

Test ID	Product Form	Aging Temp. (°C)	Aging Time (hours)	Test Temp. (°C)	Prop. Limit (MPa)	Yield Strength (MPa)	Ultimate Tensile Strength (MPa)	Uniform Elong. (%)	Elong. (%)	Red. of Area (%)	Failure Location
HS-03-05a	Sheet	675	24	23	476	536	1008	62.0	67.8	50.8	GL

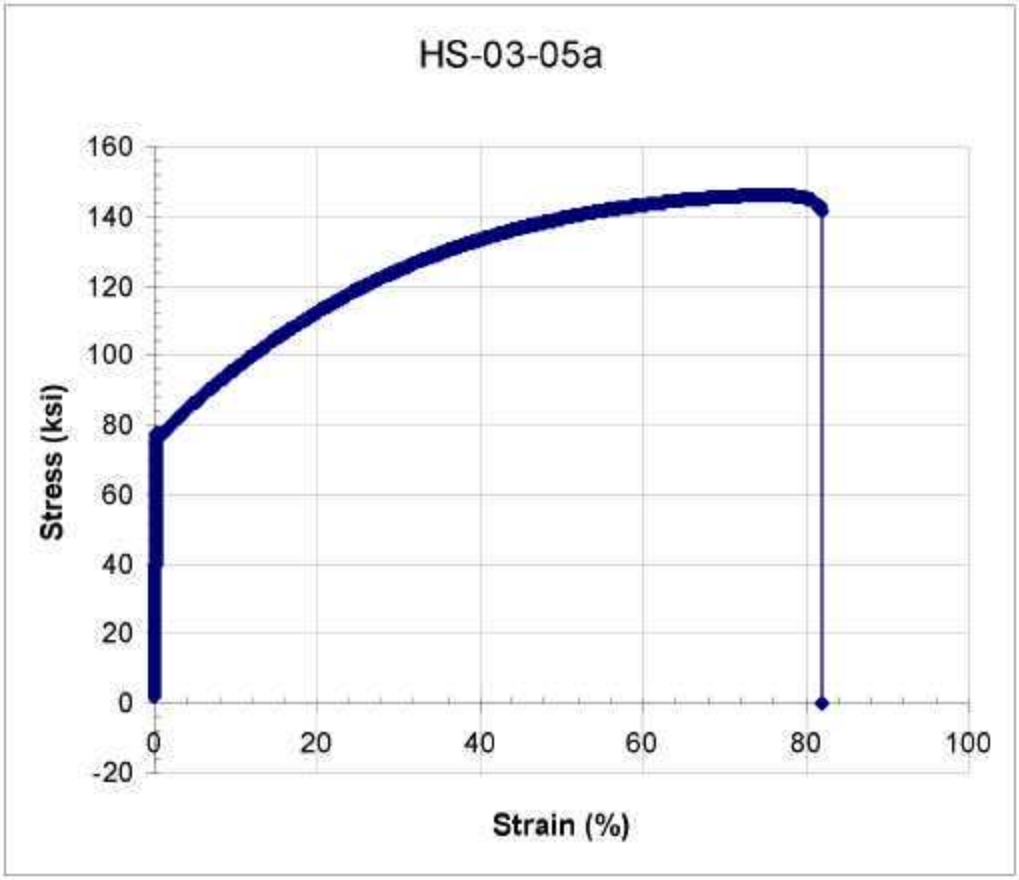

Test ID	Product Form	Aging Temp. (°C)	Aging Time (hours)	Test Temp. (°C)	Prop. Limit (MPa)	Yield Strength (MPa)	Ultimate Tensile Strength (MPa)	Uniform Elong. (%)	Elong. (%)	Red. of Area (%)	Failure Location
HS-03-03a	Sheet	675	240	23	421	536	970	38.0	38.4	26.3	GL

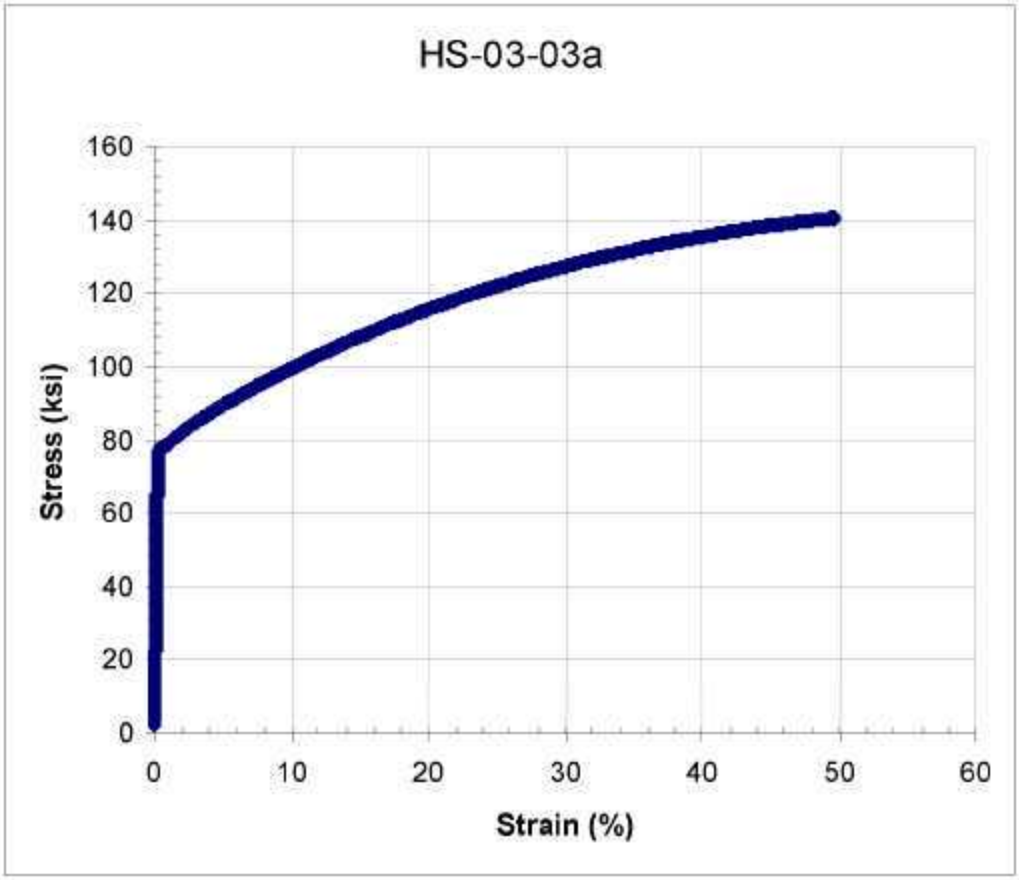

Test ID	Product Form	Aging Temp. (°C)	Aging Time (hours)	Test Temp. (°C)	Prop. Limit (MPa)	Yield Strength (MPa)	Ultimate Tensile Strength (MPa)	Uniform Elong. (%)	Elong. (%)	Red. of Area (%)	Failure Location
HS-03-01b	Sheet	675	1000	23	510	744	1047	20.9	20.9	17.4	GL

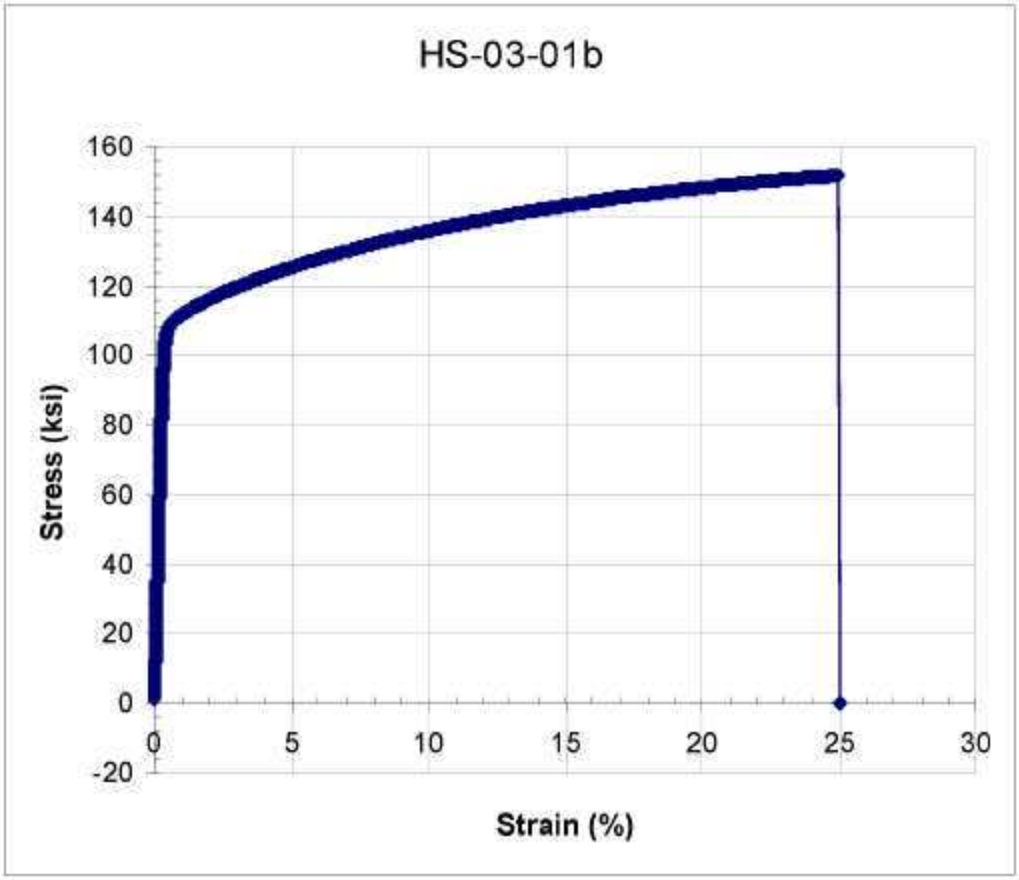

Test ID	Product Form	Aging Temp. (°C)	Aging Time (hours)	Test Temp. (°C)	Prop. Limit (MPa)	Yield Strength (MPa)	Ultimate Tensile Strength (MPa)	Uniform Elong. (%)	Elong. (%)	Red. of Area (%)	Failure Location
HS-03-01a	Sheet	675	2000	23	496	756	1017	9.8	9.8	10.7	GL

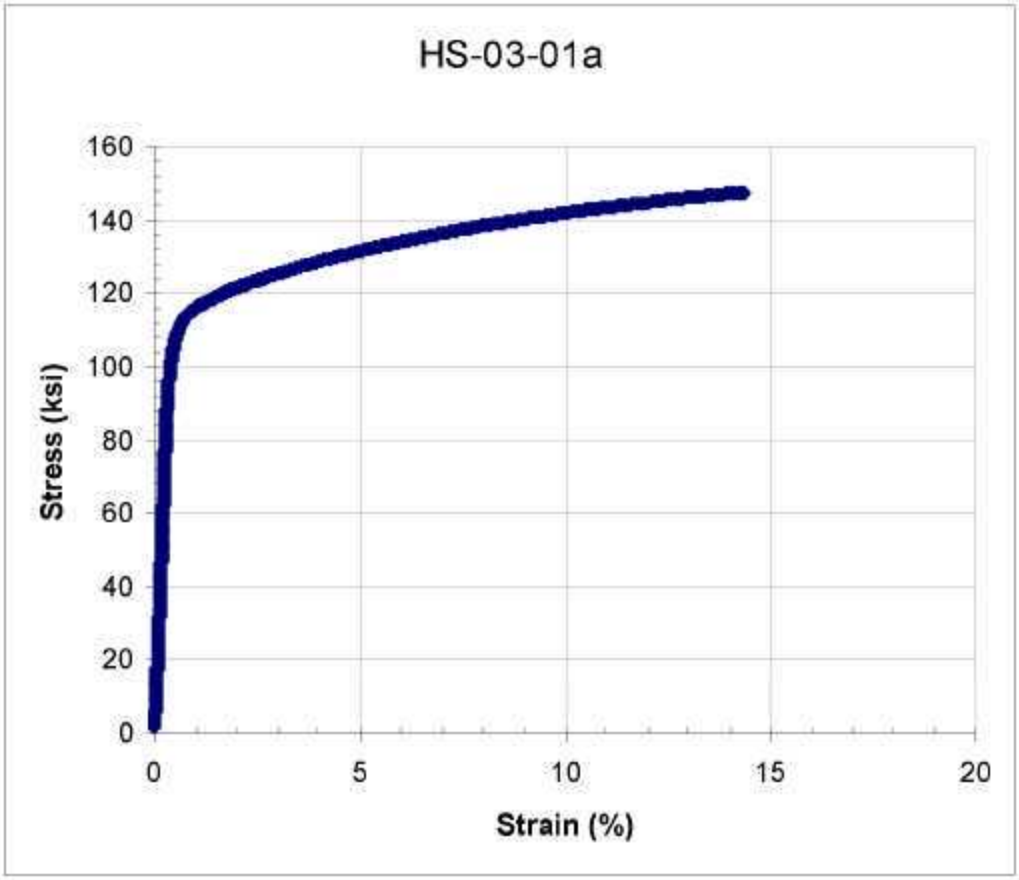

Test ID	Product Form	Aging Temp. (°C)	Aging Time (hours)	Test Temp. (°C)	Prop. Limit (MPa)	Yield Strength (MPa)	Ultimate Tensile Strength (MPa)	Uniform Elong. (%)	Elong. (%)	Red. of Area (%)	Failure Location
HS-03-08a	Sheet	675	2.4	650	207	260	776	56.6	56.6	37.9	GL

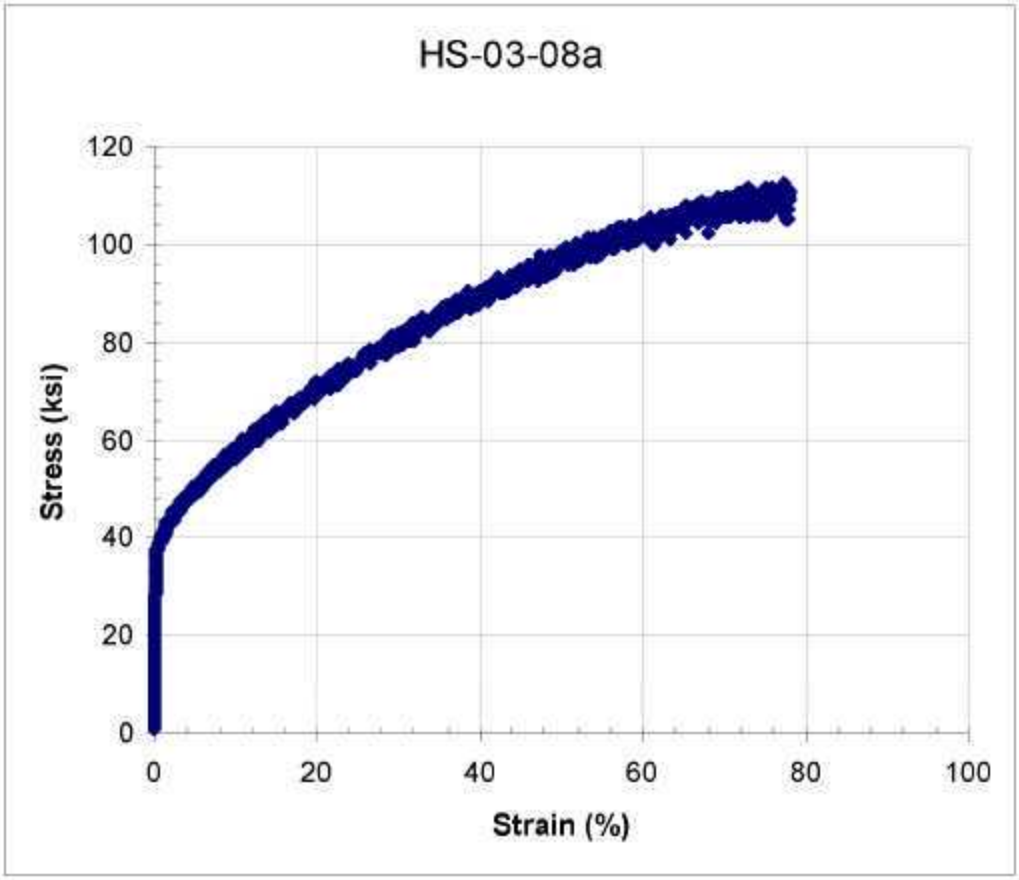

Test ID	Product Form	Aging Temp. (°C)	Aging Time (hours)	Test Temp. (°C)	Prop. Limit (MPa)	Yield Strength (MPa)	Ultimate Tensile Strength (MPa)	Uniform Elong. (%)	Elong. (%)	Red. of Area (%)	Failure Location
HS-03-06a	Sheet	675	24	650	207	280	795	61.4	61.4	39.4	GL

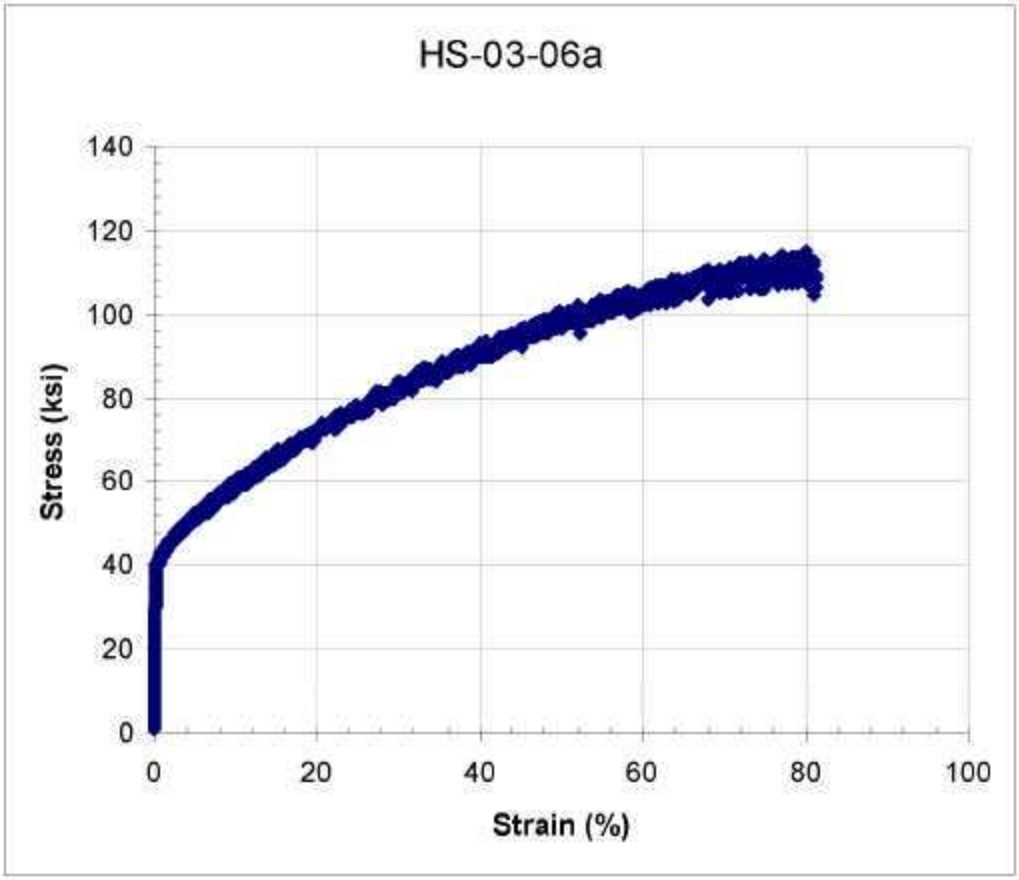

Test ID	Product Form	Aging Temp. (°C)	Aging Time (hours)	Test Temp. (°C)	Prop. Limit (MPa)	Yield Strength (MPa)	Ultimate Tensile Strength (MPa)	Uniform Elong. (%)	Elong. (%)	Red. of Area (%)	Failure Location
HS-03-04a	Sheet	675	240	650	221	328	818	44.2	44.2	38.0	GL

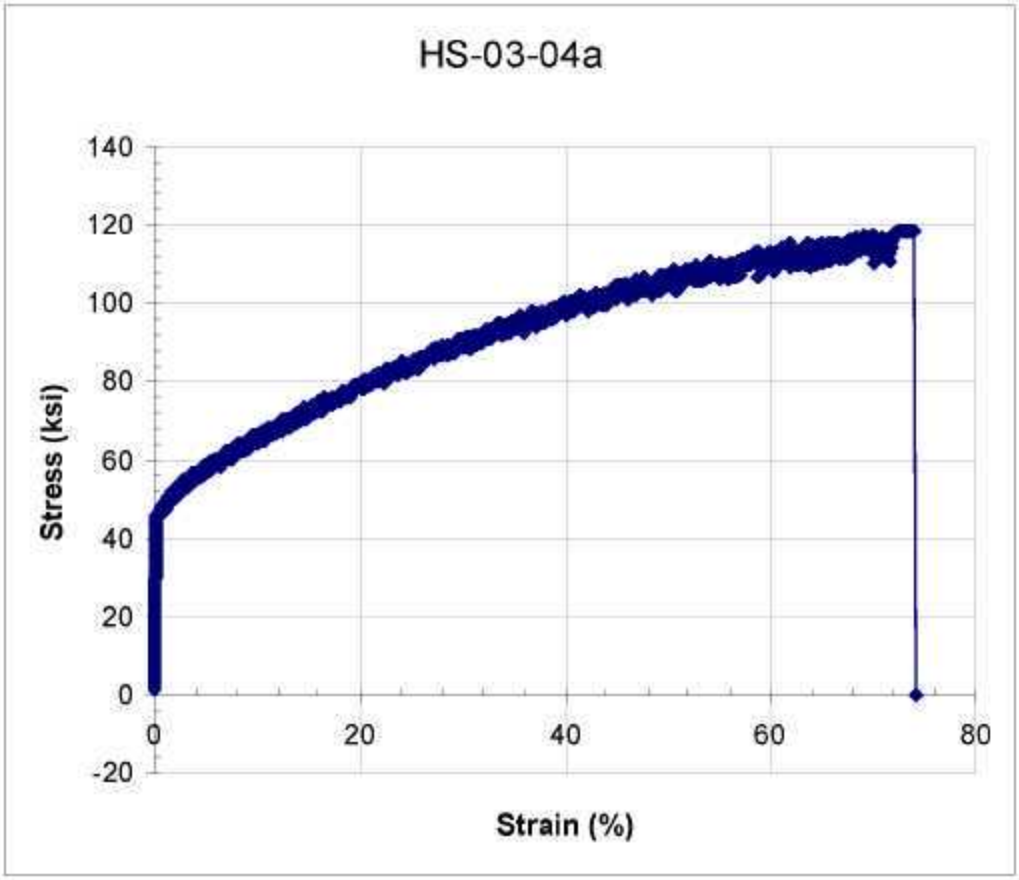

Test ID	Product Form	Aging Temp. (°C)	Aging Time (hours)	Test Temp. (°C)	Prop. Limit (MPa)	Yield Strength (MPa)	Ultimate Tensile Strength (MPa)	Uniform Elong. (%)	Elong. (%)	Red. of Area (%)	Failure Location
HS-03-02b	Sheet	675	1000	650	345	445	837	38.6	38.6	28.6	GL

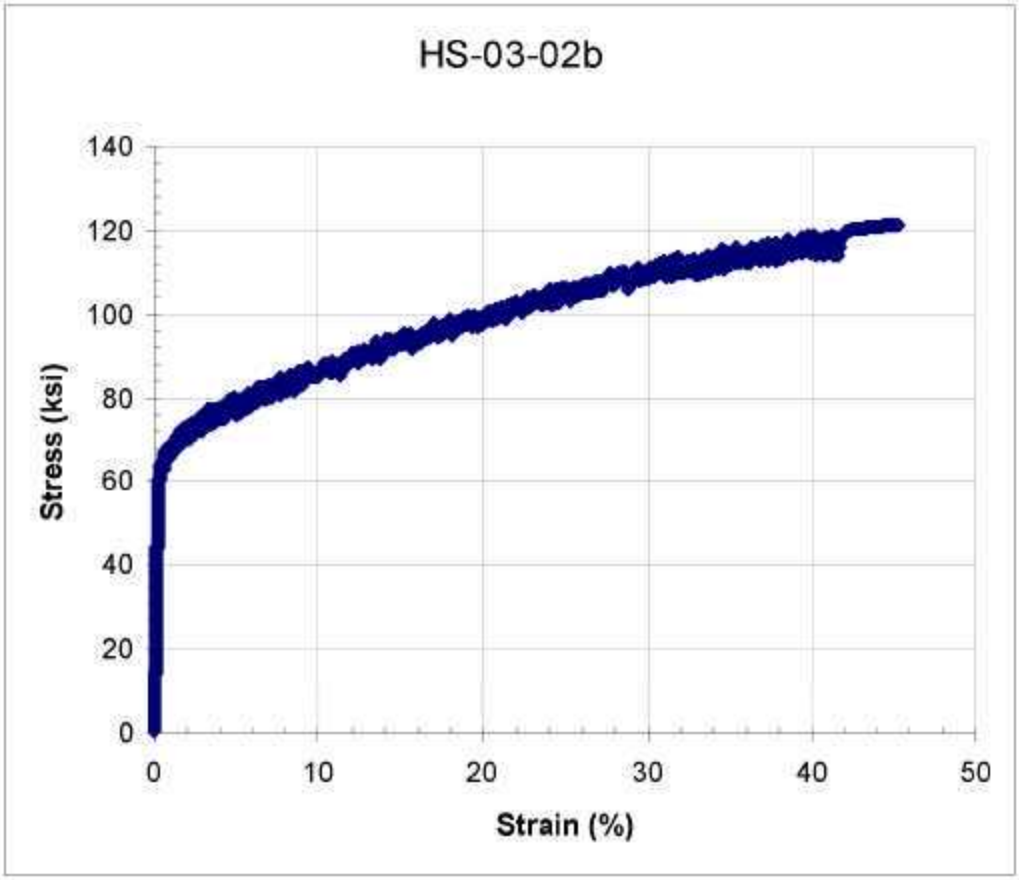

Test ID	Product Form	Aging Temp. (°C)	Aging Time (hours)	Test Temp. (°C)	Prop. Limit (MPa)	Yield Strength (MPa)	Ultimate Tensile Strength (MPa)	Uniform Elong. (%)	Elong. (%)	Red. of Area (%)	Failure Location
HS-03-02a	Sheet	675	2000	650	345	568	891	23.6	23.6	22.9	GL

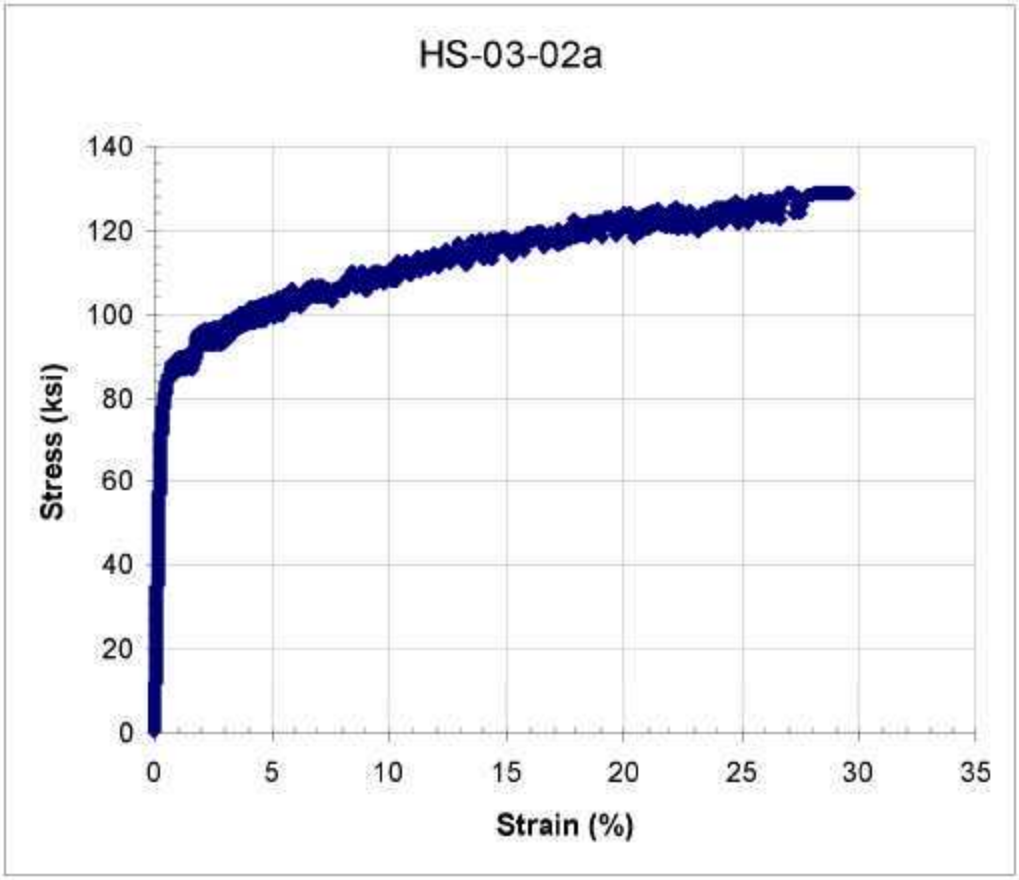

Test ID	Product Form	Aging Temp. (°C)	Aging Time (hours)	Test Temp. (°C)	Prop. Limit (MPa)	Yield Strength (MPa)	Ultimate Tensile Strength (MPa)	Uniform Elong. (%)	Elong. (%)	Red. of Area (%)	Failure Location
TT-WM-01	Sheet Weld	none	none	23		495	1008	50.0	50.0	40.7	BM

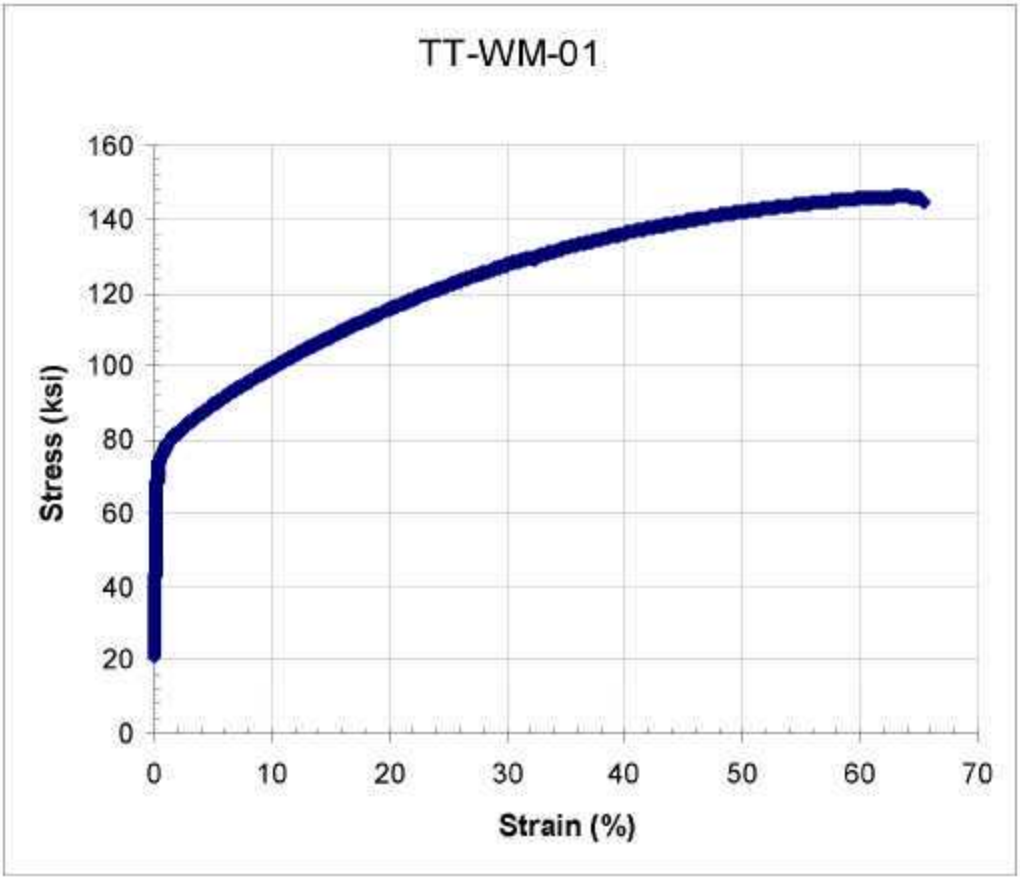

Test ID	Product Form	Aging Temp. (°C)	Aging Time (hours)	Test Temp. (°C)	Prop. Limit (MPa)	Yield Strength (MPa)	Ultimate Tensile Strength (MPa)	Uniform Elong. (%)	Elong. (%)	Red. of Area (%)	Failure Location
TT-WM-02	Sheet Weld	none	none	300	219	307	888	70.0	74.5	57.1	BM

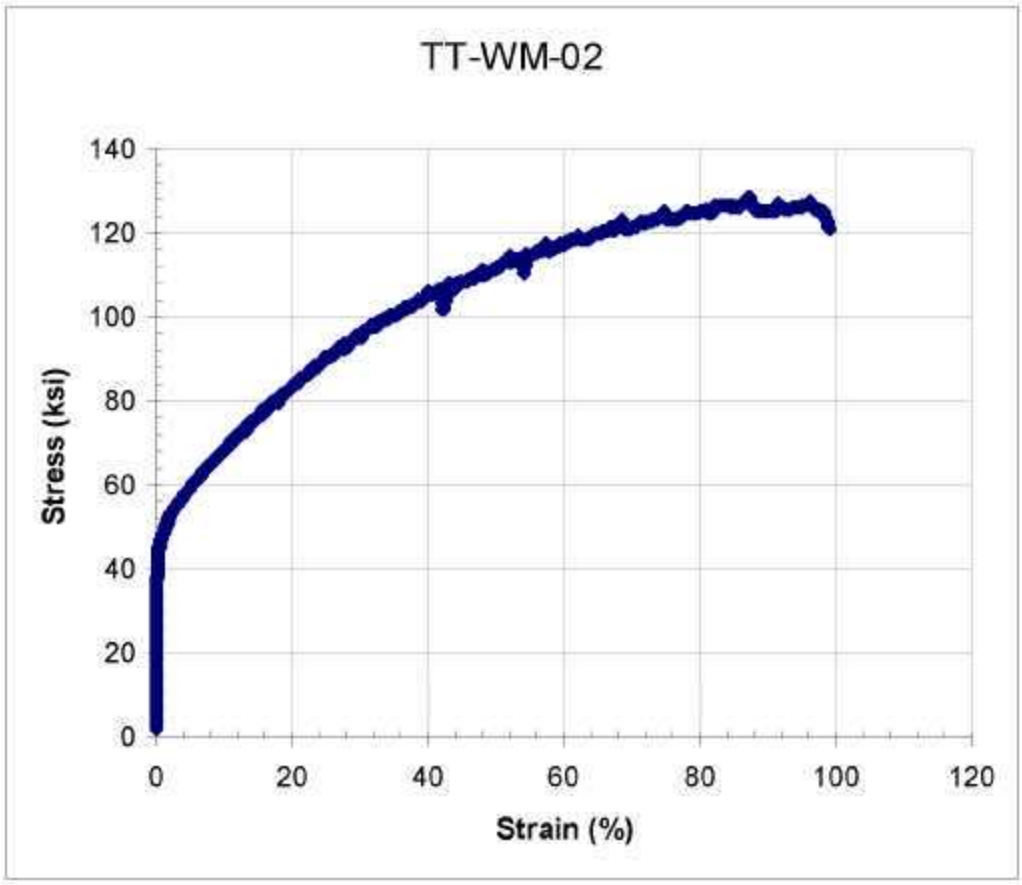

Test ID	Product Form	Aging Temp. (°C)	Aging Time (hours)	Test Temp. (°C)	Prop. Limit (MPa)	Yield Strength (MPa)	Ultimate Tensile Strength (MPa)	Uniform Elong. (%)	Elong. (%)	Red. of Area (%)	Failure Location
TT-WM-03	Sheet Weld	none	none	500	196	289	809	66.2	72.5	51.7	BM

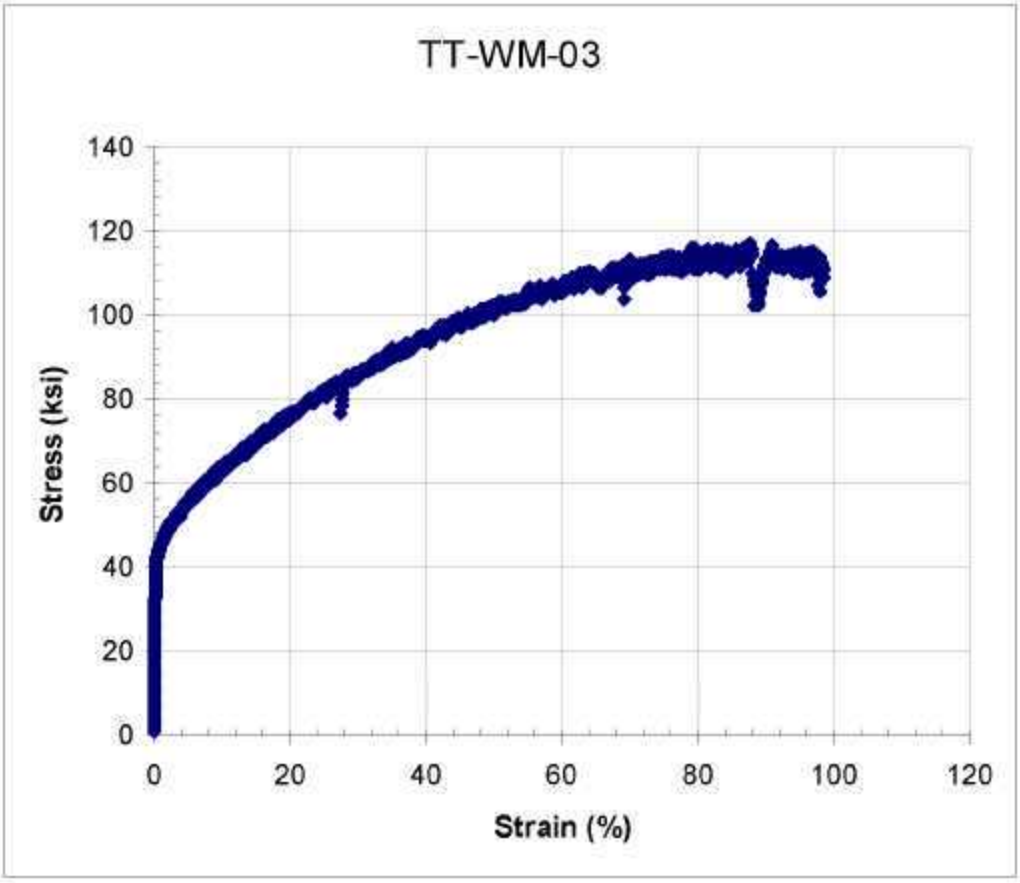

Test ID	Product Form	Aging Temp. (°C)	Aging Time (hours)	Test Temp. (°C)	Prop. Limit (MPa)	Yield Strength (MPa)	Ultimate Tensile Strength (MPa)	Uniform Elong. (%)	Elong. (%)	Red. of Area (%)	Failure Location
TT-WM-04	Sheet Weld	none	none	650	191	279	768	49.7	49.7	32.4	BM

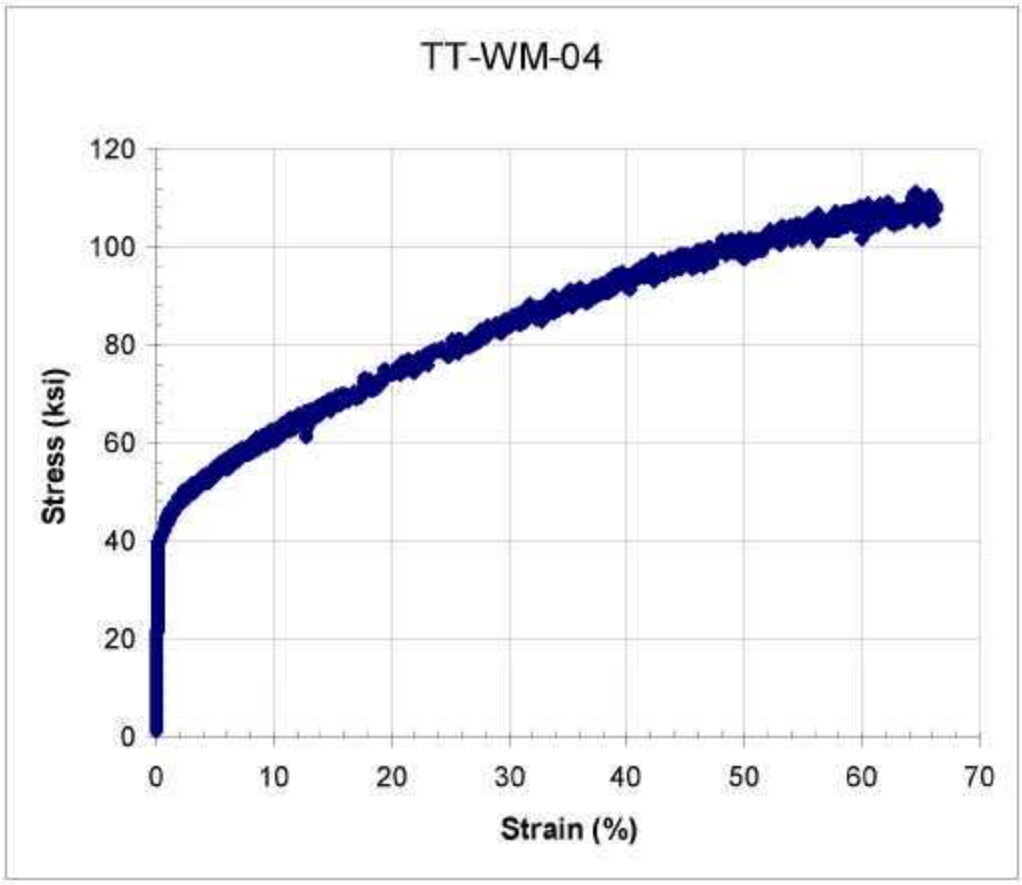

Test ID	Product Form	Aging Temp. (°C)	Aging Time (hours)	Test Temp. (°C)	Prop. Limit (MPa)	Yield Strength (MPa)	Ultimate Tensile Strength (MPa)	Uniform Elong. (%)	Elong. (%)	Red. of Area (%)	Failure Location
TT-WM-05	Sheet Weld	none	none	800	153	245	480	22.5	50.0	45.7	BM

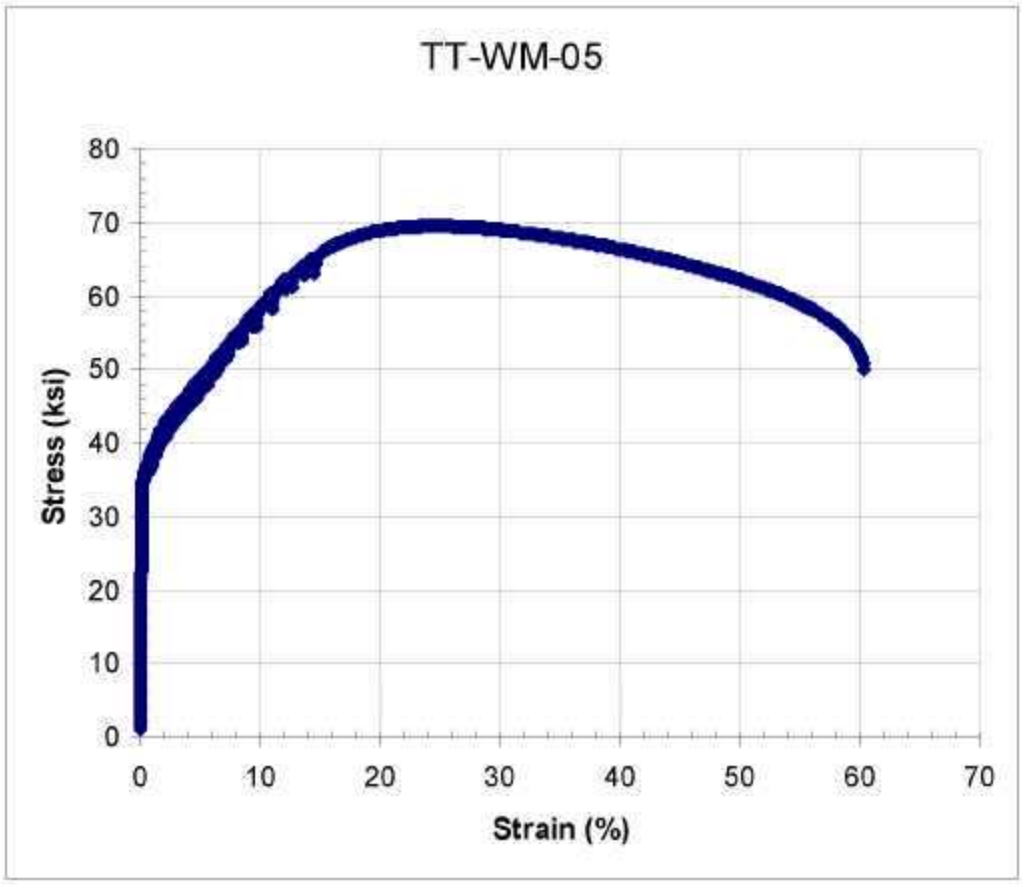

Test ID	Product Form	Aging Temp. (°C)	Aging Time (hours)	Test Temp. (°C)	Prop. Limit (MPa)	Yield Strength (MPa)	Ultimate Tensile Strength (MPa)	Uniform Elong. (%)	Elong. (%)	Red. of Area (%)	Failure Location
TT-WM-06	Sheet Weld	none	none	1000	90	165	170	4.0	72.8	62.0	BM

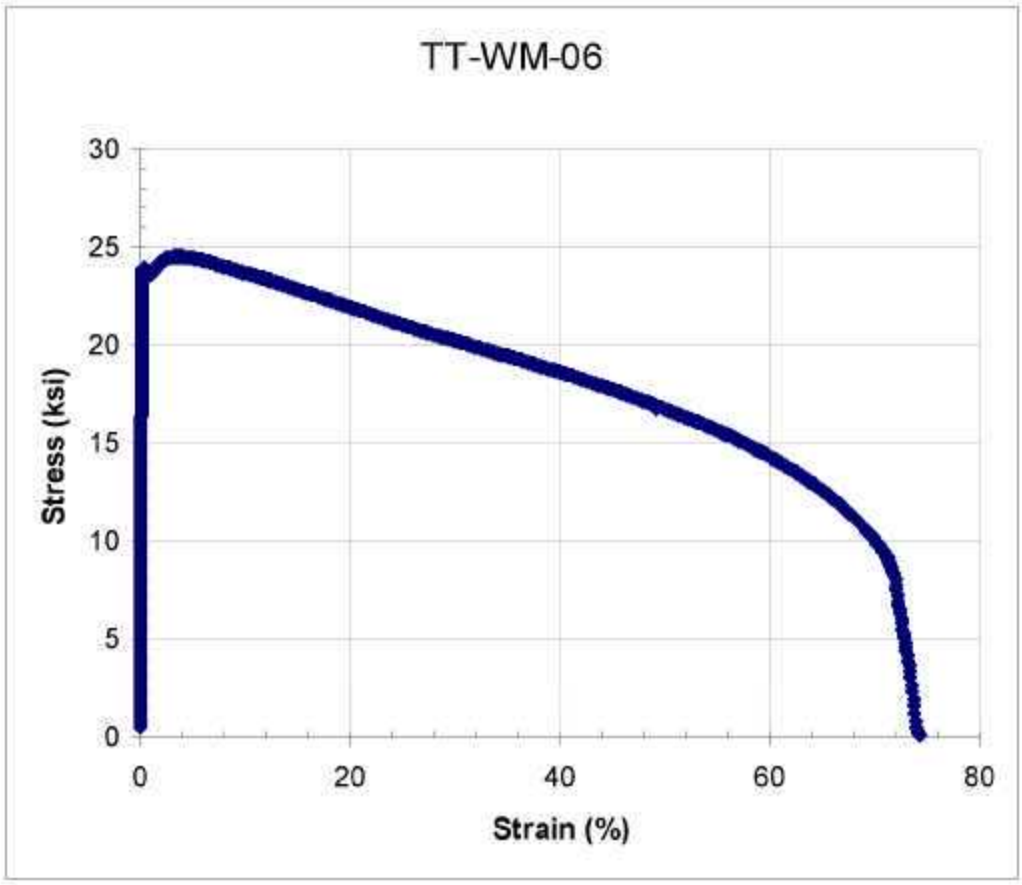

Test ID	Product Form	Aging Temp. (°C)	Aging Time (hours)	Test Temp. (°C)	Prop. Limit (MPa)	Yield Strength (MPa)	Ultimate Tensile Strength (MPa)	Uniform Elong. (%)	Elong. (%)	Red. of Area (%)	Failure Location
TT-WM-07	Sheet Weld	none	none	1100	54	94	96	1.5	53.0	58.7	BM

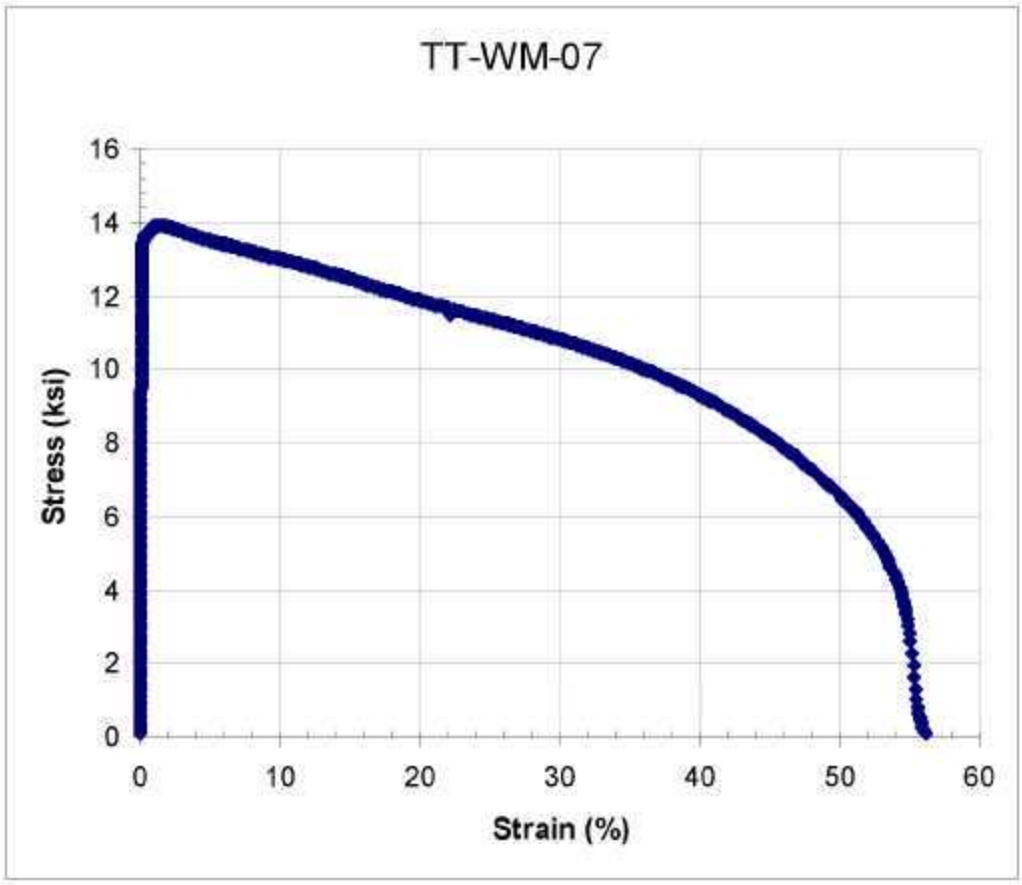

Test ID	Product Form	Aging Temp. (°C)	Aging Time (hours)	Test Temp. (°C)	Prop. Limit (MPa)	Yield Strength (MPa)	Ultimate Tensile Strength (MPa)	Uniform Elong. (%)	Elong. (%)	Red. of Area (%)	Failure Location
TT-WM-08	Sheet Weld	675	6000	23	552	762	1004	5.6	5.6	5.2	BM

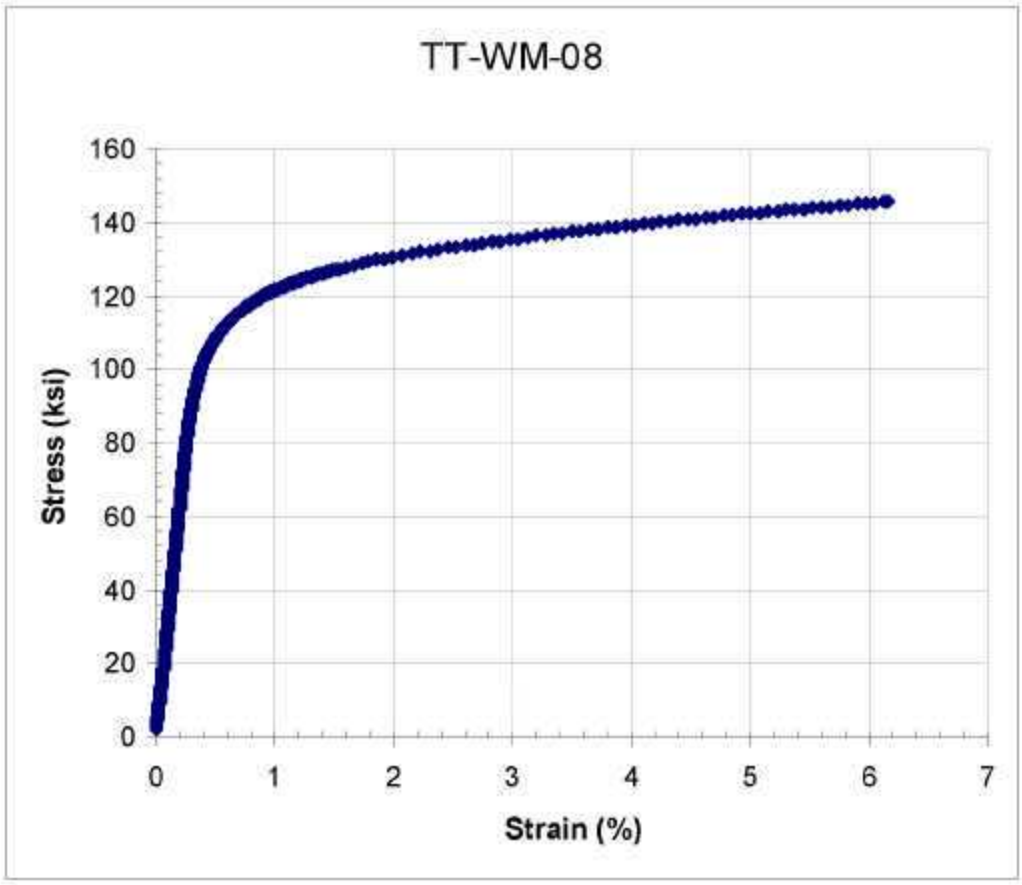

Test ID	Product Form	Aging Temp. (°C)	Aging Time (hours)	Test Temp. (°C)	Prop. Limit (MPa)	Yield Strength (MPa)	Ultimate Tensile Strength (MPa)	Uniform Elong. (%)	Elong. (%)	Red. of Area (%)	Failure Location
TT-WM-09	Sheet Weld	675	6000	300	448	601	936	12.8	12.8	13.2	BM

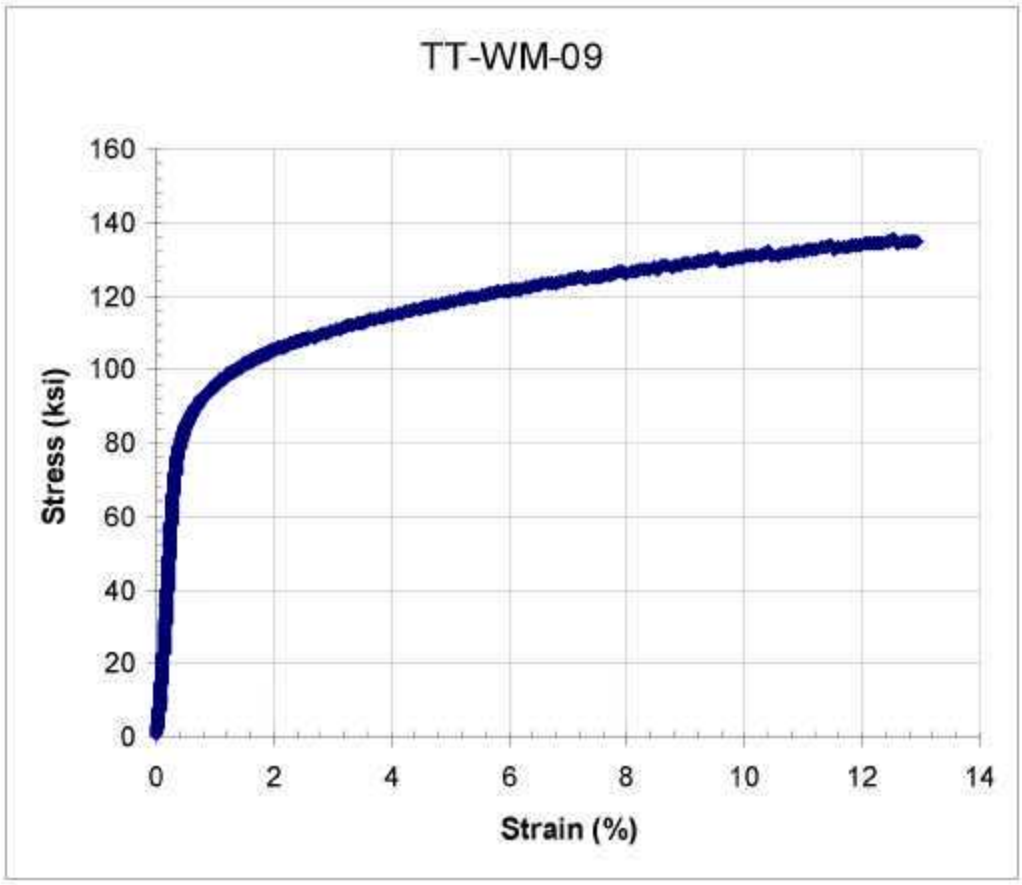

Test ID	Product Form	Aging Temp. (°C)	Aging Time (hours)	Test Temp. (°C)	Prop. Limit (MPa)	Yield Strength (MPa)	Ultimate Tensile Strength (MPa)	Uniform Elong. (%)	Elong. (%)	Red. of Area (%)	Failure Location
TT-WM-10	Sheet Weld	675	6000	500	372	542	927	16.3	16.3	15.0	BM

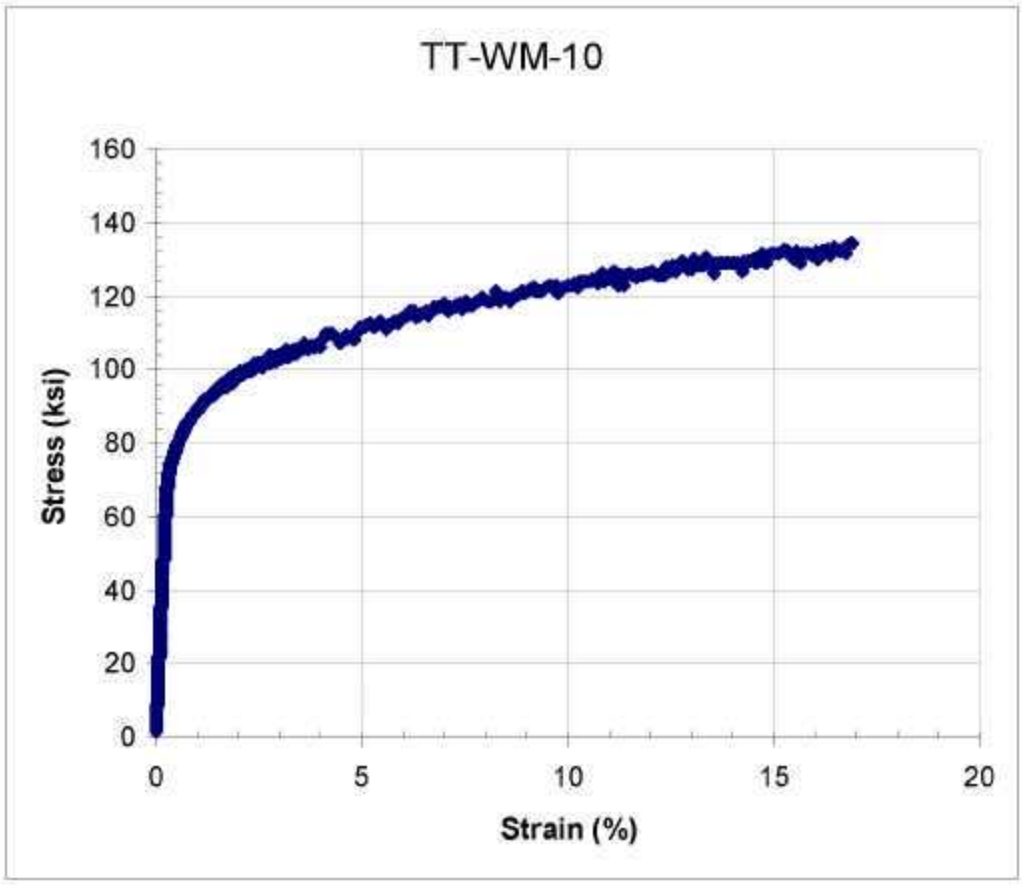

Test ID	Product Form	Aging Temp. (°C)	Aging Time (hours)	Test Temp. (°C)	Prop. Limit (MPa)	Yield Strength (MPa)	Ultimate Tensile Strength (MPa)	Uniform Elong. (%)	Elong. (%)	Red. of Area (%)	Failure Location
TT-WM-11	Sheet Weld	675	6000	650	241	549	895	16.7	16.7	17.5	BM

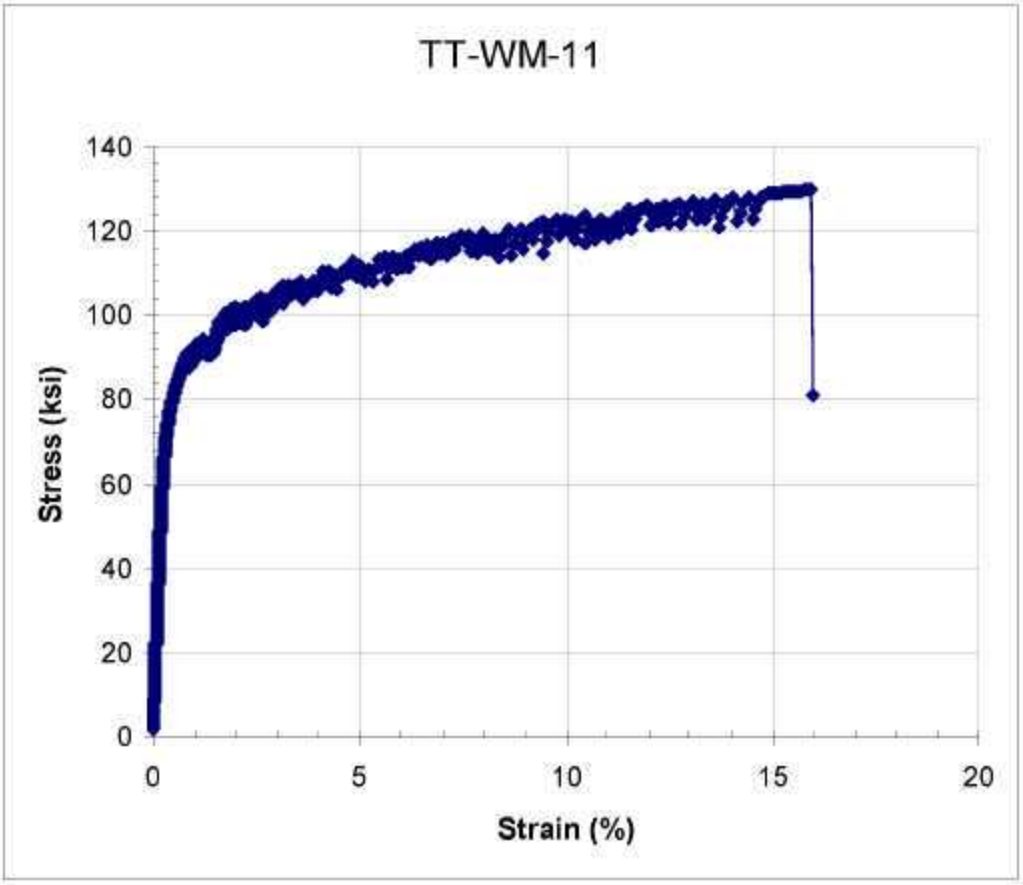

Test ID	Product Form	Aging Temp. (°C)	Aging Time (hours)	Test Temp. (°C)	Prop. Limit (MPa)	Yield Strength (MPa)	Ultimate Tensile Strength (MPa)	Uniform Elong. (%)	Elong. (%)	Red. of Area (%)	Failure Location
TT-WM-12	Sheet Weld	675	6000	800		402	554	7.2	13.4	18.3	BM

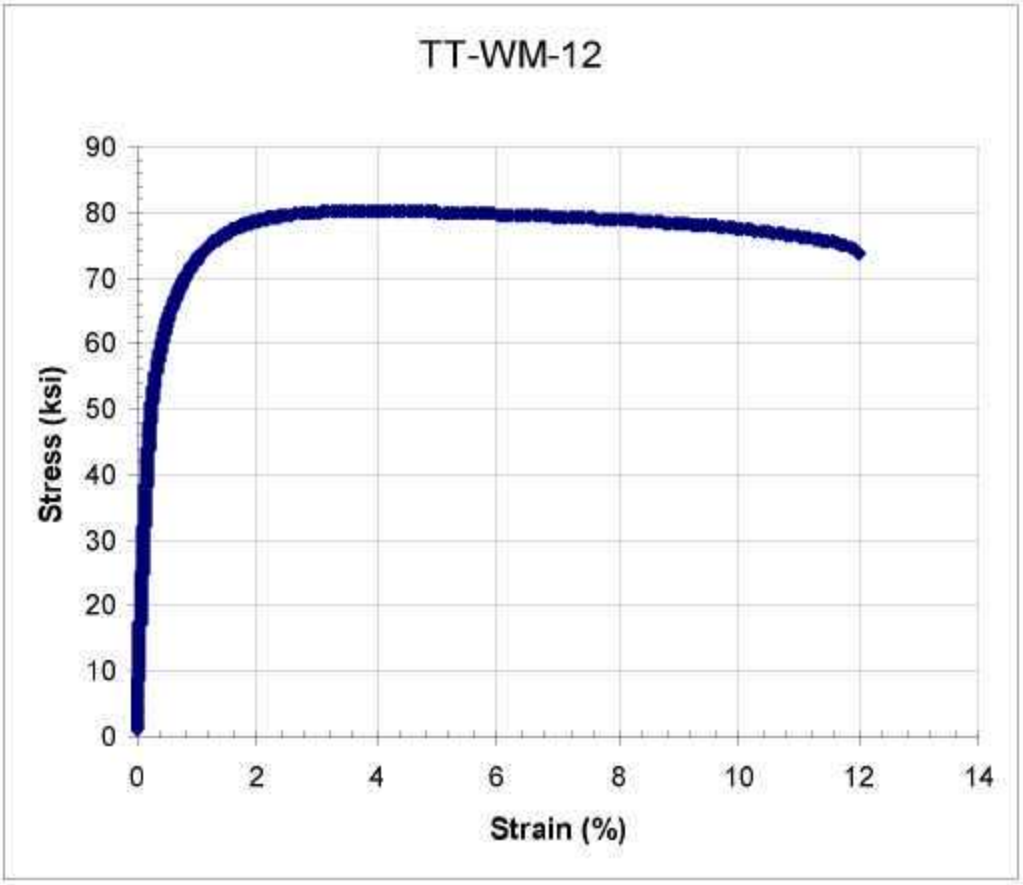

Test ID	Product Form	Aging Temp. (°C)	Aging Time (hours)	Test Temp. (°C)	Prop. Limit (MPa)	Yield Strength (MPa)	Ultimate Tensile Strength (MPa)	Uniform Elong. (%)	Elong. (%)	Red. of Area (%)	Failure Location
TT-WM-13	Sheet Weld	675	6000	1000	83	174	177	0.5	47.3	45.2	BM

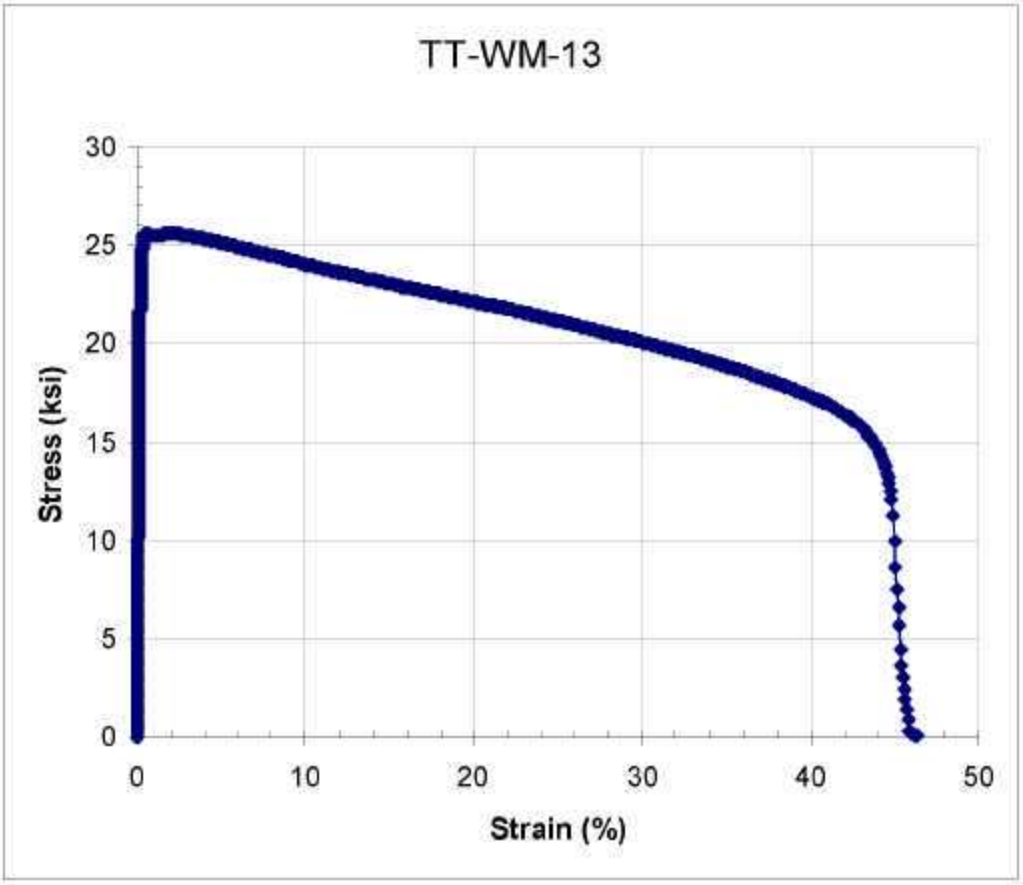

Test ID	Product Form	Aging Temp. (°C)	Aging Time (hours)	Test Temp. (°C)	Prop. Limit (MPa)	Yield Strength (MPa)	Ultimate Tensile Strength (MPa)	Uniform Elong. (%)	Elong. (%)	Red. of Area (%)	Failure Location
TT-WM-14	Sheet Weld	675	6000	1100	48	99	99	0.5	44.5	45.5	BM

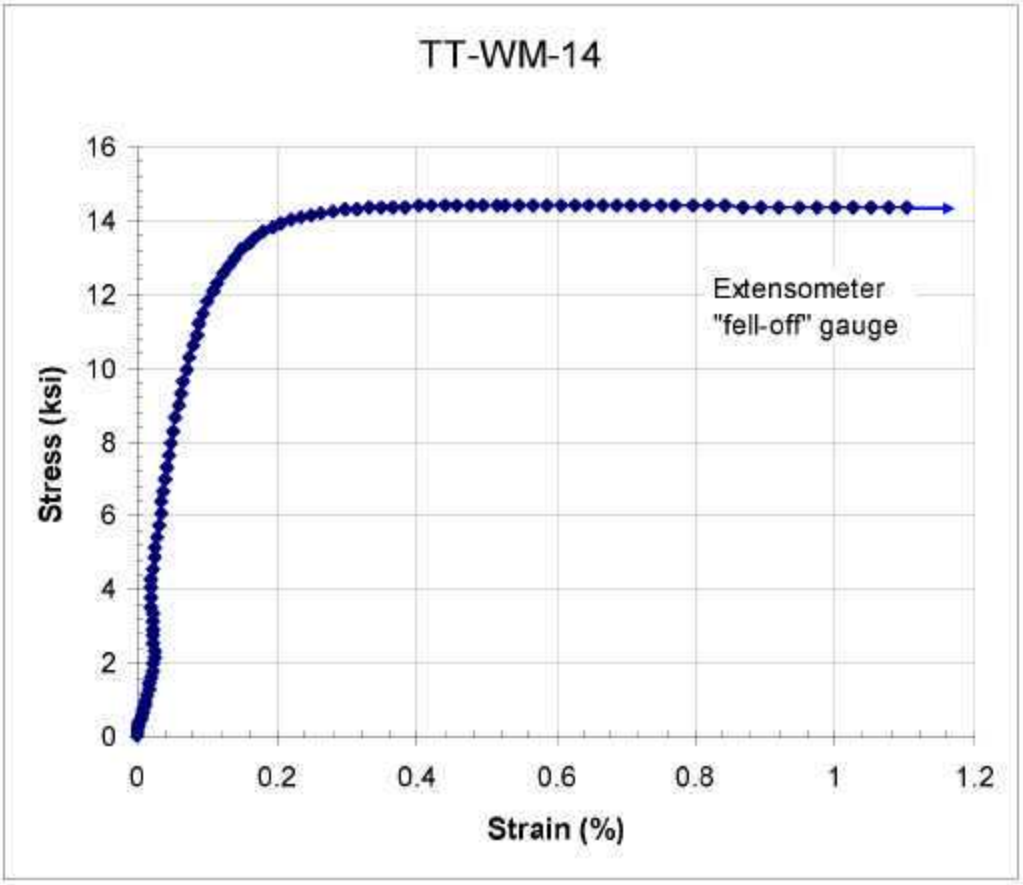

Test ID	Product Form	Aging Temp. (°C)	Aging Time (hours)	Test Temp. (°C)	Prop. Limit (MPa)	Yield Strength (MPa)	Ultimate Tensile Strength (MPa)	Uniform Elong. (%)	Elong. (%)	Red. of Area (%)	Failure Location
TT-WM-15	Sheet Weld	675	12000	23	414	753	1009	5.0	5.0	6.3	BM

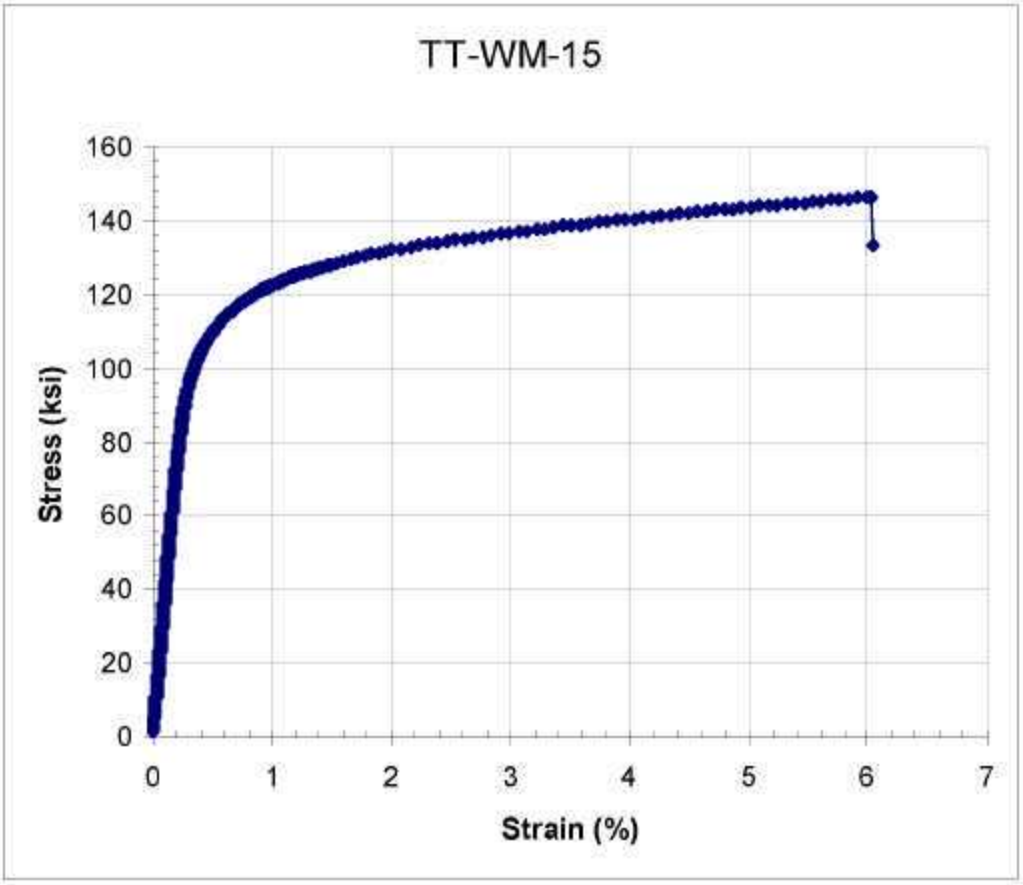

Test ID	Product Form	Aging Temp. (°C)	Aging Time (hours)	Test Temp. (°C)	Prop. Limit (MPa)	Yield Strength (MPa)	Ultimate Tensile Strength (MPa)	Uniform Elong. (%)	Elong. (%)	Red. of Area (%)	Failure Location
TT-WM-16	Sheet Weld	675	12000	300	372	615	926	7.8	7.8	8.4	BM

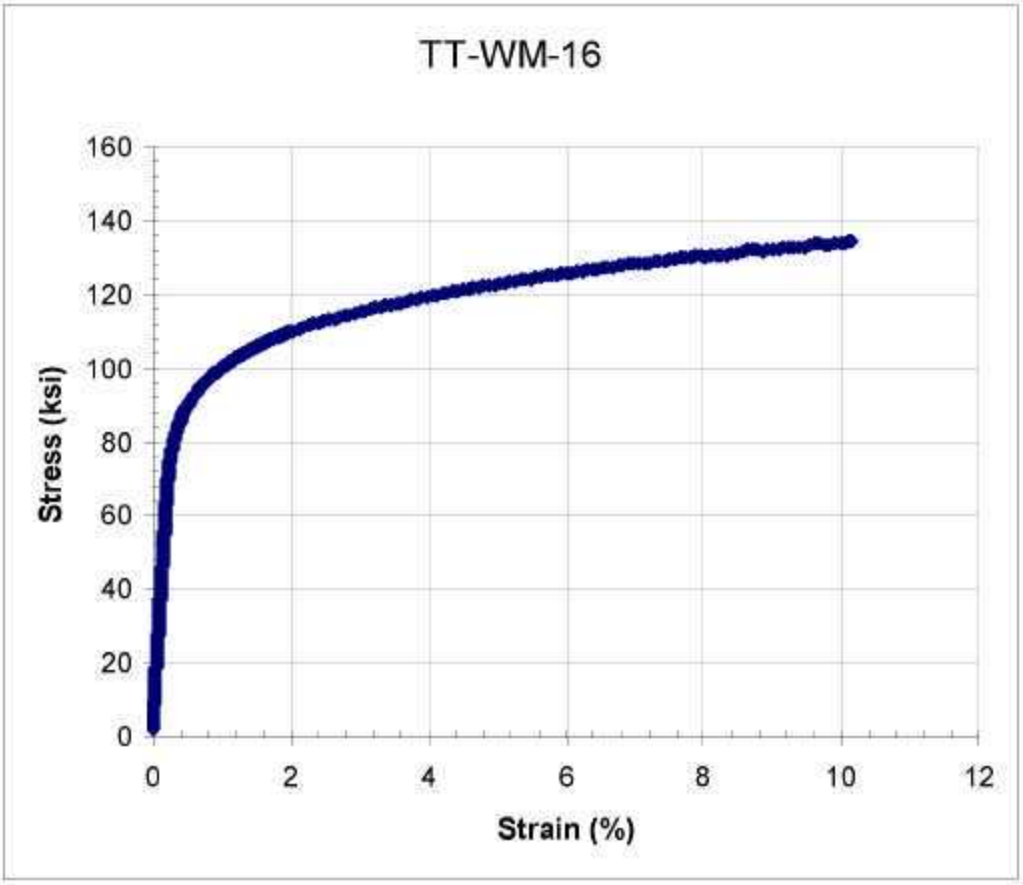

Test ID	Product Form	Aging Temp. (°C)	Aging Time (hours)	Test Temp. (°C)	Prop. Limit (MPa)	Yield Strength (MPa)	Ultimate Tensile Strength (MPa)	Uniform Elong. (%)	Elong. (%)	Red. of Area (%)	Failure Location
TT-WM-17	Sheet Weld	675	12000	500	310	564	918	12.0	12.0	13.3	BM

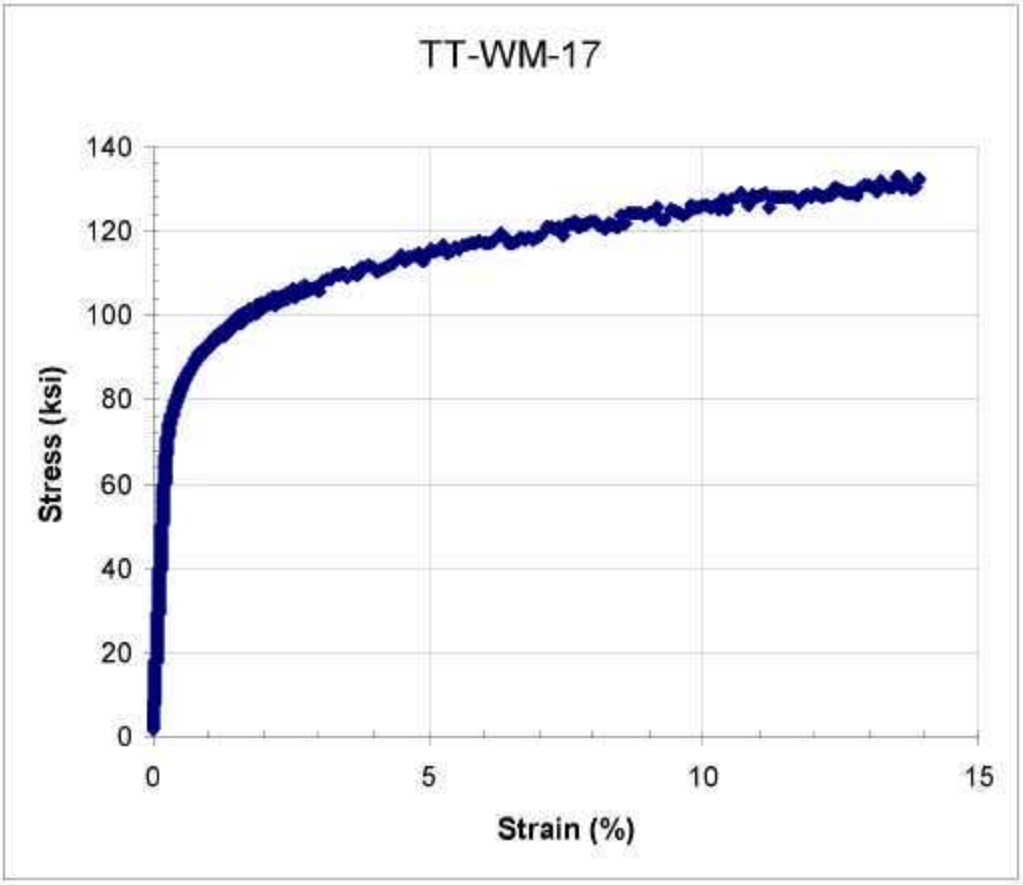

Test ID	Product Form	Aging Temp. (°C)	Aging Time (hours)	Test Temp. (°C)	Prop. Limit (MPa)	Yield Strength (MPa)	Ultimate Tensile Strength (MPa)	Uniform Elong. (%)	Elong. (%)	Red. of Area (%)	Failure Location
TT-WM-18	Sheet Weld	675	12000	650	310	572	899	11.0	11.0	12.2	BM

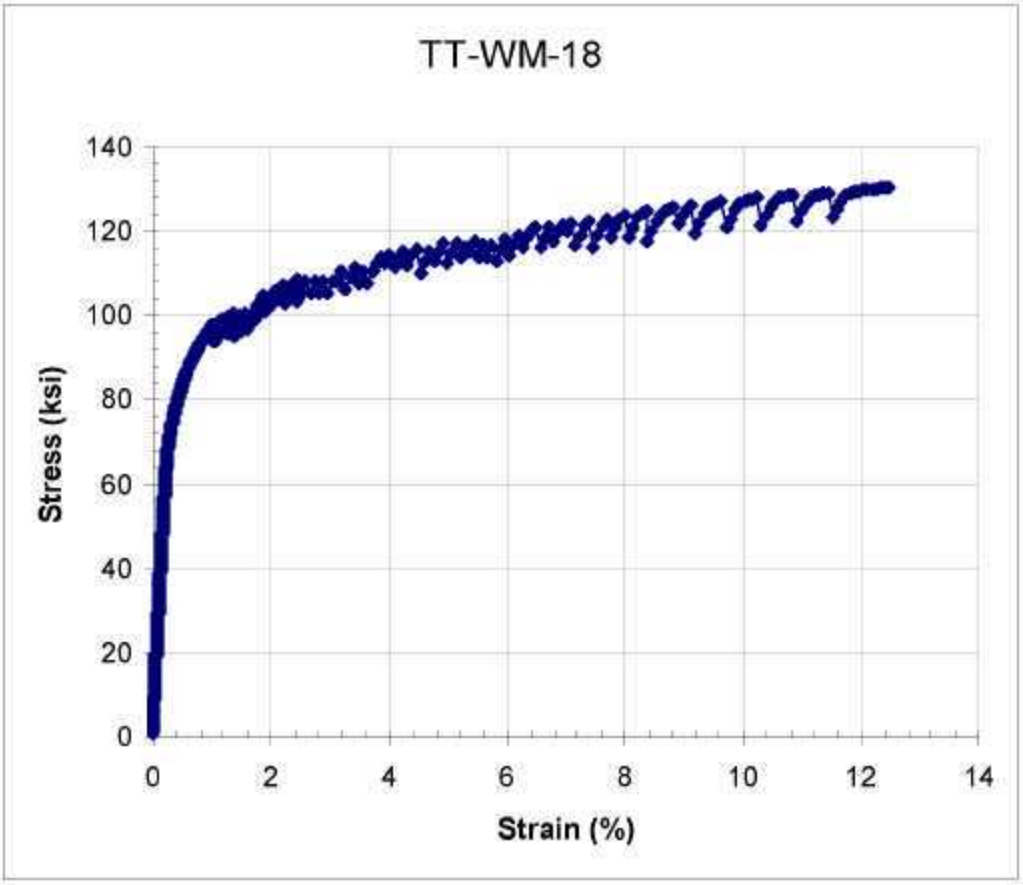

Test ID	Product Form	Aging Temp. (°C)	Aging Time (hours)	Test Temp. (°C)	Prop. Limit (MPa)	Yield Strength (MPa)	Ultimate Tensile Strength (MPa)	Uniform Elong. (%)	Elong. (%)	Red. of Area (%)	Failure Location
TT-WM-19	Sheet Weld	675	12000	800	193	438	562	2.8	8.7	10.9	BM

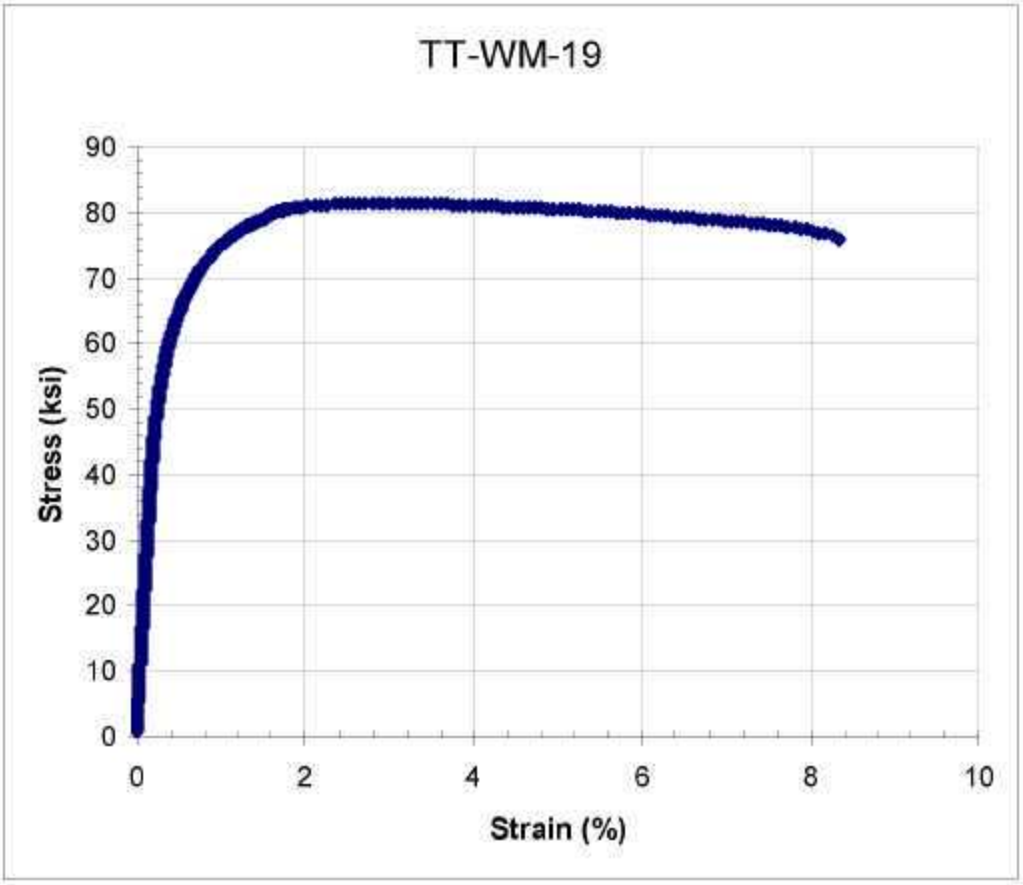

Test ID	Product Form	Aging Temp. (°C)	Aging Time (hours)	Test Temp. (°C)	Prop. Limit (MPa)	Yield Strength (MPa)	Ultimate Tensile Strength (MPa)	Uniform Elong. (%)	Elong. (%)	Red. of Area (%)	Failure Location
TT-WM-20	Sheet Weld	675	12000	1000		171	172	0.3	38.6	37.1	BM

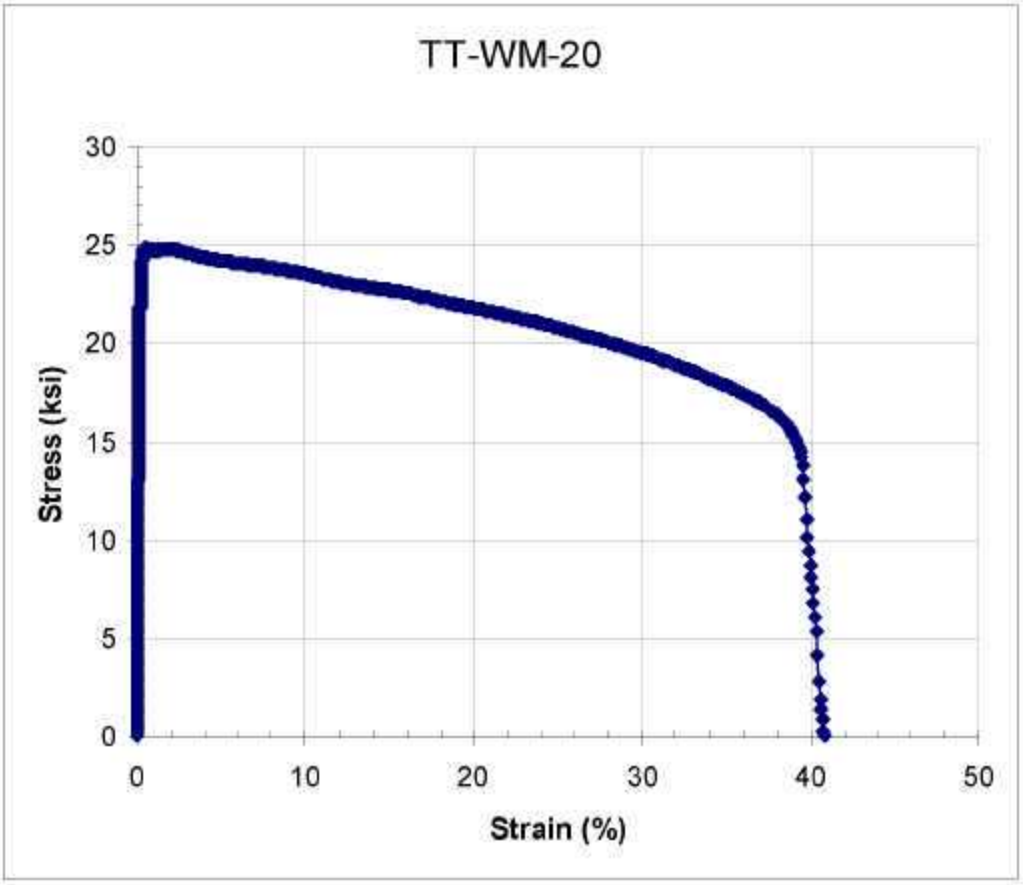

Test ID	Product Form	Aging Temp. (°C)	Aging Time (hours)	Test Temp. (°C)	Prop. Limit (MPa)	Yield Strength (MPa)	Ultimate Tensile Strength (MPa)	Uniform Elong. (%)	Elong. (%)	Red. of Area (%)	Failure Location
TT-WM-21	Sheet Weld	675	12000	1100		101	101	0.3	43.8	33.4	BM

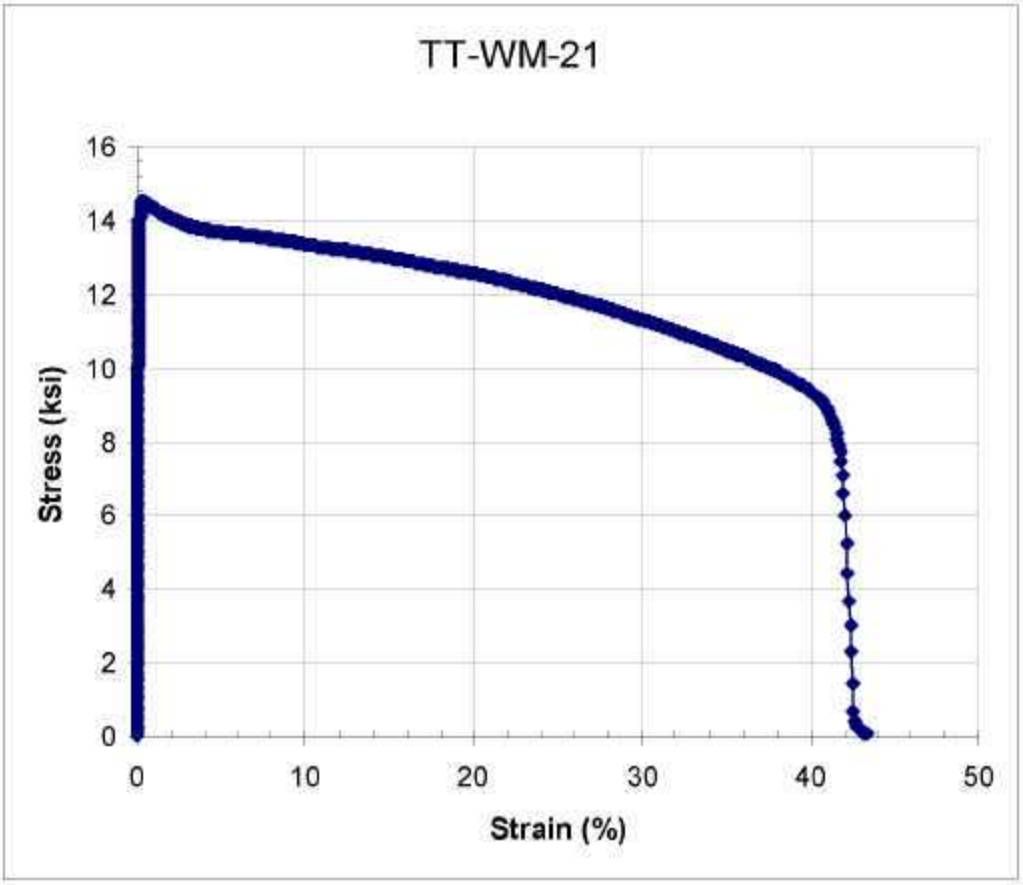

Test ID	Product Form	Aging Temp. (°C)	Aging Time (hours)	Test Temp. (°C)	Prop. Limit (MPa)	Yield Strength (MPa)	Ultimate Tensile Strength (MPa)	Uniform Elong. (%)	Elong. (%)	Red. of Area (%)	Failure Location
LWT-1	Bar Weld	none	none	20		595	1147	629.0	63.1		WM

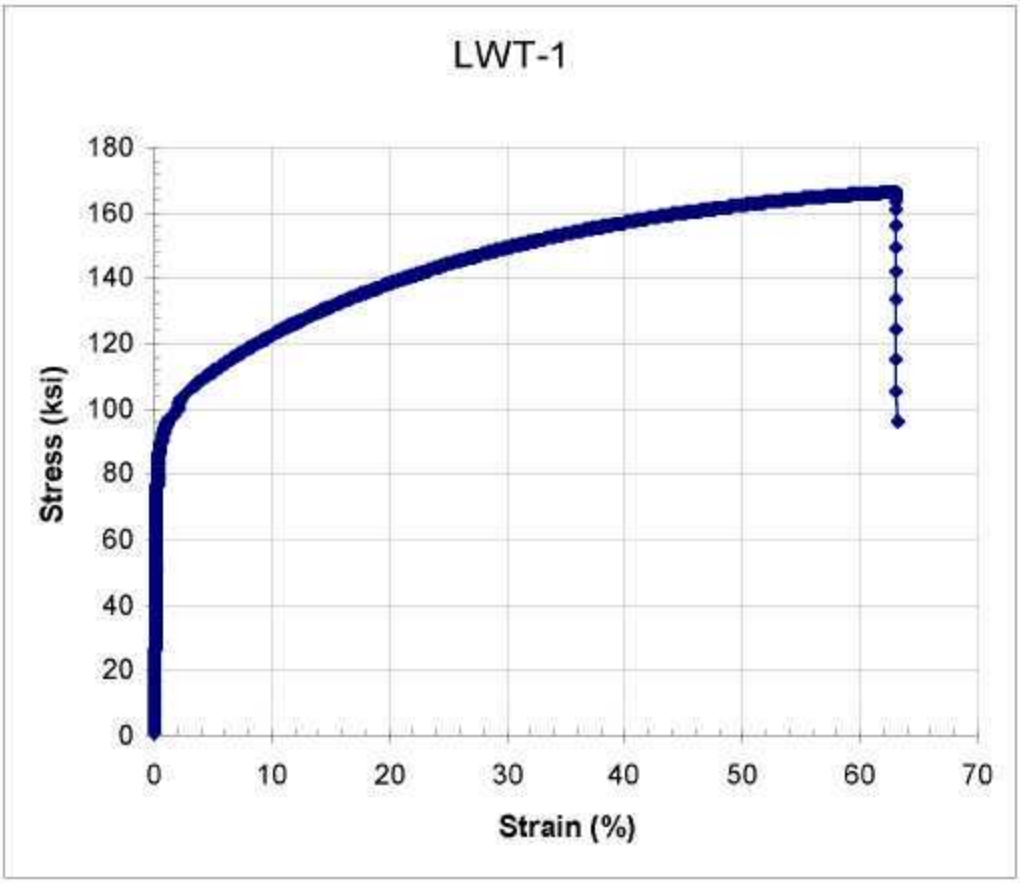

Test ID	Product Form	Aging Temp. (°C)	Aging Time (hours)	Test Temp. (°C)	Prop. Limit (MPa)	Yield Strength (MPa)	Ultimate Tensile Strength (MPa)	Uniform Elong. (%)	Elong. (%)	Red. of Area (%)	Failure Location
AWT-1	Bar Weld	none	none	20		593	1122	53.7	56.8		WM

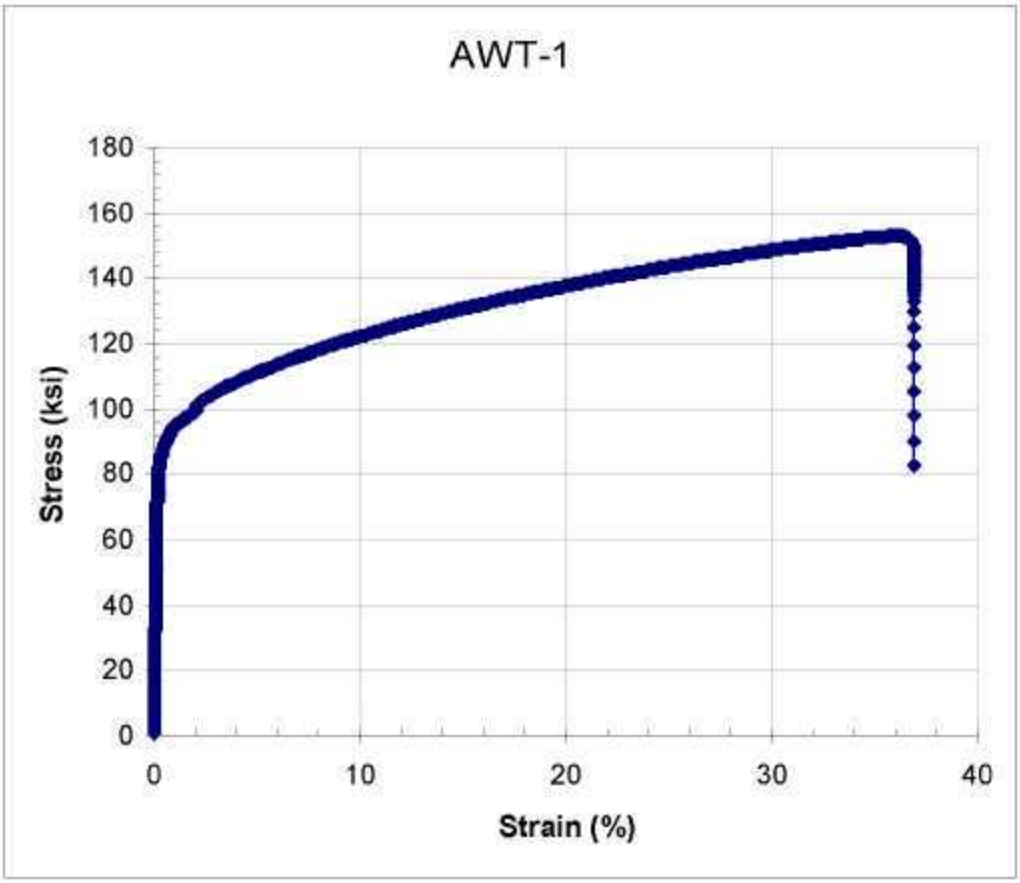

Test ID	Product Form	Aging Temp. (°C)	Aging Time (hours)	Test Temp. (°C)	Prop. Limit (MPa)	Yield Strength (MPa)	Ultimate Tensile Strength (MPa)	Uniform Elong. (%)	Elong. (%)	Red. of Area (%)	Failure Location
LWT-2	Bar Weld	none	none	650		330	736	25.5	26.2		WM

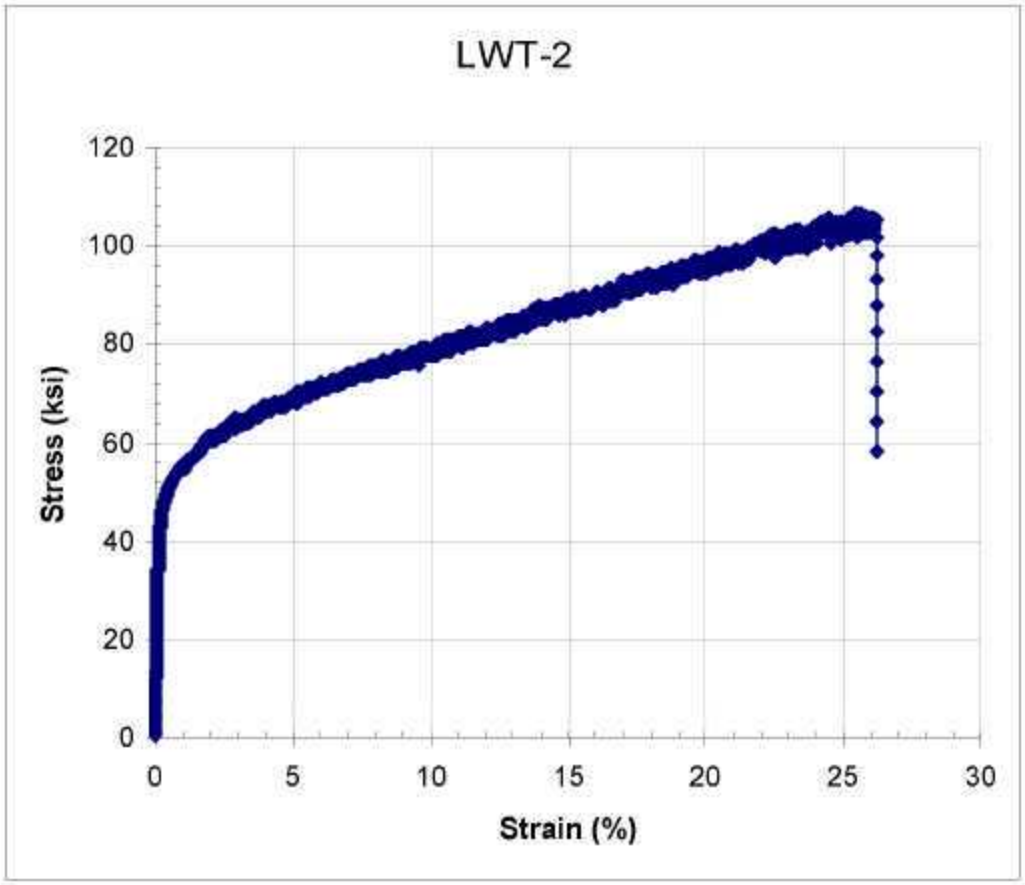

Test ID	Product Form	Aging Temp. (°C)	Aging Time (hours)	Test Temp. (°C)	Prop. Limit (MPa)	Yield Strength (MPa)	Ultimate Tensile Strength (MPa)	Uniform Elong. (%)	Elong. (%)	Red. of Area (%)	Failure Location
AWT-2	Bar Weld	none	none	650		367	851	47.7	47.4		WM

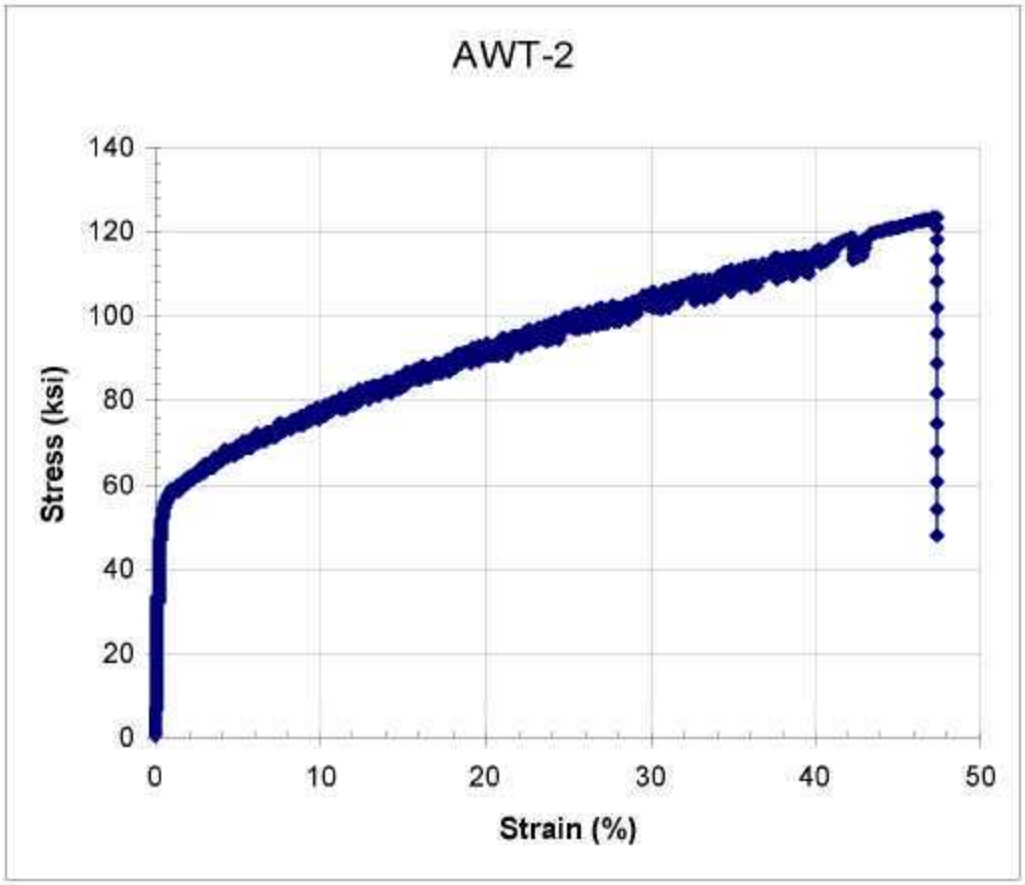

Test ID	Product Form	Aging Temp. (°C)	Aging Time (hours)	Test Temp. (°C)	Prop. Limit (MPa)	Yield Strength (MPa)	Ultimate Tensile Strength (MPa)	Uniform Elong. (%)	Elong. (%)	Red. of Area (%)	Failure Location
LWT-3	Bar Weld	850	50	20		533	1012	30.0	30.0		WM

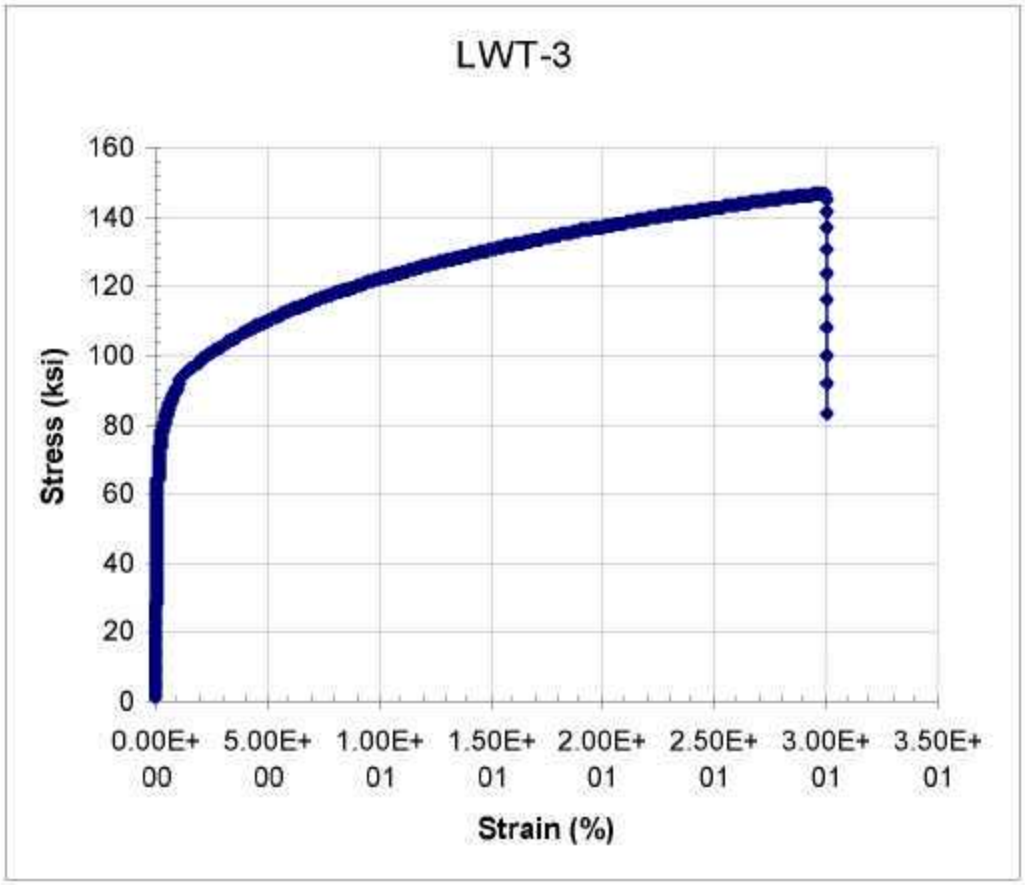

Test ID	Product Form	Aging Temp. (°C)	Aging Time (hours)	Test Temp. (°C)	Prop. Limit (MPa)	Yield Strength (MPa)	Ultimate Tensile Strength (MPa)	Uniform Elong. (%)	Elong. (%)	Red. of Area (%)	Failure Location
AWT-3	Bar Weld	850	50	20		559	1051	37.2	37.3		WM

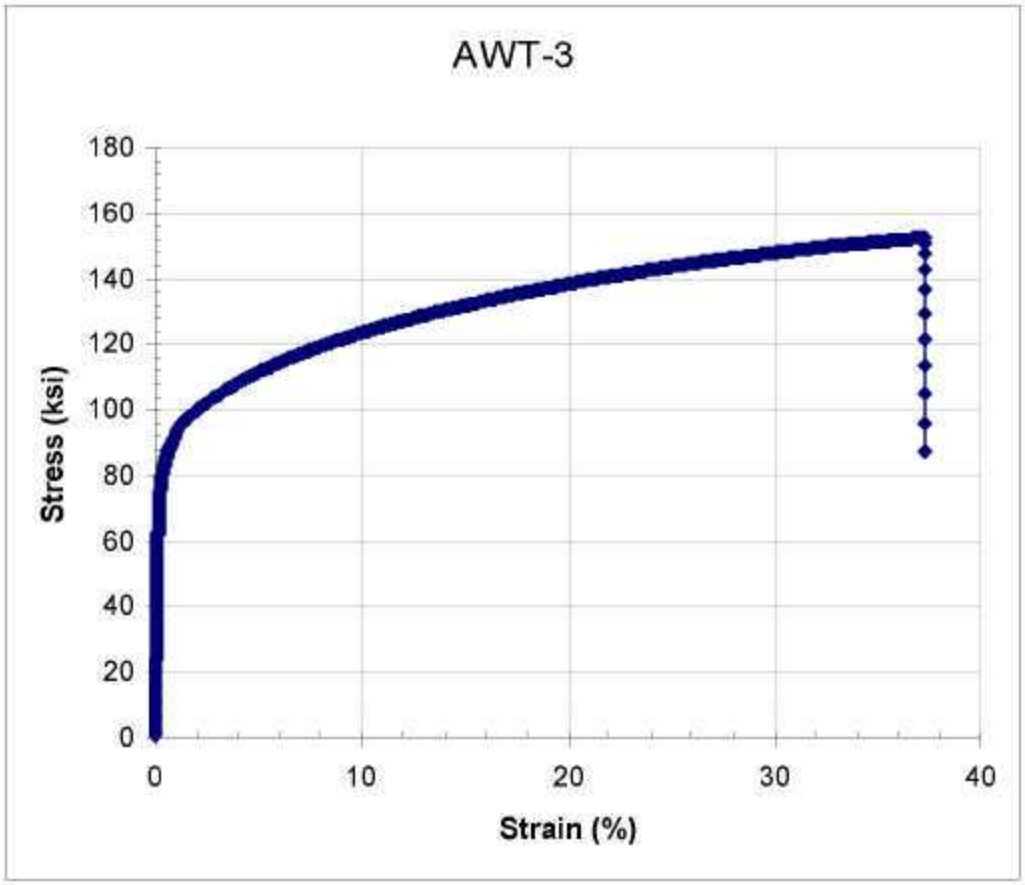

Test ID	Product Form	Aging Temp. (°C)	Aging Time (hours)	Test Temp. (°C)	Prop. Limit (MPa)	Yield Strength (MPa)	Ultimate Tensile Strength (MPa)	Uniform Elong. (%)	Elong. (%)	Red. of Area (%)	Failure Location
LWT-4	Bar Weld	850	50	650		538	831	31.7	31.7		WM

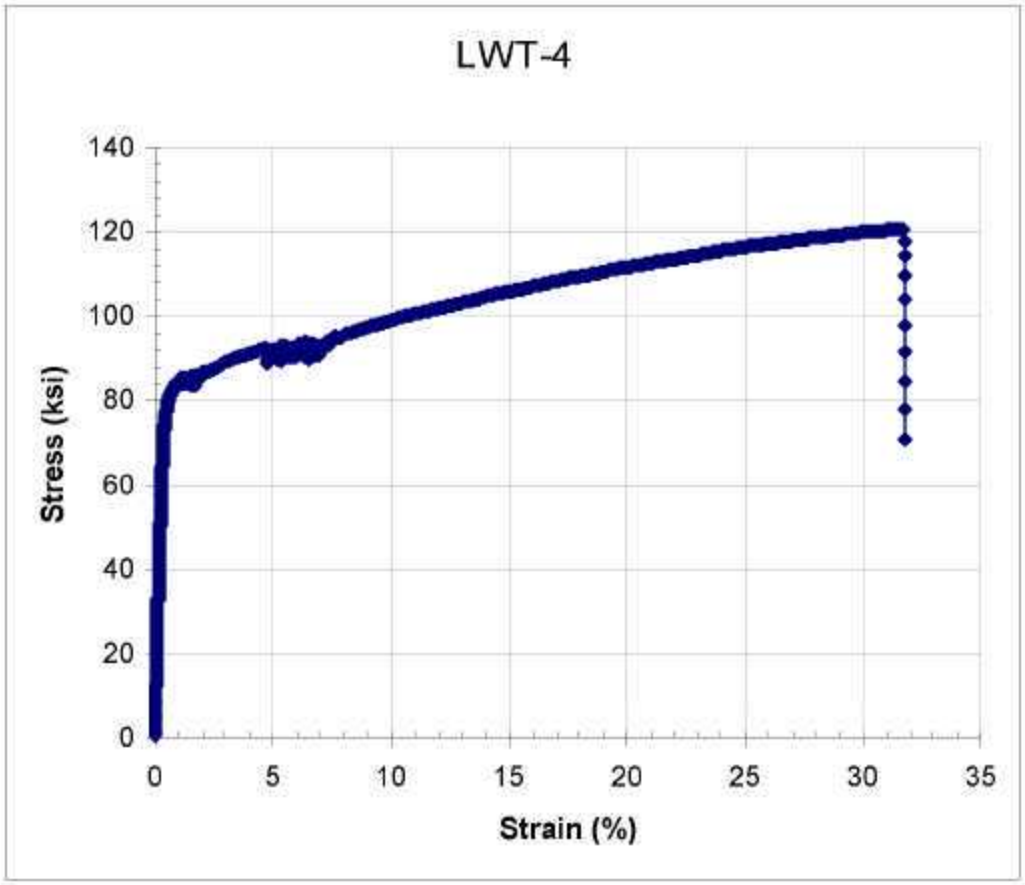

Test ID	Product Form	Aging Temp. (°C)	Aging Time (hours)	Test Temp. (°C)	Prop. Limit (MPa)	Yield Strength (MPa)	Ultimate Tensile Strength (MPa)	Uniform Elong. (%)	Elong. (%)	Red. of Area (%)	Failure Location
AWT-4	Bar Weld	850	50	650		352	873	49.2	49.3		WM

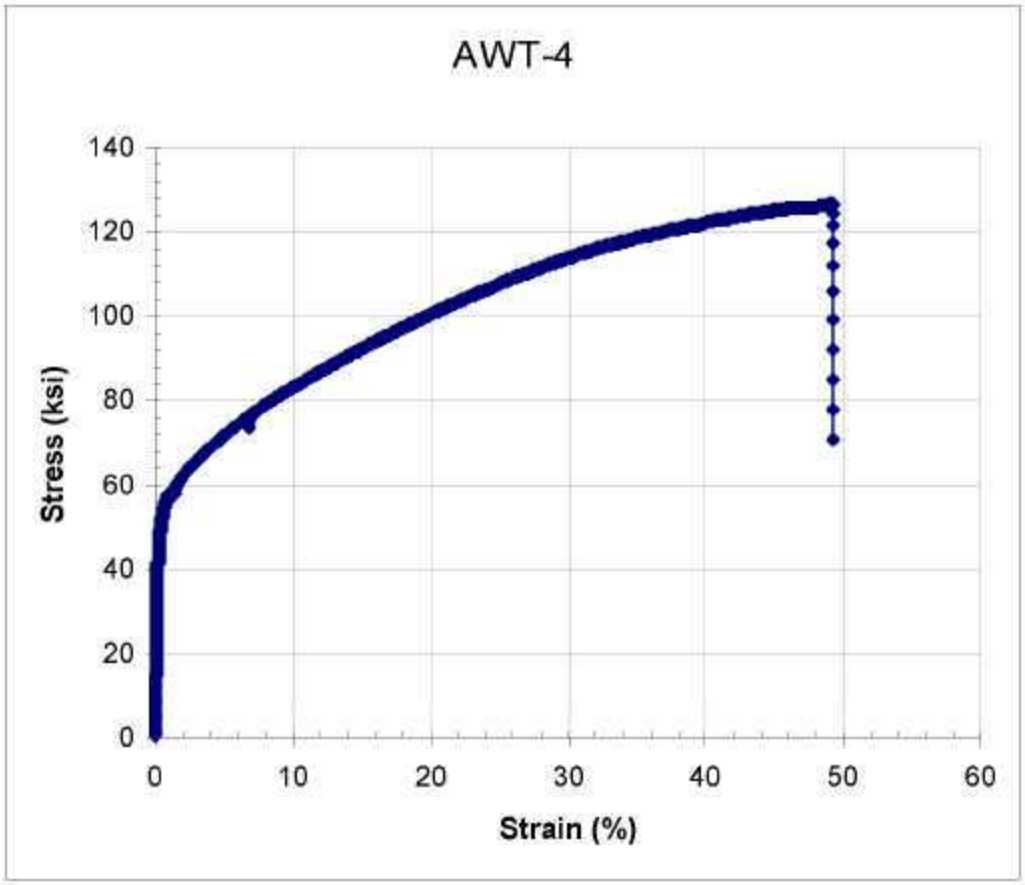

Test ID	Product Form	Aging Temp. (°C)	Aging Time (hours)	Test Temp. (°C)	Prop. Limit (MPa)	Yield Strength (MPa)	Ultimate Tensile Strength (MPa)	Uniform Elong. (%)	Elong. (%)	Red. of Area (%)	Failure Location
LWT-5	Bar Weld	675	6000	20		822	1058	4.5	4.5		BM

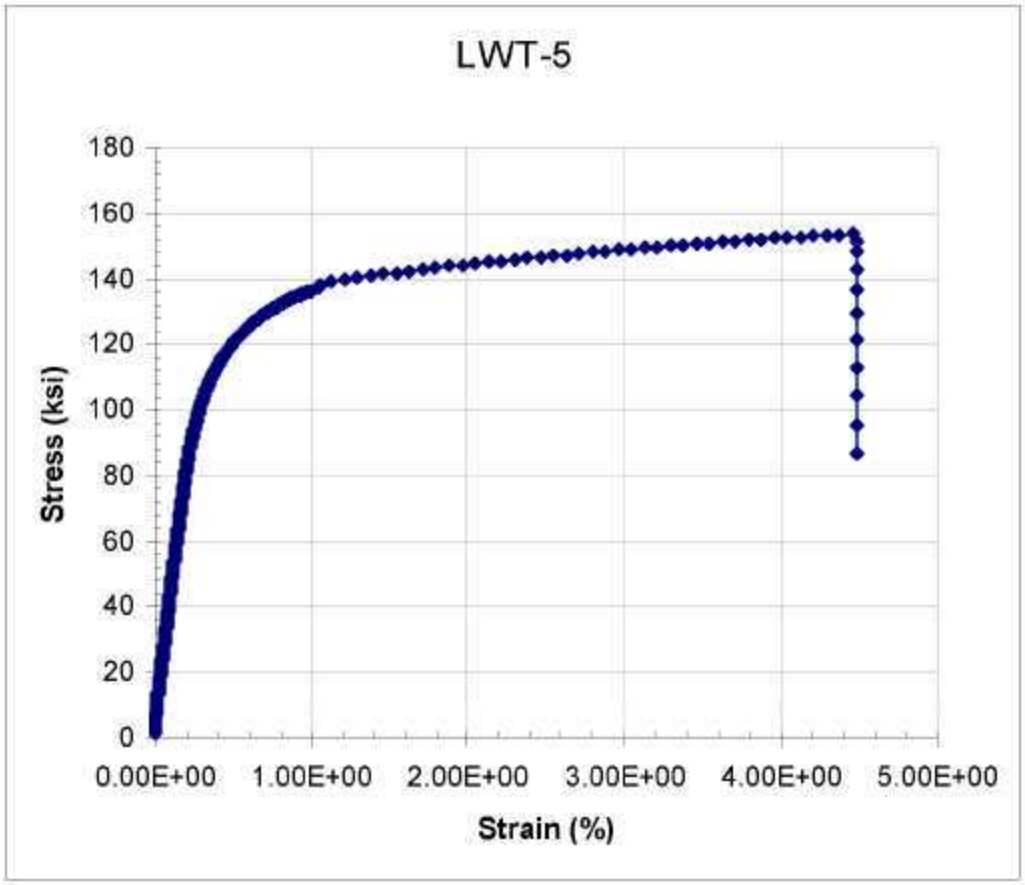

Test ID	Product Form	Aging Temp. (°C)	Aging Time (hours)	Test Temp. (°C)	Prop. Limit (MPa)	Yield Strength (MPa)	Ultimate Tensile Strength (MPa)	Uniform Elong. (%)	Elong. (%)	Red. of Area (%)	Failure Location
AWT-5	Bar Weld	675	6000	20		834	1073	4.3	4.3		BM

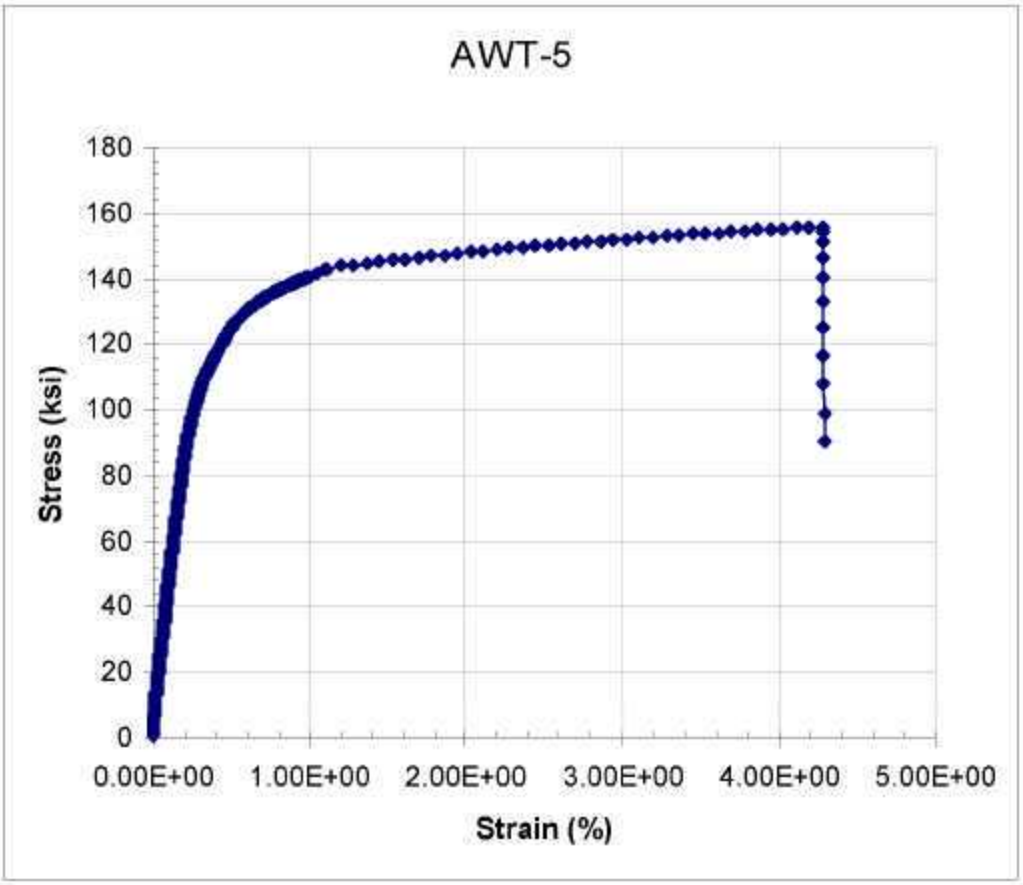

Test ID	Product Form	Aging Temp. (°C)	Aging Time (hours)	Test Temp. (°C)	Prop. Limit (MPa)	Yield Strength (MPa)	Ultimate Tensile Strength (MPa)	Uniform Elong. (%)	Elong. (%)	Red. of Area (%)	Failure Location
LWT-6	Bar Weld	675	6000	650		575	929	11.8	11.8		BM

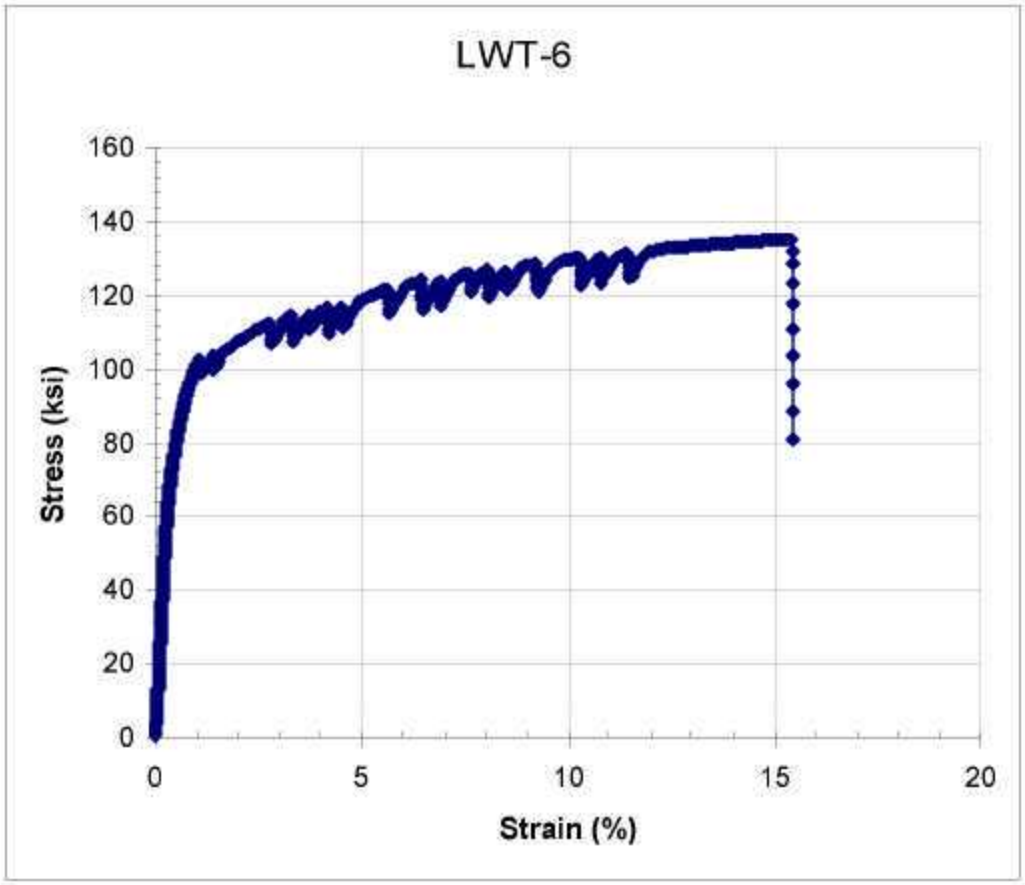

Test ID	Product Form	Aging Temp. (°C)	Aging Time (hours)	Test Temp. (°C)	Prop. Limit (MPa)	Yield Strength (MPa)	Ultimate Tensile Strength (MPa)	Uniform Elong. (%)	Elong. (%)	Red. of Area (%)	Failure Location
AWT-6	Bar Weld	675	6000	650		564	931	15.1	15.4		BM

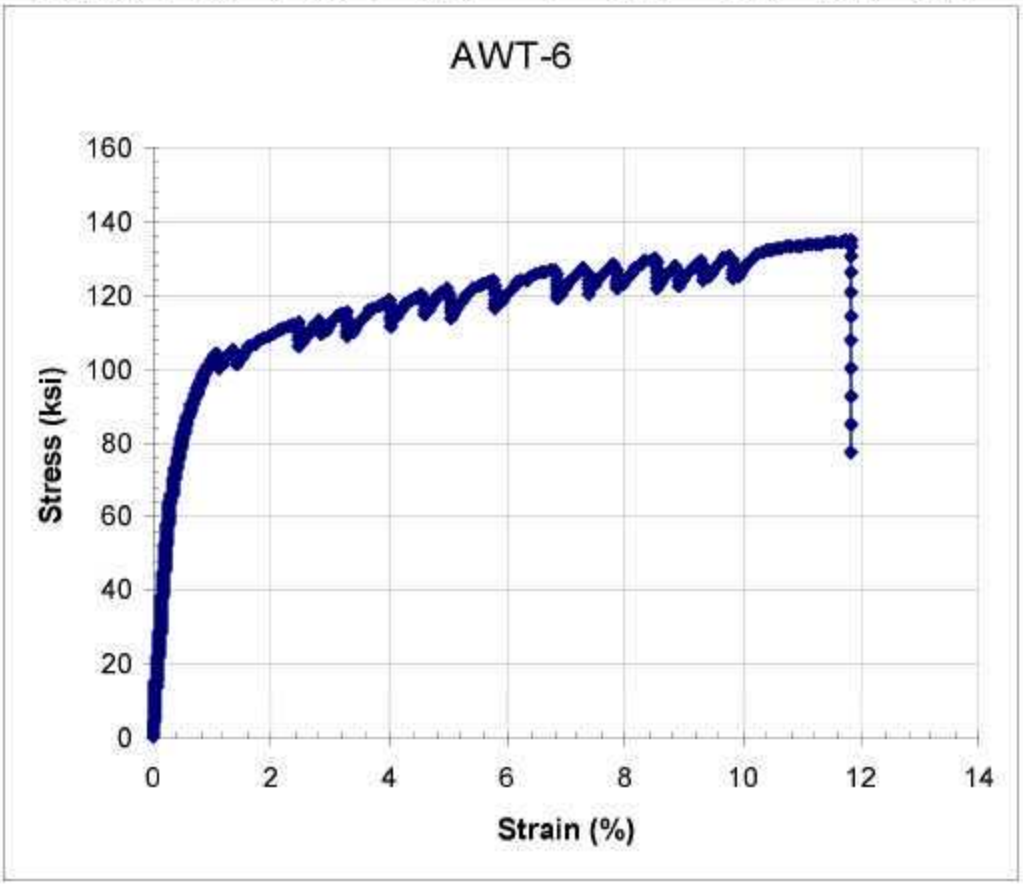

A.6 CREEP STRAIN VS. TIME CURVES

Test ID	Product Form	Aging Temp. (°C)	Aging Time (hours)	Test Temp. (°C)	Stress (MPa)	Rupture Life (hours) stopped or ongoing	Minimum Creep Rate (%/hr)	Elong. (%)	Red. of Area (%)	Failure Location
CR-BM-01	sheet	none	none	650	206.8	38557.0	2.60E-05	2.8	4.5	

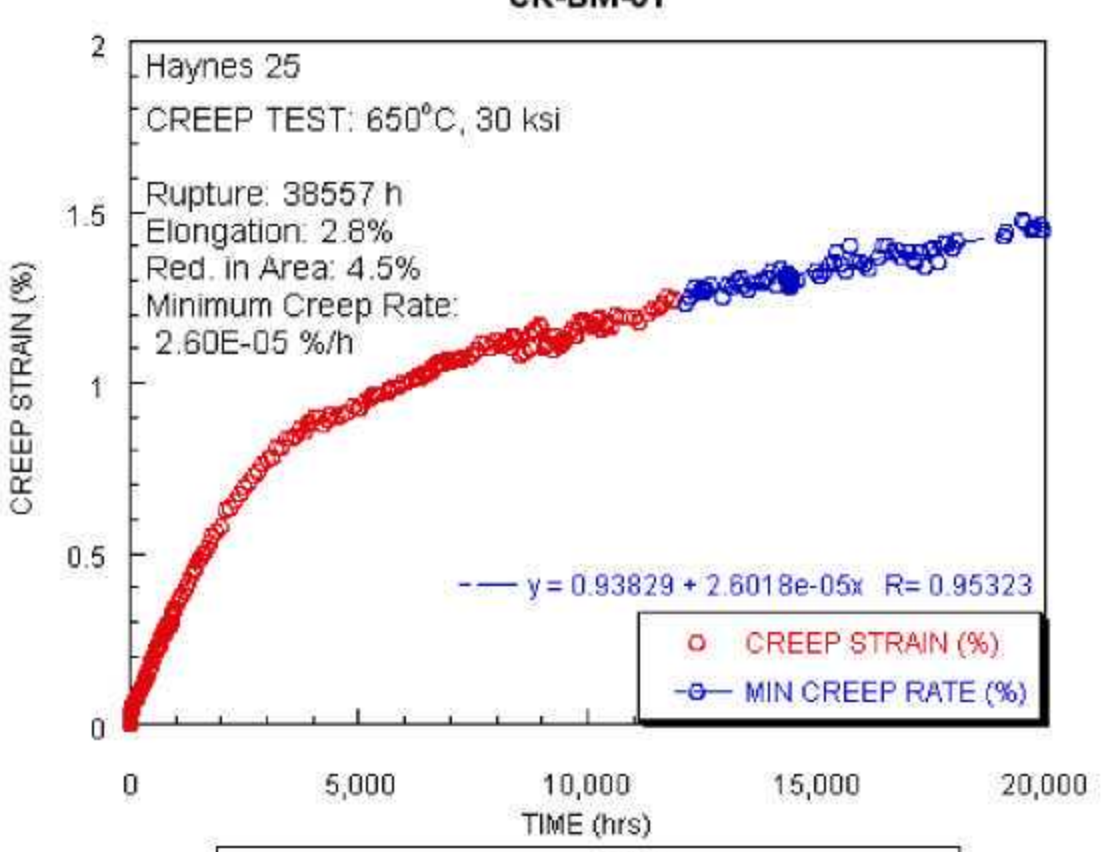

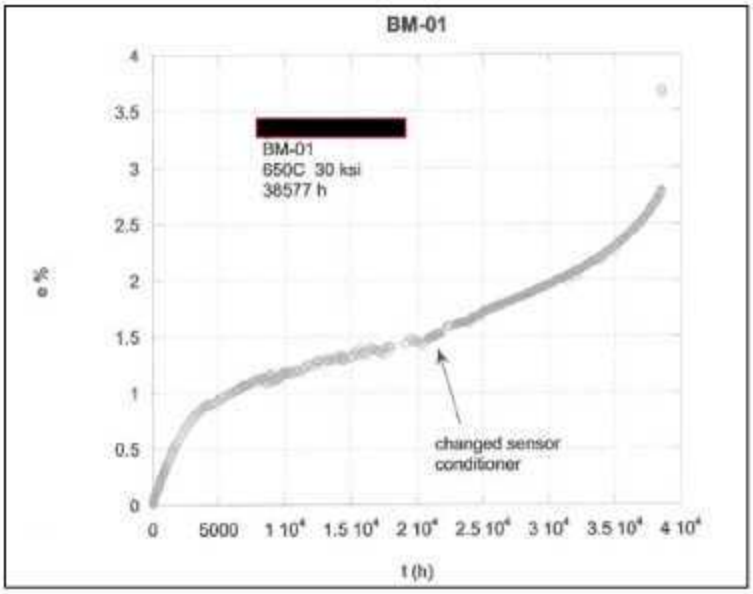

Test ID	Product Form	Aging Temp. (°C)	Aging Time (hours)	Test Temp. (°C)	Stress (MPa)	Rupture Life (hours) stopped or ongoing	Minimum Creep Rate (%/hr)	Elong. (%)	Red. of Area (%)	Failure Location
CR-BM-02	sheet	none	none	700	165.5	20637.0	1.00E-05	4.9	3.9	

CR-BM-02

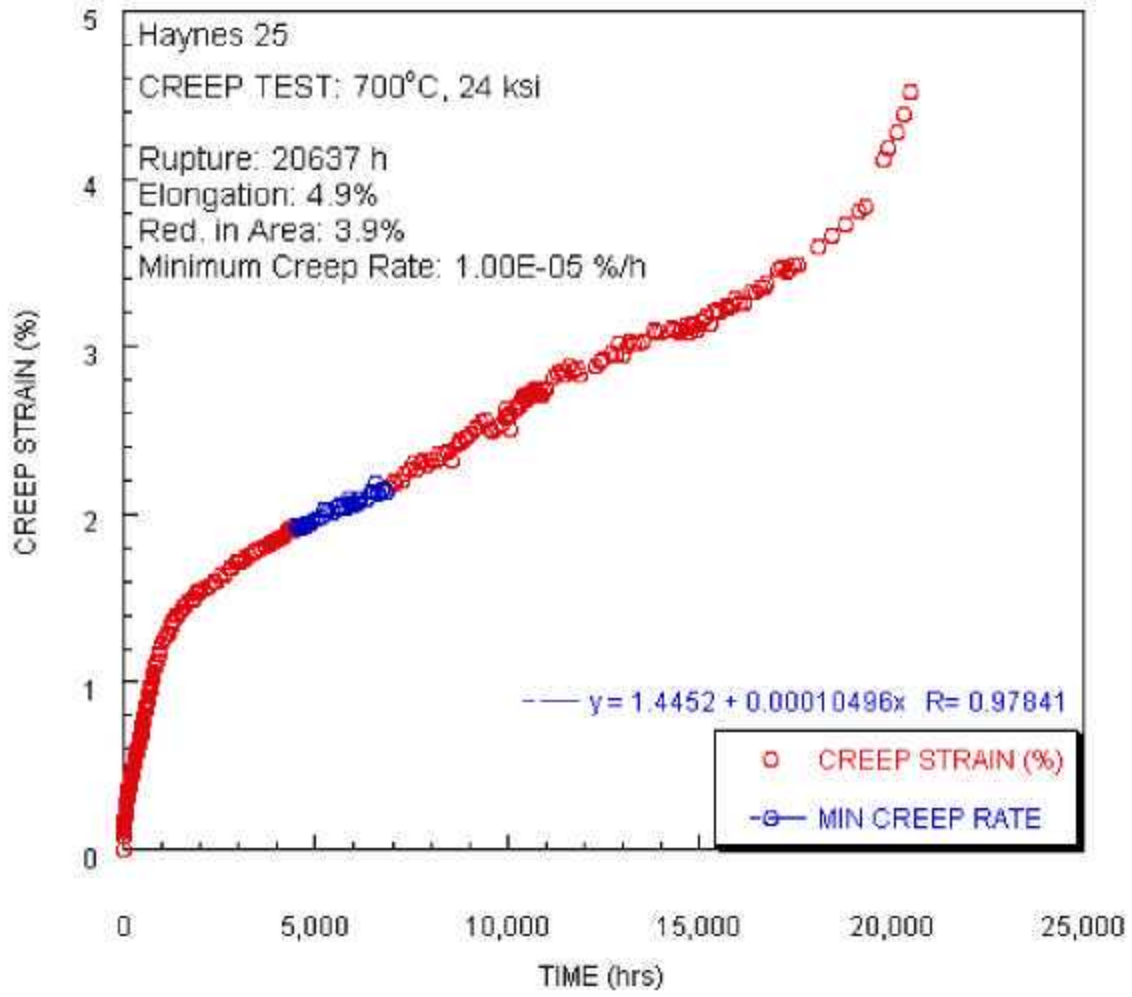

Test ID	Product Form	Aging Temp. (°C)	Aging Time (hours)	Test Temp. (°C)	Stress (MPa)	Rupture Life (hours) stopped or ongoing	Minimum Creep Rate (%/hr)	Elong. (%)	Red. of Area (%)	Failure Location
CR-BM-03	sheet	none	none	750	127.6	8786.0	5.30E-04	10.9	8.3	

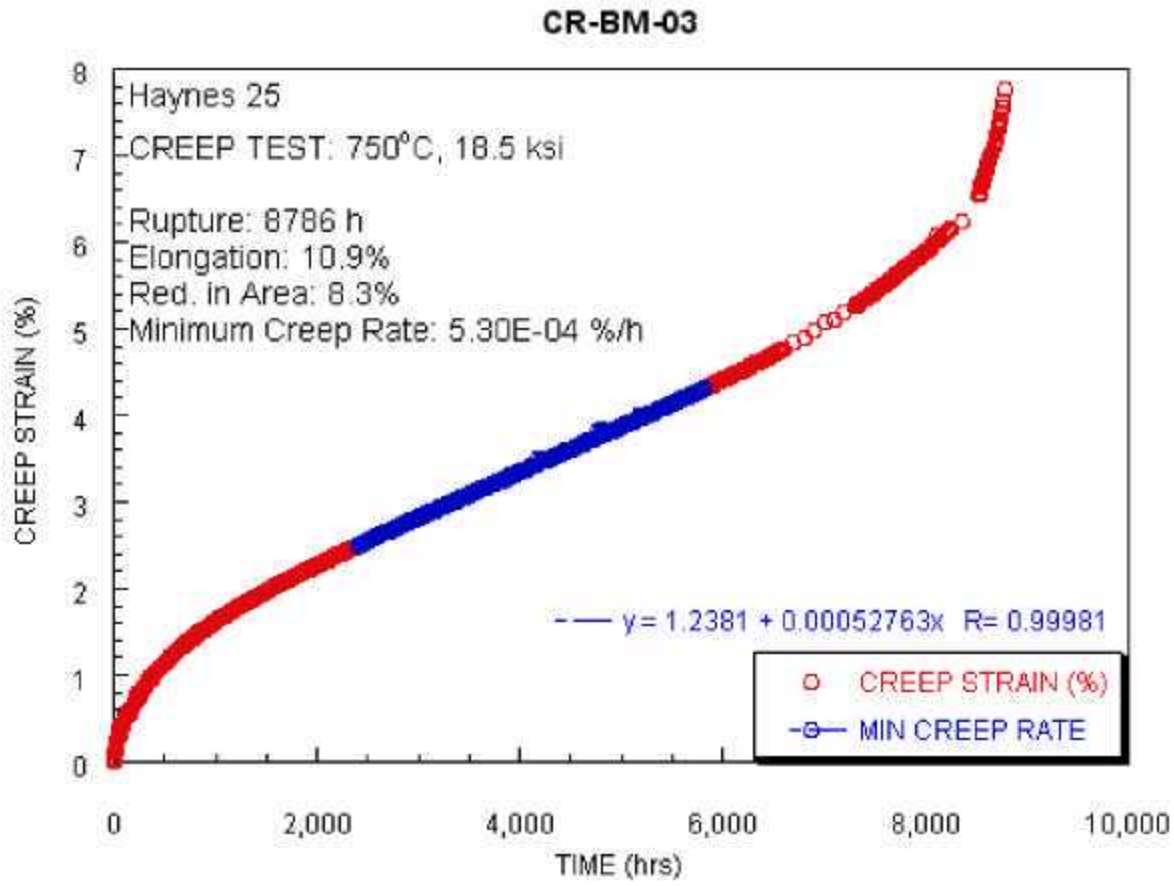

Test ID	Product Form	Aging Temp. (°C)	Aging Time (hours)	Test Temp. (°C)	Stress (MPa)	Rupture Life (hours) stopped or ongoing	Minimum Creep Rate (%/hr)	Elong. (%)	Red. of Area (%)	Failure Location
CR-BM-04	sheet	none	none	800	99.3	4983.0	8.50E-04	11.5	10.2	

CR-BM-04

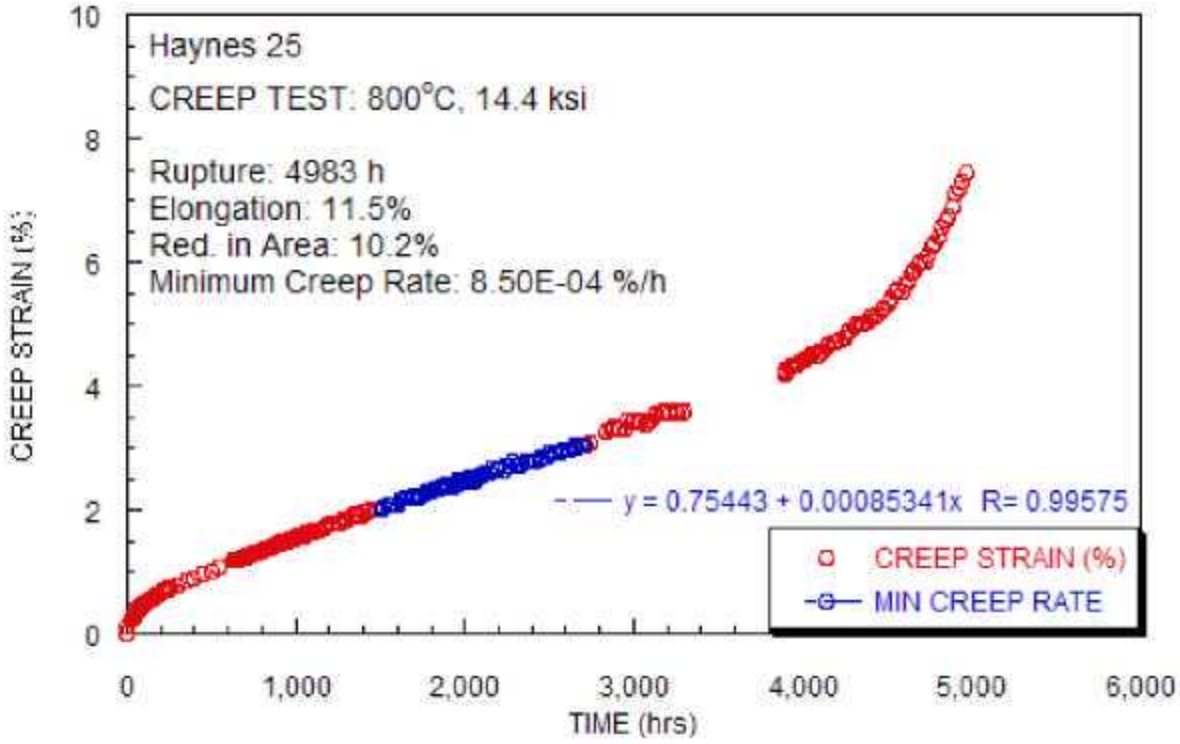

Test ID	Product Form	Aging Temp. (°C)	Aging Time (hours)	Test Temp. (°C)	Stress (MPa)	Rupture Life (hours) stopped or ongoing	Minimum Creep Rate (%/hr)	Elong. (%)	Red. of Area (%)	Failure Location
CR-BM-05	sheet	none	none	800	103.4	3626.0	1.10E-03	12.8	12.2	

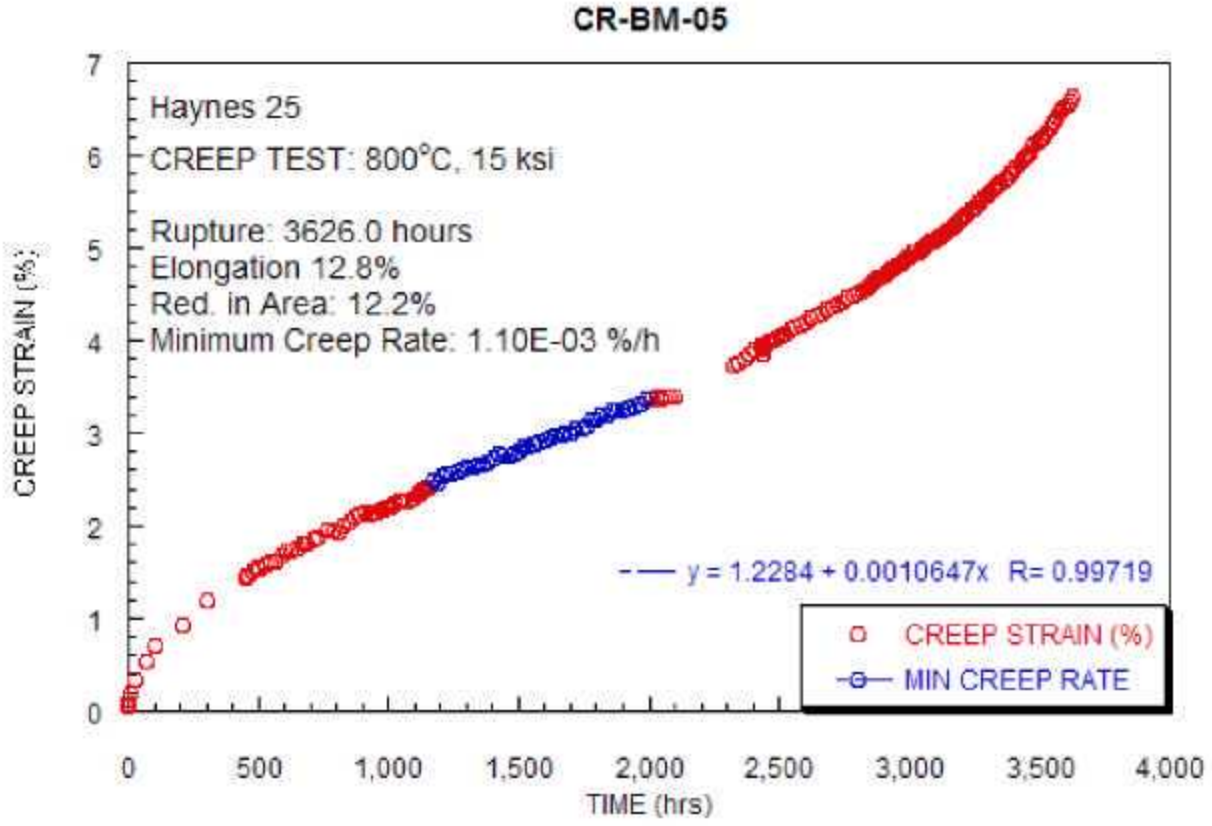

Test ID	Product Form	Aging Temp. (°C)	Aging Time (hours)	Test Temp. (°C)	Stress (MPa)	Rupture Life (hours) stopped or ongoing	Minimum Creep Rate (%/hr)	Elong. (%)	Red. of Area (%)	Failure Location
CR-BM-06	sheet	none	none	850	62.1	8975.0	1.30E-04	6.9	2.7	

CR-BM-06

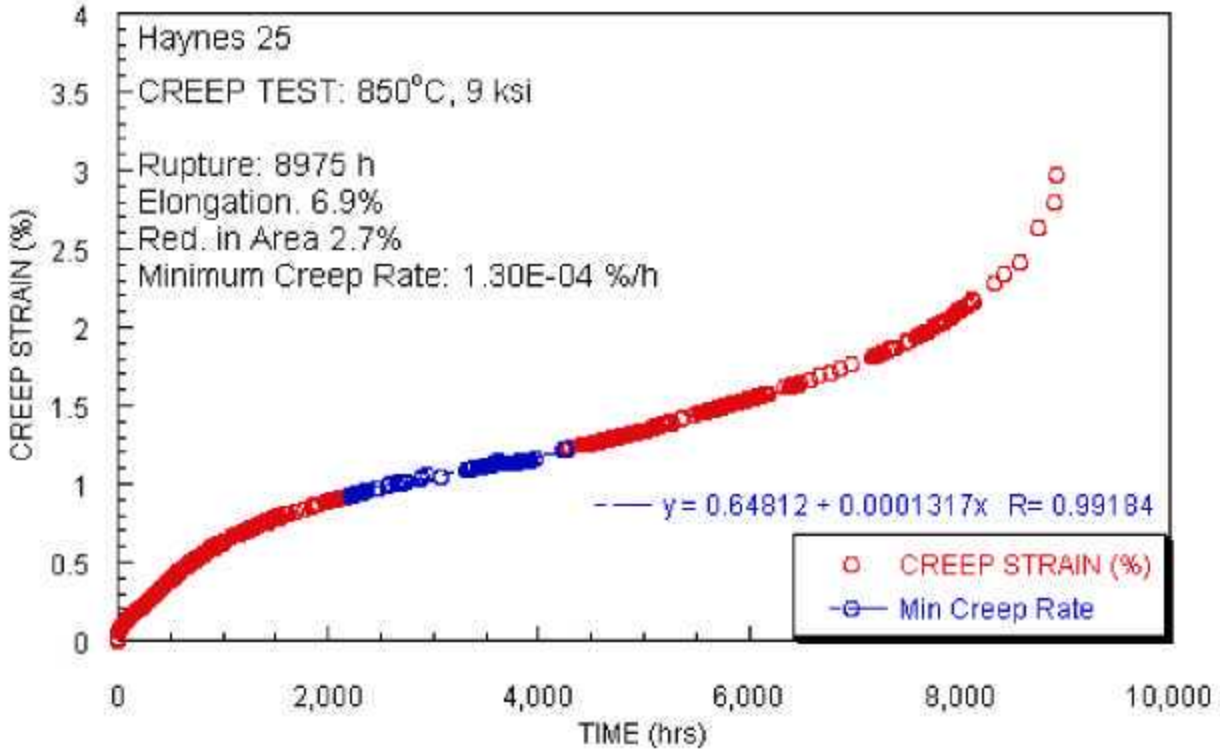

Test ID	Product Form	Aging Temp. (°C)	Aging Time (hours)	Test Temp. (°C)	Stress (MPa)	Rupture Life (hours) stopped or ongoing	Minimum Creep Rate (%/hr)	Elong. (%)	Red. of Area (%)	Failure Location
CR-BM-07	sheet	none	none	875	53.8	5763.0	1.90E-04	7.0	5.0	

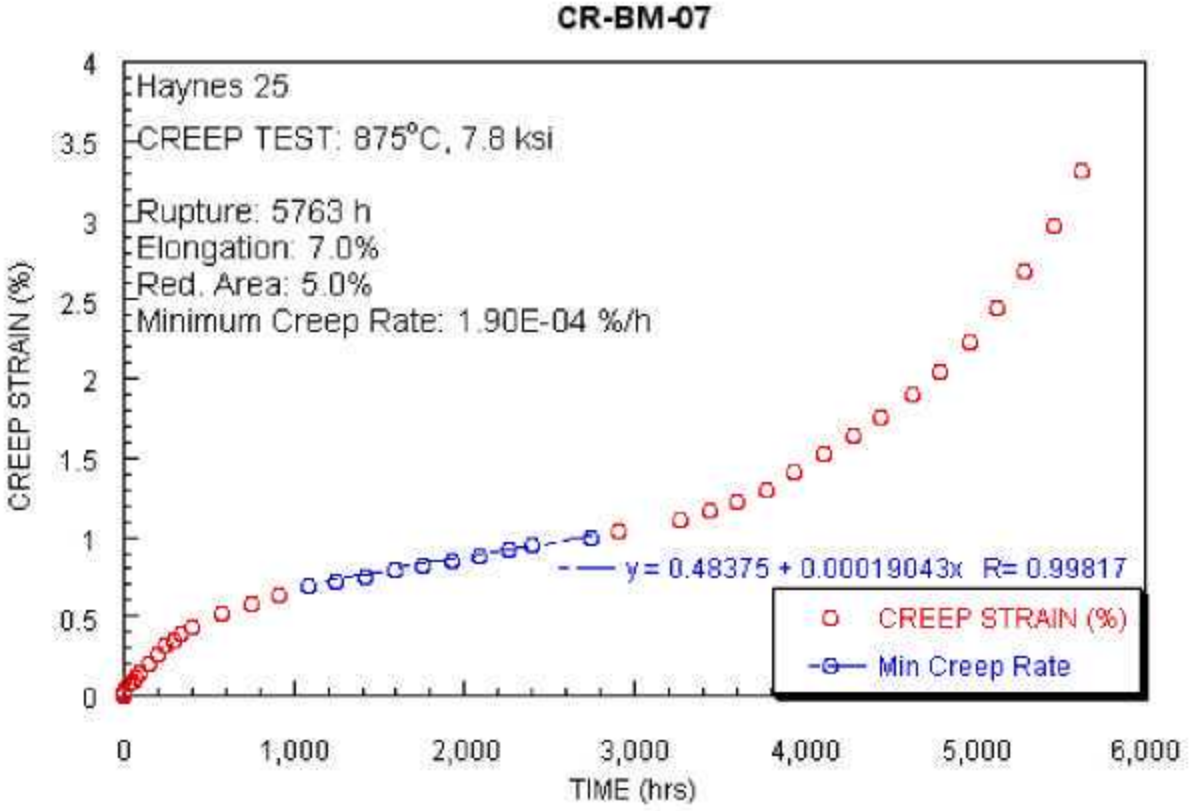

Test ID	Product Form	Aging Temp. (°C)	Aging Time (hours)	Test Temp. (°C)	Stress (MPa)	Rupture Life (hours) stopped or ongoing	Minimum Creep Rate (%/hr)	Elong. (%)	Red. of Area (%)	Failure Location
CR-BM-08	sheet	none	none	900	44.8	6232.0	2.70E-04	12.0	8.4	

CR-BM-08

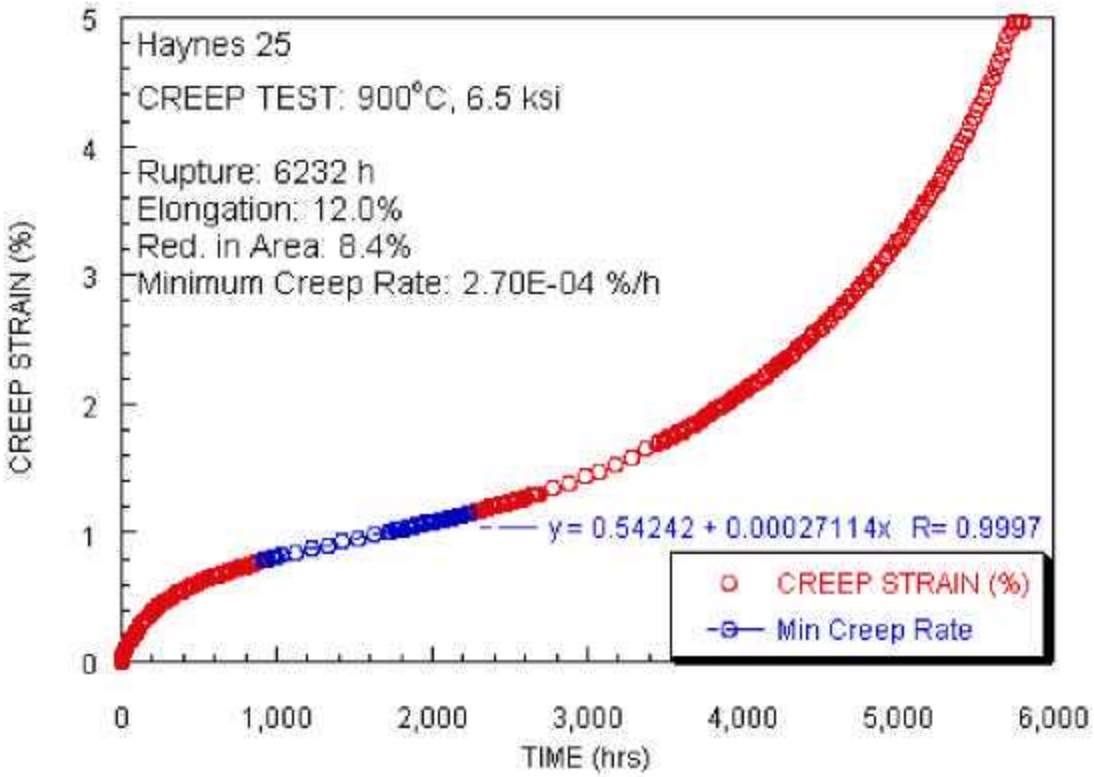

Test ID	Product Form	Aging Temp. (°C)	Aging Time (hours)	Test Temp. (°C)	Stress (MPa)	Rupture Life (hours) stopped or ongoing	Minimum Creep Rate (%/hr)	Elong. (%)	Red. of Area (%)	Failure Location
CR-BM-09	sheet	none	none	900	42.7	6585.0	1.50E-04	6.1	5.7	

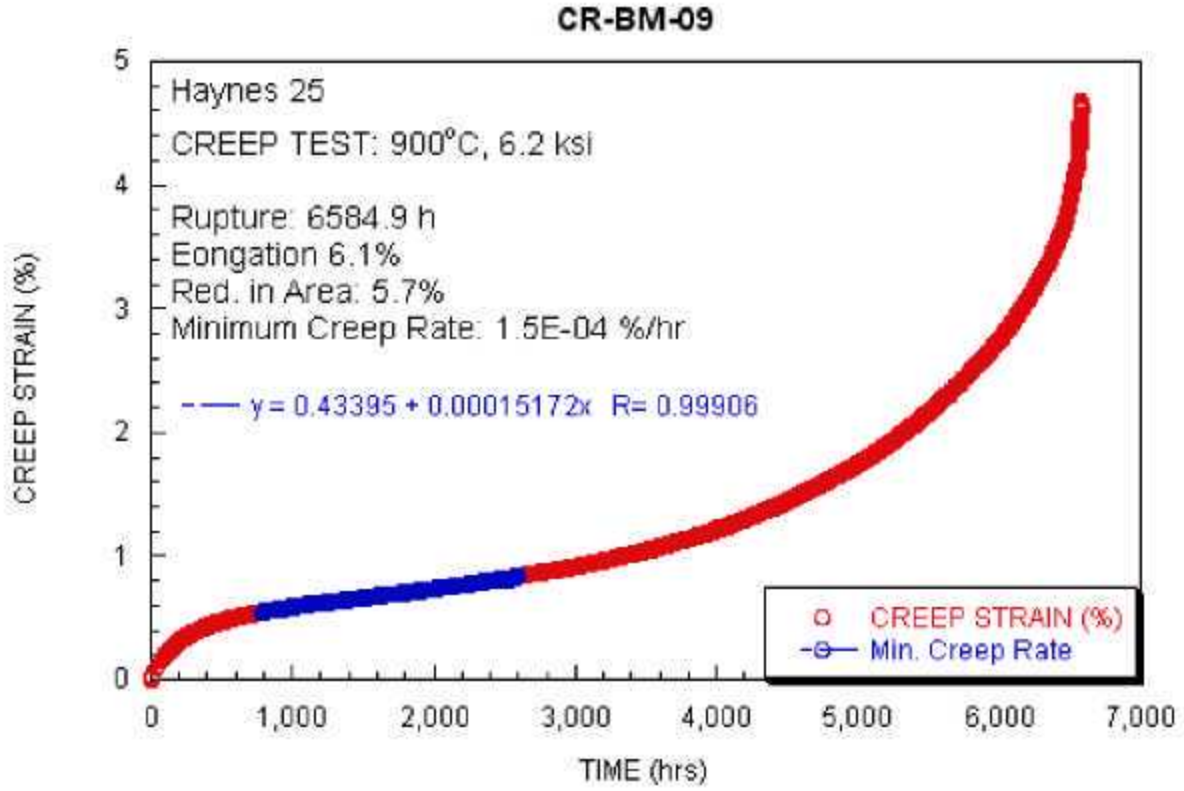

Test ID	Product Form	Aging Temp. (°C)	Aging Time (hours)	Test Temp. (°C)	Stress (MPa)	Rupture Life (hours) stopped or ongoing	*Minimum Creep Rate (%/hr)*	Elong. (%)	Red. of Area (%)	Failure Location
CR-BM-11*	sheet	none	none	925	34.5	6253.0	*2.7E-04*	10.6	8.8	

CR-BM-11

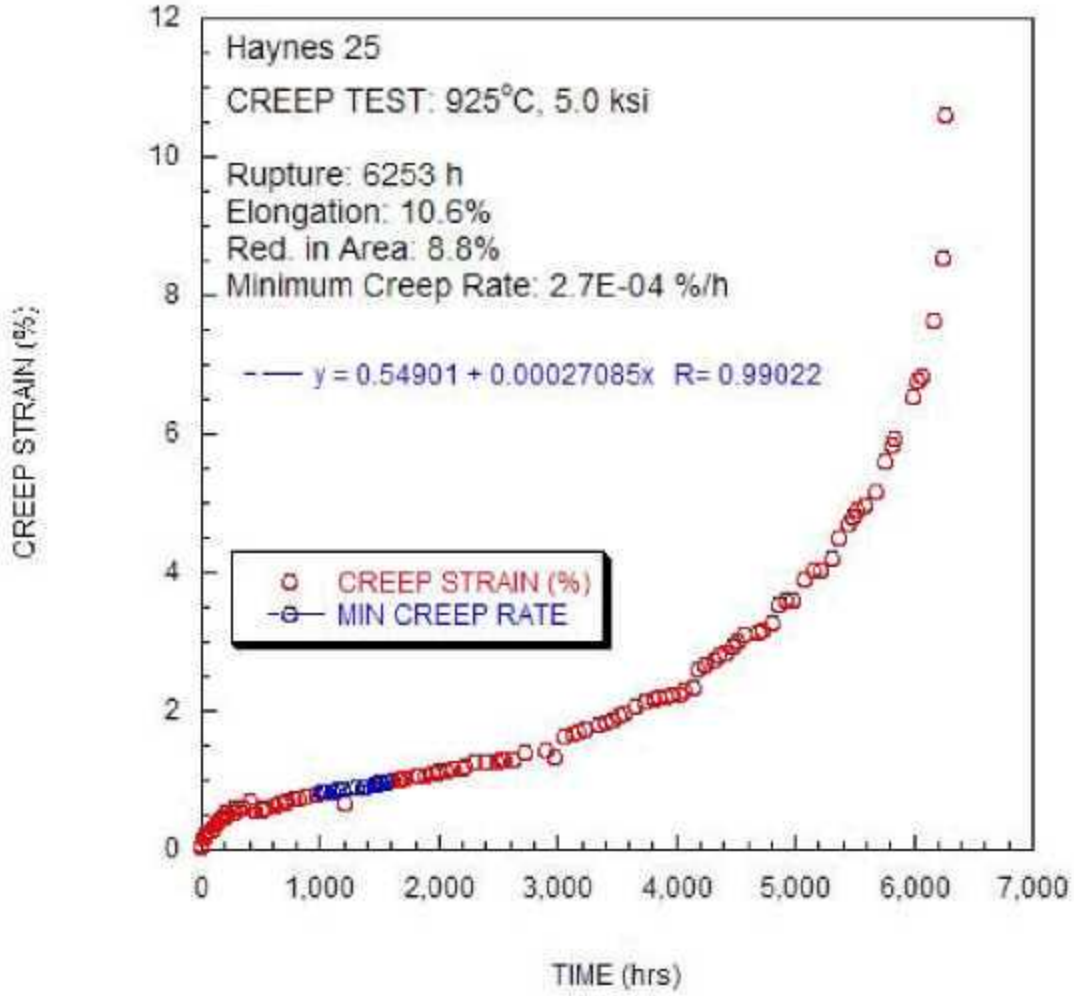

** Test performed in Argon, creep strain and minimum creep rate based on load-line displacement*

Test ID	Product Form	Aging Temp. (°C)	Aging Time (hours)	Test Temp. (°C)	Stress (MPa)	Rupture Life (hours) stopped or ongoing	*Minimum Creep Rate (%/hr)*	Elong. (%)	Red. of Area (%)	Failure Location
CR-BM-12*	sheet	none	none	925	33.1	7436.8	*1.70E-04*	9.0	6.5	

CR-BM-12

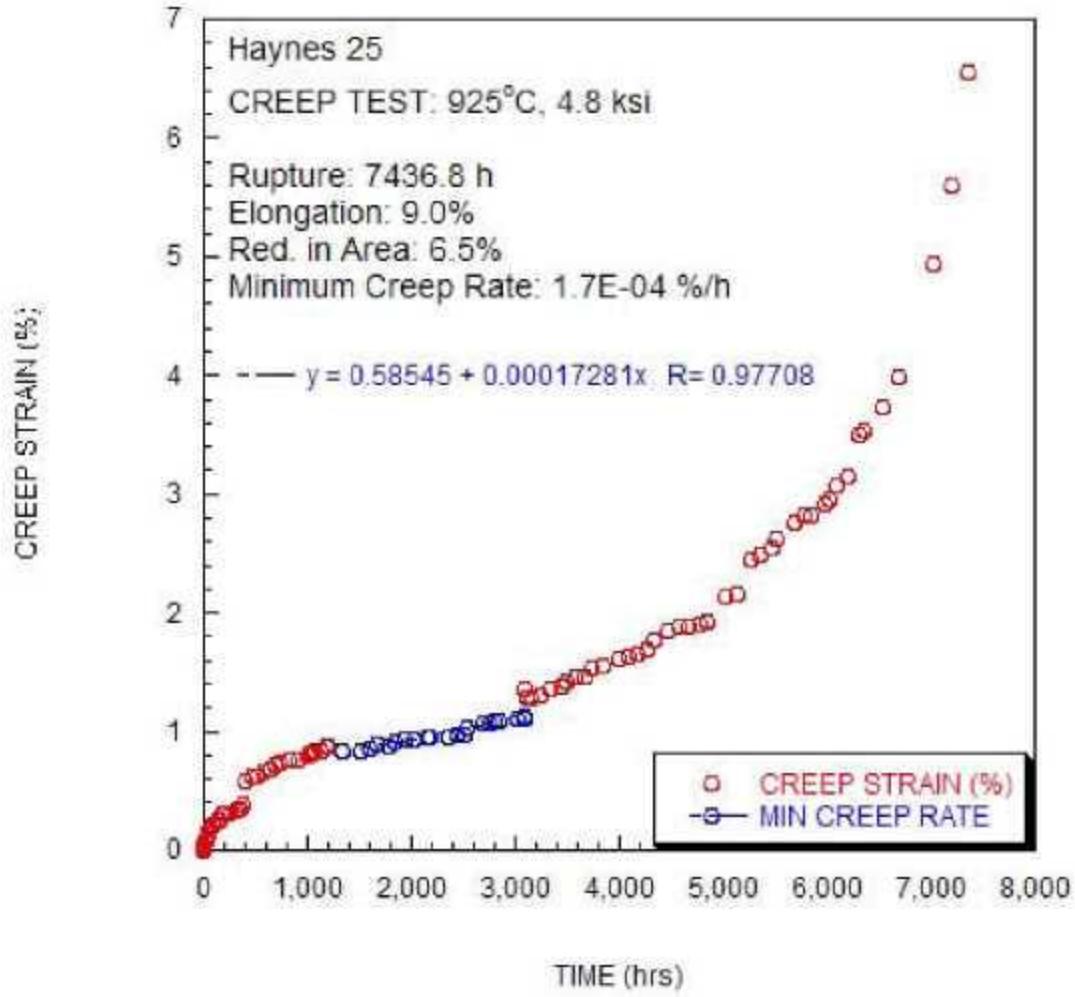

** Test performed in Argon, creep strain and minimum creep rate based on load-line displacement*

Test ID	Product Form	Aging Temp. (°C)	Aging Time (hours)	Test Temp. (°C)	Stress (MPa)	Rupture Life (hours) stopped or ongoing	*Minimum Creep Rate (%/hr)*	Elong. (%)	Red. of Area (%)	Failure Location
CR-BM-14*	sheet	none	none	950	29.0	4095.0	*3.60E-04*	8.1	9.3	

CR-BM-14

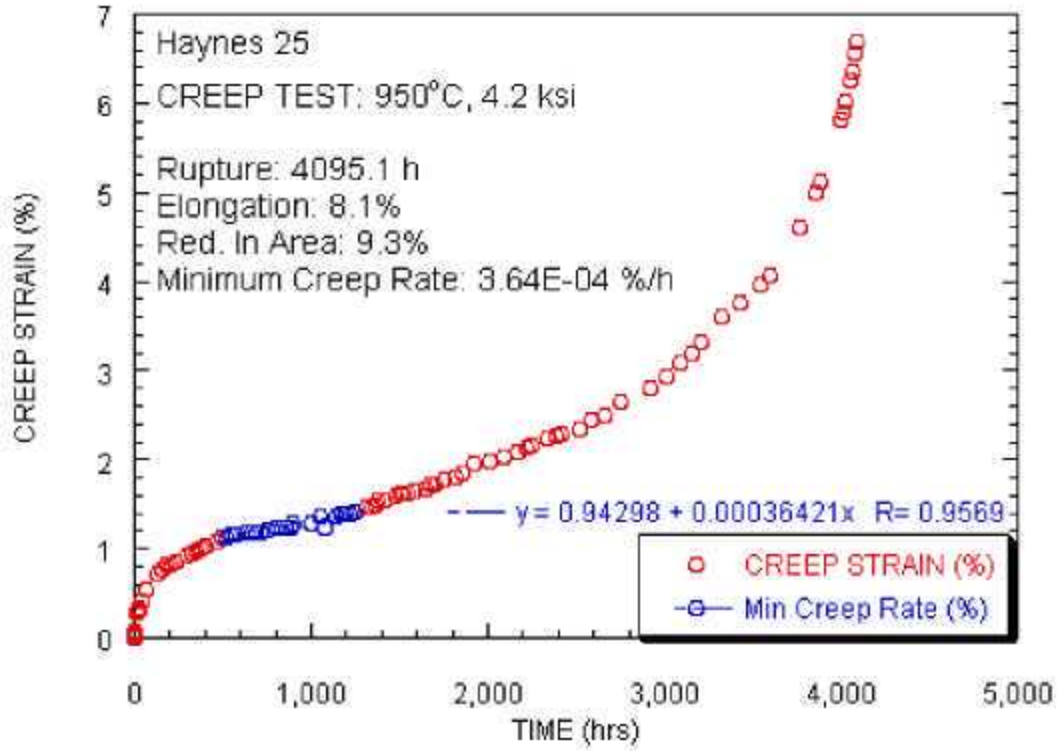

** Test performed in Argon, creep strain and minimum creep rate based on load-line displacement*

Test ID	Product Form	Aging Temp. (°C)	Aging Time (hours)	Test Temp. (°C)	Stress (MPa)	Rupture Life (hours) stopped or ongoing	Minimum Creep Rate (%/hr)	Elong. (%)	Red. of Area (%)	Failure Location
TN30440	sheet	none	none	750	220.6	498.4	3.90E-02	33.6	25.2	

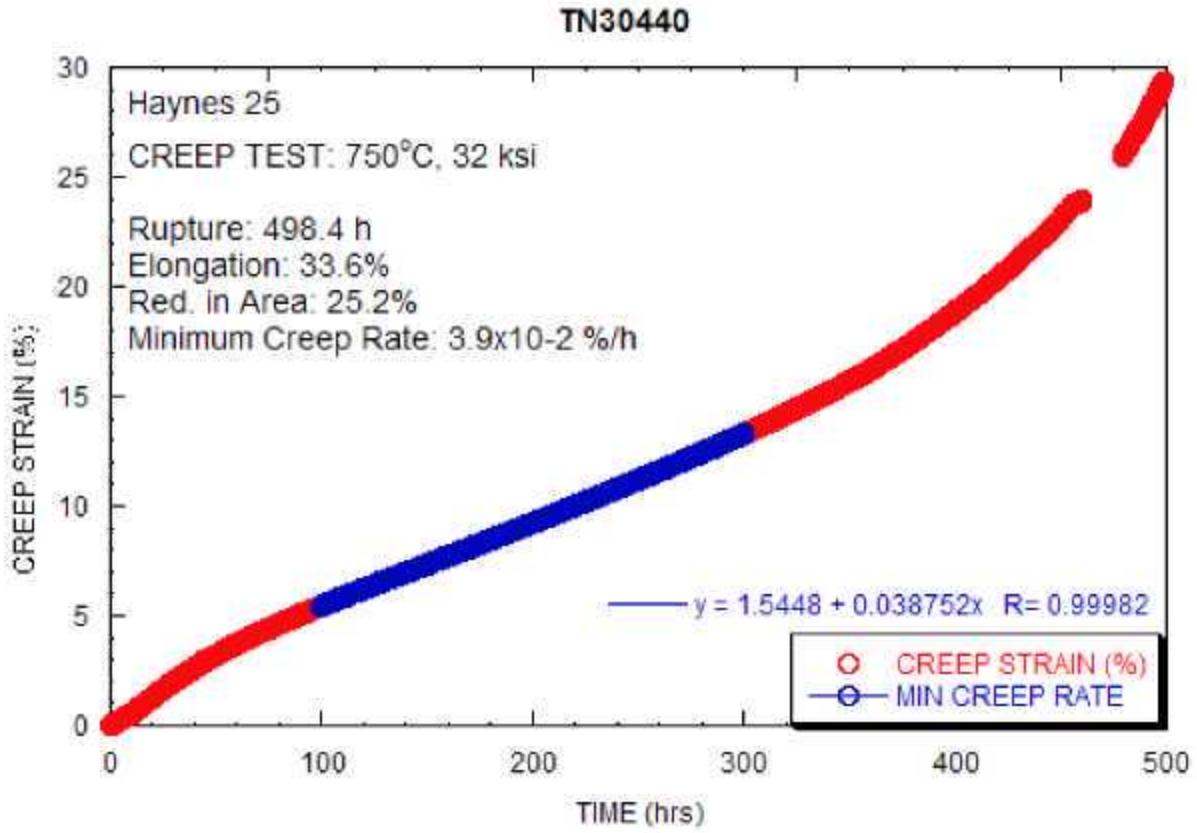

Test ID	Product Form	Aging Temp. (°C)	Aging Time (hours)	Test Temp. (°C)	Stress (MPa)	Rupture Life (hours) stopped or ongoing	Minimum Creep Rate (%/hr)	Elong. (%)	Red. of Area (%)	Failure Location
TN29885	sheet	none	none	800	186.2	144.4	1.70E-01	45.3	47.6	

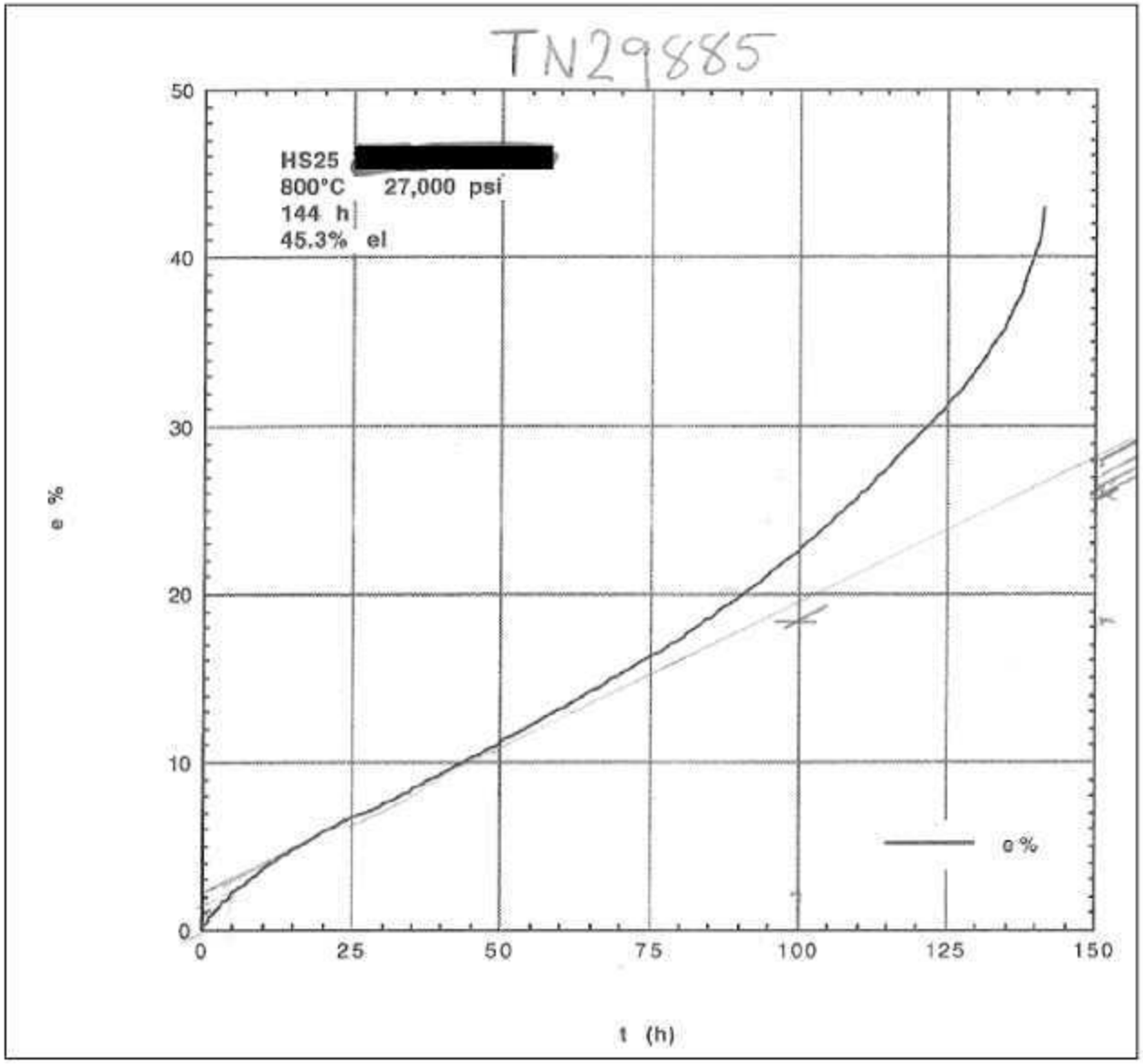

Test ID	Product Form	Aging Temp. (°C)	Aging Time (hours)	Test Temp. (°C)	Stress (MPa)	Rupture Life (hours) stopped or ongoing	Minimum Creep Rate (%/hr)	Elong. (%)	Red. of Area (%)	Failure Location
TN30215	sheet	none	none	750	217.2	436.8	4.90E-02	32.0	32.7	

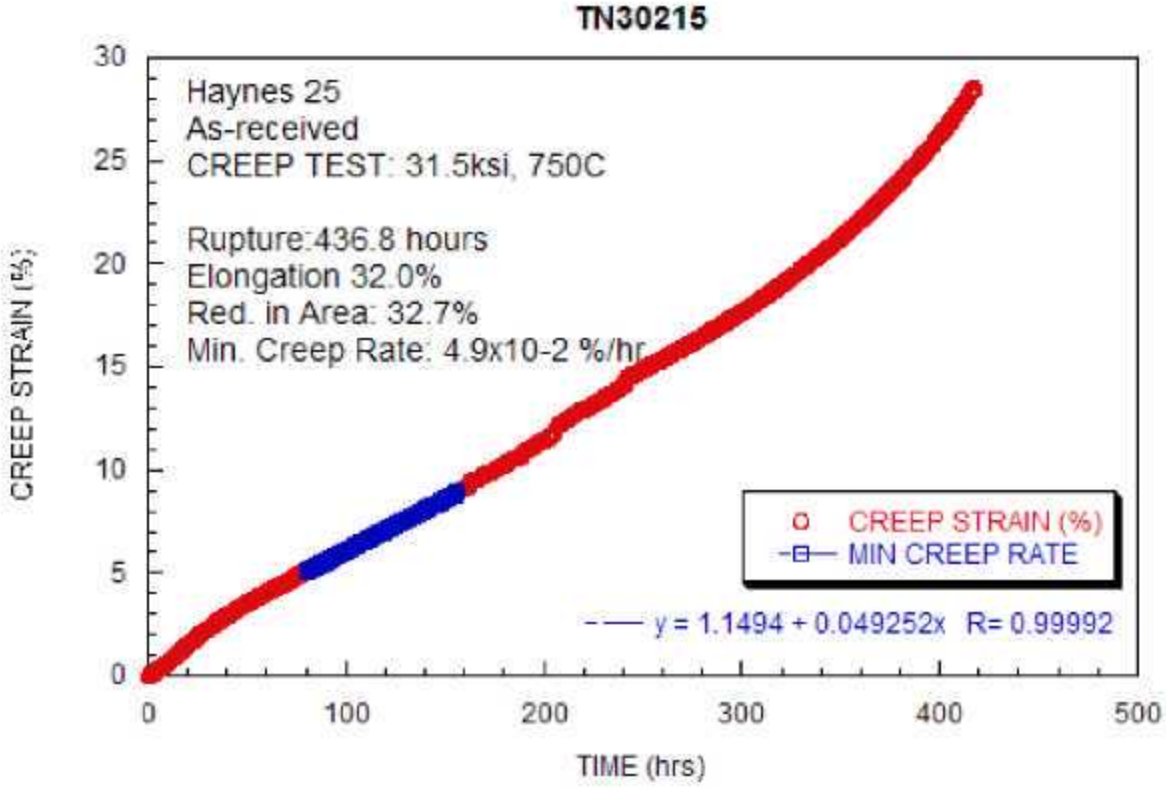

Test ID	Product Form	Aging Temp. (°C)	Aging Time (hours)	Test Temp. (°C)	Stress (MPa)	Rupture Life (hours) stopped or ongoing	Minimum Creep Rate (%/hr)	Elong. (%)	Red. of Area (%)	Failure Location
TN30420	sheet	none	none	850	151.7	57.6	3.60E-01	46.7	48.3	

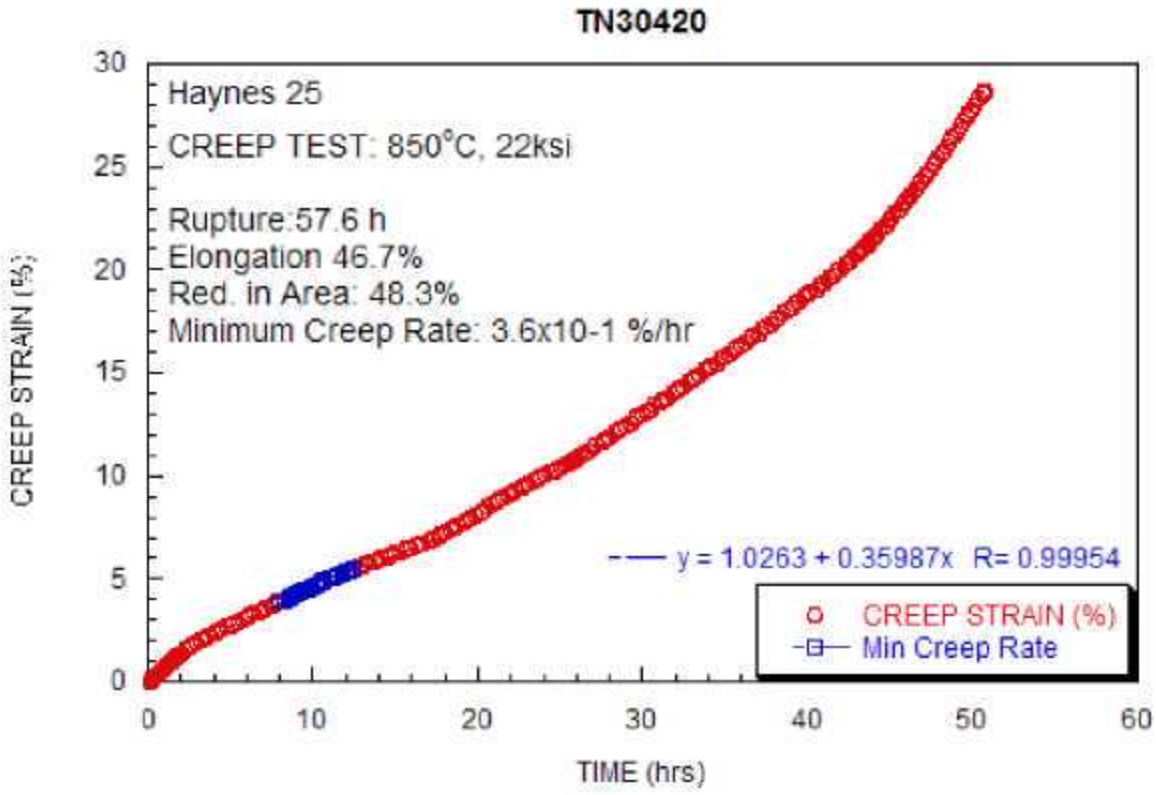

Test ID	Product Form	Aging Temp. (°C)	Aging Time (hours)	Test Temp. (°C)	Stress (MPa)	Rupture Life (hours) stopped or ongoing	Minimum Creep Rate (%/hr)	Elong. (%)	Red. of Area (%)	Failure Location
TN30138	sheet	none	none	750	193.1	745.0	1.60E-02	21.3	19.7	

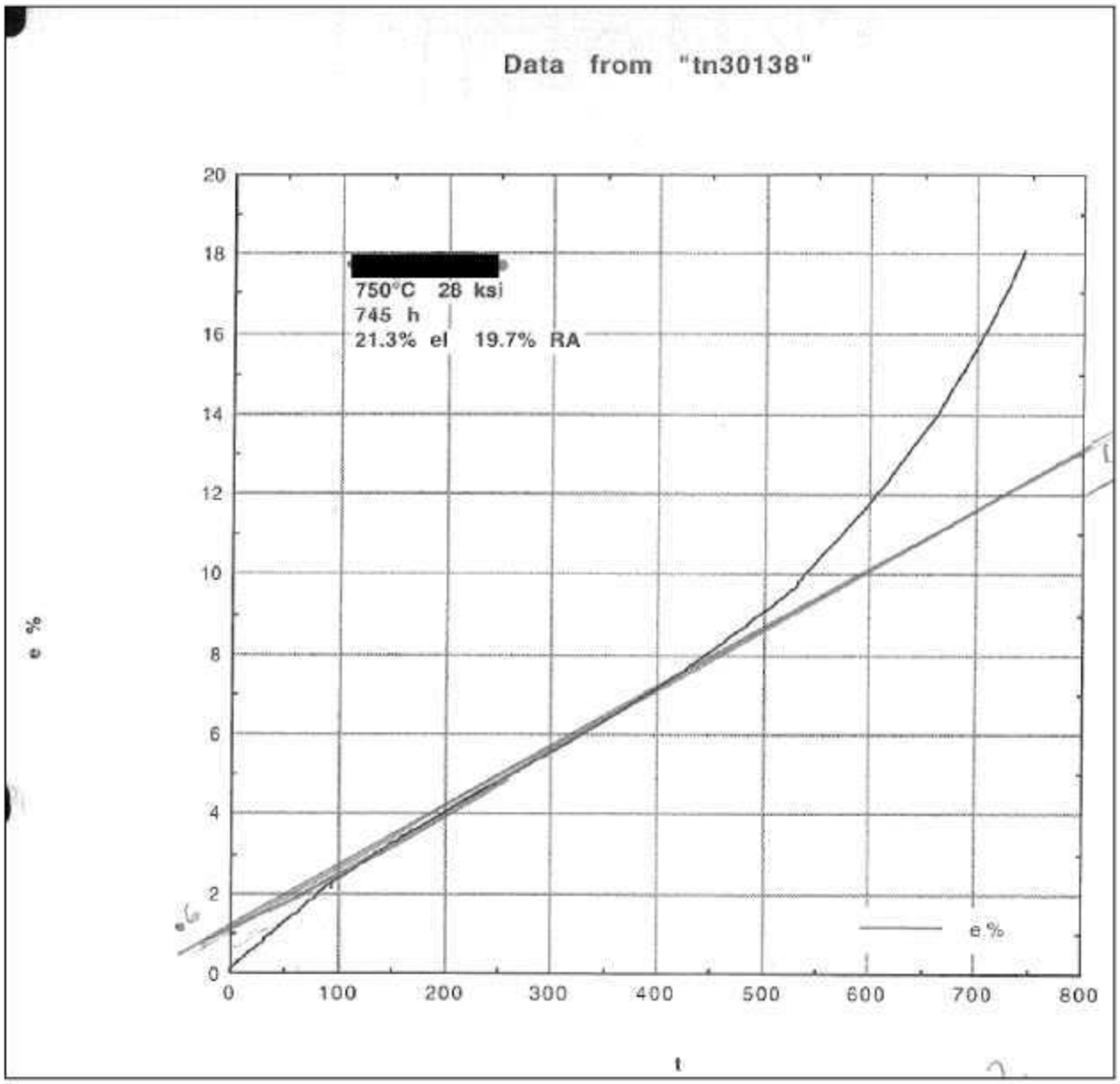

Test ID	Product Form	Aging Temp. (°C)	Aging Time (hours)	Test Temp. (°C)	Stress (MPa)	*Rupture Life (hours) stopped or ongoing*	Minimum Creep Rate (%/hr)	Elong. (%)	Red. of Area (%)	Failure Location
MG-13	sheet	none	none	600	179.3	*9000.0*	1.8E-05			

MG-13

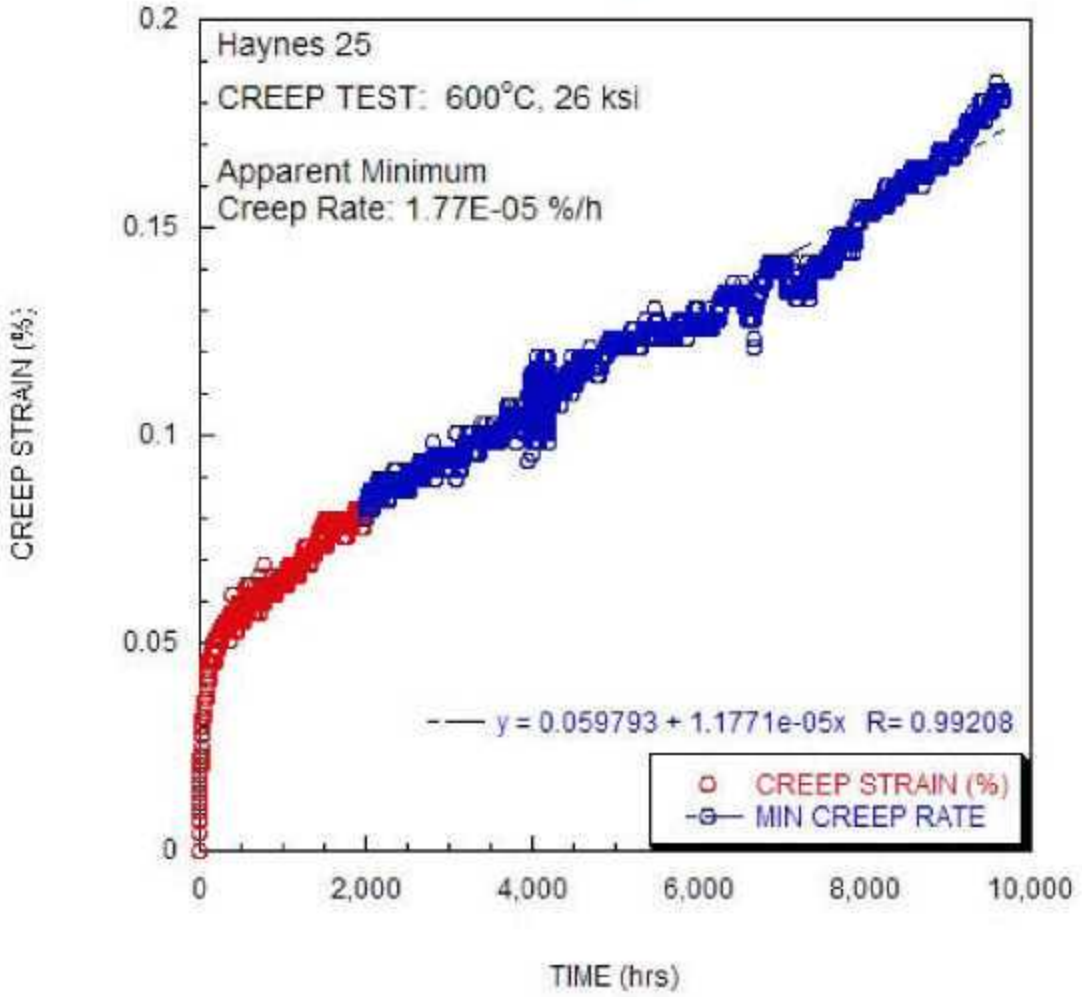

Test ID	Product Form	Aging Temp. (°C)	Aging Time (hours)	Test Temp. (°C)	Stress (MPa)	Rupture Life (hours) stopped or ongoing	Minimum Creep Rate (%/hr)	Elong. (%)	Red. of Area (%)	Failure Location
MG-14	sheet	none	none	600	206.8	12311.0	2.0E-05			

MG-14

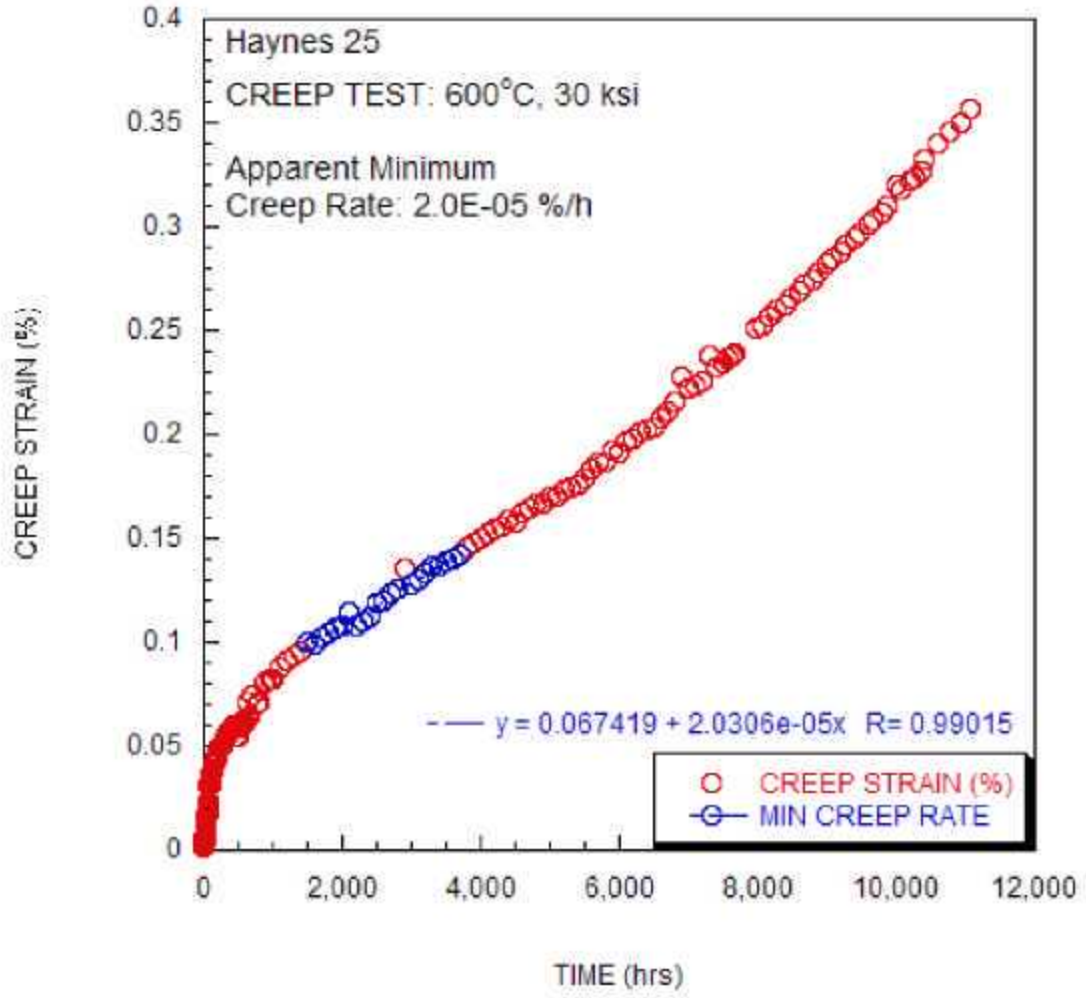

Test ID	Product Form	Aging Temp. (°C)	Aging Time (hours)	Test Temp. (°C)	Stress (MPa)	*Rupture Life (hours) stopped or ongoing*	Minimum Creep Rate (%/hr)	Elong. (%)	Red. of Area (%)	Failure Location
MG-15	sheet	none	none	625	144.8	*30000.0*	1.3E-05			

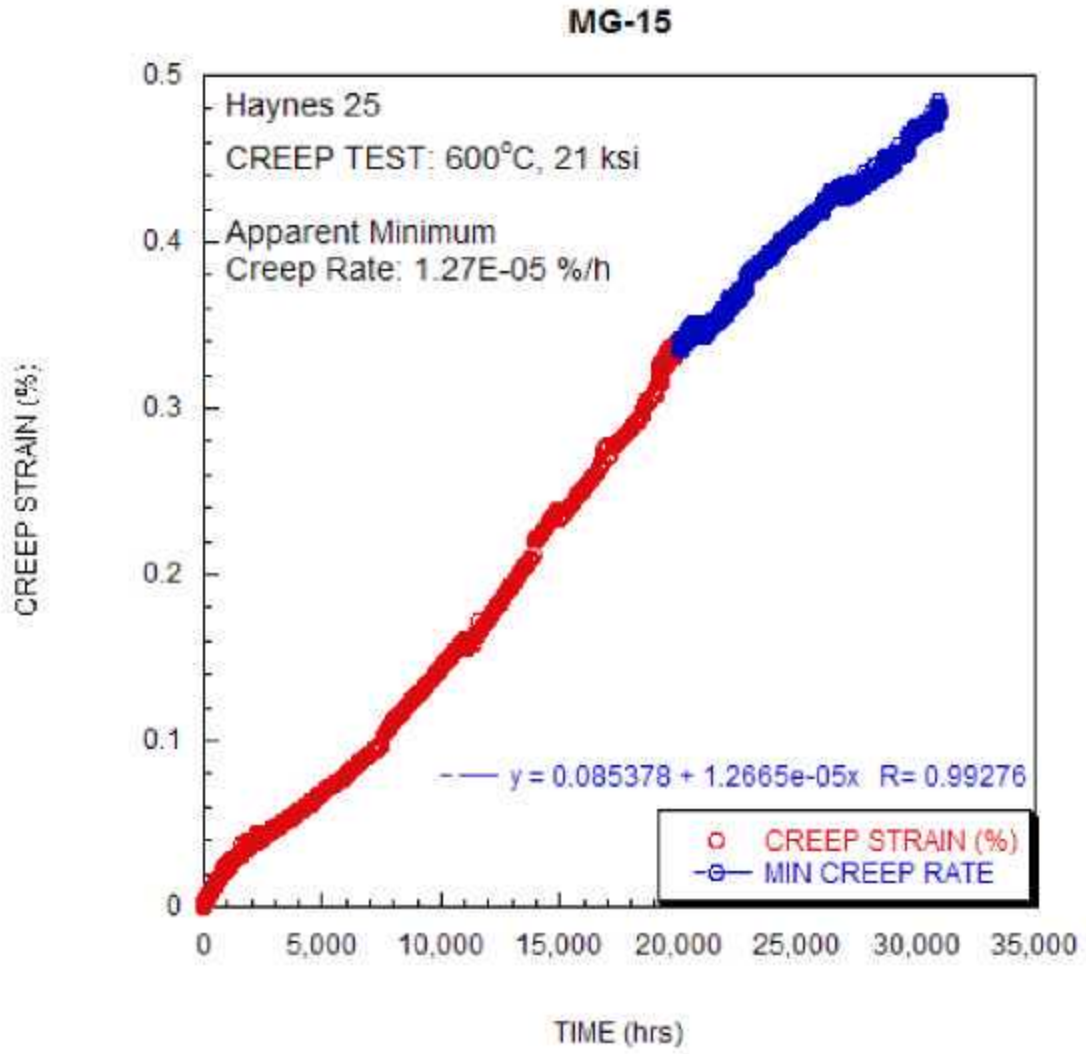

Test ID	Product Form	Aging Temp. (°C)	Aging Time (hours)	Test Temp. (°C)	Stress (MPa)	Rupture Life (hours) stopped or ongoing	Minimum Creep Rate (%/hr)	Elong. (%)	Red. of Area (%)	Failure Location
MG-17	sheet	none	none	625	206.8	12614.0	2.1E-05			

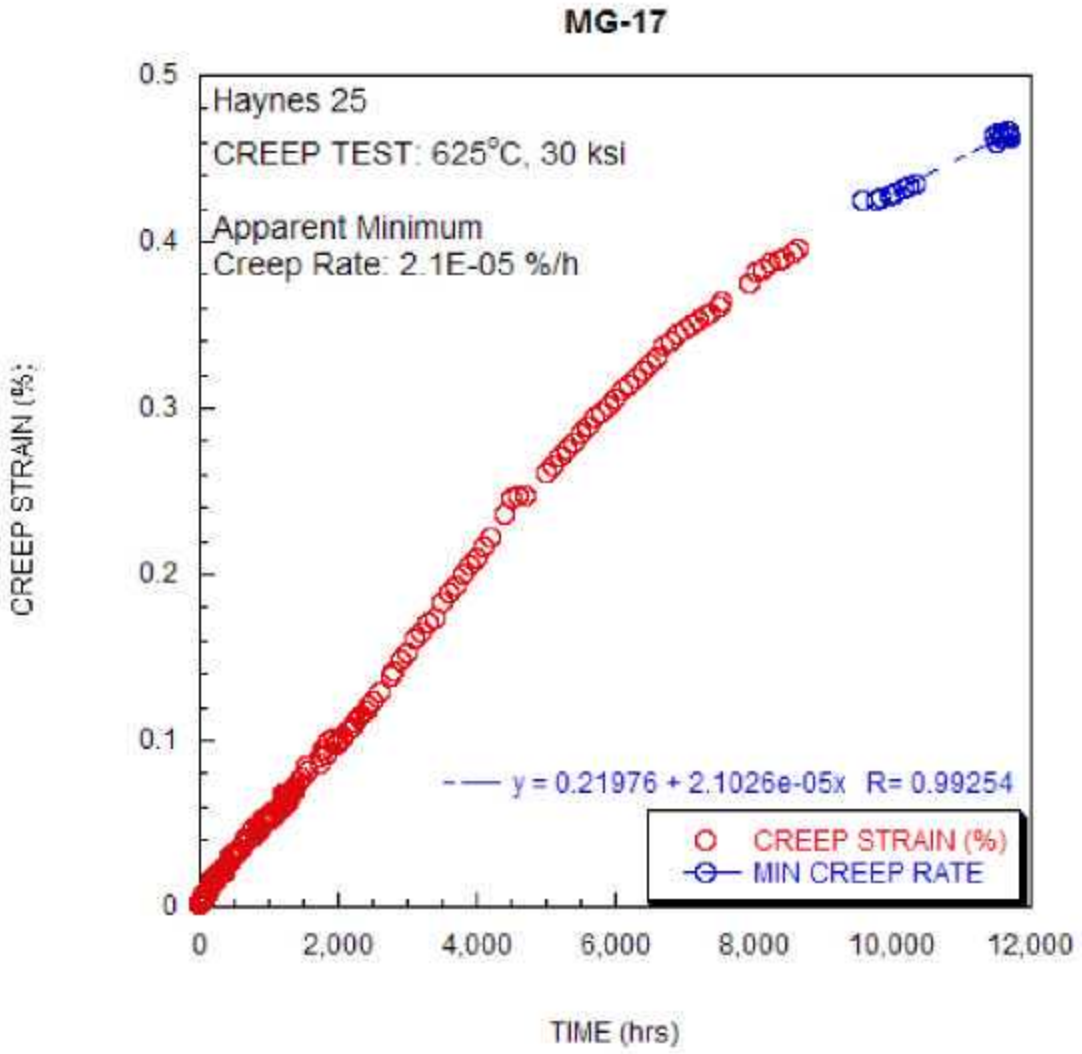

Test ID	Product Form	Aging Temp. (°C)	Aging Time (hours)	Test Temp. (°C)	Stress (MPa)	Rupture Life (hours) stopped or ongoing	Minimum Creep Rate (%/hr)	Elong. (%)	Red. of Area (%)	Failure Location
MG-18	sheet	none	none	650	124.1	10507.0	4.5E-05			

MG-18

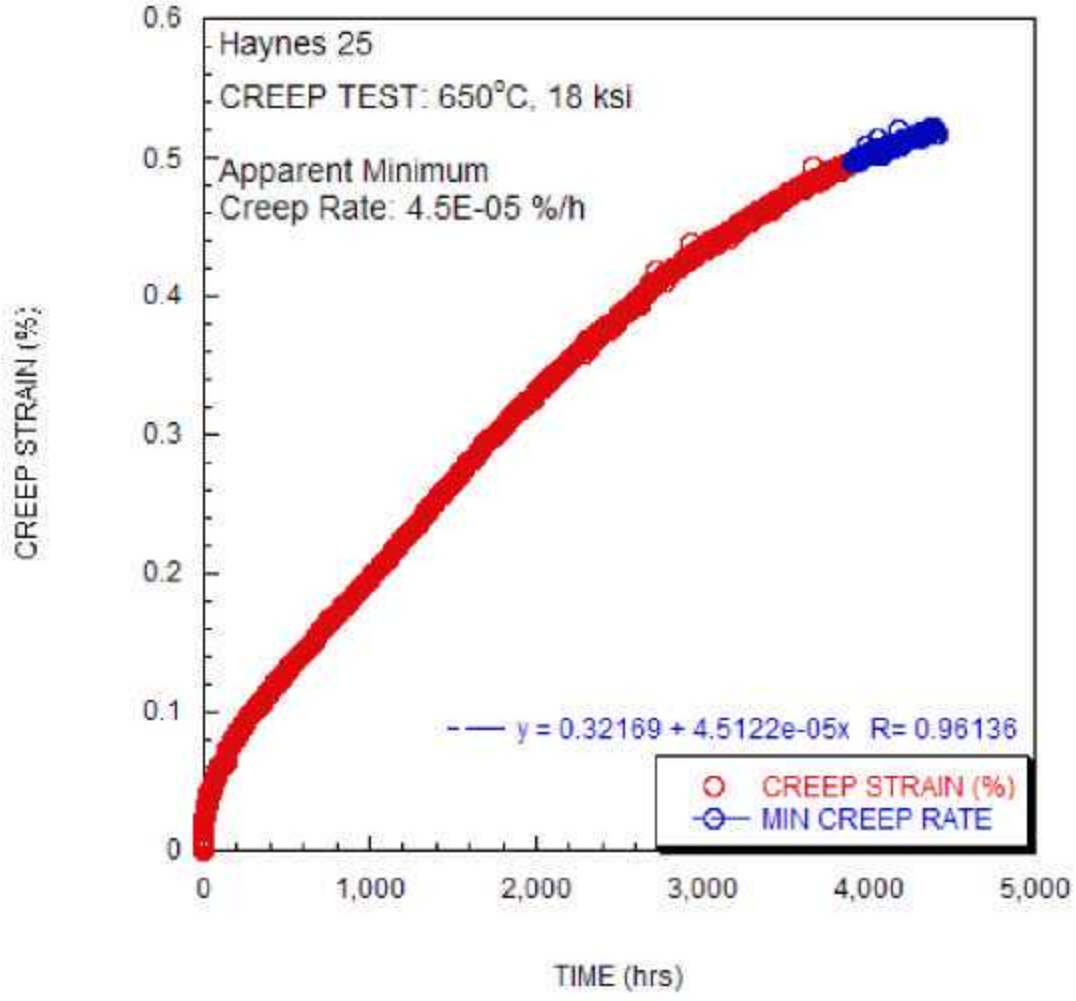

Test ID	Product Form	Aging Temp. (°C)	Aging Time (hours)	Test Temp. (°C)	Stress (MPa)	Rupture Life (hours) stopped or ongoing	Minimum Creep Rate (%/hr)	Elong. (%)	Red. of Area (%)	Failure Location
MG-21	sheet	none	none	650	186.2	11080.0	4.2E-05			

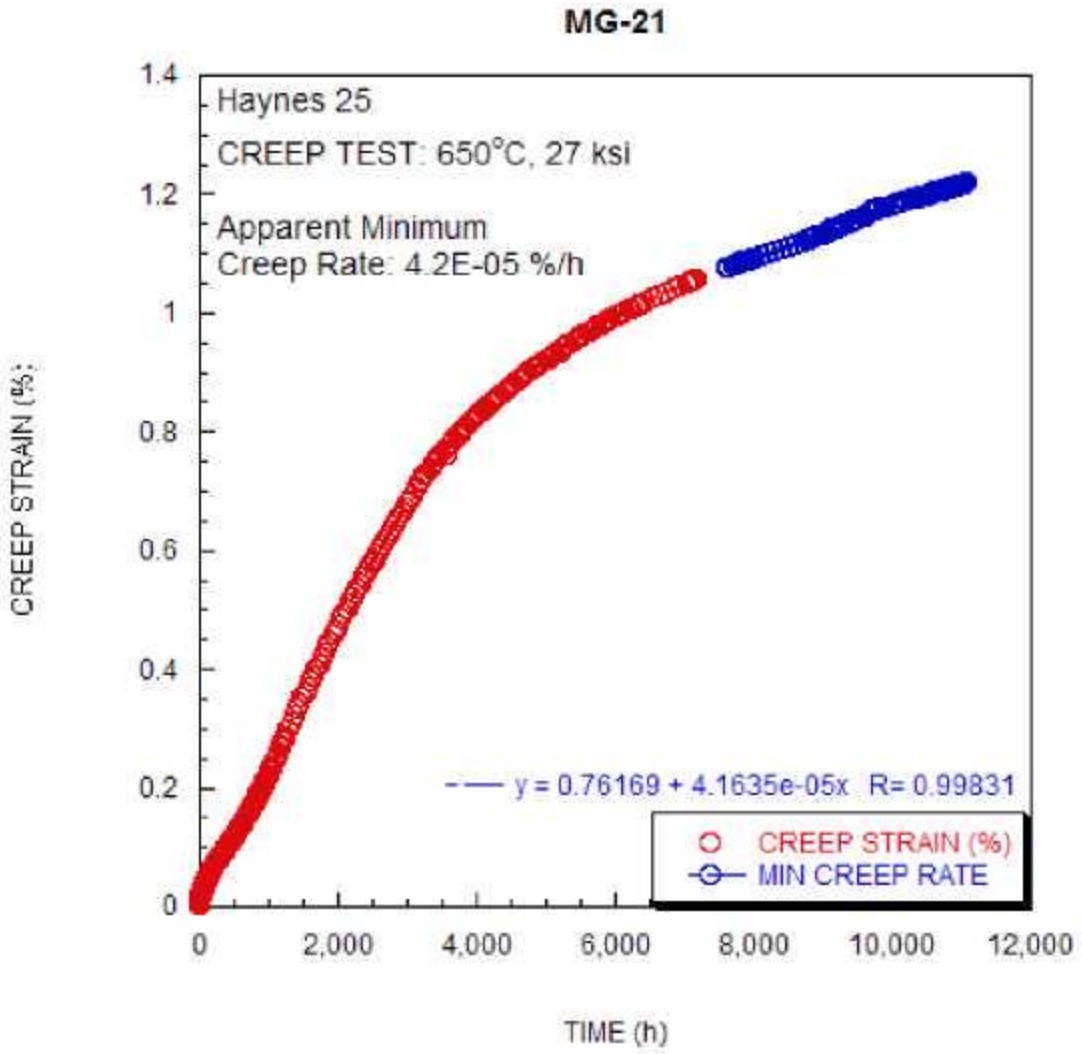

Test ID	Product Form	Aging Temp. (°C)	Aging Time (hours)	Test Temp. (°C)	Stress (MPa)	Rupture Life (hours) stopped or ongoing	Minimum Creep Rate (%/hr)	Elong. (%)	Red. of Area (%)	Failure Location
MG-22	sheet	none	none	675	103.4	11117.0	4.2E-06			

MG-22

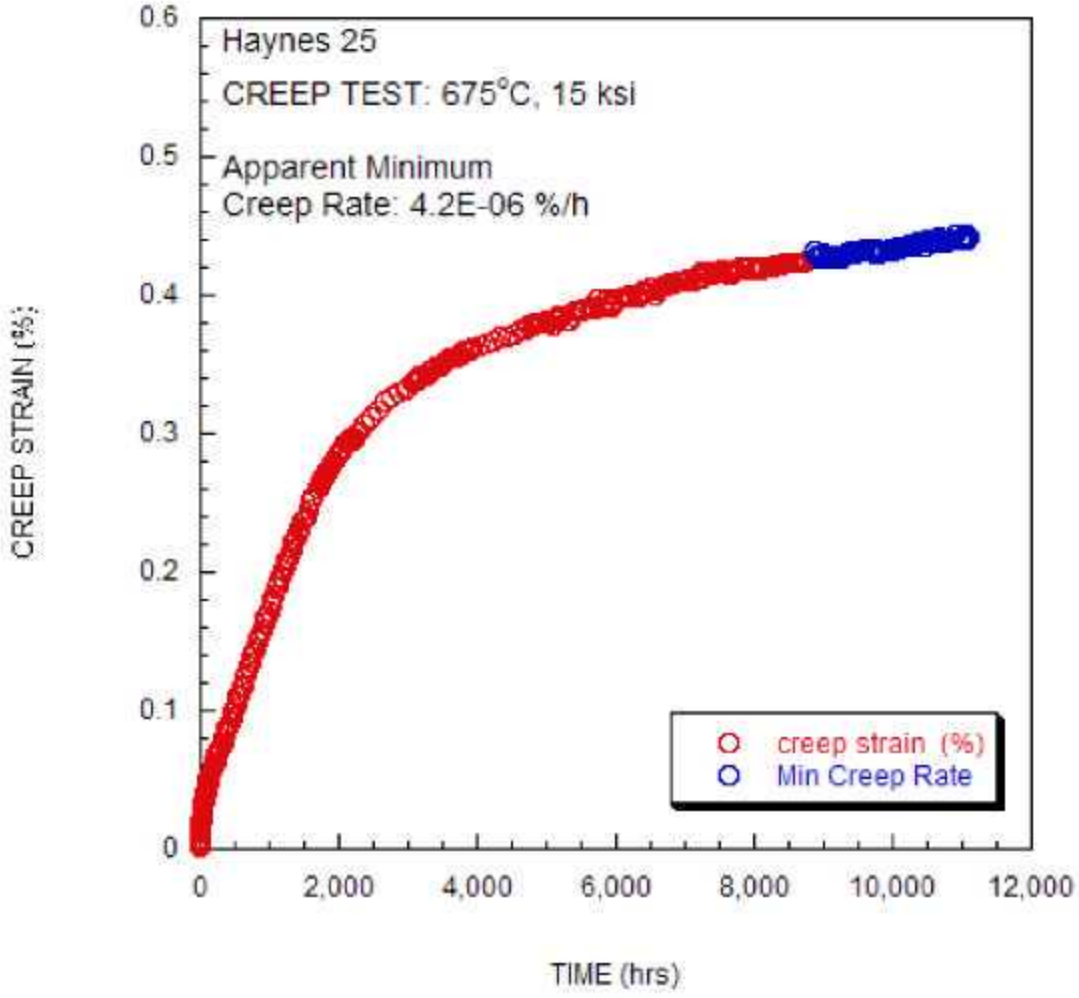

Test ID	Product Form	Aging Temp. (°C)	Aging Time (hours)	Test Temp. (°C)	Stress (MPa)	*Rupture Life (hours) stopped or ongoing*	Minimum Creep Rate (%/hr)	Elong. (%)	Red. of Area (%)	Failure Location
MG-24	sheet	none	none	675	151.7	*38000.0*	1.6E-05			

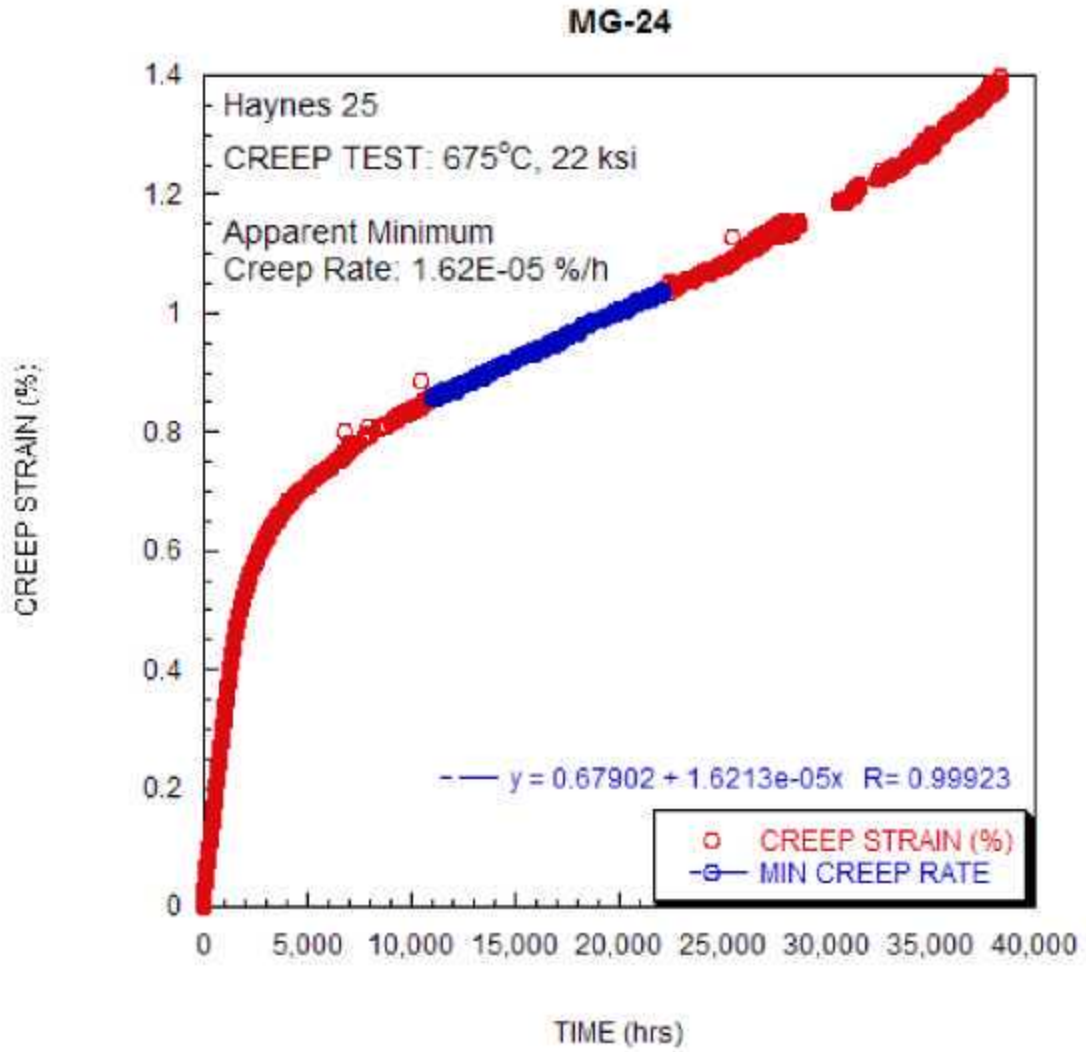

Test ID	Product Form	Aging Temp. (°C)	Aging Time (hours)	Test Temp. (°C)	Stress (MPa)	Rupture Life (hours) stopped or ongoing	Minimum Creep Rate (%/hr)	Elong. (%)	Red. of Area (%)	Failure Location
MG22b	sheet	none	none	675	103.4	15976.0	5.5E-06			
				675	0.0	16262.0				
				675	103.4	20591.0	5.70E-06			
				700	103.4	22892.0	6.80E-06			
				725	103.4	24496.0	2.10E-05			
				700	103.4	25574.0	1.10E-05			
				675	103.4	39841.0	6.30E-06			
				675	117.2	*42000.0*	8.70E-06			

MG-22b

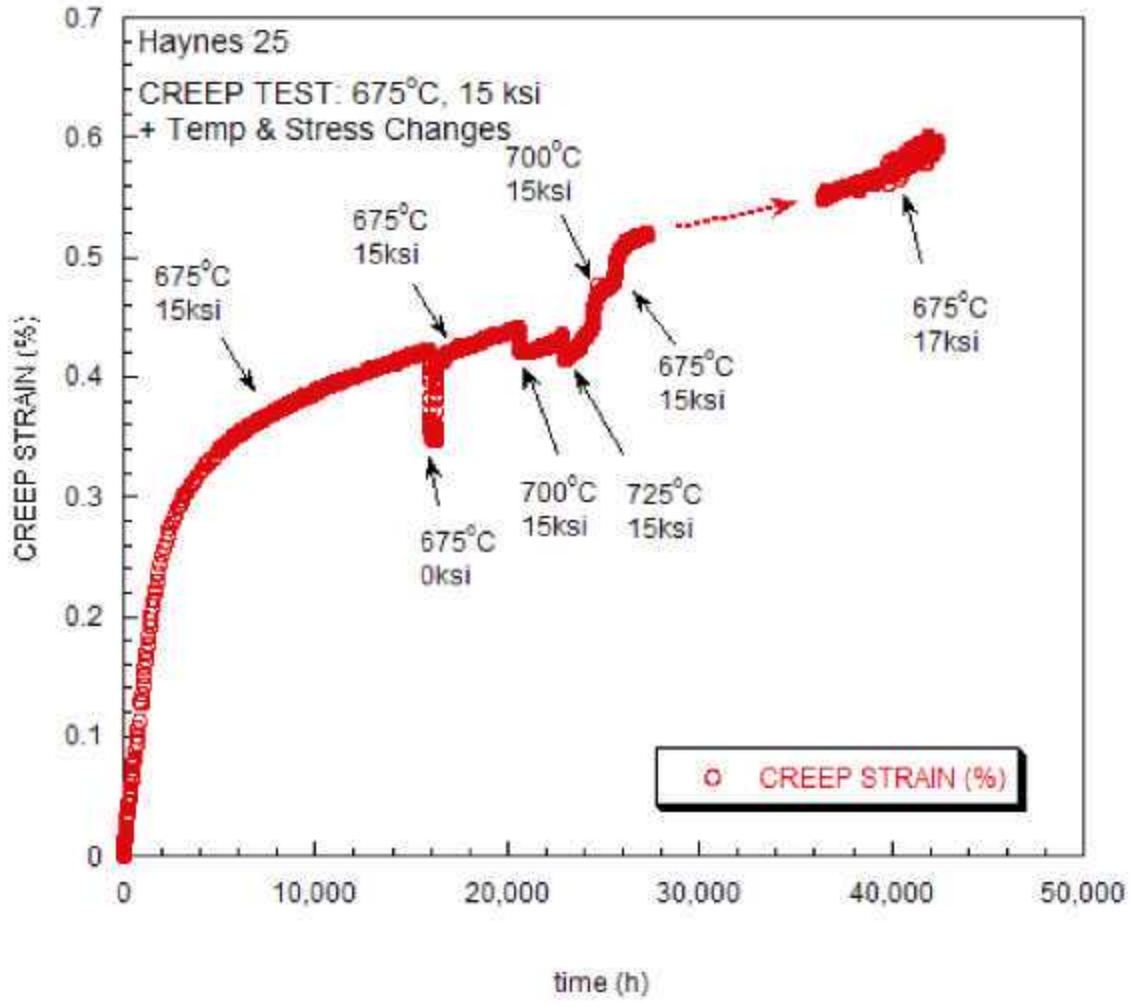

Test ID	Product Form	Aging Temp. (°C)	Aging Time (hours)	Test Temp. (°C)	Stress (MPa)	*Rupture Life (hours) stopped or ongoing*	Minimum Creep Rate (%/hr)	Elong. (%)	Red. of Area (%)	Failure Location
CR-BM-15	sheet	675	6000	650	206.8	*38300.0*	2.50E-05			

CR-BM-15

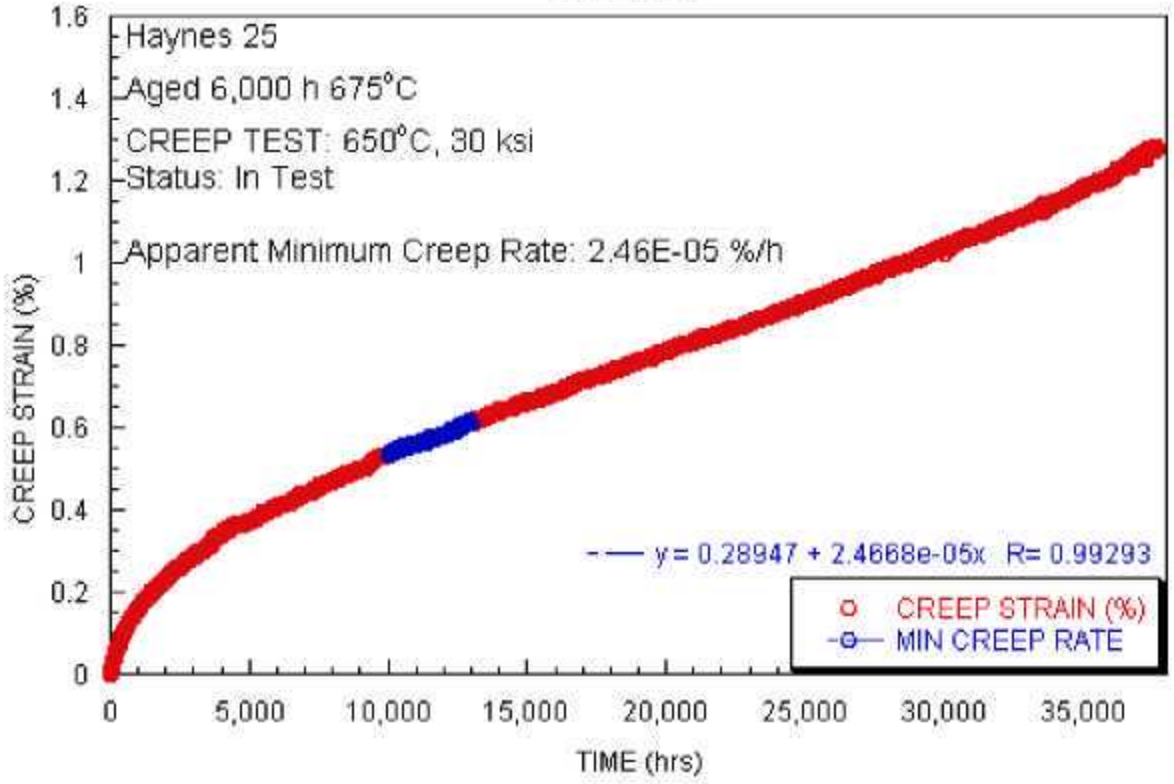

Test ID	Product Form	Aging Temp. (°C)	Aging Time (hours)	Test Temp. (°C)	Stress (MPa)	Rupture Life (hours) stopped or ongoing	Minimum Creep Rate (%/hr)	Elong. (%)	Red. of Area (%)	Failure Location
CR-BM-16	sheet	675	6000	700	165.5	20670	6.90E-05	3.8	3.1	

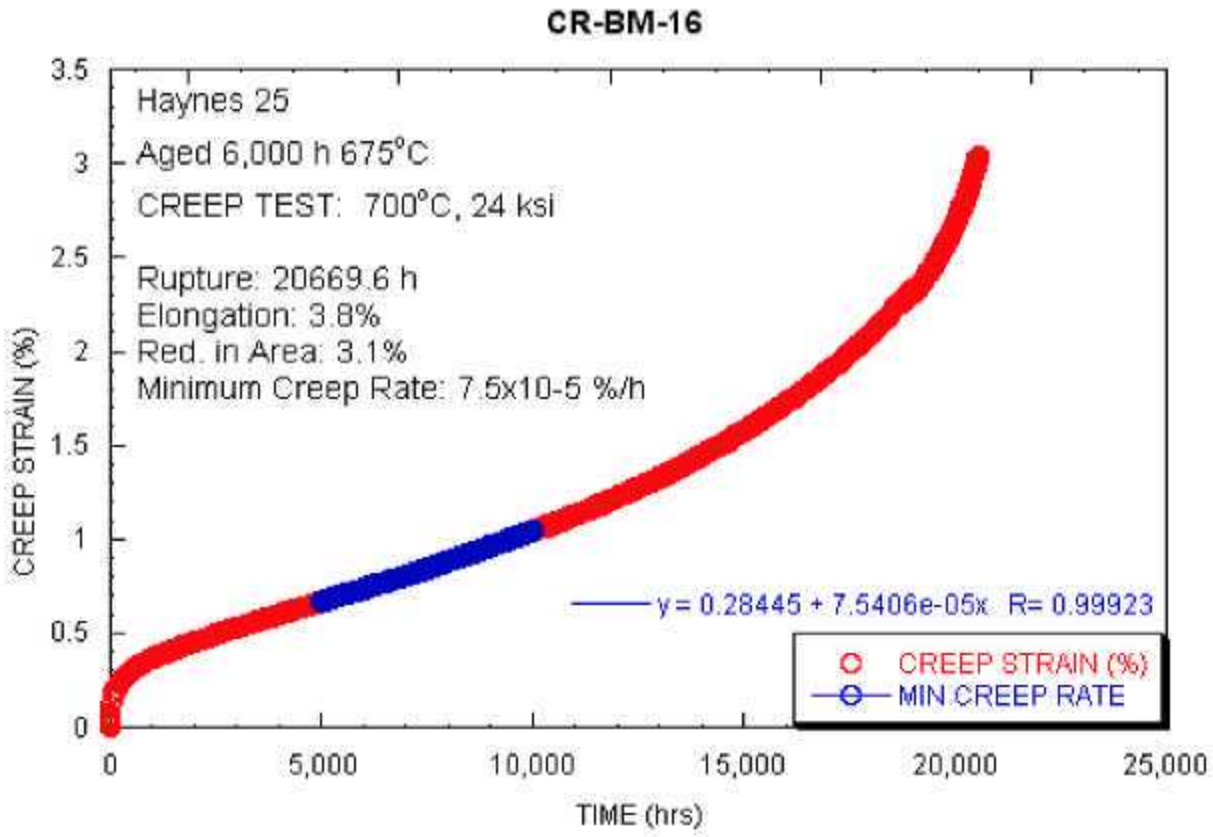

Test ID	Product Form	Aging Temp. (°C)	Aging Time (hours)	Test Temp. (°C)	Stress (MPa)	Rupture Life (hours) stopped or ongoing	Minimum Creep Rate (%/hr)	Elong. (%)	Red. of Area (%)	Failure Location
CR-BM-17	sheet	675	6000	750	127.6	9536	3.90E-05	5.8	4.8	

CR-BM-17

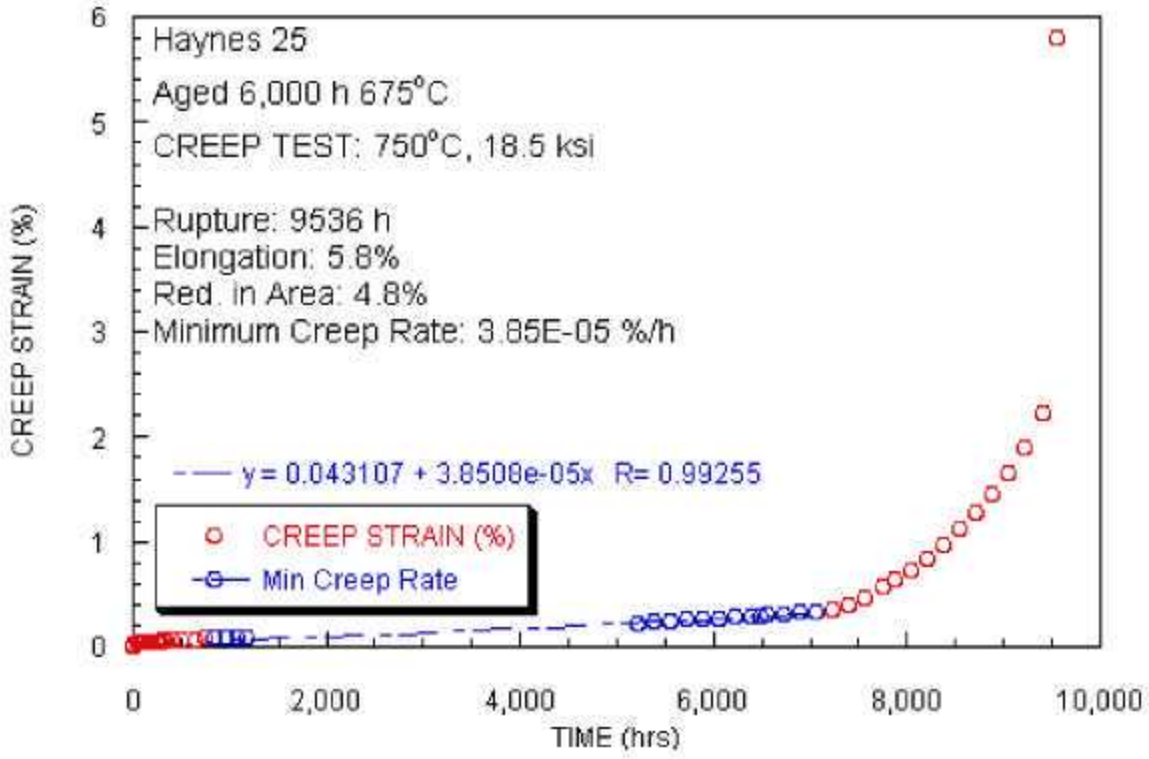

Test ID	Product Form	Aging Temp. (°C)	Aging Time (hours)	Test Temp. (°C)	Stress (MPa)	Rupture Life (hours) stopped or ongoing	Minimum Creep Rate (%/hr)	Elong. (%)	Red. of Area (%)	Failure Location
CR-BM-18	sheet	675	6000	800	99.3	8863	1.90E-04	9.3	7.1	

CR-BM-18

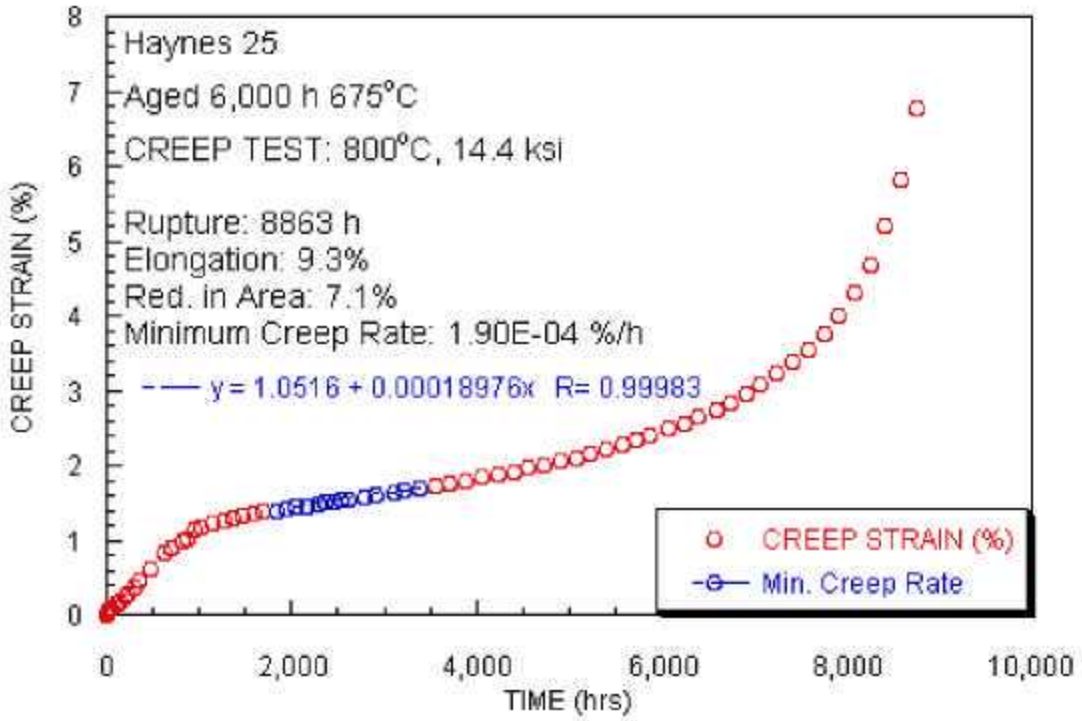

Test ID	Product Form	Aging Temp. (°C)	Aging Time (hours)	Test Temp. (°C)	Stress (MPa)	Rupture Life (hours) stopped or ongoing	Minimum Creep Rate (%/hr)	Elong. (%)	Red. of Area (%)	Failure Location
CR-BM-19	sheet	675	6000	800	103.4	4626	3.00E-04	6.9	6.4	

CR-BM-19

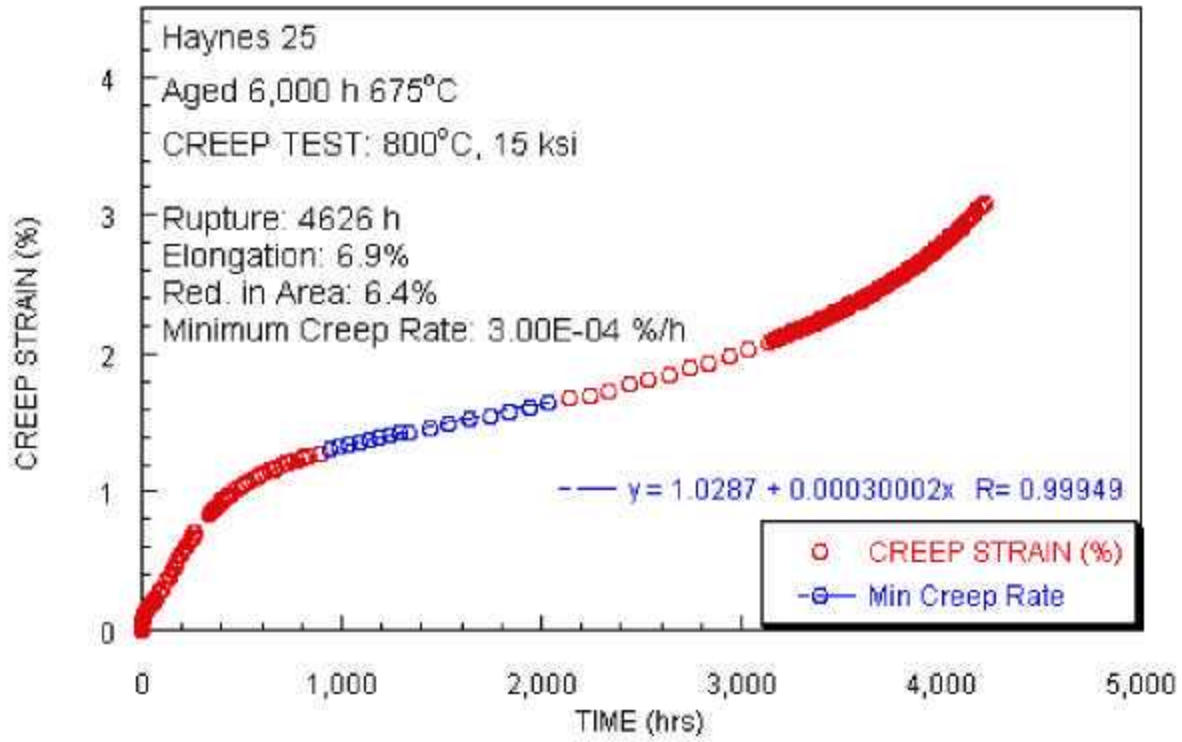

Test ID	Product Form	Aging Temp. (°C)	Aging Time (hours)	Test Temp. (°C)	Stress (MPa)	Rupture Life (hours) stopped or ongoing	Minimum Creep Rate (%/hr)	Elong. (%)	Red. of Area (%)	Failure Location
CR-BM-20	sheet	675	6000	850	62.1	6092	1.30E-04	4.2	1.2	

CR-BM-20

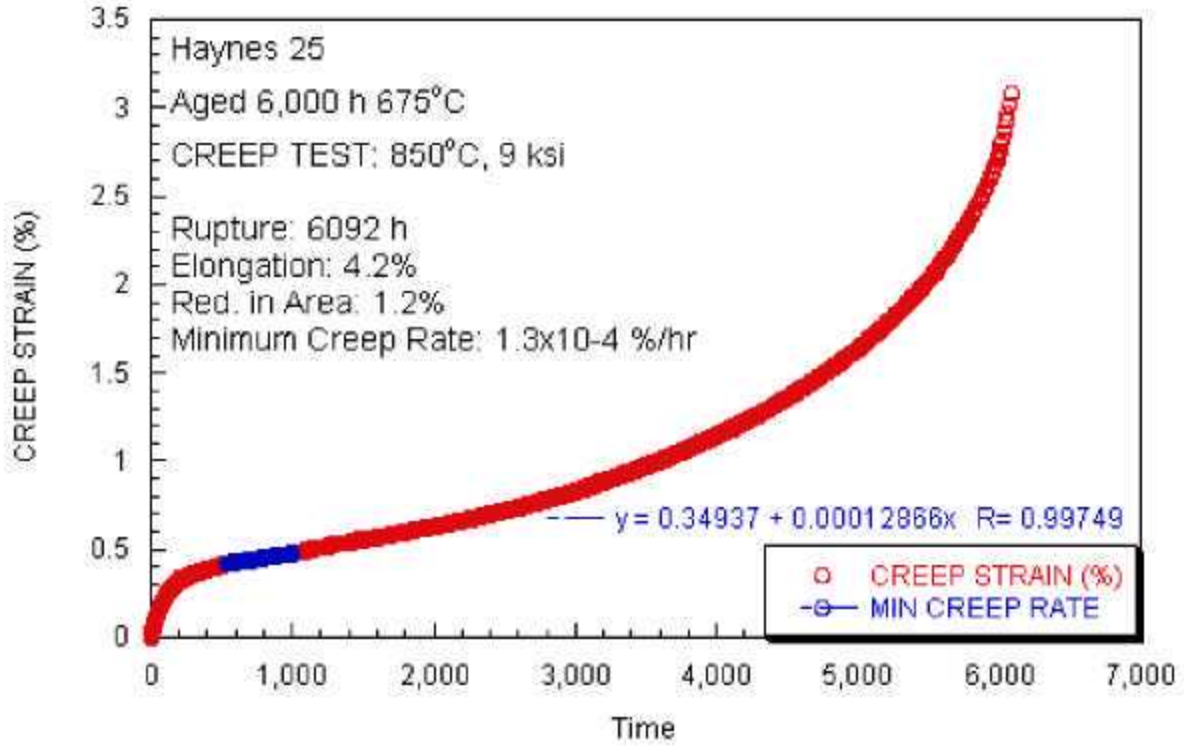

Test ID	Product Form	Aging Temp. (°C)	Aging Time (hours)	Test Temp. (°C)	Stress (MPa)	Rupture Life (hours) stopped or ongoing	Minimum Creep Rate (%/hr)	Elong. (%)	Red. of Area (%)	Failure Location
CR-BM-22	sheet	675	6000	900	44.8	6105	1.60E-04	11.0	5.1	

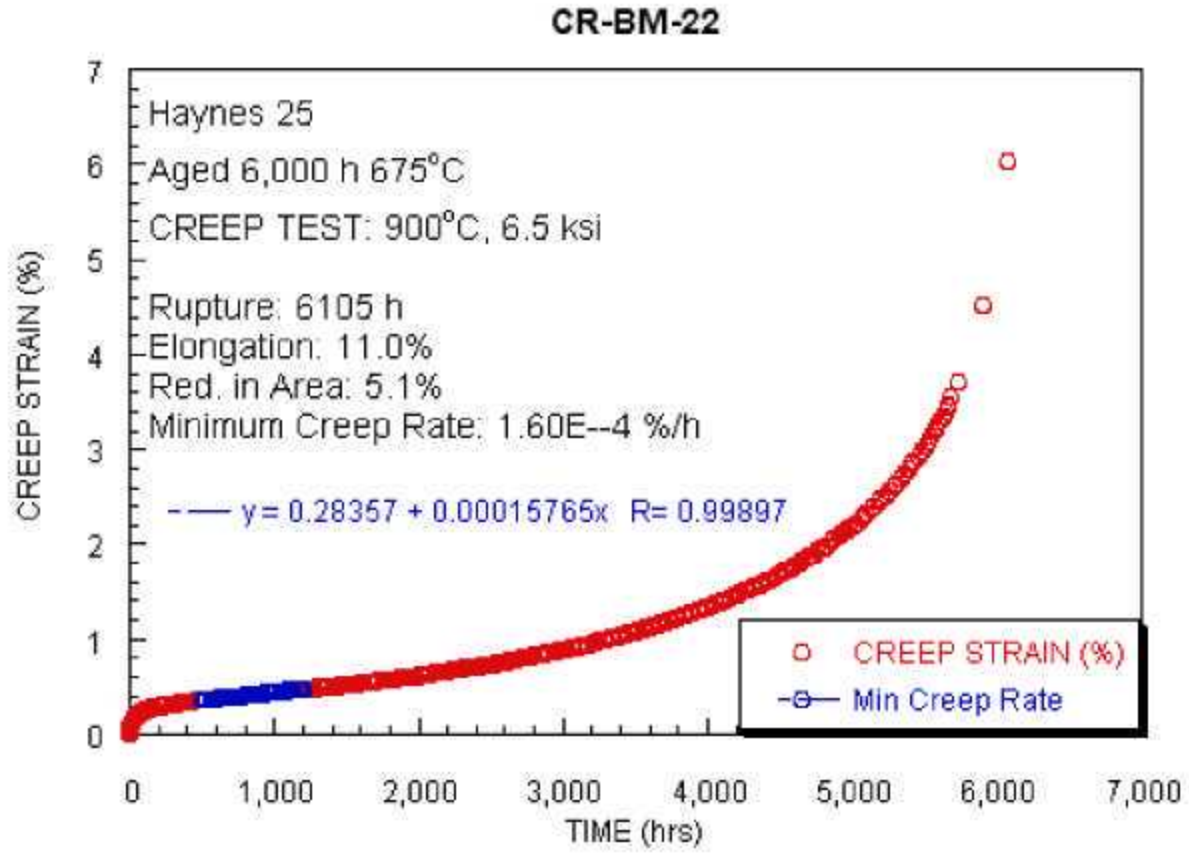

Test ID	Product Form	Aging Temp. (°C)	Aging Time (hours)	Test Temp. (°C)	Stress (MPa)	Rupture Life (hours) stopped or ongoing	Minimum Creep Rate (%/hr)	Elong. (%)	Red. of Area (%)	Failure Location
CR-WM-02	sheet weld	none	none	700	165.5	21339.3	3.45E-05	4.4	1.9	BM

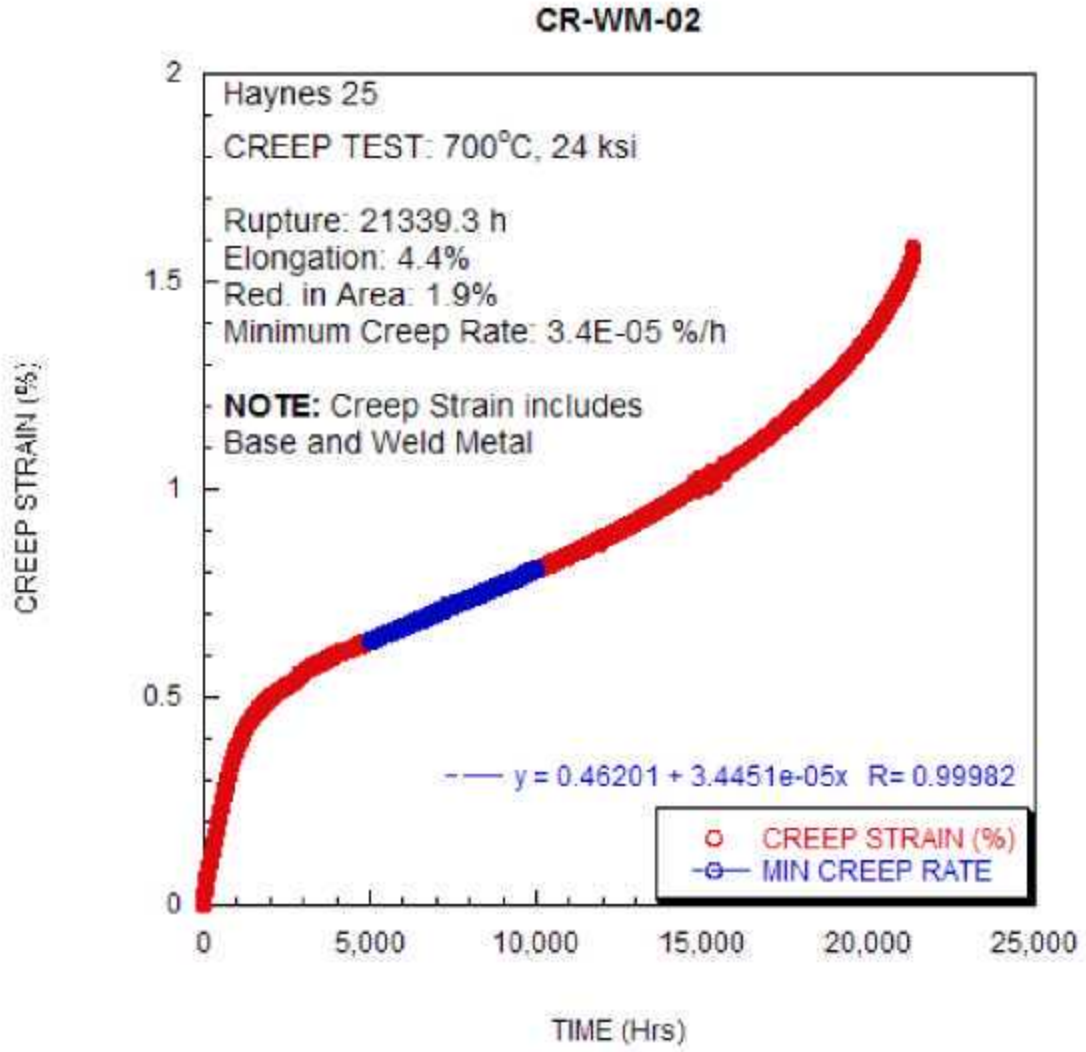

Test ID	Product Form	Aging Temp. (°C)	Aging Time (hours)	Test Temp. (°C)	Stress (MPa)	Rupture Life (hours) stopped or ongoing	Minimum Creep Rate (%/hr)	Elong. (%)	Red. of Area (%)	Failure Location
CR-WM-03	sheet weld	none	none	750	127.6	9588	3.50E-04	8.1	9.6	BM

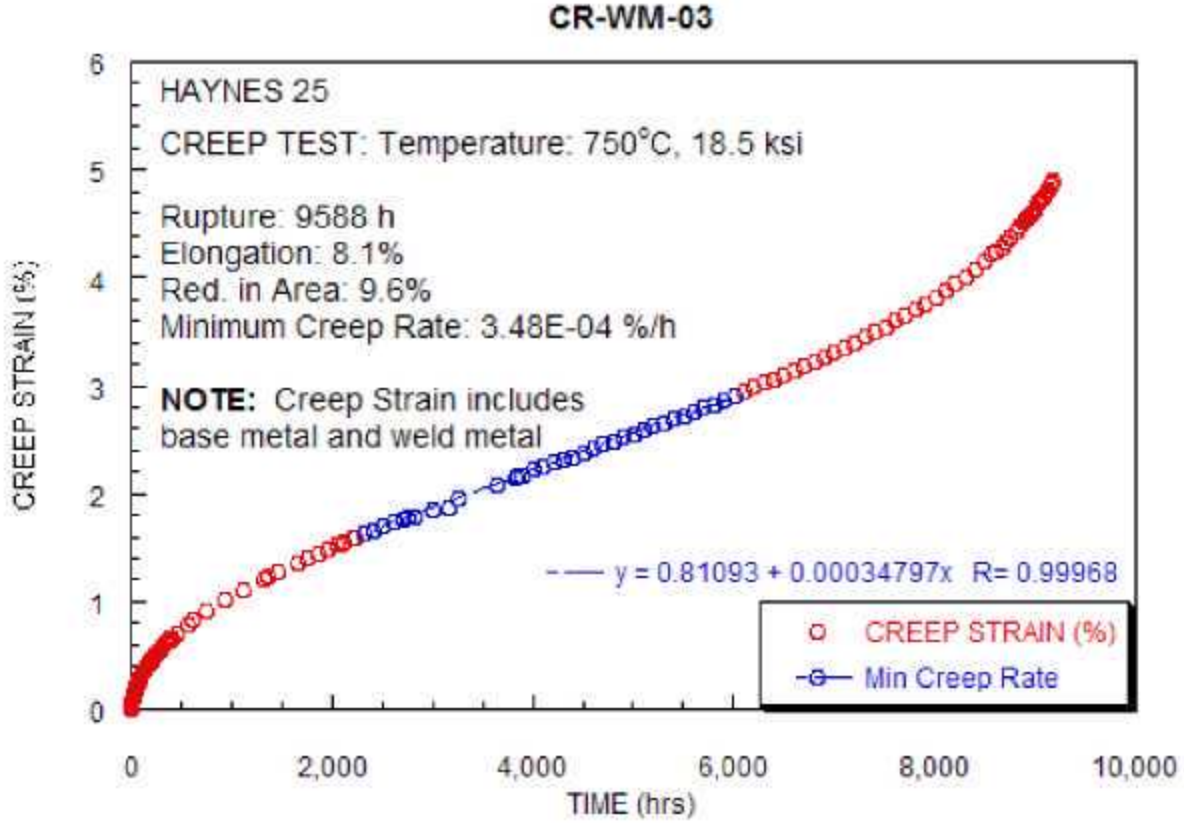

Test ID	Product Form	Aging Temp. (°C)	Aging Time (hours)	Test Temp. (°C)	Stress (MPa)	Rupture Life (hours) stopped or ongoing	Minimum Creep Rate (%/hr)	Elong. (%)	Red. of Area (%)	Failure Location
CR-WM-04	sheet weld	none	none	800	99.3	6620	4.40E-04	6.7	10.3	BM

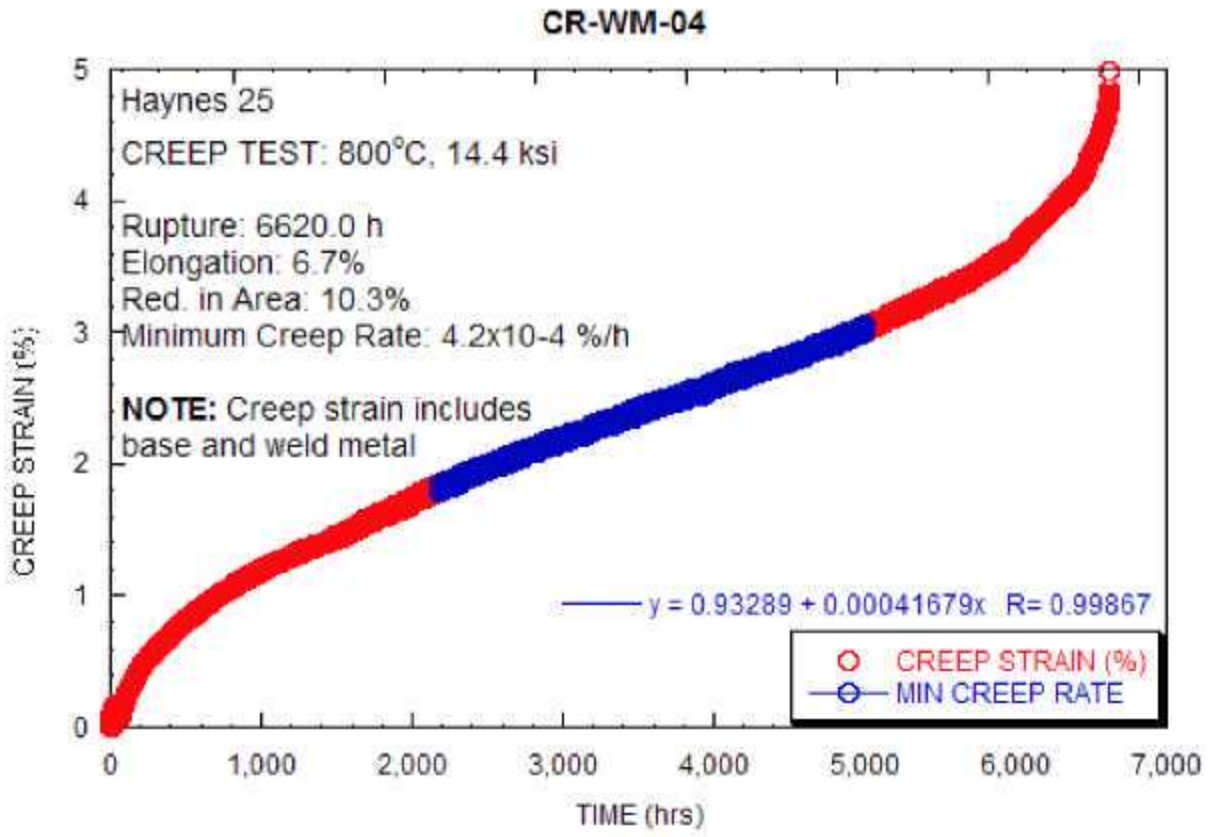

Test ID	Product Form	Aging Temp. (°C)	Aging Time (hours)	Test Temp. (°C)	Stress (MPa)	Rupture Life (hours) stopped or ongoing	Minimum Creep Rate (%/hr)	Elong. (%)	Red. of Area (%)	Failure Location
CR-WM-05	sheet weld	none	none	800	103.4	4550	8.40E-04	9.2	5.4	BM

CR-WM-05

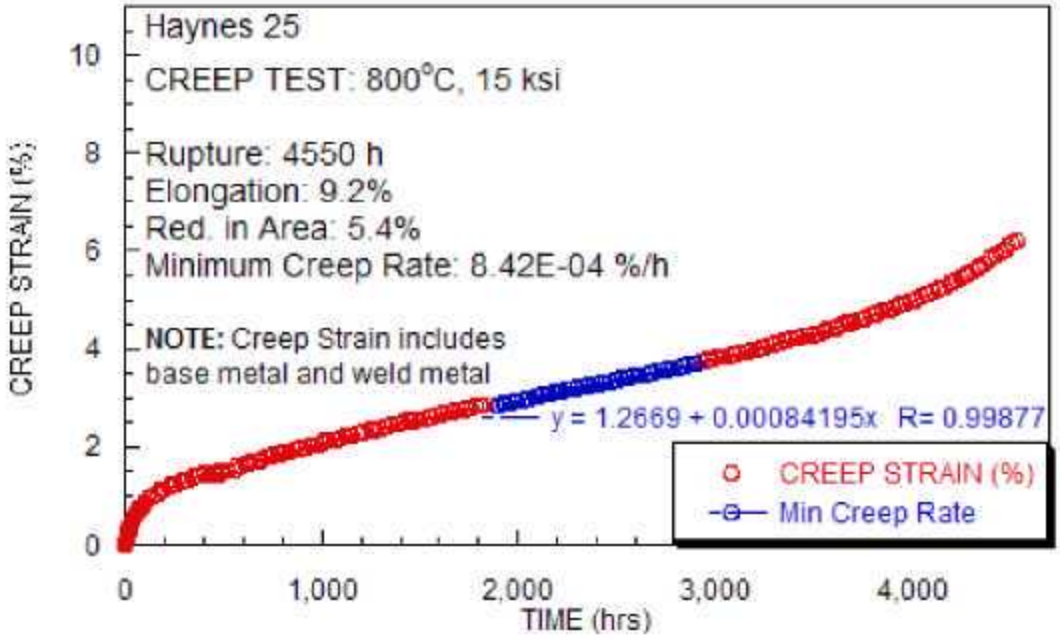

Test ID	Product Form	Aging Temp. (°C)	Aging Time (hours)	Test Temp. (°C)	Stress (MPa)	Rupture Life (hours) stopped or ongoing	Minimum Creep Rate (%/hr)	Elong. (%)	Red. of Area (%)	Failure Location
CR-WM-06	sheet weld	none	none	850	62.1	8710	1.20E-04	6.5	4.1	BM

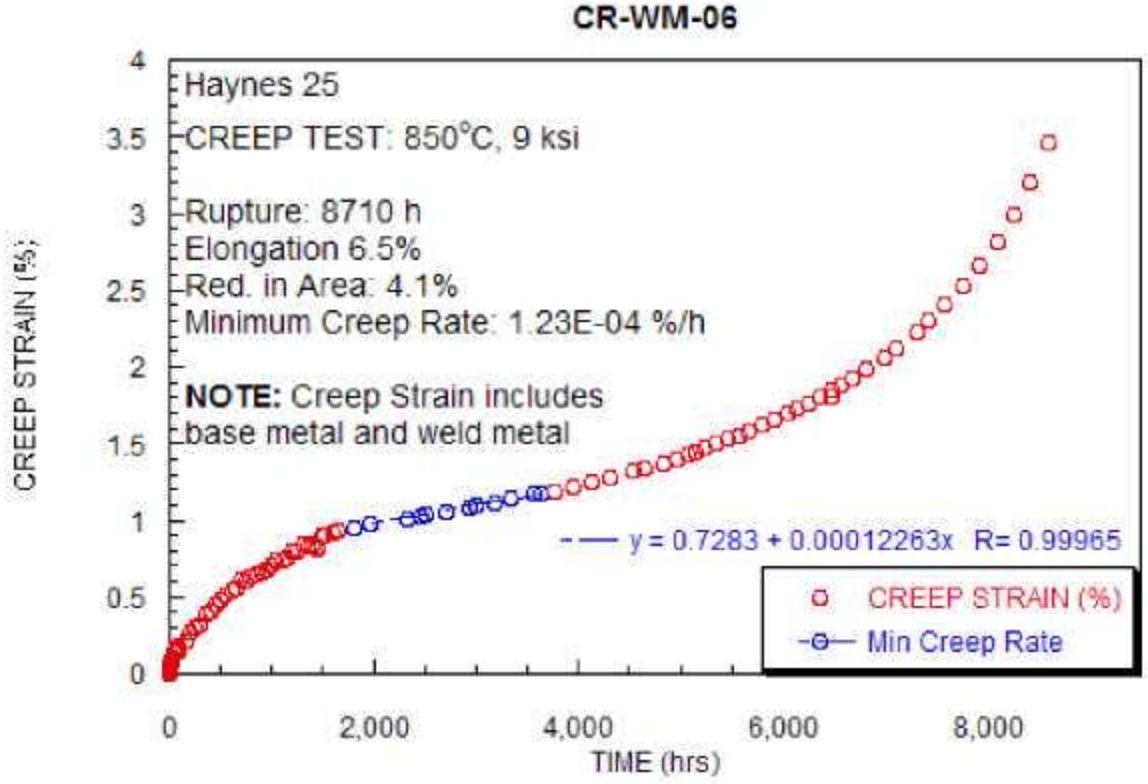

Test ID	Product Form	Aging Temp. (°C)	Aging Time (hours)	Test Temp. (°C)	Stress (MPa)	Rupture Life (hours) stopped or ongoing	Minimum Creep Rate (%/hr)	Elong. (%)	Red. of Area (%)	Failure Location
CR-WM-07	sheet weld	none	none	875	53.8	6000	1.30E-04			

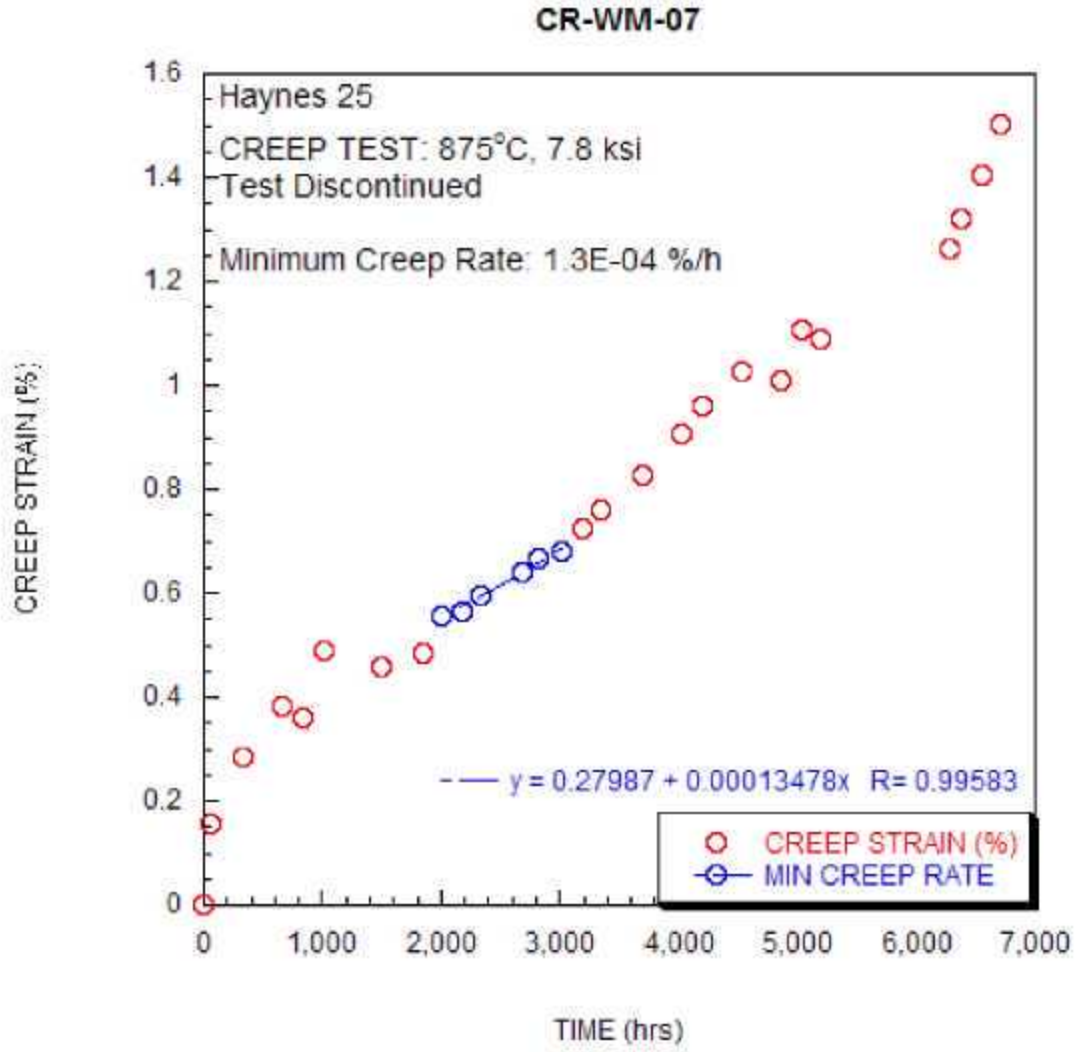

Test ID	Product Form	Aging Temp. (°C)	Aging Time (hours)	Test Temp. (°C)	Stress (MPa)	Rupture Life (hours) stopped or ongoing	Minimum Creep Rate (%/hr)	Elong. (%)	Red. of Area (%)	Failure Location
CR-WM-08	sheet weld	none	none	900	44.8	4372	2.50E-04	5.2	1.2	BM

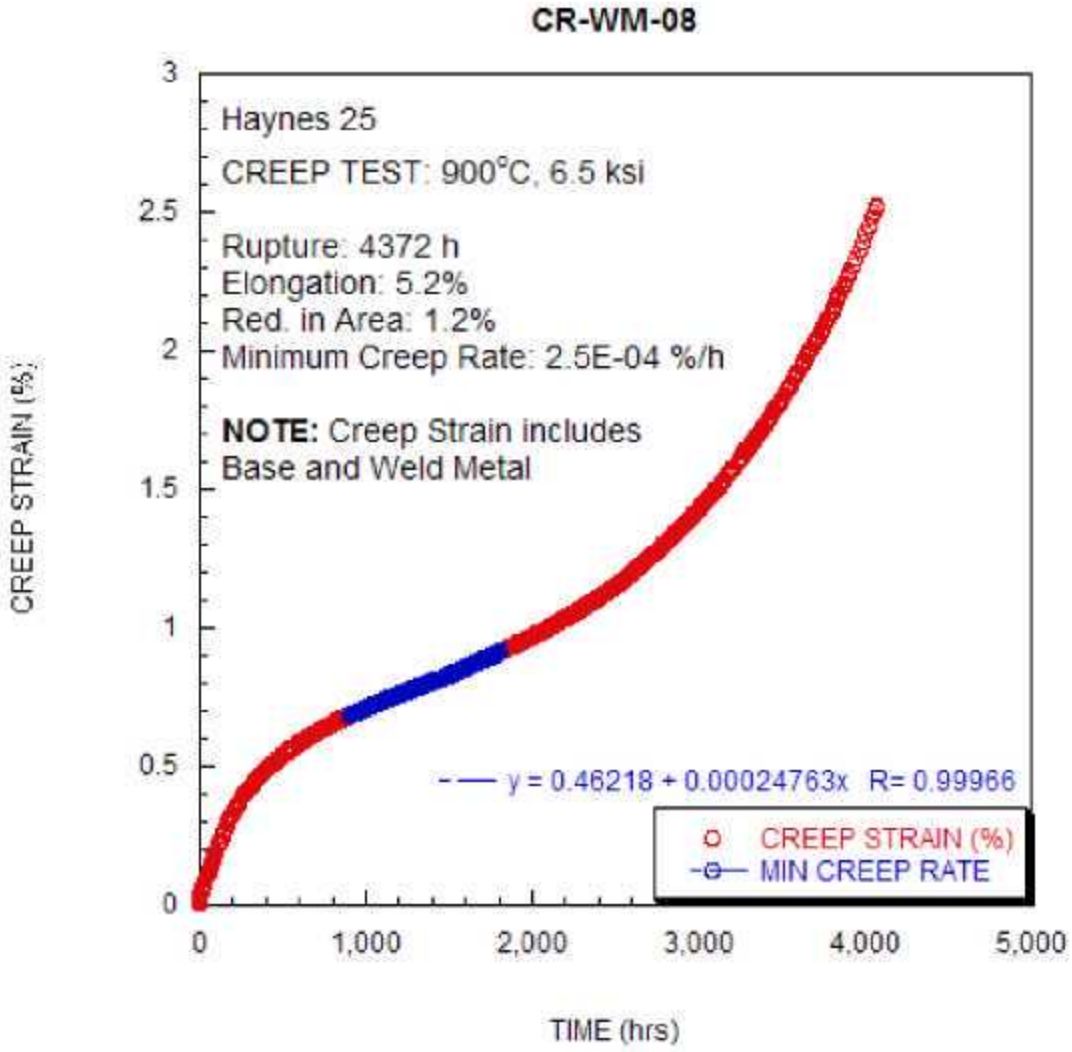

Test ID	Product Form	Aging Temp. (°C)	Aging Time (hours)	Test Temp. (°C)	Stress (MPa)	Rupture Life (hours) stopped or ongoing	Minimum Creep Rate (%/hr)	Elong. (%)	Red. of Area (%)	Failure Location
CR-WM-09	sheet weld	none	none	900	42.7	6470	1.30E-04	9.8	7.2	BM

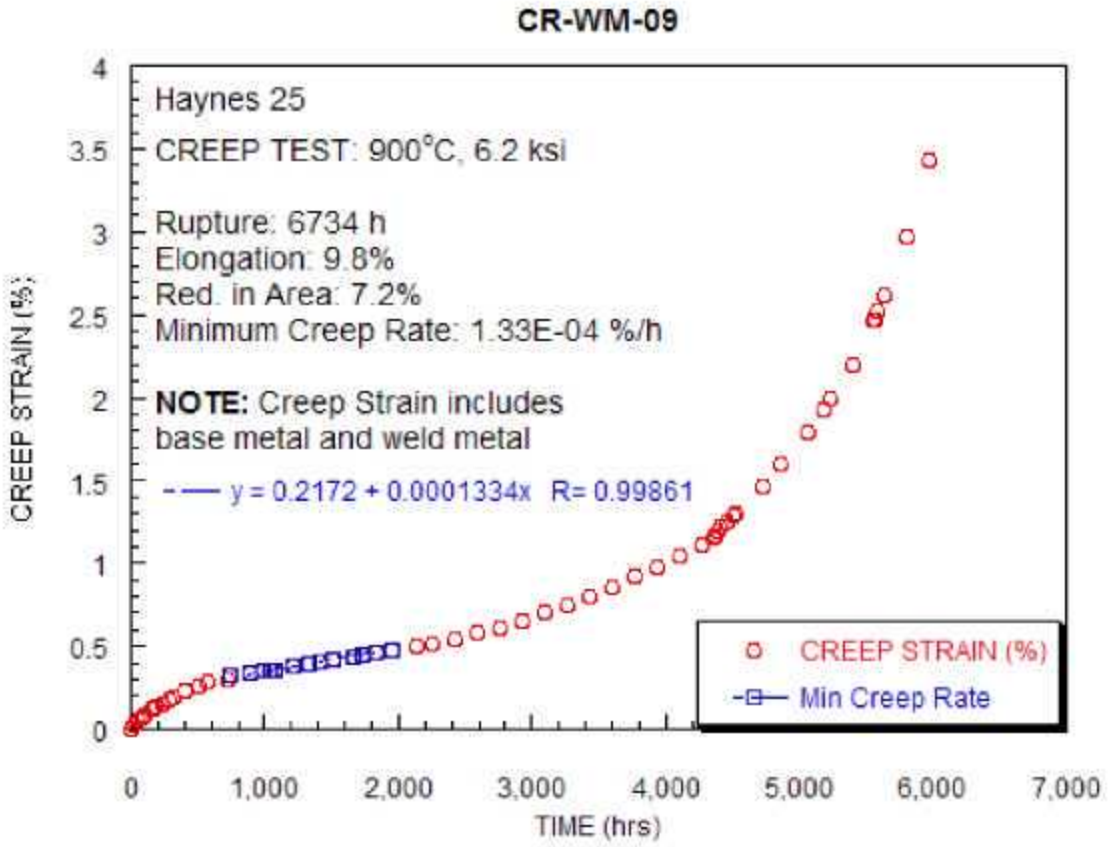

Test ID	Product Form	Aging Temp. (°C)	Aging Time (hours)	Test Temp. (°C)	Stress (MPa)	*Rupture Life (hours) stopped or ongoing*	Minimum Creep Rate (%/hr)	Elong. (%)	Red. of Area (%)	Failure Location
MG-01	sheet weld	none	none	600	179.3	*32128*	1.5E-05			

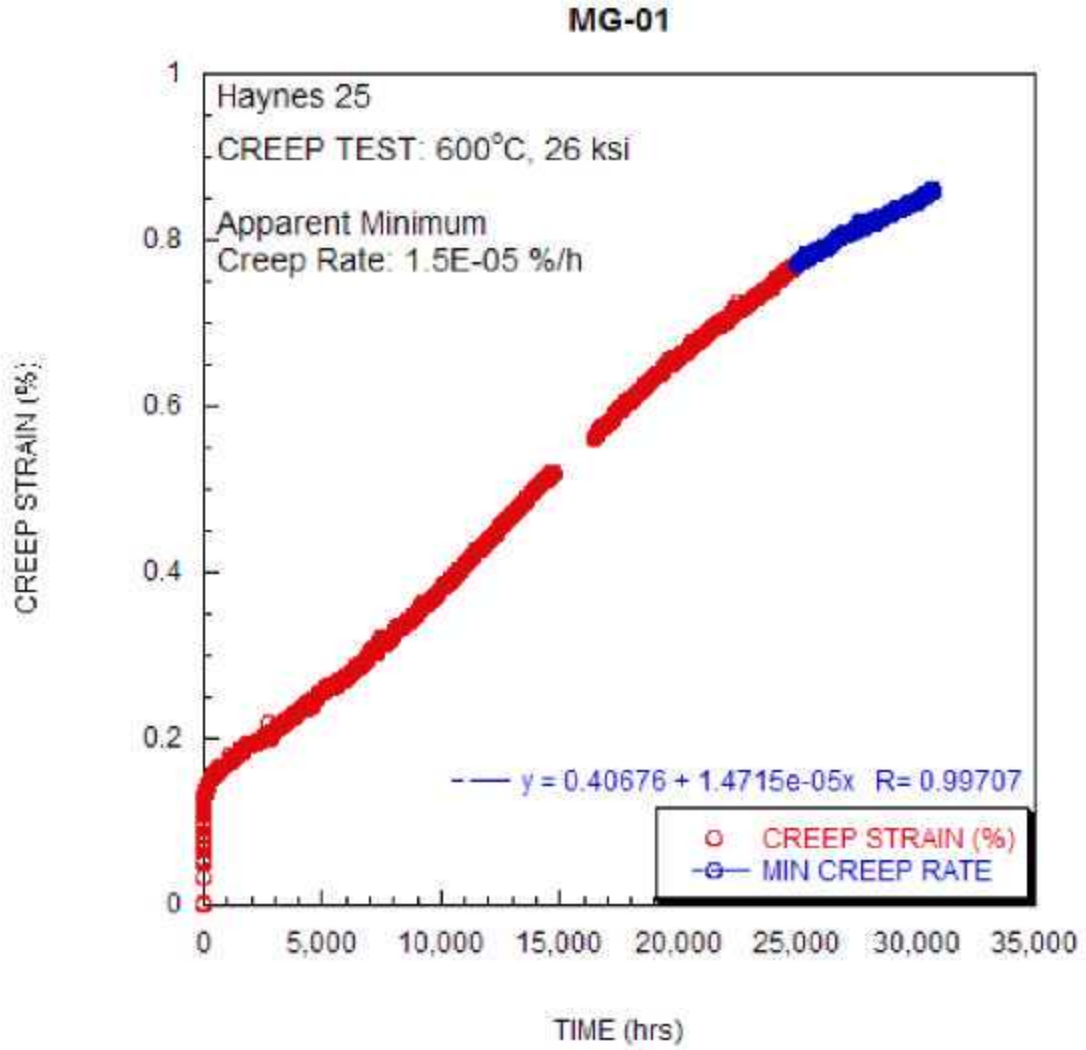

Test ID	Product Form	Aging Temp. (°C)	Aging Time (hours)	Test Temp. (°C)	Stress (MPa)	*Rupture Life (hours) stopped or ongoing*	Minimum Creep Rate (%/hr)	Elong. (%)	Red. of Area (%)	Failure Location
MG-03	sheet weld	none	none	625	144.8	*32440*	4.5E-06			

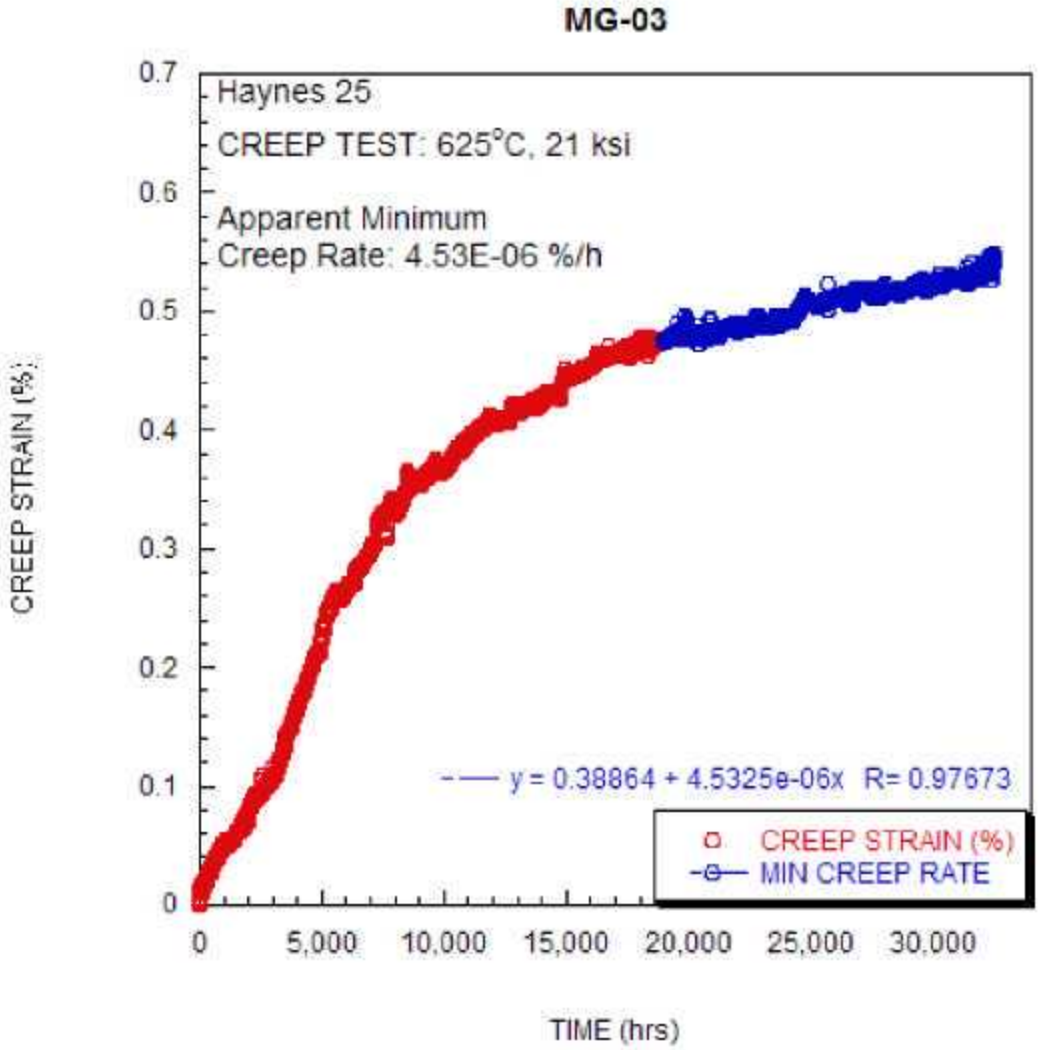

Test ID	Product Form	Aging Temp. (°C)	Aging Time (hours)	Test Temp. (°C)	Stress (MPa)	Rupture Life (hours) stopped or ongoing	Minimum Creep Rate (%/hr)	Elong. (%)	Red. of Area (%)	Failure Location
MG-06	sheet weld	none	none	650	124.1	11782	1.4E-05			

MG-06

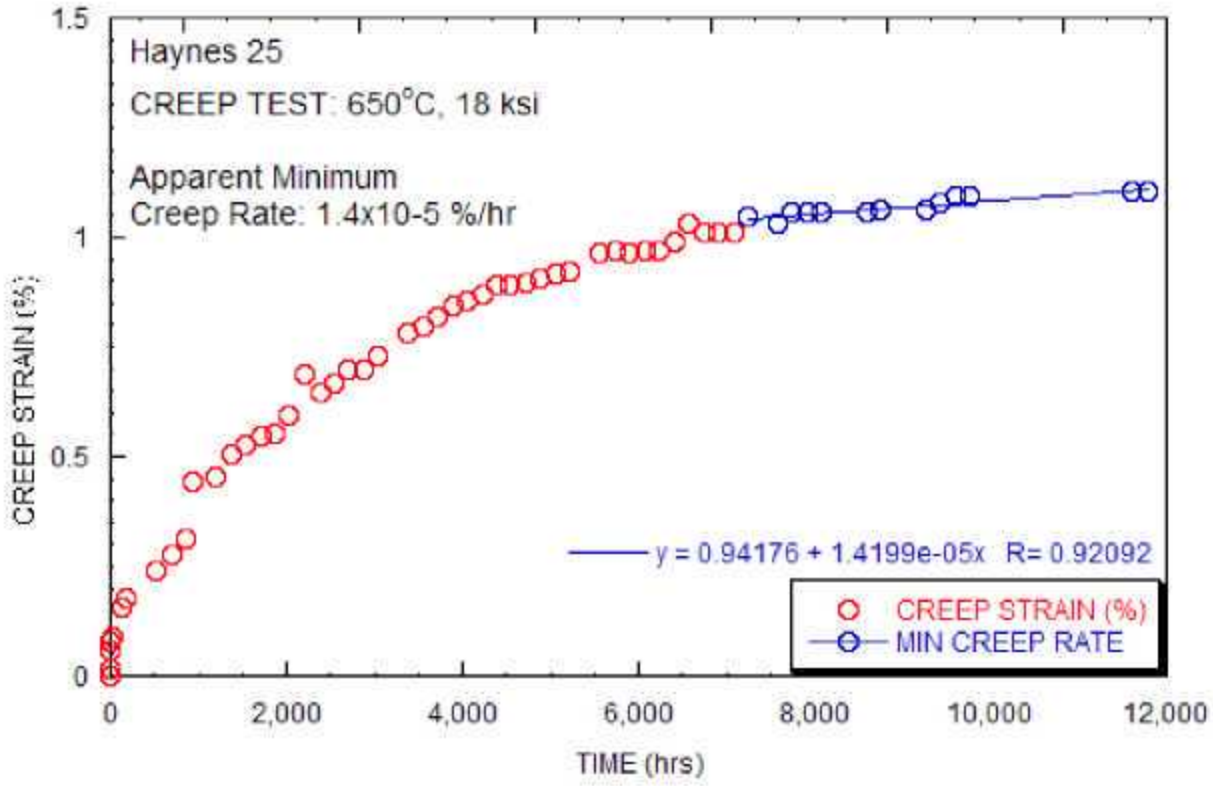

Test ID	Product Form	Aging Temp. (°C)	Aging Time (hours)	Test Temp. (°C)	Stress (MPa)	Rupture Life (hours) stopped or ongoing	Minimum Creep Rate (%/hr)	Elong. (%)	Red. of Area (%)	Failure Location
MG-09	sheet weld	none	none	650	186.2	10292	7.0E-05			

MG-09

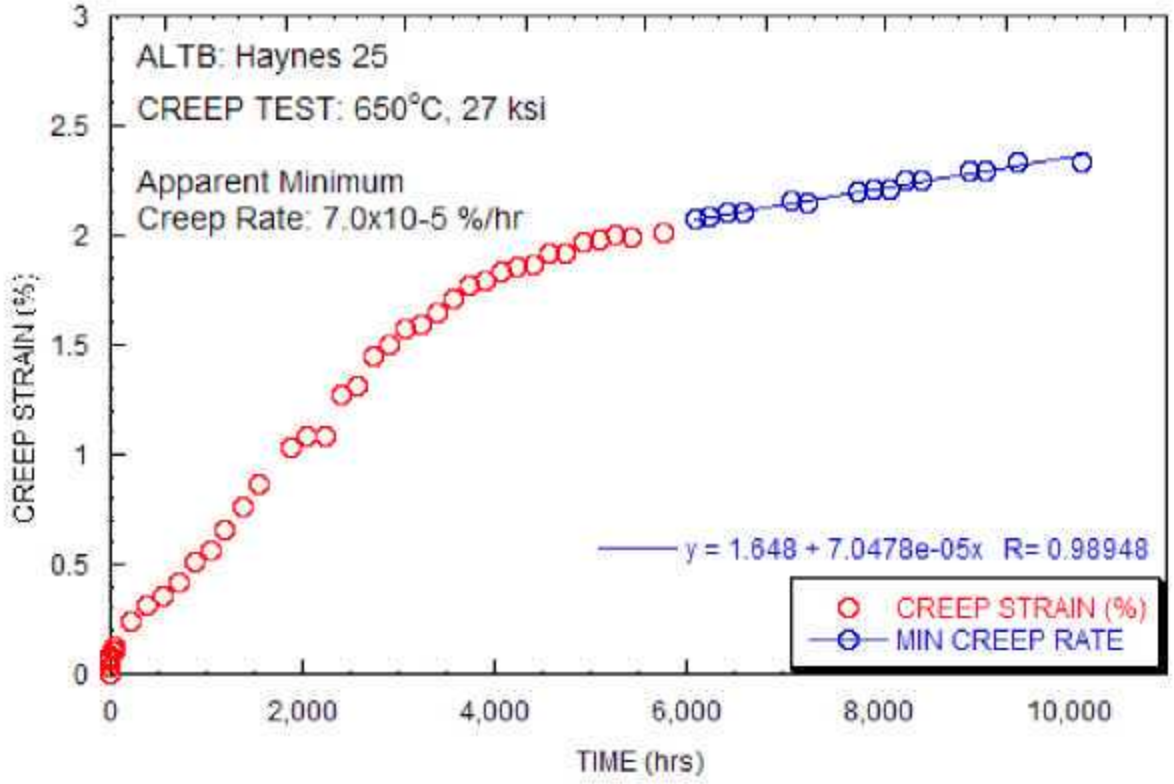

Test ID	Product Form	Aging Temp. (°C)	Aging Time (hours)	Test Temp. (°C)	Stress (MPa)	Rupture Life (hours) stopped or ongoing	Minimum Creep Rate (%/hr)	Elong. (%)	Red. of Area (%)	Failure Location
MG-10	sheet weld	none	none	675	103.4	11295	4.6E-06			

MG-10

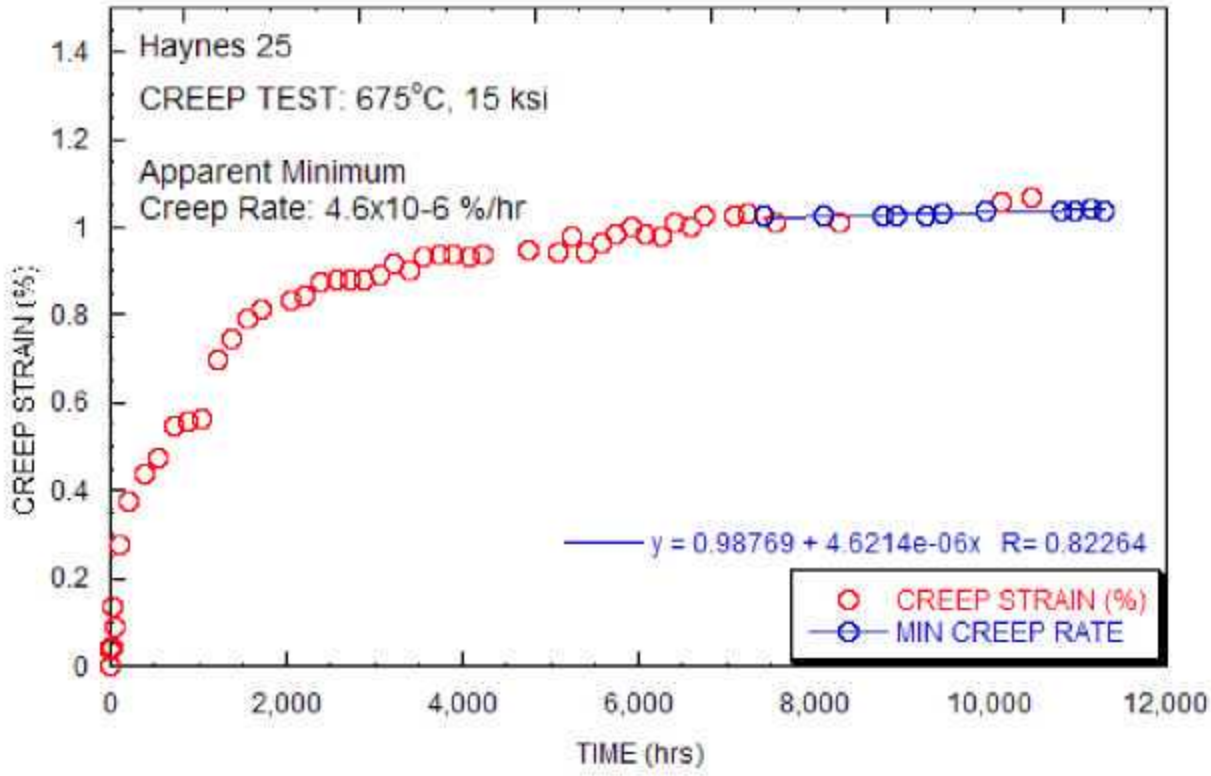

Test ID	Product Form	Aging Temp. (°C)	Aging Time (hours)	Test Temp. (°C)	Stress (MPa)	Rupture Life (hours) stopped or ongoing	Minimum Creep Rate (%/hr)	Elong. (%)	Red. of Area (%)	Failure Location
CR-WM-15	sheet weld	675	6000	650	206.8	32136	1.30E-05	2.6	2.1	BM

CR-WM-15

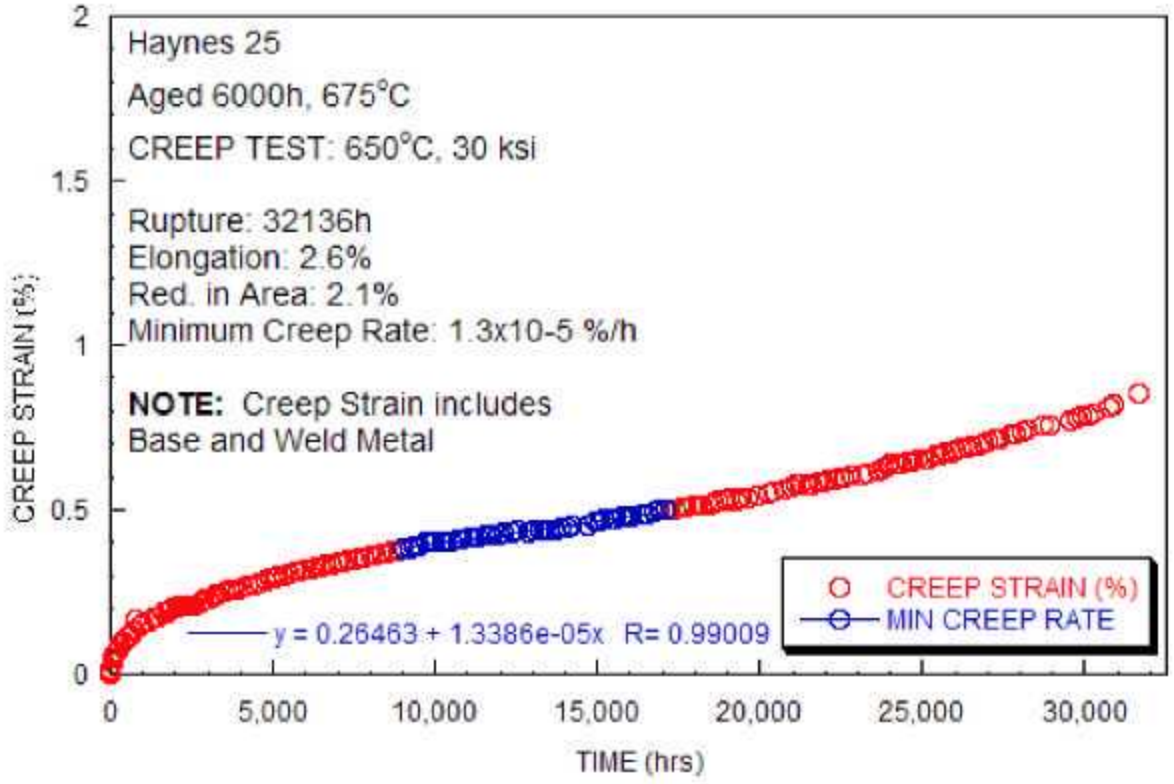

Test ID	Product Form	Aging Temp. (°C)	Aging Time (hours)	Test Temp. (°C)	Stress (MPa)	Rupture Life (hours) stopped or ongoing	Minimum Creep Rate (%/hr)	Elong. (%)	Red. of Area (%)	Failure Location
CR-WM-16	sheet weld	675	6000	700	165.5	16896	3.10E-05	1.8	1.0	HAZ

CR-WM-16

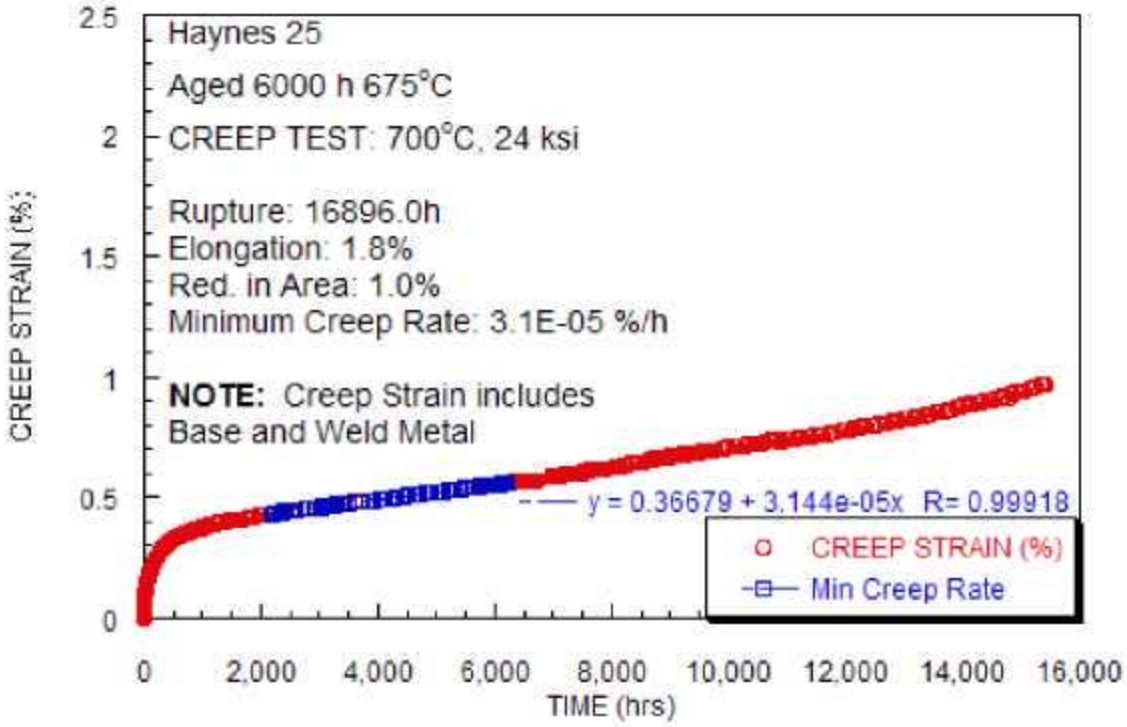

Test ID	Product Form	Aging Temp. (°C)	Aging Time (hours)	Test Temp. (°C)	Stress (MPa)	Rupture Life (hours) stopped or ongoing	Minimum Creep Rate (%/hr)	Elong. (%)	Red. of Area (%)	Failure Location
CR-WM-17	sheet weld	675	6000	750	127.6	11990	8.10E-05	4.5	3.1	BM

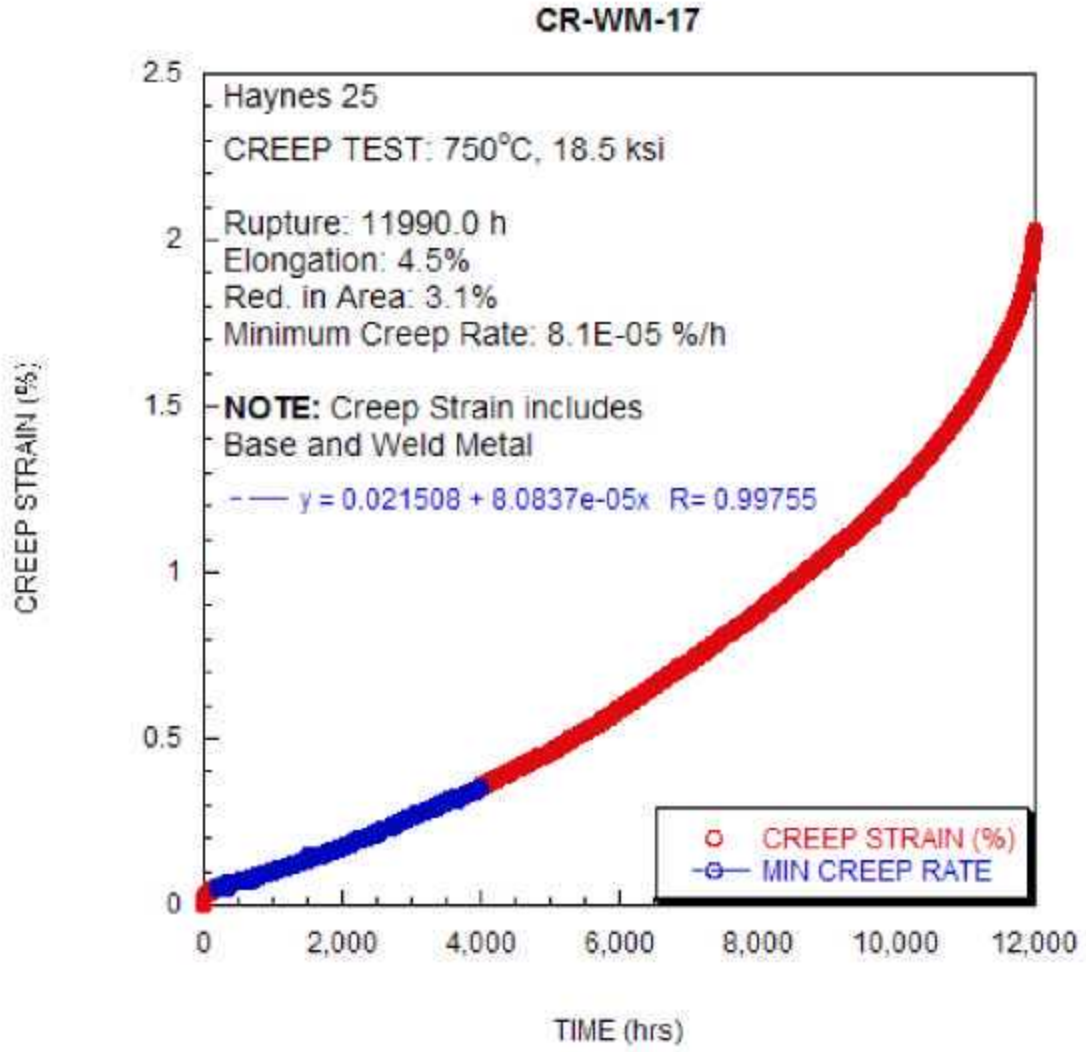

Test ID	Product Form	Aging Temp (°C)	Aging Time (hours)	Test Temp (°C)	Stress (MPa)	Rupture Life (hours) stopped or ongoing	Minimum Creep Rate (%/hr)	Elong (%)	Red of Area (%)	Failure Location
CR-VM-18	sheet weld	675	6000	800	99 3	8568	1 30E-04			BM

Test ID	Product Form	Aging Temp. (°C)	Aging Time (hours)	Test Temp. (°C)	Stress (MPa)	Rupture Life (hours) stopped or ongoing	Minimum Creep Rate (%/hr)	Elong. (%)	Red. of Area (%)	Failure Location
CR-WM-19	sheet weld	675	6000	800	103.4	4011	2.60E-04	4.2	6.2	BM

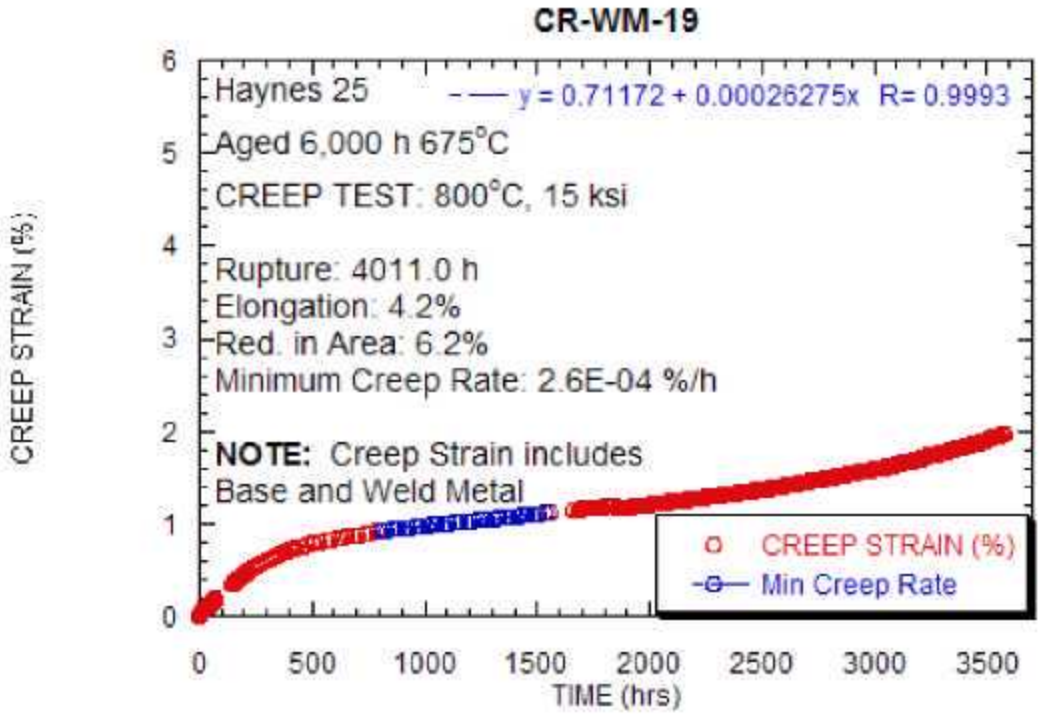

Test ID	Product Form	Aging Temp. (°C)	Aging Time (hours)	Test Temp. (°C)	Stress (MPa)	Rupture Life (hours) stopped or ongoing	Minimum Creep Rate (%/hr)	Elong. (%)	Red. of Area (%)	Failure Location
CR-WM-20	sheet weld	675	6000	850	62.1	11117	1.10E-04	5.2	2.4	BM

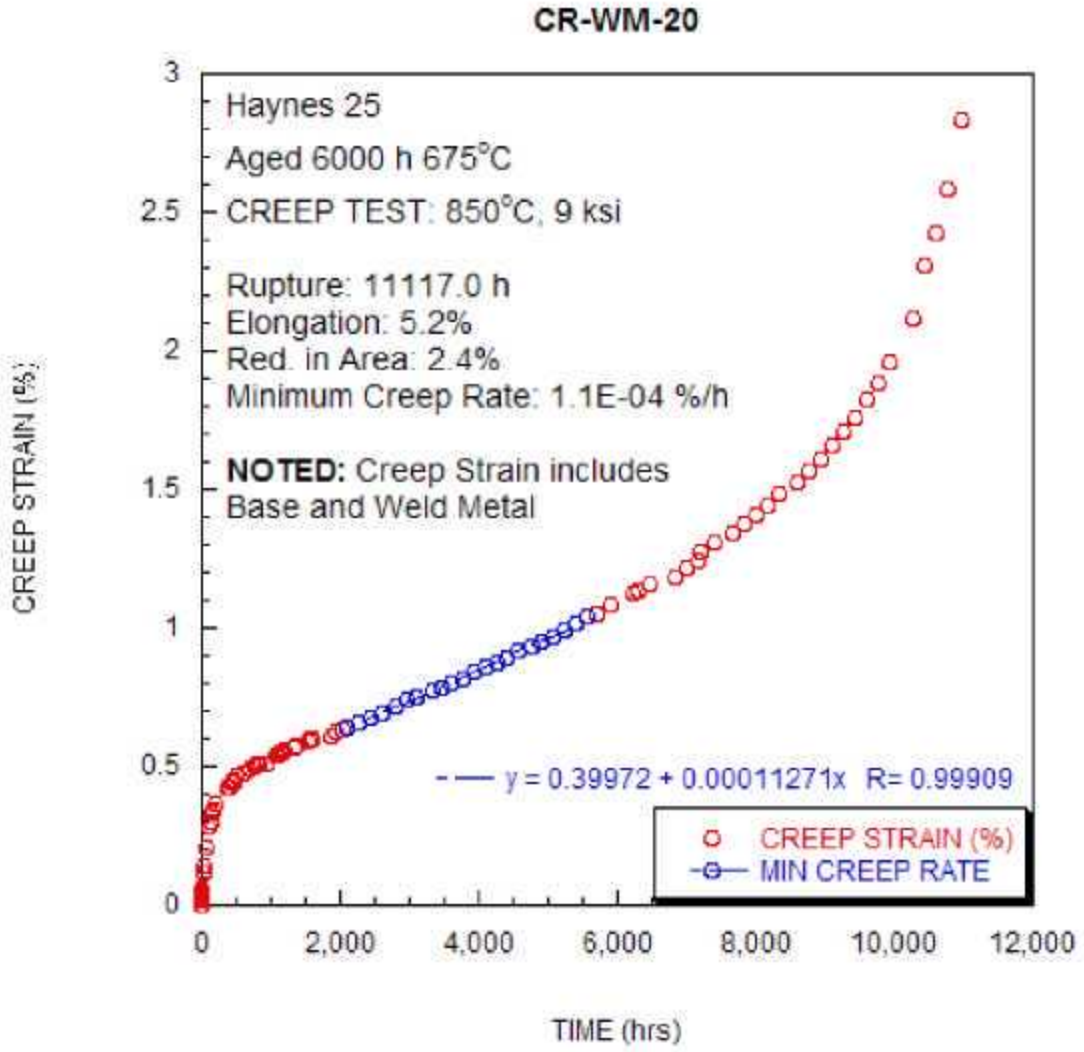

Test ID	Product Form	Aging Temp. (°C)	Aging Time (hours)	Test Temp. (°C)	Stress (MPa)	Rupture Life (hours) stopped or ongoing	Minimum Creep Rate (%/hr)	Elong. (%)	Red. of Area (%)	Failure Location
LWC-9	bar weld	none	none	800	103.4	6464.1	6.34E-04	11.2	27.3	BM

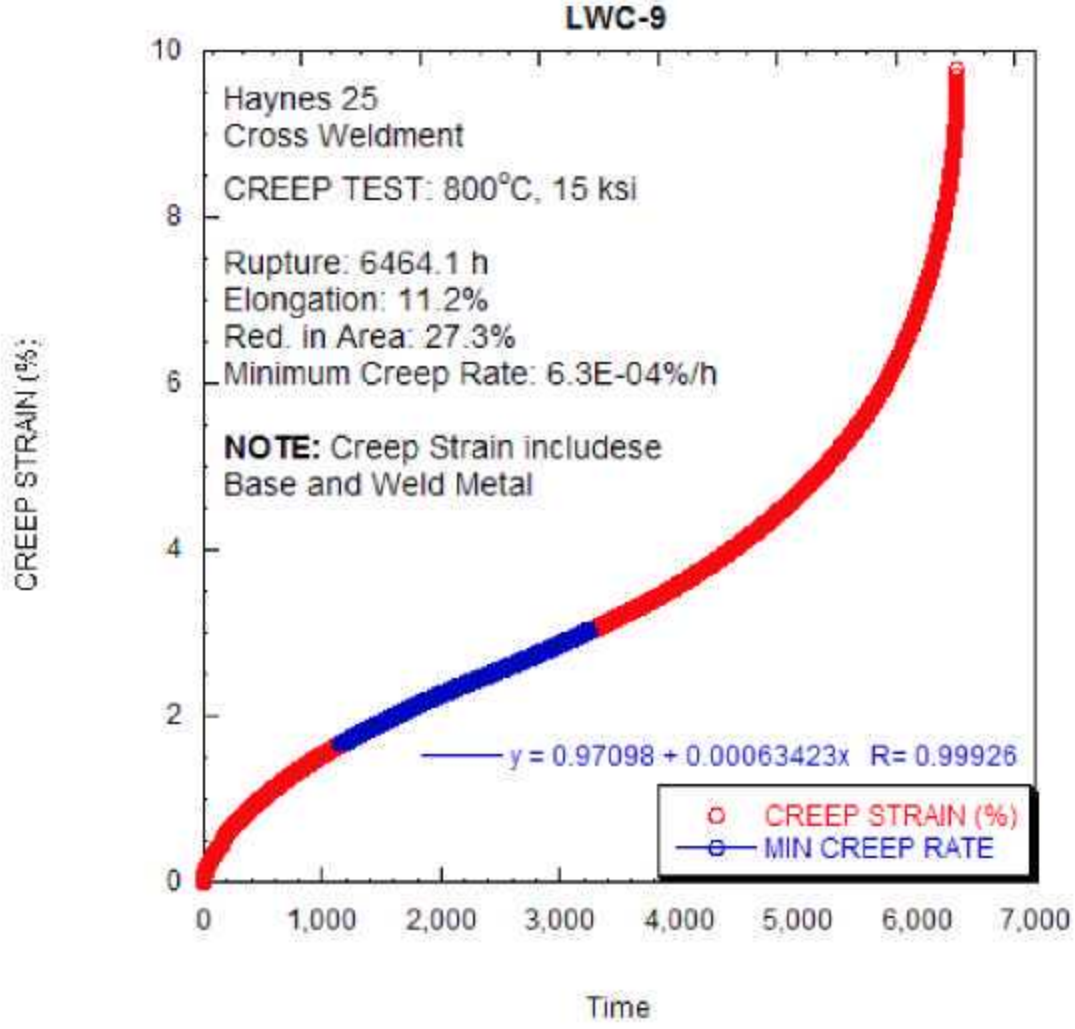

Test ID	Product Form	Aging Temp. (°C)	Aging Time (hours)	Test Temp. (°C)	Stress (MPa)	*Rupture Life (hours) stopped or ongoing*	Minimum Creep Rate (%/hr)	Elong. (%)	Red. of Area (%)	Failure Location
AWC-7	bar weld	none	none	650	124.1	*8326.0*	7.12E-06			

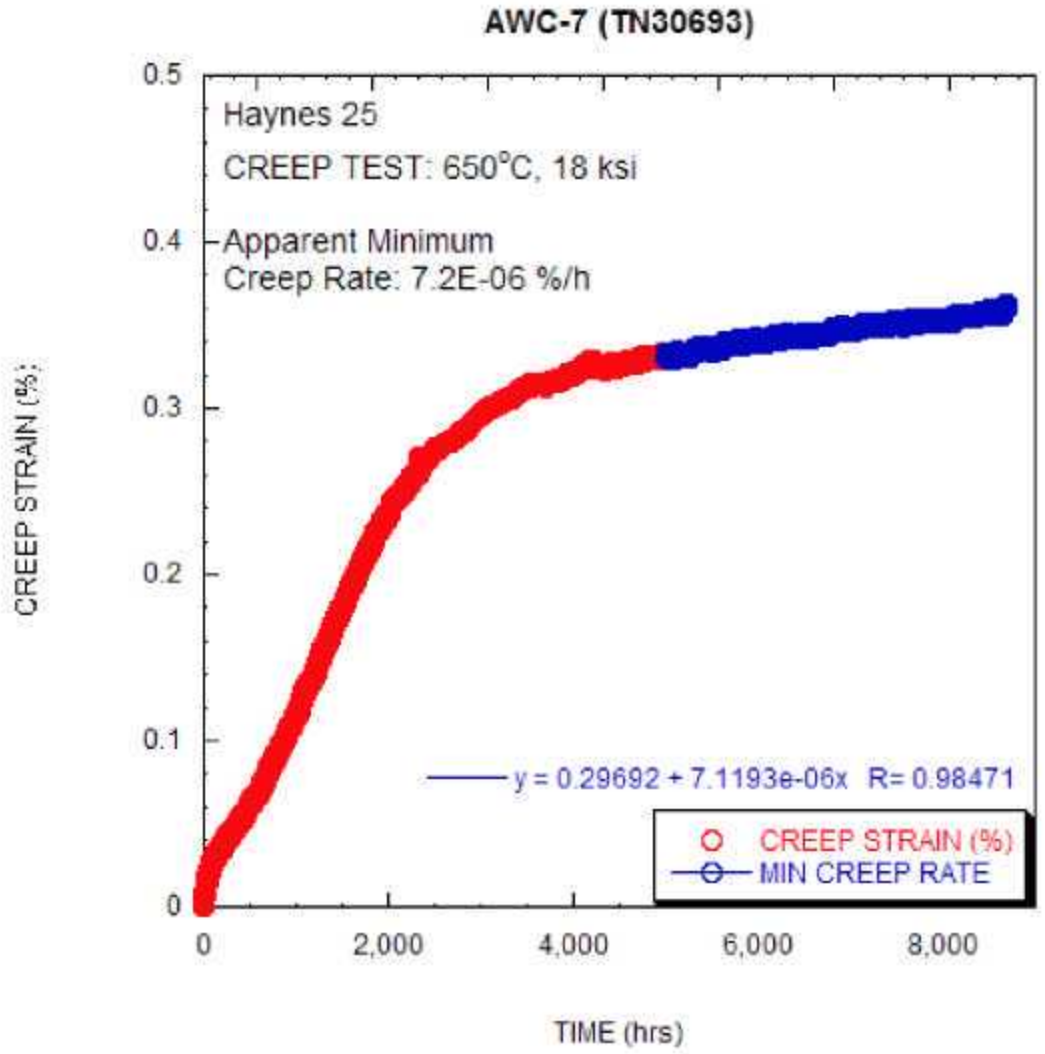

Test ID	Product Form	Aging Temp. (°C)	Aging Time (hours)	Test Temp. (°C)	Stress (MPa)	*Rupture Life (hours) stopped or ongoing*	Minimum Creep Rate (%/hr)	Elong. (%)	Red. of Area (%)	Failure Location
AWC-8	bar weld	none	none	650	206.8	*8186.0*	7.99E-05			

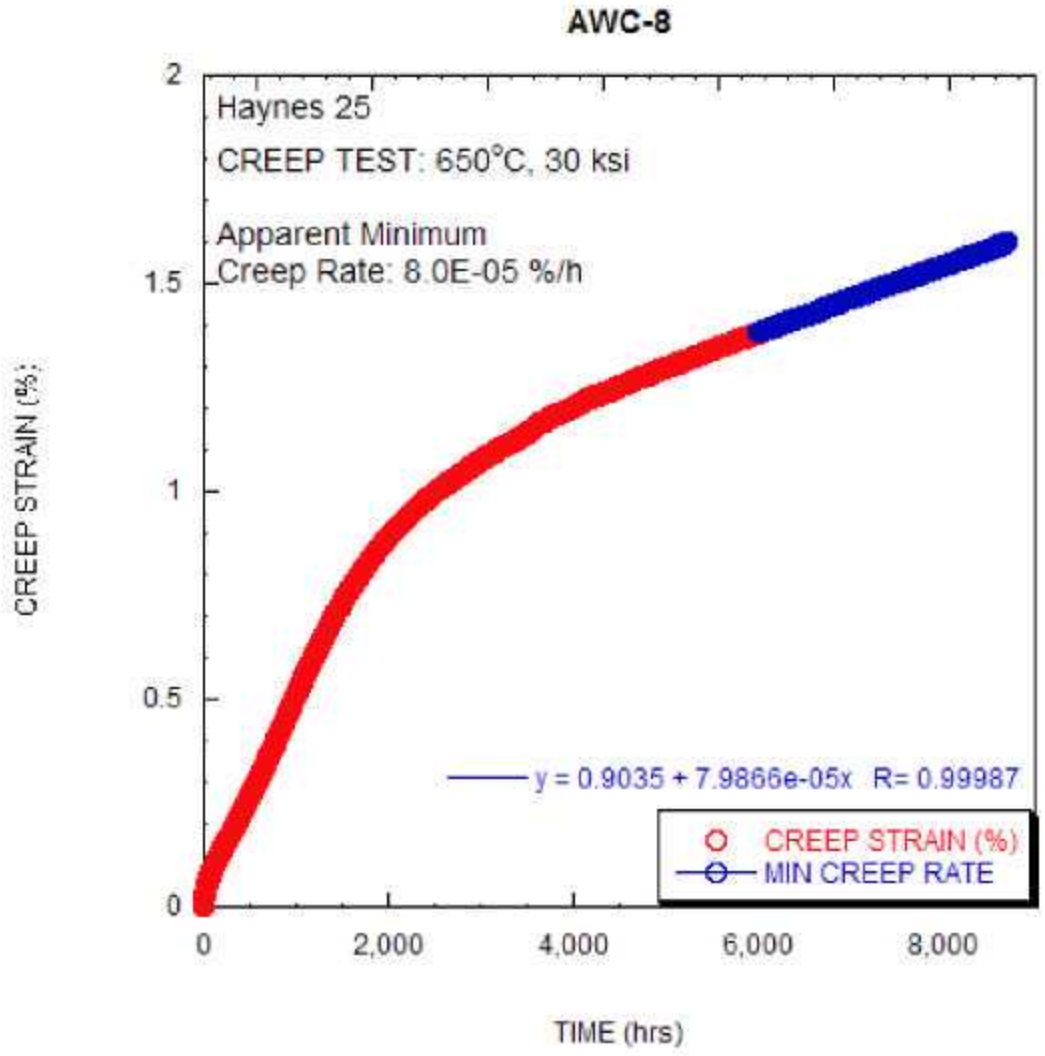

Test ID	Product Form	Aging Temp. (°C)	Aging Time (hours)	Test Temp. (°C)	Stress (MPa)	Rupture Life (hours) stopped or ongoing	Minimum Creep Rate (%/hr)	Elong. (%)	Red. of Area (%)	Failure Location
AWC-9	bar weld	none	none	800	103.4	5718.9	5.71E-04	14.5	19.2	BM

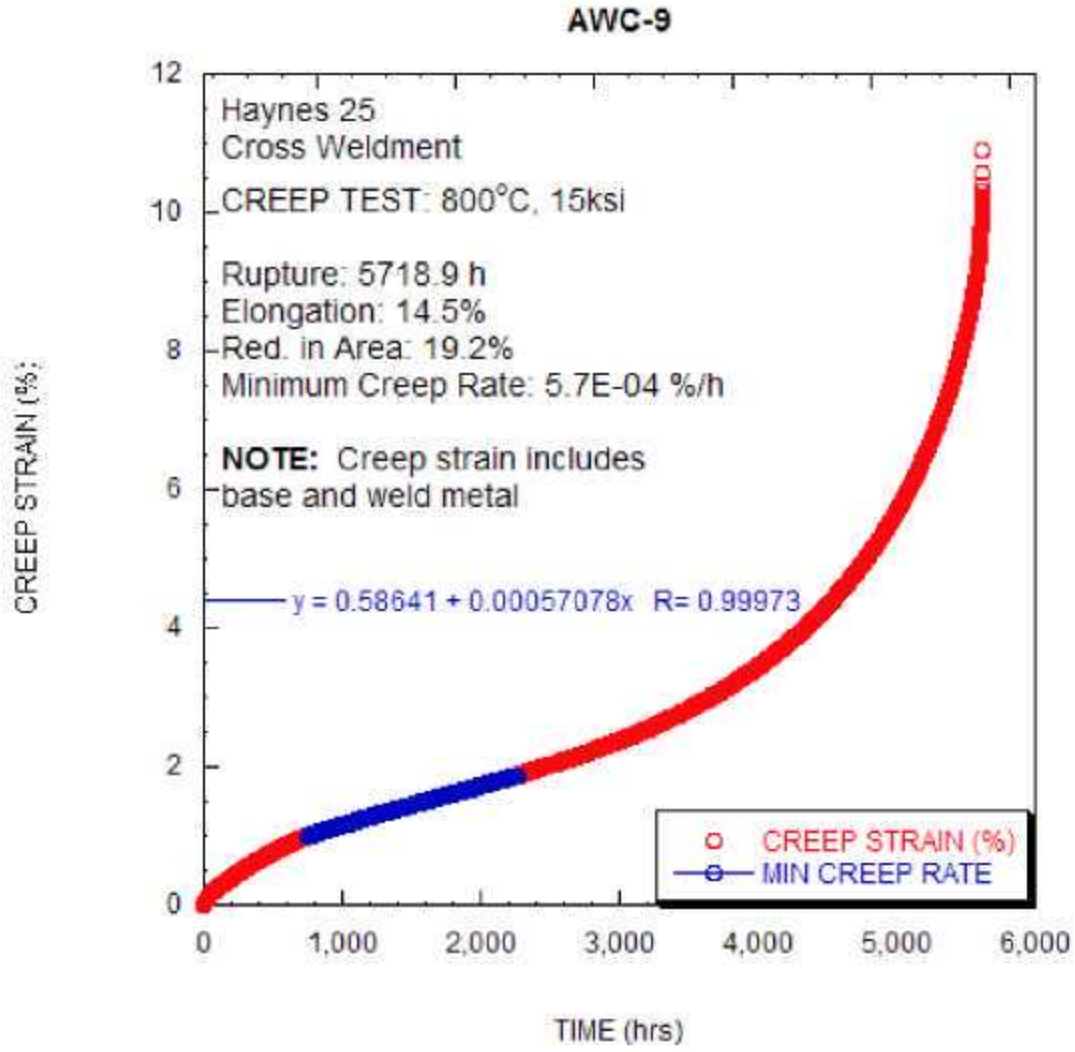

A.7 HISTORICAL SUMMARY OF HAYNES 25 TENSILE DATA

Table A.7.1. Alloy 25 (L-605) historical tensile data for annealed material

Heat ID / Source	Product Form	Temperature (°C)	Yield Strength (MPa)	Ultimate Tensile Strength (MPa)	Elongation (%)
astm 1		24	483	1069	55
astm 1		649	272	514	25
astm 1		816	241	345	15
astm 1		982	145	157	16
astm 1		1149		62	24
astm 2		24	592	1110	47
astm 2		399	385	952	40
astm 2		538	372	903	40
astm 2		649	379	648	29
astm 2		732	354	578	11
astm 2		816	310	381	16
astm 2		899	220	236	30
astm 2		982	190	201	37
astm 4		24	396	1020	36
astm 4		649		731	34
astm 4		816		477	42
astm 5		24	407	958	
ht 1716	sheet	24	492	869	43
ht 1931	sheet	24	459	993	68
ht 1843	sheet	24	385	876	77
ht 1335	sheet	24	476	1034	65
ht 1813	sheet	24	494	952	43.6
ht 1816	sheet	24	448	931	60
ht 1816	sheet	316	305	827	80
ht 1816	sheet	760	242	583	28
ht 1816	sheet	982	125	231	40
xxx	sheet	649	241	483	24
xxx	sheet	982	159	179	39
xxx	sheet	24	424	993	85
xxx	sheet	24	385	896	94
xxx	sheet	650	195	686	64
xxx	sheet	700	191	636	50
xxx	sheet	800	183	388	28.8
xxx	sheet	850	186	300	20.8
DMIC-32	sheet	24	462	1007	64
DMIC-32	sheet	316		814	77.5
DMIC-32	Sheet	427		772	72
DMIC-32	sheet	538		690	68
DMIC-32	sheet	593		669	53.5

Table A.7.1. Alloy 25 (L-605) historical tensile data for annealed material (Continued)

Heat ID / Source	Product Form	Temperature (°C)	Yield Strength (MPa)	Ultimate Tensile Strength (MPa)	Elongation (%)
DMIC-32	sheet	649		514	25
DMIC-32	sheet	732		372	13
DMIC-32	sheet	816		345	15
DMIC-32	sheet	899		228	16
DMIC-32	sheet	982		157	16
DMIC-32	sheet	1093		97	23.3
DMIC-32	sheet	1149		62	24
DMIC-32	sheet	1204		50	22.6
DMIC-32	sheet	1260		35	18.6
DMIC-33	sheet	24	483	1069	55
DMIC-33	sheet	93		979	62
DMIC-33	sheet	149		924	67
DMIC-33	sheet	204		876	71
DMIC-33	sheet	260		841	75
DMIC-33	sheet	316		814	77
DMIC-33	sheet	371		786	75
DMIC-33	sheet	427		772	72
DMIC-33	sheet	482		745	71
DMIC-33	sheet	538	241	703	68
DMIC-33	sheet	760	255	365	13
DMIC-33	sheet	871	234	276	14
DMIC-33	sheet	982		159	18
DMIC-33	sheet	649	241	524	25
DMIC-33	sheet	1093		90	23
DMIC-34	sheet	24	463	1007	64

Table A.7.1 Alloy 25 (L-605) historical tensile data for annealed material (Continued)

Heat ID / Source	Product Form	Temperature (°C)	Yield Strength (MPa)	Ultimate Tensile Strength (MPa)	Elongation (%)
DMIC-34	sheet	316	279	883	72
DMIC-34	sheet	427	269	855	74
DMIC-34	sheet	538	247	800	59
DMIC-34	sheet	649	244	710	35
DMIC-34	sheet	760	260	455	12
DMIC-34	sheet	871	238	321	30
DMIC-34	sheet	982	159	237	41
DMIC-34	sheet	1093	83	135	34
DMIC-34	sheet	1149	61	72	21
DMIC-34	sheet	1204	39	47	14
DMIC-34	sheet	1260		32	13
DMIC-34	sheet	1316		21	6
DMIC-39	sheet	24	592	1110	47
DMIC-39	sheet	399	385	952	40
DMIC-39	sheet	538	372	903	40
DMIC-39	sheet	649	379	648	29
DMIC-39	sheet	732	354	578	11
DMIC-39	sheet	816	310	381	16
DMIC-39	sheet	899	219	236	30
DMIC-39	sheet	982	190	201	37
DMIC-39	sheet	1149		82	24
DMIC-38	sheet	24	474	972	43
DMIC-38	sheet	538	245	758	59
DMIC-38	sheet	538	249	710	45
DMIC-38	sheet	649	230	651	40

Table A.7.1. Alloy 25 (L-605) historical tensile data for annealed material (Continued)

Heat ID / Source	Product Form	Temperature (°C)	Yield Strength (MPa)	Ultimate Tensile Strength (MPa)	Elongation (%)
DMIC-38	sheet	649	239	696	43.5
DMIC-38	sheet	732	208	520	23
DMIC-38	sheet	732	228	556	28
DMIC-38	sheet	816	220	445	27
DMIC-38	sheet	816	227	441	27.5
DMIC-38	sheet	899	226	328	28
DMIC-38	sheet	899	223	300	26
DMIC-38	sheet	982	151	169	35
DMIC-38	sheet	982	183	219	35
DMIC-38	sheet	1038	51	85	18
DMIC-38	sheet	1038	79	103	16.5
DMIC-38	sheet	1093	68	90	17
DMIC-38	sheet	1093	48	73	22.5
DMIC-38	sheet	1149	32	55	13
DMIC-38	sheet	1149	40	54	22
DMIC-56	sheet	24	496	938	59
DMIC-56	sheet	649	234	621	66
DMIC-56	sheet	649	254	696	70
DMIC-56	sheet	871	217	433	31
DMIC-56	sheet	871	200	410	40
DMIC-56	sheet	982	200	270	35
DMIC-56	sheet	982	155	227	25
DMIC-56	sheet	1149	54	103	25
DMIC-56	sheet	1149	66	109	25

Table A.7.2. Alloy 25 (L-605) historical tensile data for welded material

Heat ID / Source	Product Form (Thickness in inches)	Weld Process	Temperature (°C)	Yield Strength (MPa)	Ultimate Tensile Strength (MPa)	Elongation (%)	Failure Location
haynes	.094 sht	sma	24	505	898	30	
haynes	.094 sht	sma	816	247	452	16	
haynes	.125 sht	sma	24	486	920	35	
haynes	.125 sht	sma	816	232	445	15	
haynes	.094 sht	gta	24	512	935	38	
haynes	.094 sht	gta	816	249	472	19	
haynes	.125 sht	gta	24	496	945	40	
haynes	.125 sht	gta	816	232	477	23	
DMIC 25	.062 sht	gta	24	402	958	58.5	weldment
DMIC 25	.062 sht	gta	24	461	949	55	weldment
DMIC 25	.062 sht	gta	538	248	696	50.5	weldment
DMIC 25	.062 sht	gta	538	250	667		
DMIC 25	.062 sht	gta	649	261	605	25	weldment
DMIC 25	.062 sht	gta	649	261	618		
DMIC 25	.062 sht	gta	732	226	527	18.5	weldment
DMIC 25	.062 sht	gta	732	233	583	22	weldment
DMIC 25	.062 sht	gta	816	220	419	23	
DMIC 25	.062 sht	gta	816	206	416	22	weldment
DMIC 25	.062 sht	gta	900	220	241	30	weldment
DMIC 25	.062 sht	gta	900	225	239	30	weldment
DMIC 25	.062 sht	gta	982	14.4	158	17	weldment
DMIC 25	.062 sht	gta	982	152	161	22	weldment
DMIC 25	.062 sht	gta	1038	68	119	15	weldment
DMIC 25	.062 sht	gta	1038	66	128	14	weldment
DMIC 25	.062 sht	gta	1038	54	68	14	weldment
DMIC 25	.062 sht	gta	1038	55	63	15.5	
DMIC 25	.062 sht	gta	1149		57	6.5	weldment
DMIC 25	.062 sht	gta	1149	32	41	7	weldment

Table A.7.2. Alloy 25 (L-605) historical tensile data for welded material (Continued)

Heat ID / Source	Product Form (Thickness in inches)	Weld Process	Temperature (°C)	Yield Strength (MPa)	Ultimate Tensile Strength (MPa)	Elongation (%)	Failure Location
DMIC 6	0.04 sht	gta	24	505	787	18.2	
DMIC 6	0.04 sht	gta	871	237	245	9.6	
DMIC 6	0.04 sht	gta	1093	75	80	12.4	
1931	.062 sht	gta	24	481	910	35	
1843	.062 sht	gta	24	432	864	34	
1335	.060 sht	gta	24	490	972	40	

Table A.7.3. Alloy 25 (L-605) historical tensile data for aged material

Heat ID / Source	Aging Temperature (°C)	Aging Time (hours)	Test Temperature (°C)	Yield Strength (MPa)	Ultimate Tensile Strength (MPa)	Elongation (%)	Reduction of Area (%)
DMIC 39	760	0	760	228	324	9	
DMIC 39	760	0	760	193	386	18	
DMIC 39	760	120	760	283	579	24	
DMIC 39	760	120	760	214	510	31	
DMIC 39	760	350	760	421	641	10	
DMIC 39	760	350	760	393	676	18	
DMIC 39	871	0	871	172	324	19	
DMIC 39	871	0	871	179	386	19	
DMIC 39	871	120	871	186	414	38	
DMIC 39	871	120	871	269	372	25	
DMIC 39	871	350	871	186	386	30	
DMIC 39	871	350	871	179	386	37	
DMIC39	982	0	982	103	200	17	
DMIC 39	982	0	982	110	248	12	
DMIC 39	982	120	982	103	179	22	
DMIC 39	982	120	982	138	248	35	
DMIC39	982	350	982	83	228	35	
DMIC 39	982	350	982	110	248	32	
ORNL 1816	816	0	24	448	931	60	
ORNL 1816	816	11448	24	427	821	7.9	7.9
ORNL 1816	816	11448	24	427	848	8.8	8.8
ORNL 1816	816	0	316	303	827	80	
ORNL 1816	816	11448	316	317	772	20	20
ORNL 1816	816	11448	316	303	758	18.3	18.3
ORNL 1816	816	0	760	241	586	28	
ORNL 1816	816	11448	760	241	552	53.1	20
ORNL 1816	816	11448	760	255	558	53	18.4
ORNL 1816	816	0	982	124	234	40	
ORNL 1816	816	11448	982	152	179	48	6
ORNL 1816	816	0	24	448	931	60	
ORNL 1816	816	11448	24	400	931	10.2	10.2
ORNL 1816	816	11448	24	379	1020	10.8	10.8
ORNL 1816	816	0	316	303	827	80	

Table A.7.3. Alloy 25 (L-605) historical tensile data for aged material (continued)

Heat ID / Source	Aging Temperature (°C)	Aging Time (hours)	Test Temperature (°C)	Yield Strength (MPa)	Ultimate Tensile Strength (MPa)	Elongation (%)	Reduction of Area (%)
ORNL 1816	816	11448	316	331	821	20.2	20.2
ORNL 1816	816	11448	316	324	765	13.8	13.8
ORNL 1816	816	0	760	241	586	28	
ORNL 1816	816	11448	760	262	586	57.7	16.7
ORNL 1816	816	11448	760	262	586	59.4	16.6
ORNL 1816	816	0	982	124	234	40	
ORNL 1816	816	11448	982	152	179	47.1	6
ORNL 1816	816	11448	982	76	90	75	7.7
ORNL 1813	850	0	24	496	952	43.6	43.2
ORNL 1813	850	50	24	552	779	14.6	
ORNL 1813	850	4843	24	607	917	12.9	12.7
SNAP 29	760	0	24	407	883	56.6	
SNAP 29	760	500	24	427	724	17	
SNAP 29	760	1000	24	483	793	10	
SNAP 29	760	4000	24		793	2	
SNAP 29	760	0	538	179	655	71.2	
SNAP 29	760	500	538	200	600	41.3	
SNAP 29	760	1000	538	296	690	27.8	
SNAP 29	760	4000	538	359	752	10	
SNAP 29	816	0	24	407	883	56.6	
SNAP 29	816	500	24	462	765	8	
SNAP 29	816	1000	24	522	851	3	
SNAP 29	816	4000	24	490	821	2	
SNAP 29	816	0	538	179	655	71.2	
SNAP 29	816	500	538	262	621	15	
SNAP 29	816	1000	538	359			
SNAP 29	816	4000	538	338	627	5	
SNAP 29	871	0	24	407	883	56.6	
SNAP 29	871	500	24	517	876	8	
SNAP 29	871	1000	24	476	807	3	
SNAP 29	871	4000	24	462	731	2	
SNAP 29	871	0	538	179	655	71.2	
SNAP 29	871	500	538	317	765	10	
SNAP 29	871	1000	538	310	676	8.3	
SNAP 29	871	4000	538	296	607	4	

Table A.7.3. Alloy 25 (L-605) historical tensile data for aged material (continued)

Heat ID / Source	Aging Temperature (°C)	Aging Time (hours)	Test Temperature (°C)	Yield Strength (MPa)	Ultimate Tensile Strength (MPa)	Elongation (%)	Reduction of Area (%)
Wlodek A	871	4	24	600		35	
Wlodek A	871	15	24	607		27	
Wlodek A	871	25	24	614		18	
Wlodek A	871	50	24	607		18	
Wlodek A	871	100	24	565		12	
Wlodek A	871	1000	24	586	1117	9	
Wlodek B	871	1000	24	531	1034	7	
Wlodek C	871	1000	24	565	1069	5	
Wlodek C	871	1000	260	414		12	
Wlodek C	871	1000	538	372		15	
Wlodek D	871	1000	24	586	1055	5	
Wlodek E	871	15	24	469		16	
Wlodek E	871	25	24	469		10	
Wlodek E	871	50	24	496		10	
Wlodek E	871	100	24	538		10	
Wlodek E	871	1000	24	565	979	5	
Wlodek F	871	1000	24	531	910	2	
Wlodek F	871	1000	260	365		7	
Wlodek F	871	1000	538	331		11	
Wlodek F	871	1000	871	179		34	
Wlodek G	871	1000	24	593	917	1	
Wlodek G	871	1000	260	496		1	
Wlodek G	871	1000	538	434		2	
Bourgette	650	0	24	386	896	94	91
Bourgette	650	1000	24	393	786	53	53
Bourgette	650	1000	24	386	834	60	60
Bourgette	650	2000	24	427	841	34	34
Bourgette	650	2000	650	255	724	47	47
Bourgette	700	0	24	386	896	94	91
Bourgette	700	1000	24	758	917	5	5
Bourgette	700	1000	24	758	952	8	8
Bourgette	700	2000	24	917	1027	2.5	2.5
Bourgette	700	2000	700	703	855	16	6.5
Bourgette	800	0	24	386	896	94	91
Bourgette	800	1000	24	545	938	15	15
Bourgette	800	1000	800		648	20.5	20.5
Bourgette	800	2000	24	545	924	10.5	10.5
Bourgette	800	2000	800	310	483	33.5	12
Bourgette	850	0	24	386	896	94	91
Bourgette	850	1000	650	193	690	64	63
Bourgette	850	1000	700	193	634	50	50
Bourgette	850	1000	850		352	44.5	7.5
Bourgette	850	2000	24	483	772	5.2	5.2
Bourgette	850	2000	850	255	290	43.5	8

A.8 HISTORICAL SUMMARY OF HAYNES 25 CREEP-RUPTURE DATA

Table A.8.1. Alloy 25 (L-605) historical creep and stress-rupture data

Heat ID / Source	Temperature (°C)	Stress (MPa)	Rupture Life (MPa)	Minimum Creep Rate (%/hr)	Elongation (%)
astm1	982	28	686	5.00E-04	4.0
astm1	982	34	269	3.60E-03	4.0
astm1	927	41	569	9.00E-04	6.0
astm1	982	41	198	5.50E-03	2.0
astm1	871	55	1671	2.60E-04	6.0
astm1	927	55	283	6.40E-03	13.0
astm1	871	69	582	2.60E-03	10.0
astm1	927	69	123	1.07E-02	13.0
astm1	871	83	506	6.40E-03	7.6
astm1	927	83	73.2	2.67E-01	10.0
astm1	816	97	2850	1.90E-04	4.0
astm1	871	97	186	4.04E-02	10.0
astm1	871	103	139	4.50E-02	19.0
astm1	816	124	389	1.93E-02	15.0
astm1	816	124	324	2.81E-02	11.0
astm1	871	124	51.5	1.39E-01	17.5
astm1	816	131	431	1.42E-02	20.0
astm1	816	148	269	2.57E-02	17.0
astm1	816	165	107	9.33E-02	17.0
astm1	649	310	121	5.80E-03	7.0
astm2	899	69	324		6.0
astm2	899	103	36		16.0
astm2	816	138	437		15.0
astm2	899	138	10.7		20.0
astm2	816	172	128		21.0
astm2	899	172	2		24.0
astm2	816	241	9.1		28.0
astm2	649	345	71.9		6.0
astm2	649	394	4.4		7.0
astm2	649	446	4		8.0
astm2	649	483	1.2		11.0
astm3	982	34	420	5.30E-03	3.5
astm3	982	41	165	1.40E-02	4.0
astm3	982	55	30	1.80E-01	9.0
astm3	982	69	11.5	7.10E-01	9.0
astm3	982	90	1.9	3.10E+00	13.5
astm3	816	103	752	3.80E-03	5.0
astm3	816	138	90	4.60E-02	6.0
astm3	816	172	20	2.80E-01	7.5
astm3	816	207	5	1.35E+00	10.5
astm4	816	129	302.9		14.0
astm4	816	150	115.5		22.0
astm4	816	172	64.5		15.0

Table A.8.1. Alloy 25 (L-605) historical creep and stress-rupture data (continued)

Heat ID / Source	Temperature (°C)	Stress (MPa)	Rupture Life (MPa)	Minimum Creep Rate (%/hr)	Elongation (%)
astm4	816	207	15.4		20.0
astm4	649	455	193.5		8.0
astm4	649	481	113.5		9.0
Baughman	1038	34	6.8		11.0
Baughman	982	55	5		9.0
Baughman	982	69	1.6		14.0
Baughman	982	69	1.4		13.0
Baughman	1038	69	0.2		19.0
Baughman	982	103	0.2		22.0
Flagella	1093	10	595	7.00E-04	
Flagella	1093	14	424.6	5.67E-04	4.1
Flagella	1093	14	329.7	5.88E-04	3.7
Flagella	1093	14	219.8	6.55E-04	4.0
Flagella	1093	18	223	1.25E-03	
Flagella	1093	23	150.8	8.00E-03	6.2
Flagella	1093	24	170	2.10E-03	3.8
Flagella	1093	24	39.6	4.00E-03	
Flagella	1093	24	132	5.21E-03	7.0
Flagella	1093	25	64	3.80E-03	
Flagella	1093	41	13.6	1.28E-01	12.1
Flagella	1093	41	9.8	2.59E-01	10.6
Flagella	1093	41	5.4	9.12E-01	
Flagella	1093	42	14.5	7.78E-02	10.5
Flagella	927	76	1057	1.76E-03	15.9
Flagella	927	83	729	2.30E-03	21.3
Flagella	927	83	652	3.80E-03	26.6
Flagella	927	83	554	2.67E-03	23.8
Flagella	927	117	92.7	1.74E-02	22.3
Flagella	927	117	81.3	4.35E-02	21.0
Flagella	927	117	79.2	1.46E-02	28.0
Flagella	927	117	74.9	5.77E-02	20.0
Flagella	927	138	24.1	2.53E-01	33.3
Flagella	927	138	23.6	1.89E-01	22.9
Flagella	927	138	17	5.87E-01	23.5
Flagella	927	138	13.6	3.76E-01	25.2
Flagella	760	234	2053	6.60E-04	11.5
Flagella	760	234	1584	1.43E-03	10.2
Flagella	760	241	1289	2.50E-03	12.8
Flagella	760	241	1002	2.60E-03	6.9
Flagella	760	276	184	1.40E-02	7.7
Flagella	760	290	103	2.90E-02	6.8
Flagella	760	290	194	1.60E-02	6.5
Flagella	760	290	152.5	2.30E-02	5.1
Flagella	760	310	83.1	3.40E-02	6.4
Flagella	760	345	29.2	1.27E-01	4.0
Flagella	760	379	16.9	2.57E-01	7.4

Table A.8.1. Alloy 25 (L-605) historical creep and stress-rupture data (continued)

Heat ID / Source	Temperature (°C)	Stress (MPa)	Rupture Life (MPa)	Minimum Creep Rate (%/hr)	Elongation (%)
Flagella	760	379	9.1	2.93E-01	4.3
Greene	982	40	87		5.0
Greene	982	59	58		9.0
Greene	982	69	14		19.0
Greene	982	76	7.1		16.0
Greene	982	79	8.8		21.0
Greene	982	79	7.8		14.0
Greene	982	79	5		18.0
Greene	982	103	1.8		32.0
Greene	982	138	0.3		30.0
Greene	982	159	0.2		31.0
HW80794	1149	17	10		
HW80794	1108	21	46		
HW80794	1149	21	3.6		
HW80794	1108	22	34		
HW80794	1108	26	10		
HW80794	1149	28	1.6		
HW80794	1108	29	8.2		
HW80794	1108	30	7		
HW80794	1149	30	0.8		
HW80794	1108	33	6		
HW80794	1108	38	2.7		
HW80794	1108	41	0.7		
ORNL 1335	816	121	474	2.00E-02	15.0
ORNL 1335	760	155	522	1.70E-02	13.0
ORNL 1335	704	276	151	8.00E-03	5.0
ORNL 1716	1316	14	0.6	1.50E+01	12.5
ORNL 1716	1204	21	1.3	5.80E+00	10.0
ORNL 1716	1149	28	3	3.00E-01	4.0
ORNL 1716	1177	28	0.8	6.50E+00	7.0
ORNL 1716	1204	28	0.4	2.70E+01	11.0
ORNL 1716	1260	28	0.2	9.00E+01	15.0
ORNL 1716	1149	41	0.5	4.50E+00	5.0
ORNL 1716	1177	41	0.2	5.50E+01	15.0
ORNL 1716	1204	41	0.1	1.30E+02	16.0
ORNL 1716	1093	48	2.4	1.20E+01	6.0
ORNL 1716	1093	69	0.3	2.20E+01	12.0
ORNL 1716	1149	69	0	1.80E+02	7.5
ORNL 1716	871	79	164		3.5
ORNL 1716	982	103	1	5.00E+00	9.0
ORNL 1716	1093	103	0	4.00E+02	13.0
ORNL 1716	816	121	386	1.20E-02	6.0
ORNL 1716	982	138	0.3	4.00E+01	16.0
ORNL 1716	760	190	33		3.0
ORNL 1843	871	79	515		20.0
ORNL 1843	816	121	382	4.00E-02	23.0

Table A.8.1. Alloy 25 (L-605) historical creep and stress-rupture data (continued)

Heat ID / Source	Temperature (°C)	Stress (MPa)	Rupture Life (MPa)	Minimum Creep Rate (%/hr)	Elongation (%)
ORNL 1843	760	155	1296	1.10E-02	20.0
ORNL 1931	1204	28	0.6	2.60E+01	22.0
ORNL 1931	1149	41	0.3	4.20E+01	17.0
ORNL 1931	1093	48	0.8	1.00E+01	9.0
ORNL 1931	1093	69	0.2	3.30E+01	14.0
ORNL 1931	982	103	1.5	7.90E+00	15.0
ORNL 1931	816	121	595	1.30E-02	10.0
ORNL 1931	760	190	155	4.00E-02	8.0
ORNL 1931	704	276	248	2.20E-02	5.0
Widmer	982	28	1463.5	6.60E-04	5.2
Widmer	982	34	921.9	1.00E-03	9.1
Widmer	982	38	528	1.60E-03	9.3
Widmer	982	41	447.2	2.80E-03	10.0
Widmer	982	48	160	1.30E-02	9.6
Widmer	982	55	51	7.80E-02	6.3
Widmer	982	59	65.8	7.60E-02	10.7
Widmer	982	61	56.6	8.00E-02	7.8
Widmer	899	62	892	1.20E-03	4.0
Widmer	899	69	965.9	1.60E-03	6.4
Widmer	982	69	28.6		19.1
Widmer	899	76	287.8	1.60E-02	8.0
Widmer	816	79	13018	8.50E-05	4.9
Widmer	899	83	235	1.50E-02	8.9
Widmer	982	83	7.8	1.40E+00	20.8
Widmer	899	90	123.5	5.60E-02	12.7
Widmer	982	90	5.2	2.80E+00	32.4
Widmer	816	103	3883.8	4.00E-04	10.0
Widmer	857	103	368.4	1.60E-02	10.3
Widmer	899	103	70.9	1.20E-01	11.0
Widmer	982	103	2.1	6.90E+00	29.4
Widmer	899	110	46.6	2.90E-01	27.0
Widmer	816	117	1157	4.70E-03	9.4
Widmer	816	117	1203		11.1
Widmer	816	117	1661.8		15.3
Widmer	816	117	1729.4		8.2
Widmer	816	117	1764.7		10.3
Widmer	816	117	1802		14.5
Widmer	816	117	2010		11.7
Widmer	899	121	15.3	1.20E+00	26.6
Widmer	982	124	0.8	1.40E+01	32.9
Widmer	816	128	748.3	9.80E-03	15.1
Widmer	899	131	12.7	1.20E+00	23.6
Widmer	816	138	305.7	7.10E-02	13.9
Widmer	899	138	8.7	1.60E+00	23.5
Widmer	816	148	301	7.50E-02	16.5
Widmer	816	152	146	7.20E-02	14.5

Table A.8.1. Alloy 25 (L-605) historical creep and stress-rupture data (continued)

Heat ID / Source	Temperature (°C)	Stress (MPa)	Rupture Life (MPa)	Minimum Creep Rate (%/hr)	Elongation (%)
Widmer	899	152	4.2	3.60E+00	19.9
Widmer	732	172	6055	5.70E-04	7.2
Widmer	816	172	96.5	9.50E-02	23.4
Widmer	857	172	9.6	1.60E+00	19.7
Widmer	732	179	5654	4.10E-04	7.0
Widmer	649	183	21789	9.60E-06	1.2
Widmer	732	190	2098.8	1.10E-03	5.0
Widmer	816	190	25.7	2.60E-01	15.0
Widmer	649	193	10192	4.50E-05	1.4
Widmer	732	200	1969.1	1.20E-03	5.6
Widmer	649	203	17867	5.20E-05	2.2
Widmer	732	203	374.6	3.80E-03	2.4
Widmer	732	207	218.2	4.00E-03	8.5
Widmer	732	207	815.9	1.50E-03	3.7
Widmer	816	207	13.8	2.80E-01	12.1
Widmer	816	207	16.2		22.7
Widmer	816	207	10.4		12.8
Widmer	816	207	11.3		11.7
Widmer	816	207	11.9		14.9
Widmer	816	207	13.4		14.1
Widmer	816	207	15.2		15.0
Widmer	816	207	23.4		12.4
Widmer	649	214	3294	2.60E-04	1.6
Widmer	732	221	243.7	8.80E-03	3.9
Widmer	816	221	5.5	7.80E-01	18.3
Widmer	732	234	114.2	3.30E-02	5.7
Widmer	649	241	3445	3.90E-04	3.2
Widmer	691	241	539.7	1.80E-03	2.0
Widmer	732	241	40.7	2.30E-02	2.7
Widmer	816	241	2.7	1.30E+00	12.3
Widmer	649	259	1693	5.40E-04	2.1
Widmer	816	259	1.7	3.60E+00	17.1
Widmer	816	259	1.1	8.40E+00	15.1
Widmer	649	276	686		3.7
Widmer	649	276	797		5.1
Widmer	649	276	1160		2.0
Widmer	649	276	1200		4.0
Widmer	649	276	1295		4.0
Widmer	649	276	1636		3.8
Widmer	732	276	18	6.00E-02	4.1
Widmer	649	283	823	1.20E-03	4.3
Widmer	732	283	10.2	1.30E-01	5.3
Widmer	649	293	200	1.60E-03	4.3
Widmer	732	296	5.9		7.6
Widmer	649	310	136.9	2.90E-03	8.2
Widmer	732	310	3.7	5.30E-01	7.5

Table A.8.1. Alloy 25 (L-605) historical creep and stress-rupture data (continued)

Heat ID / Source	Temperature (°C)	Stress (MPa)	Rupture Life (MPa)	Minimum Creep Rate (%/hr)	Elongation (%)
Widmer	649	331	74.9	6.50E-03	7.9
Widmer	649	345	51.6	7.50E-03	5.3
Widmer	691	345	5.3	1.10E-01	10.1
Widmer	732	345	1.3	5.70E-01	8.7
Widmer	649	352	64.4	8.00E-03	8.3
Widmer	649	372	23.1	2.70E-02	14.1
Widmer	649	414	3.9		24.8
Widmer	649	414	5.4		13.5
Widmer	649	414	5.6		16.0
Widmer	649	414	6.2		16.4
Widmer	649	414	8		13.8
Widmer	649	414	8.6		16.5
Widmer	649	414	10.1		16.7
Widmer	649	414	11.8		13.4
Widmer	649	414	12.7		14.3
Widmer	649	431	12	9.30E-02	18.4
Widmer	649	431	8.5	7.50E-02	19.9
Widmer	649	448	5.1		20.8

Table A.8.2. Alloy 25 (L-605) historical creep and stress-rupture data for weldments

Heat ID / Source	Temperature (°C)	Stress (MPa)	Rupture Life (MPa)	Minimum Creep Rate (%/hr)	Elongation (%)	Rupture Location
flagella	760	241	532.9	3.50E-03	22.5	
flagella	760	241	315.7	1.69E-02	8.8	
flagella	760	290	150.1	4.70E-02	11.3	
flagella	760	290	24.1	7.40E-02	6.3	
flagella	760	379	1.9	1.51E-01	37.5	
flagella	760	379	0.2		21.0	
flagella	760	234	555.0		36.3	
flagella	760	241	300.5	4.34E-03	13.8	
flagella	760	290	16.8		22.5	
flagella	760	290	11.0	1.25E-01	32.5	
flagella	760	379	5.0	9.70E-01	21.3	
flagella	760	379	1.6	1.34E+00	16.3	
flagella	760	379	1.4	6.25E-01	8.8	
flagella	927	83	392.9	3.30E-02	31.3	
flagella	927	83	320.9	1.55E-03	10.0	
flagella	927	117	27.4	9.37E-02	2.5	
flagella	927	117	15.6		21.3	
flagella	927	138	26.9	2.91E-01	7.1	
flagella	927	138	17.9	4.48E-01	17.5	
flagella	927	83	364.9	3.27E-02	35.0	
flagella	927	83	81.2		16.3	
flagella	927	117	66.1	1.28E-01	42.5	
flagella	927	117	31.5	1.57E-01	27.5	
flagella	927	117	5.8		27.5	
flagella	927	138	21.4	4.07E-01	61.3	
flagella	927	165	4.3	1.66E+00	21.0	
flagella	1093	10	1614.2	5.77E-04		
flagella	1093	10	874.4	8.75E-03		
flagella	1093	24	74.6	1.99E-02	7.5	
flagella	1093	24	38.3			
flagella	1093	41	7.2	8.20E-01	38.8	
flagella	1093	41	1.0		34.0	
flagella	1093	10	424.3	6.91E-03		
flagella	1093	13	129.8		20.0	
flagella	1093	24	75.1	8.00E-02	22.5	
flagella	1093	24	17.6		18.8	
flagella	1093	24	17.0		23.8	
flagella	1093	41	6.1	9.11E-01	25.0	
flagella	1093	41	2.8	1.44E+00		
flagella	1093	41	2.1	2.21E+00	21.3	
ht 1931	649	345	105.0	2.50E-02	5.0	base
ht 1931	649	293		2.00E-03		
ht 1931	704	276	173.0	1.50E-02	2.0	haz
ht 1931	704	248	432.0	1.00E-02	2.0	haz
ht 1931	760	190	226.0	3.50E-02	10.0	haz

Table A.8.2. Alloy 25 (L-605) historical creep and stress-rupture data for weldments (continued)

Heat ID / Source	Temperature (°C)	Stress (MPa)	Rupture Life (MPa)	Minimum Creep Rate (%/hr)	Elongation (%)	Rupture Location
ht 1931	816	121	296.0	1.50E-02	7.5	haz
ht 1931	816	103	897.0	6.00E-03	7.0	haz
ht 1931	871	93	143.0		4.0	haz
ht 1931	871	79	558.0		7.0	haz
ht 1931	982	138	0.2	3.30E+01	9.0	haz
ht 1931	982	103	1.2	8.40E+00	15.0	base
ht 1931	1093	69	0.1		17.0	base
ht 1931	1093	69	0.1		15.0	base
ht 1931	1093	48	0.9	5.00E+00	17.0	base
ht 1931	1149	41	0.3	2.20E+01	10.0	base
ht 1931	1204	28	0.5	3.00E+01	30.0	base
ht 1843	760	155	1693.0	1.00E-02	9.0	base
ht 1843	816	121	1798.0	5.00E-03	10.0	base
ht 1843	871	79	1194.0		10.0	base
ht 1843	816	121	1374.0	4.00E-03	6.0	haz
ht 1335	649	345	372.0	4.00E-03	6.0	base
ht 1335	704	276	20.0		20.0	base
ht 1335	704	276	86.0	2.50E-02	3.0	weld
ht 1335	760	190	106.0	8.00E-02	9.0	base
ht 1335	760	155	755.0	1.00E-02	12.0	base
ht 1335	816	121	269.0	3.00E-02	11.0	base
ht 1335	816	103	542.0		11.0	base
ht 1335	871	78	410.0			base
astm	816	207	28.5		16.0	base
astm	816	148	409.7		15.0	base
astm	816	138	19.0		13.0	base
astm	871	96.5	369.7		5.0	base
astm	927	96.5	41.7		10.0	base
astm	927	55.7	405.8		5.0	base
astm	982	69	43.1		10.0	base
astm	982	41.4	135.0			

INTERNAL DISTRIBUTION

1. E. P. George
2. D. B. Glanton
3-4. J. F. King
5. E. Lara-Curzio
6. R. L. Martin
7. T. E. McGreevy
8. R. G. Miller
9. W. Ren
10-11. J. P. Shingledecker
12. B. L. Sparks
13. R. W. Swindeman
14. G. B. Ulrich
15. ORNL Technical Information Office (RC)

EXTERNAL DISTRIBUTION

16. Robert T. Carpenter, Orbital Sciences Corporation
20030 Century Blvd., Suite 102, Germantown, MD 20874

17. John Dowicki, Office of Radioisotope Power Systems, NE-34/GTN
U. S. Department of Energy, 1000 Independence Avenue SW, Washington, DC 20585-1290

18. Lloyd. Edgerly, Office of Radioisotope Power Systems, NE-34/GTN
U. S. Department of Energy, 1000 Independence Avenue SW, Washington, DC 20585-1290

19. R. G. Hanson, Idaho National Laboratory, P. O. Box 1625, MS-6122, Idaho Falls, ID 83415

20. Stephen G. Johnson, Idaho National Laboratory, P. O. Box 1625, MS-6122, Idaho Falls, ID 83415

21. Robert Lange, Office of Radioisotope Power Systems, NE-34/GTN
U. S. Department of Energy, 1000 Independence Avenue SW, Washington, DC 20585-1290

22. Andrew Leanna, Teledyne Energy Systems, 10707 Gilroy Road. Hunt Valley, MD 21031-1311

23. Michael Katcher, Haynes International, P.O. Box 9013, Kokomo, IN 46904-9013

24. Dwaine Klarstrom, Haynes International, P.O. Box 9013, Kokomo, IN 46904-9013

25-26. Michael McKittrick, Teledyne Energy Systems, 10707 Gilroy Road, Hunt Valley, MD 21031-1311

27. Office of Scientific and Technical Information (PDF file to ORNL Releasing Official, D. R. Hamrin)

28. Emil Skrabek, Orbital Sciences Corporation
20030 Century Blvd., Suite 102, Germantown, MD 20874

29. Craig E. Van Pelt, Los Alamos National Laboratory, P. O. Box 1633, Los Alamos, NM 87545

30. John Vogt, Teledyne Energy Systems, 10707 Gilroy Road, Hunt Valley, MD 21031-1311